

# Topics in fluid mechanics

A. C. Fowler  
Mathematical Institute, Oxford University

December 7, 2020

# Contents

Preface . . . . .	iv
<b>1 Thin film flows</b>	<b>1</b>
1.1 Lubrication theory . . . . .	1
1.2 Droplet dynamics . . . . .	3
1.2.1 Gravity . . . . .	5
1.2.2 Surface tension . . . . .	5
1.2.3 The capillary droplet . . . . .	9
1.2.4 Stability . . . . .	10
1.2.5 Advance and retreat . . . . .	13
1.3 Elongational flows . . . . .	14
1.3.1 Steady flow . . . . .	16
1.3.2 Capillary effects . . . . .	18
Exercises . . . . .	19
<b>2 Porous media</b>	<b>25</b>
2.1 Darcy's law . . . . .	26
2.1.1 Homogenisation . . . . .	28
2.1.2 Empirical measures . . . . .	30
2.2 Basic groundwater flow . . . . .	31
2.2.1 Boundary conditions . . . . .	32
2.2.2 Dupuit approximation . . . . .	32
2.3 Unsaturated soils . . . . .	36
2.3.1 The Richards equation . . . . .	37
2.3.2 Non-dimensionalisation . . . . .	38
2.3.3 Snow melting . . . . .	40
2.3.4 Similarity solutions . . . . .	43
2.4 Immiscible two-phase flows: the Buckley-Leverett equation . . . . .	45
2.5 Consolidation . . . . .	47
Exercises . . . . .	53
<b>3 Convection</b>	<b>59</b>
3.1 Mantle convection . . . . .	59
3.2 The Earth's core . . . . .	61
3.3 Magma chambers . . . . .	63

3.4	Rayleigh–Bénard convection . . . . .	64
3.4.1	Linear stability . . . . .	67
3.5	High Rayleigh number convection . . . . .	69
3.5.1	Boundary layer theory . . . . .	70
3.6	Double-diffusive convection . . . . .	76
3.6.1	Linear stability . . . . .	77
3.6.2	Layered convection . . . . .	80
3.7	Parameterised convection . . . . .	83
3.7.1	Plumes . . . . .	83
3.8	Turbulent convection . . . . .	91
3.9	Notes and references . . . . .	92
	Exercises . . . . .	93
<b>4</b>	<b>Rotating fluid flows</b>	<b>103</b>
4.1	Basic equations . . . . .	105
4.1.1	Spin-up . . . . .	107
4.2	Stratified flow . . . . .	108
4.2.1	Earth’s atmosphere . . . . .	109
4.2.2	Governing equations . . . . .	110
4.2.3	Eddy viscosity . . . . .	111
4.2.4	Potential temperature . . . . .	111
4.2.5	Coordinates . . . . .	112
4.3	Gravity waves . . . . .	115
4.3.1	Kelvin waves . . . . .	117
4.4	Non-dimensionalisation . . . . .	118
4.4.1	Parameter estimates . . . . .	120
4.4.2	A reduced model . . . . .	122
4.4.3	Geostrophic flow . . . . .	123
4.5	The quasi-geostrophic potential vorticity equation . . . . .	124
4.6	Rossby waves . . . . .	127
4.7	Baroclinic instability . . . . .	128
4.7.1	The Eady model . . . . .	129
4.7.2	The Charney model . . . . .	132
4.8	Frontogenesis . . . . .	132
4.9	Depressions and hurricanes . . . . .	134
4.10	Notes and references . . . . .	135
	Exercises . . . . .	135
<b>5</b>	<b>Two-phase flows</b>	<b>142</b>
5.1	Flow régimes . . . . .	143
5.2	A simple two-phase flow model . . . . .	144
5.2.1	Boundary conditions . . . . .	146
5.2.2	Characteristics . . . . .	146
5.2.3	Modifications . . . . .	148

5.2.4	Constitution of the pressures . . . . .	150
5.2.5	Phase change and the energy equation . . . . .	152
5.3	Averaging: two-fluid models . . . . .	153
5.3.1	Jump conditions . . . . .	157
5.3.2	Constitutive laws . . . . .	157
5.3.3	One-dimensional flows: cross-sectional averaging . . . . .	158
5.3.4	Scaling the model . . . . .	160
5.3.5	Homogeneous and drift-flux models . . . . .	162
5.3.6	A simple model for annular flow . . . . .	163
5.3.7	Disturbance waves . . . . .	167
5.4	Density wave oscillations . . . . .	167
5.4.1	Sub-cooled region . . . . .	169
5.4.2	Two-phase region . . . . .	169
5.4.3	Non-dimensionalisation . . . . .	170
5.4.4	A reduced model . . . . .	171
5.4.5	Steady states . . . . .	173
5.4.6	Instability and ill-posedness . . . . .	173
5.4.7	Stability analysis . . . . .	177
	Exercises . . . . .	179
	<b>References</b>	<b>185</b>

# Preface

These notes have been produced to accompany the section C course ‘Topics in fluid mechanics’, introduced into the Oxford curriculum for the first time in Michaelmas Term 2007. The aim of the course is to show how fluid mechanics is used in real applications. The notes describe five topics of current interest, and the course treats each of these in turn. The separate chapters of the notes follow the scheme of the lectures. The present edition of these notes will continue to be updated; the date of this version is as shown below. All advice on errors will be gratefully received.

A. C. Fowler

Oxford, December 7, 2020

# Chapter 1

## Thin film flows

### 1.1 Lubrication theory

Lubrication theory refers to a class of approximations of the Navier–Stokes equations which are based on a large *aspect ratio* of the flow. The aspect ratio is the ratio of two different directional length scales of the flow, as for example the depth and the width. Typical examples of flows where the aspect ratio is large (or small, depending on which length is in the numerator) are lakes, rivers, atmospheric winds, waterfalls, lava flows, and in an industrial setting, oil flows in bearings (whence the term lubrication theory). Lubrication theory forms a basic constituent of a viscous flow course and will not be dwelt on here.

In brief the Navier–Stokes equations for an incompressible take the form

$$\begin{aligned}\nabla \cdot \mathbf{u} &= 0, \\ \rho[\mathbf{u}_t + (\mathbf{u} \cdot \nabla)\mathbf{u}] &= -\nabla p + \mu \nabla^2 \mathbf{u},\end{aligned}\tag{1.1}$$

at least in Cartesian coordinates. It should be recalled that the actual definition of  $\nabla^2 \equiv \nabla \cdot \nabla - \nabla \times \nabla \times$ , and the components of  $\nabla^2 \mathbf{u} = \nabla^2 u_i \mathbf{e}_i$  (we use the summation convention) is only applicable in Cartesian coordinates. For other systems, one can for example consult the appendix in Batchelor (1967).

We begin by non-dimensionalising the equations by choosing scales

$$\mathbf{x} \sim l, \quad t \sim \frac{l}{U}, \quad \mathbf{u} \sim U, \quad p - p_a \sim \frac{\mu U}{l};\tag{1.2}$$

this is the usual way to scale the equations, except that we have chosen to balance the pressure with the viscous terms. The pressure  $p_a$  is an ambient pressure, commonly atmospheric pressure. The resulting dimensionless equations are

$$\begin{aligned}\nabla \cdot \mathbf{u} &= 0, \\ Re \dot{\mathbf{u}} \equiv Re [\mathbf{u}_t + (\mathbf{u} \cdot \nabla)\mathbf{u}] &= -\nabla p + \nabla^2 \mathbf{u},\end{aligned}\tag{1.3}$$

where

$$Re = \frac{\rho U l}{\mu}\tag{1.4}$$

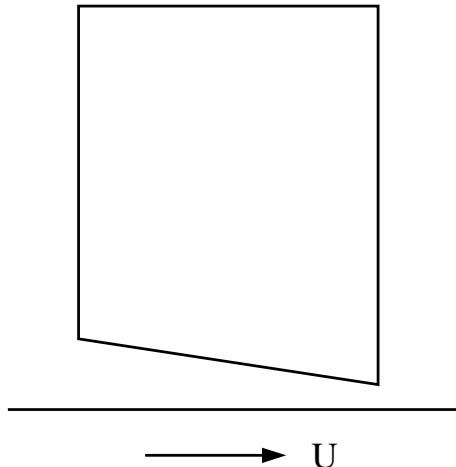


Figure 1.1: A slider bearing.

is the Reynolds number; the overdot denotes the material derivative. For  $Re \ll 1$  we have Stokes flow, where the inertial terms can be neglected, and for  $Re \gg 1$ , boundary layers generally occur (and the pressure would be rescaled to balance the inertia terms, thus  $p \sim Re$ ).

Lubrication theory describes a situation where the geometry of the flow allows the neglect of the inertial terms, even if the Reynolds number is not small. Suppose for example that  $l$  measures the extent of the flow in the  $x$  direction, but the fluid thickness in the (say)  $z$  direction is small. A simple example is the slider bearing, shown in figure 1.1, in which the fluid is confined between two surfaces, which we might take to be  $z = 0$  and  $z = h(x)$ , and one of the surfaces moves at speed  $U$  relative to the other. To be specific, we assume a two-dimensional flow in which the coordinates are  $(x, z)$ , the velocity components are  $(u, w)$ , the bearing ( $z = h$ ) is of finite length  $l$  and lies above a flat surface  $z = 0$  which moves at speed  $U$ ; the bearing is open to the atmosphere at each end, and the gap width  $h \sim d \ll l$ . We define the small parameter

$$\varepsilon = \frac{d}{l}, \quad (1.5)$$

so that in non-dimensional terms, the bearing is at  $z = \varepsilon h(x)$  (where we scaled the dimensional  $h$  with  $d$ , so that the dimensionless  $h$  is  $O(1)$ ). It is then appropriate to rescale the variables as follows:

$$z \sim \varepsilon, \quad w \sim \varepsilon, \quad p \sim \frac{1}{\varepsilon^2}, \quad (1.6)$$

and the equations then take the form

$$\begin{aligned} u_x + w_z &= 0, \\ \varepsilon^2 Re \dot{u} &= -p_x + u_{zz} + \varepsilon^2 u_{xx}, \\ \varepsilon^4 Re \dot{w} &= -p_z + \varepsilon^2 (w_{zz} + \varepsilon^2 w_{xx}), \end{aligned} \quad (1.7)$$

with boundary conditions

$$\begin{aligned} u = 1, \quad w = 0 \quad \text{at} \quad z = 0, \\ u = w = 0 \quad \text{at} \quad z = h, \\ p = 0 \quad \text{at} \quad x = 0, 1. \end{aligned} \tag{1.8}$$

At leading order we then have  $p = p(x, t)$ , and thus, integrating, we obtain

$$u = \frac{z}{h} - \frac{1}{2}p_x(hz - z^2). \tag{1.9}$$

The final part of the solution comes from integrating the mass conservation equation from  $z = 0$  to  $z = h$ . This gives

$$0 = -[w]_0^h = - \int_0^h w_z dz = \int_0^h u_x dz = \frac{\partial}{\partial x} \int_0^h u dz, \tag{1.10}$$

where we can take the differentiation outside the integral because  $u$  is zero at  $z = h$ . In fact we can write down (1.10) directly since it is an expression of conservation of mass across the layer; and this applies more generally, even if the base is not flat, and indeed even if both surfaces depend on time, and the result can be extended to three dimensions; see question 1.2. Calculating the flux from (1.9), we obtain

$$\int_b^s u dz = \frac{1}{2}h - \frac{1}{12}h^3 p_x = K \tag{1.11}$$

is constant. Given  $h$ , the solution for  $p$  can be found as a quadrature, and is

$$p = 6 \left[ f_2(x) - \frac{f_2(1)f_3(x)}{f_3(1)} \right], \quad f_n(x) = \int_0^x \frac{dx}{h^n}. \tag{1.12}$$

In three dimensions, exactly the same procedure leads to the equation

$$\frac{1}{12} \nabla_H \cdot (h^3 \nabla_H p) = \frac{1}{2} h_x, \tag{1.13}$$

where the plate flow direction is taken along the  $x$  axis; derivation of this is left as an exercise.

## 1.2 Droplet dynamics

When one of the surfaces is a free surface (meaning it is free to deform), such as a droplet of liquid resting on a surface, or a rivulet flowing down a window pane, there are two differences which must be accounted for in formulating the problem. One is that the free surface is usually a material surface, so that a kinematic condition is appropriate. In three dimensions, this takes the form

$$w = s_t + us_x + vs_y - a. \tag{1.14}$$

Here,  $z = s$  is the free surface, and  $(u, v, w)$  is the velocity; the term  $a$  is normally absent, but a non-zero value describes surface accumulation (which might for example be due to condensation); if  $a < 0$  it describes ablation due for example to evaporation.

The other difference is that the boundary conditions at the free surface are generally not ones of prescribed velocity but of prescribed stress. In the common case of a droplet of liquid with air above, these conditions take the form

$$\sigma_{nn} = -p_a, \quad \sigma_{nt} = 0, \quad (1.15)$$

representing the fact that the atmosphere exerts a constant pressure on the surface, and no shear stress. Commonly the pressure is taken as *gauge* pressure, i. e., measured relative to atmospheric pressure, which is equivalent to taking  $p_a = 0$  in (1.15). To unravel these conditions, we will consider the case of a two-dimensional incompressible flow. In this case, the components of the stress tensor are

$$\sigma_{11} = -p + \tau_1, \quad \sigma_{13} = \sigma_{31} = \tau_3, \quad \sigma_{33} = -p - \tau_1, \quad (1.16)$$

where

$$\tau_1 = 2\mu u_x, \quad \tau_3 = \mu(u_z + w_x), \quad (1.17)$$

and then with

$$\mathbf{n} = \frac{(-s_x, 1)}{(1 + s_x^2)^{1/2}}, \quad \mathbf{t} = \frac{(1, s_x)}{(1 + s_x^2)^{1/2}}, \quad (1.18)$$

we have

$$\begin{aligned} \sigma_{nn} = \sigma_{ij}n_i n_j &= -p - \frac{[\tau_1(1 - s_x^2) + 2\tau_3 s_x]}{1 + s_x^2}, \\ \sigma_{nt} = \sigma_{ij}n_i t_j &= \frac{[\tau_3(1 - s_x^2) - 2\tau_1 s_x]}{1 + s_x^2}. \end{aligned} \quad (1.19)$$

The dimensionless equations are virtually the same, as we initially scale  $p - p_a$ ,  $\tau_1$  and  $\tau_3$  with  $\mu U/l$ , and then when the rescaling in (1.6) is done (note that consequently we rescale  $\tau_3 \sim 1/\varepsilon$ ), the surface boundary conditions become

$$\begin{aligned} p + \frac{\varepsilon^2[\tau_1(1 - \varepsilon^2 s_x^2) + 2\tau_3 s_x]}{1 + \varepsilon^2 s_x^2} &= 0, \\ \tau_3(1 - \varepsilon^2 s_x^2) - 2\varepsilon^2 \tau_1 s_x &= 0, \end{aligned} \quad (1.20)$$

where

$$\tau_1 = 2u_x, \quad \tau_3 = u_z + \varepsilon^2 w_x. \quad (1.21)$$

Putting  $\varepsilon = 0$ , we thus obtain the leading order conditions

$$p = \tau_3 = 0 \quad \text{on} \quad z = s. \quad (1.22)$$

We can then integrate  $u_{zz} = p_x$ , assuming also a no slip base at  $z = b$ , to obtain an expression for the flux

$$\int_b^s u dz = -\frac{1}{3}h^3 p_x, \quad (1.23)$$

and the conservation of mass equation then integrates (see question 1.2) to give the evolution equation for  $h = s - b$  in the form

$$h_t = \frac{1}{3} \frac{\partial}{\partial x} [h^3 p_x]. \quad (1.24)$$

### 1.2.1 Gravity

The astute reader will notice that something is missing. Unlike the slider bearing, nothing is driving the flow! Indeed, since  $p = p(x, t)$  and  $p = 0$  at  $z = s$ ,  $p = 0$  everywhere. Related to this is the fact that there is nothing to determine the velocity scale  $U$ . Commonly such droplet flows are driven by gravity. If we include gravity in the  $z$  momentum equation, then it takes the dimensional form  $\dots = -p_z - \rho g \dots$ , and since in the rescaled model all the other terms are negligible, the pressure will be hydrostatic,  $p \approx p_a + \rho g(s - z)$ , and this gives a natural scale for  $p - p_a \sim \rho g d$ , and equating this with the eventual pressure scale  $\mu U l / d^2$  determines the velocity scale as

$$U = \frac{\rho g d^3}{\mu l}. \quad (1.25)$$

The dimensionless pressure then becomes  $p = s - z$ , so that  $p_x = s_x$ , and (1.24) now takes the form of a nonlinear diffusion equation,

$$h_t = \frac{1}{3} \frac{\partial}{\partial x} [h^3 s_x]. \quad (1.26)$$

One might wonder how the length scales  $l$  and  $d$  should be chosen; the answer to this, at least if the base is flat, is that it can be taken from the initial condition for  $s$ . The reason for this is that, since (1.26) is a diffusion equation, the drop will simply continue to spread out: there is no natural length scale in the model. Associated with this is the consequent fact that for an initial concentration of liquid at the origin (again on a flat base), the solution takes the form of a similarity solution (see question 1.6). On the other hand, if  $b$  is variable, then it provides a natural length scale. Indeed, for a basin shaped  $b$  (for example  $x^2$ , dimensionlessly), the initial volume (or cross-sectional area) determines the eventual steady state as a lake with  $s$  constant, and both  $d$  and  $l$  prescribed.

### 1.2.2 Surface tension

Another way in which a natural length scale can occur in the model is through the introduction of surface tension at the interface. Let us digress for a moment to consider how surface tension arises. Surface tension is a property of interfaces, whereby they have an apparent strength. This is most simply manifested by the ability of small objects which are themselves heavier than water to float on the interface. The experiment is relatively easily done using a paper clip, and certain insects (water striders) have the ability to stay on the surface of a pond.

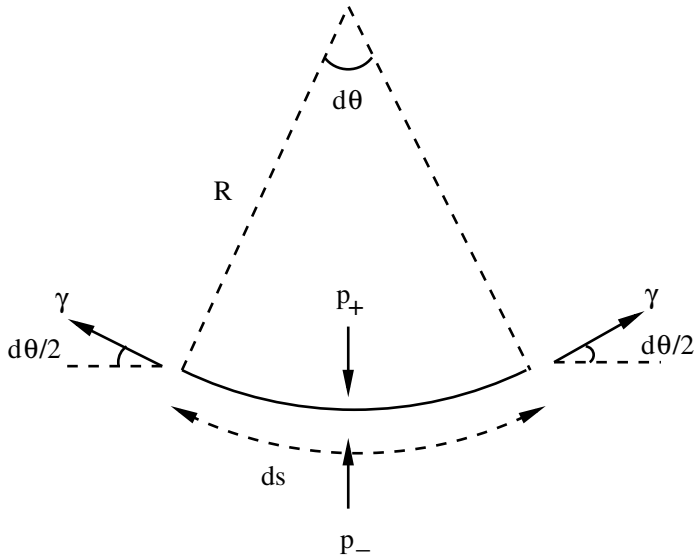


Figure 1.2: The simple mechanical interpretation of surface tension.

The simplest way to think about surface tension is mechanically. The interface between two fluids has an associated tension, such that if one draws a line in the interface of length  $l$ , then there is a force of magnitude  $\gamma l$  which acts along this line:  $\gamma$  is the surface tension, and is a force per unit length. The presence of a surface tension causes an imbalance in the normal stress across the interface, as is indicated in figure 1.2, which also provides a means of calculating it. Taking  $ds$  as a short line segment in an interface subtending an angle  $d\theta$  at its centre of curvature, a force balance normal to the interface leads to the condition

$$p_+ - p_- = \frac{\gamma}{R}, \quad (1.27)$$

where

$$R = \frac{ds}{d\theta} \quad (1.28)$$

is the *radius of curvature*, and its inverse  $1/R$  is the curvature.

For a two-dimensional surface, the curvature is described by two *principal radii of curvature*  $R_1$  and  $R_2$ , the mean curvature is defined by

$$\kappa = \frac{1}{2} \left( \frac{1}{R_1} + \frac{1}{R_2} \right), \quad (1.29)$$

and the pressure jump condition is

$$p_+ - p_- = 2\gamma\kappa = \gamma \left( \frac{1}{R_1} + \frac{1}{R_2} \right), \quad (1.30)$$

although this is not much use to us unless we have a way of calculating the curvature of a surface. This leads us off into the subject of differential geometry, and we do not want to go there. A better way lies along the following path.

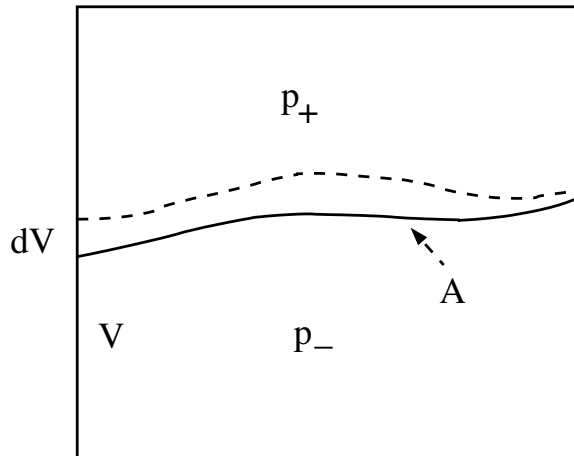


Figure 1.3: The energetic basis of surface tension.

The sceptical reader will in any case wonder what this surface tension actually is. It manifests itself as a force, but along a *line*? And what is its physical origin? The answer to this question veers towards the philosophical. We think we understand force, after all it pops up in Newton's second law, but how do we measure it? Pressure, for example, we conceive of as being due to the collision of molecules with a surface, and the measure of the force they exert is due to the momentum exchange at the surface. We pull on a rope, exerting a force, but the measure of the force is in the extension of the rope via Hooke's law. Force is apparently something we measure via its effect on momentum exchange, or on mechanical displacement; we can actually define force through these laws.

The more basic quantity is energy, which has a direct interpretation, whether as kinetic energy or internal energy (the vibration of molecules). And in fact Newton's second law for a particle is equivalent to the statement that the rate of change of energy is equal to the rate of doing work, and this might be taken as the fundamental law.

The meaning of surface tension actually arises through the property of an interface, which has a surface energy  $\gamma$  with units of energy per unit area. The interfacial condition then arises through the (thermodynamic) statement that in equilibrium the energy of the system is minimised.

To be specific, consider the situation in figure 1.3, where two fluids at pressures  $p_-$  and  $p_+$  are separated by an interface with area  $A$ . Consider a displacement of the interface causing a change of volume  $dV$  as shown. Evidently the work done on the upper fluid is  $p_+ dV$ , which is thus its change of energy, and correspondingly the change for the lower fluid is  $-p_- dV$ . If the change of interfacial surface area is  $dA$ , then the total change of energy<sup>1</sup> is

$$dF = (p_+ - p_-) dV + \gamma dA, \quad (1.31)$$

<sup>1</sup>This energy is the *Helmholtz free energy*.

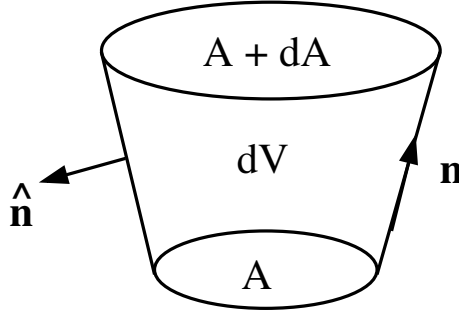


Figure 1.4: Calculation of  $\frac{\partial A}{\partial V}$ .

and at equilibrium this must be zero (since  $F$  is minimised). The equilibrium interfacial boundary condition is therefore

$$p_+ - p_- = -\gamma \frac{\partial A}{\partial V}, \quad (1.32)$$

which, it turns out, is equivalent to (1.30).

Computation of  $\frac{\partial A}{\partial V}$  can be done as follows. We consider a displacement of the interface as shown in figure 1.4. An element of surface  $A$  is displaced to  $A + dA$ , and we can form a connecting volume  $dV$  such that the normal  $\mathbf{n}$  to the interface is always parallel to the connecting surface between the end faces  $A$  and  $A + dA$ . We need to distinguish between the normal  $\hat{\mathbf{n}}$  to the surface of the connecting volume and the normal to the interfacial surface. Evidently we have  $\mathbf{n} = \hat{\mathbf{n}}$  at the end faces, but  $\mathbf{n} \cdot \hat{\mathbf{n}} = 0$  on the connecting cylindrical surface.

Applying the divergence theorem, we see that the change in area is

$$dA = \int_{\partial(dV)} \mathbf{n} \cdot \hat{\mathbf{n}} dS = \int_{dV} \nabla \cdot \mathbf{n} dV, \quad (1.33)$$

and thus

$$\frac{\partial A}{\partial V} = \nabla \cdot \mathbf{n}. \quad (1.34)$$

For example, if the interface is represented as  $z = s(x, y, t)$ , then

$$\nabla \cdot \mathbf{n} = -\nabla \cdot \left[ \frac{\nabla s}{(1 + |\nabla s|^2)^{1/2}} \right], \quad (1.35)$$

where on the right hand side  $\nabla = \nabla_H = \left( \frac{\partial}{\partial x}, \frac{\partial}{\partial y} \right)$ , and for small interfacial displacement, this may be linearised to obtain

$$2\kappa = -\frac{\partial A}{\partial V} = -\nabla \cdot \mathbf{n} = \nabla \cdot \left[ \frac{\nabla s}{(1 + |\nabla s|^2)^{1/2}} \right] \approx \nabla^2 s. \quad (1.36)$$

### 1.2.3 The capillary droplet

Now we use this in the droplet equation. Again we restrict attention to two-dimensional droplets. For three-dimensional droplets, see question 1.7. The surface boundary condition is now approximately  $p - p_a = -\gamma s_{xx}$ , and non-dimensionally

$$p = -\frac{1}{B}s_{xx} \quad \text{on} \quad z = s, \quad (1.37)$$

where  $B$  (commonly also written  $Bo$ ) is the Bond number, given by

$$B = \frac{\rho g l^2}{\gamma}. \quad (1.38)$$

This gives a natural length scale for the droplet, by choosing  $B = 1$ , thus

$$l = \left(\frac{\gamma}{\rho g}\right)^{1/2}; \quad (1.39)$$

in this case the dimensionless pressure is  $p = s - z - s_{xx}$ , and thus mass conservation leads to

$$h_t = \frac{1}{3} \frac{\partial}{\partial x} [h^3(s_x - s_{xxx})], \quad (1.40)$$

and the surface tension term acts as a further stabilising term.<sup>2</sup>

Surface tension acts to limit the spread of a droplet. Indeed there is a steady state of (1.40) which is easily found. Suppose the base is flat, so  $s = h$ . We prescribe the cross-sectional area of the drop,  $A$ . In dimensionless terms, we thus require

$$\int h \, dx = 2\alpha = \left(\frac{\rho g}{\gamma}\right)^{1/2} \frac{A}{d}. \quad (1.41)$$

Let us choose  $d$  so that the maximum depth is one (note that the value of  $d$  remains to be determined). We can suppose that the drop is symmetric about the origin, and that its dimensionless half-width is  $\lambda$ , also to be determined. Thus

$$h(\pm\lambda) = 0, \quad h(0) = 1, \quad (1.42)$$

as well as (1.41), and both  $\alpha$  and  $\lambda$  are to be determined.

A further condition is necessary at the margins. This is the prescription of a contact angle, which can be construed as arising through a balance of the surface tension forces at the three interfaces at the contact line: gas/liquid, liquid/solid, and solid/gas. All three interfaces have a surface energy, and minimisation of this corresponds to prescription of a contact angle. Specifically, if  $\theta$  is the angle between the

---

<sup>2</sup>This can be seen by considering small perturbations about a uniform solution  $h = s = 1$  (with a flat base), for which the linearised equation has normal mode solutions  $\propto \exp(\sigma t + ikx)$ , with  $\sigma = -\frac{1}{3}(k^2 + k^4)$ .

gas/liquid and liquid/solid interfaces, then resolution of the surface tension tangential to the wall leads to

$$\gamma_{\text{SL}} + \gamma \cos \theta = \gamma_{\text{SG}}, \quad (1.43)$$

where  $\gamma_{\text{SL}}$  is the solid/liquid surface energy, and  $\gamma_{\text{SG}}$  is the solid/gas surface energy. Defining  $S = l \tan \theta / d$ , this implies that

$$h_x = \mp S \quad \text{at} \quad x = \pm \lambda. \quad (1.44)$$

The steady state of (1.40) is easily found. The flux is zero, so  $h_x - h_{xxx}$  is zero, and integration of this leads to

$$h = 1 - \left( \frac{\cosh x - 1}{\cosh \lambda - 1} \right), \quad (1.45)$$

and then (1.41) and (1.44) yield

$$\alpha = \frac{\lambda \cosh \lambda - \sinh \lambda}{\cosh \lambda - 1}, \quad \frac{\sinh \lambda}{\cosh \lambda - 1} = S. \quad (1.46)$$

$S(\lambda)$  is a monotonically decreasing function of  $\lambda$  (why?), and tends to one as  $\lambda \rightarrow \infty$ , and therefore the second relation determines  $\lambda$  providing  $S > 1$ . It seems there is a problem if  $S < 1$ , but this is illusory since both  $\alpha$  and  $S$  depend on the unknown  $d$ , so it is best to solve

$$\frac{\alpha}{S} = \frac{A}{2l^2 \tan \theta} = \frac{\lambda \cosh \lambda - \sinh \lambda}{\sinh \lambda}; \quad (1.47)$$

the right hand side increases monotonically from 0 to  $\infty$  as  $\lambda$  increases, and therefore provides a unique solution for  $\lambda$  for any values of  $A$  and  $\theta$ ;  $d$  is then determined by either expression in (1.46).

It is of interest to see when the assumption  $d \ll l$  is then valid. From (1.46),

$$\varepsilon = \tan \theta \left( \frac{\cosh \lambda - 1}{\sinh \lambda} \right). \quad (1.48)$$

The expression in  $\lambda$  increases monotonically from 0 to 1 as  $\lambda$  increases. Thus  $\varepsilon \ll 1$  if either  $\theta \ll 1$ , or (if  $\tan \theta \sim O(1)$ )  $\lambda \ll 1$ . From (1.47), this is the case provided  $A \ll l^2$ , i. e.,  $\frac{\rho g A}{\gamma} \ll 1$ . For air and water, this implies  $A \ll 7 \text{ mm}^2$ .

### 1.2.4 Stability

We now consider the stability of steady solutions of (1.40), which we take in the form

$$h_t = \left[ \frac{1}{3} h^3 (h_x - h_{xxx}) \right]_x. \quad (1.49)$$

Before doing so, we comment on the meaning of the fourth derivative term, which is present due to surface tension. The gravity term is clearly diffusive (with a nonlinear diffusion coefficient  $\frac{1}{3}h^3$ ), but what does the surface tension term represent? In other

contexts it is referred to as a long-range or non-local diffusion (or dispersion) term. To understand such a reference, suppose that the flux of a quantity having density  $\rho$  is given not by Fick's law  $\mathbf{J} = -D\nabla\rho$ , but by

$$\mathbf{J} = -D\nabla W, \quad W = \int_{\mathbf{R}^3} \rho(\mathbf{x} + \boldsymbol{\xi}, t) K(\boldsymbol{\xi}) d\boldsymbol{\xi}, \quad (1.50)$$

where the kernel function  $K = K(\xi)$  (here  $\xi = |\boldsymbol{\xi}|$ ) is spherically symmetric in an isotropic medium, and can be taken (by choice of  $D$ ) to have integral over all space equal to one. If  $K$  is a delta function,  $K = \delta(\mathbf{x} - \boldsymbol{\xi})$ , then we regain Fick's law, but more generally we might suppose it is a Gaussian, for example. (1.50) allows a diffusive motion due to non-local concentrations. An example of such dependence might be in traffic flow, where the motion of individual 'molecules' (cars) is affected by the observation of conditions further ahead. Another example might be in herd migration.

If we suppose that  $K$  is delta function-like, in the sense that it varies rapidly with  $\boldsymbol{\xi}$ , then it is appropriate to approximate (1.50) by Taylor expansion of  $\rho$ , and this leads to

$$\mathbf{J} = -D\nabla\rho - D_2\nabla\nabla^2\rho + \dots, \quad (1.51)$$

where

$$D_2 = \frac{1}{6}D \int_{\mathbf{R}^3} \xi^2 K(\xi) d\boldsymbol{\xi} = \frac{2}{3}\pi D \int_0^\infty \xi^4 K(\xi) d\xi. \quad (1.52)$$

Solutions of the conservation law  $\rho_t = -\nabla \cdot \mathbf{J}$ , using the truncated expression in (1.51), have the normal mode form

$$\rho = e^{i\mathbf{k} \cdot \mathbf{x} + \sigma t}, \quad \sigma = -Dk^2 + D_2k^4, \quad (1.53)$$

and we see that the well-posedness ( $\sigma < 0$  as  $k \rightarrow \infty$ ) in this truncated form requires  $D_2 < 0$ , which seems unlikely, unless  $K$  becomes negative at large  $\xi$ .

If we use the full expression in (1.50), then we find that (1.53) is replaced by

$$\sigma = -4\pi k D I(k), \quad I(k) = \int_0^\infty r K(r) \sin kr dr \quad (1.54)$$

(use spherical polar coordinates and take the  $z$  axis in the direction of  $\mathbf{k}$ ). For example, the (normalised) Gaussian

$$K(\xi) = \frac{1}{(\pi\nu)^{3/2}} e^{-\xi^2/\nu} \quad (1.55)$$

leads to

$$\sigma = -k^2 D e^{-\frac{1}{4}\nu k^2}, \quad (1.56)$$

and expansion of this for small  $\nu$  (or  $k$ ) leads to the truncated version above. Note that for the full expression, the limits  $\nu \rightarrow 0$  and  $k \rightarrow \infty$  do not commute.

Returning to the matter at hand (equation (1.49)), we first consider the case of an infinite uniform layer of fluid, with constant solution  $h = 1$ . In this case we write  $h = 1 + h_1$  and linearise on the basis that  $h_1 \ll 1$ . This simply gives

$$h_{1t} = \frac{1}{3}(h_{1xx} - h_{1xxx}), \quad (1.57)$$

which has the normal mode solutions  $h_1 = e^{ikx+\sigma t}$ , and

$$\sigma = -\frac{1}{3}(k^2 + k^4), \quad (1.58)$$

and the steady solution is stable.

For the case of a finite droplet with solution  $h_0(x)$  given by (1.45), we write  $h = h_0 + h_1$ , and again supposing  $h_1 \ll h_0$ , we linearise as before, which leads (since  $h_0''' = h_0'$ ) to

$$h_{1t} = \left[ \frac{1}{3} h_0^3 (h_{1x} - h_{1xxx}) \right]_x, \quad (1.59)$$

and normal mode solutions are of the form  $h_1 = H(x)e^{\sigma t}$ , and then

$$\sigma H = \left[ \frac{1}{3} h_0^3 (H_x - H_{xxx}) \right]_x. \quad (1.60)$$

This equation requires boundary conditions, but there are issues. If the margins move, then the linearisation must become invalid, since it requires the assumption that  $h_1 \ll h_0$ , which cannot in general be true if the margins move. Consideration of this case requires a more subtle approach, which uses the method of strained coordinates, but will be foregone here.

Let us suppose, then, that the margins do not move. In this case we should prescribe

$$H = H' = 0 \quad \text{at} \quad x = \pm\lambda. \quad (1.61)$$

This provides four conditions, the gradient condition occurring because of the prescribed contact angle. However, we note that the equation is degenerate since  $h_0(\pm\lambda) = 0$ , so that the full complement of boundary conditions may not be able to be satisfied. Often in such singular problems (think of Bessel's equation), one only needs to suppress singular solutions. If (1.61) can be satisfied, then automatically  $H \ll h_0$  as  $x \rightarrow \pm\lambda$ , which is required for the validity of the analysis.

Perhaps an ingenious exact solution of (1.60) can be found, but failing that, we resort to an energy-type argument. If we multiply both sides of the equation by  $H - H_{xx}$  and integrate, then we find

$$\sigma = \frac{-\int_{-\lambda}^{\lambda} \frac{1}{3} h_0^3 (H_x - H_{xxx})^2 dx}{\int_{-\lambda}^{\lambda} (H^2 + H_x^2) dx}, \quad (1.62)$$

and thus  $\sigma < 0$ : the droplet is stable. (1.62) actually provides a variational principle for  $\sigma$ : see question 1.3.

Coming back to the issue of the behaviour of  $H$  at the end points, we put, for example,  $X = x + \lambda$ , so that

$$-\alpha H \approx [X^3 (H_X - H_{XXX})]_X, \quad \alpha = \frac{3|\sigma|}{S^3}, \quad (1.63)$$

and we find possible solution behaviours as  $X \rightarrow 0$  of the form

$$\begin{aligned} H &\sim X^2 + cX^3 + \dots, \\ H &\sim 1 - bX \ln X, \end{aligned} \tag{1.64}$$

where  $b$  and  $c$  are specific constants (see exercise 1.3). Therefore it seems in fact that only one condition can be applied at each end, in keeping with the degenerate nature of the equation, but that in fact the extra gradient condition in (1.61) is satisfied automatically.

It should be mentioned that when droplets move, there are issues both with the viability of prescribing a constant contact angle, because of experimentally observed *contact angle hysteresis*, and also with the application of the no-slip condition, which causes a contact line singularity. So the above discussion of stability is slightly inaccurate.

### 1.2.5 Advance and retreat

When a droplet is of finite extent, it is possible to describe the behaviour near the margins by a local expansion. Typically the surface approaches the base with local power law behaviour, and this depends on whether the droplet is advancing or retreating. Consider, for example, the gravity-driven droplet with an accumulation or ablation term:

$$h_t = \frac{1}{3} (h^3 h_x)_x + a, \tag{1.65}$$

where  $a > 0$  for accumulation, and  $a < 0$  for ablation. (1.65) represents a simple model for the motion of an ice sheet such as Antarctica, where  $a > 0$  represents accumulation due to snowfall. If we suppose that near the margin  $x = x_s$  in a two-dimensional motion,  $h \sim C(x_s - x)^\nu$ , then a local expansion shows that if the front is advancing,  $\dot{x}_s > 0$ , then  $\nu = \frac{1}{3}$  and  $\dot{x}_s \sim \frac{1}{9}C^3$ ; in advance the front is therefore steep. On the other hand, if the front is retreating, then this can only occur if  $a < 0$  (as is in fact obvious), and in that case  $\nu = 1$  and  $\dot{x}_s \sim -|a|/C$ . The fact that the front slope is infinite in advance and finite in retreat is associated with ‘waiting time’ behaviour, which occurs when the front has to ‘fatten up’ before it can advance.

We can try and carry out the same analysis for the droplet with gravity and surface tension. If the left hand margin is  $x = x_s(t)$ , we put  $x = x_s + X$ , so that in the  $(X, t)$  coordinates,

$$h_t - \dot{x}_s h_X = \left[ \frac{1}{3} h^3 (h_X - h_{XXX}) \right]_X; \tag{1.66}$$

however, finding a local expansion is not so easy. Trying various choices, it seems that retreat ( $\dot{x}_s > 0$ ) can be described by

$$h \sim aX(-\ln X)^{1/3}, \quad \dot{x}_s \sim \frac{1}{9}a^3, \tag{1.67}$$

but no such simple (!) behaviour describes advance. However, a balance is possible when there is a non-zero flux at the front  $q_s$ , and then

$$h \sim aX^{3/4}, \quad q_s = \frac{5}{64}a^4. \tag{1.68}$$

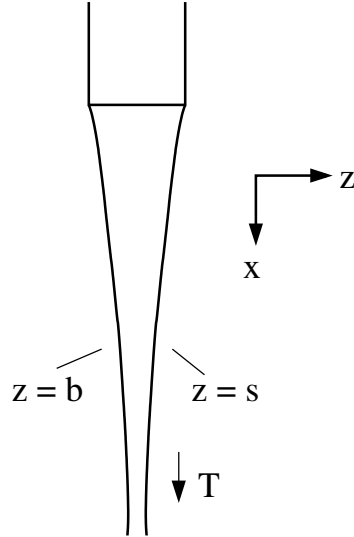


Figure 1.5: An elongational film flow.

But both these behaviours provide an infinite gradient at the margin, which is inconsistent with the prescription of a finite slope contact angle, and also with the lubrication theory linearisation of the curvature term, and for both these reasons, the model becomes suspect if the margins are allowed to move.

### 1.3 Elongational flows

A different application of lubrication theory occurs in a falling sheet of fluid, such as occurs when a tap is switched on. At low velocities, the flow is continuous and laminar (though at very low flow rates it breaks up into droplets), and is also thin, but is distinguished from surface droplets or bearing flows by the fact that *both* surfaces of the fluid have zero stress acting on them.

To be specific, we consider the situation shown in figure 1.5. We consider flow from an orifice, and we take the flow to be two-dimensional, with the  $x$  direction in the direction of flow and  $z$  transverse to it. To begin with we ignore gravity and suppose that the flow is driven by an applied tension  $T$  (force per unit width in the  $y$  direction out of the page) at  $\infty$ ; this is like drawing honey out of a jar with a spoon.

The basic equations are those as scaled in (1.3), and can be written in the form

$$\begin{aligned}
 u_x + w_z &= 0, \\
 Re \dot{u} &= -p_x + \tau_{1x} + \tau_{3z}, \\
 Re \dot{w} &= -p_z + \tau_{3x} - \tau_{1z},
 \end{aligned} \tag{1.69}$$

where

$$\tau_1 = 2u_x, \quad \tau_3 = u_z + w_x. \tag{1.70}$$

If the two free surfaces are  $z = s$  and  $z = b$ , then the boundary conditions on both surfaces are  $\sigma_{nn} = \sigma_{nt} = 0$  (we subtract off the ambient pressure), or in other words  $\sigma_{ni} = \sigma_{ij}n_j = 0$ , and for  $z = s$ , this gives

$$\begin{aligned}(p - \tau_1)s_x + \tau_3 &= 0, \\ -\tau_3 s_x - p - \tau_1 &= 0.\end{aligned}\tag{1.71}$$

(These are actually equivalent to (1.19).)

Now we rescale the variables to account for the large aspect ratio. The difference with the earlier approach is that shear stresses are uniformly small, and so we also rescale  $\tau_3$  to be small. Thus we rescale the variables as

$$z \sim \varepsilon, \quad w \sim \varepsilon, \quad \tau_3 \sim \varepsilon,\tag{1.72}$$

and this leads to the rescaled equations

$$\begin{aligned}u_x + w_z &= 0, \\ Re \dot{u} &= -p_x + \tau_{1x} + \tau_{3z}, \\ \varepsilon^2 Re \dot{w} &= -p_z + \varepsilon^2 \tau_{3x} - \tau_{1z},\end{aligned}\tag{1.73}$$

where

$$\tau_1 = 2u_x, \quad \varepsilon^2 \tau_3 = u_z + \varepsilon^2 w_x,\tag{1.74}$$

and on the free surfaces (e. g.,  $z = s$ )

$$\begin{aligned}(p - \tau_1)s_x + \tau_3 &= 0, \\ -\varepsilon^2 \tau_3 s_x - p - \tau_1 &= 0.\end{aligned}\tag{1.75}$$

At leading order, we have  $u = u(x, t)$ ,  $p + \tau_1 = 0$ ,  $p = -2u_x$ , whence we find

$$\tau_{3z} = Re \dot{u} - 4u_{xx},\tag{1.76}$$

with

$$\tau_3 = 4u_x s_x \quad \text{on } z = s, \quad \tau_3 = 4u_x b_x \quad \text{on } z = b,$$

and from these we deduce

$$\begin{aligned}Re h(u_t + uu_x) &= 4(hu_x)_x, \\ h_t + (hu)_x &= 0,\end{aligned}\tag{1.77}$$

where the second equation is derived as usual to represent conservation of mass. Note in this derivation that the inertial terms are not necessarily small; nevertheless the asymptotic procedure works in the usual way.

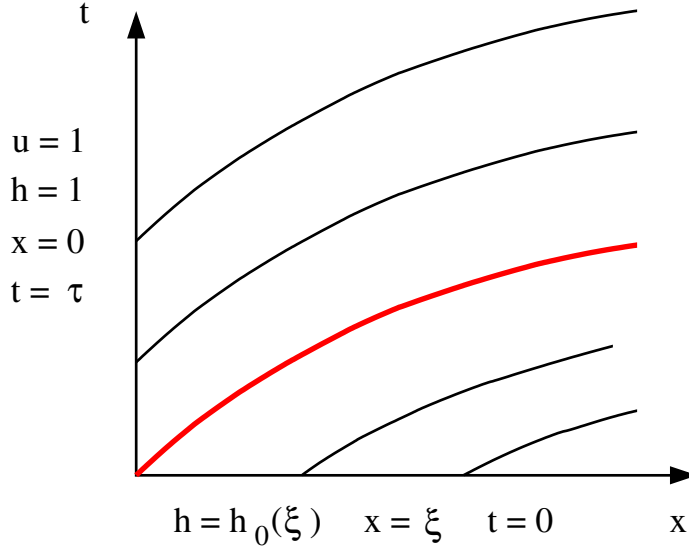


Figure 1.6: Characteristics for (1.77). The dividing characteristic from the origin is shown in red.

### 1.3.1 Steady flow

For a long filament such as that shown in figure 1.5, it is appropriate to prescribe inlet conditions, and these can be taken to be

$$h = u = 1 \quad \text{at} \quad x = 0, \quad (1.78)$$

by appropriate choice of  $U$  and  $d$ . In addition, we prescribe the force (per unit width in the third dimension) to be  $T$ , and this leads to

$$hu_x \rightarrow 1 \quad \text{as} \quad x \rightarrow \infty, \quad (1.79)$$

where the constant is set to one by choice of the length scale as

$$l = \frac{2\mu dU}{T}; \quad (1.80)$$

thus the aspect ratio is small ( $d \ll l$ ) if  $T \ll \mu U$ .

If we consider a slow, steady flow in which the inertial terms can be ignored ( $Re \rightarrow 0$ ), it is easy to solve the equations. We have  $hu = 1$  and  $hu_x = 1$ , and thus

$$u = e^x, \quad h = e^{-x}. \quad (1.81)$$

As a matter of curiosity, one can actually solve the time-dependent problem (1.77), at least when  $Re = 0$ . We write the equations in the form

$$\begin{aligned} h_t + uh_x &= -1, \\ hu_x &= 1, \end{aligned} \quad (1.82)$$

with the boundary and initial conditions as shown in figure 1.6. The characteristic form of the first equation is

$$x_t = u[x(\xi, t), t], \quad h_t = -1, \quad (1.83)$$

where the partial derivatives are holding  $\xi$  fixed, i. e., we consider  $x = x(\xi, t)$ ,  $h = h(\xi, t)$ . The dividing characteristic from the origin (which we define to be  $t = t_d(x)$ ) divides the quadrant into two regions, in which the initial data is parameterised differently. For the lower region  $t < t_d(x)$ , we have

$$h = h_0(\xi) - t. \quad (1.84)$$

We take the first equation in (1.83), and differentiate with respect to  $\xi$ . Using the definition of  $u_x$  from (1.82), we find

$$x_{\xi t} = \frac{x_\xi}{h_0(\xi) - t}. \quad (1.85)$$

We can integrate this with respect to  $t$ , *holding  $\xi$  constant*, that is, the integral with respect to  $t$  is along a characteristic. It follows that

$$x_\xi = \frac{h_0(\xi)}{h_0(\xi) - t}, \quad (1.86)$$

in which we have applied the initial condition  $x_\xi = 1$  at  $t = 0$ .

Next we integrate with respect to  $\xi$  *holding  $t$  constant*; since (1.86) only holds for  $t < t_d(x)$ , we integrate back to this, but note that this corresponds to the value  $\xi = 0$ ; we then have

$$x = x_d(t) + \int_0^\xi \frac{h_0(s) ds}{h_0(s) - t}, \quad (1.87)$$

where  $x_d$  is the inverse of  $t_d(x)$ : to calculate this we need to solve for the upper region  $t > t_d$ .

To do this, we can proceed as above, but it is quicker to note that since the boundary conditions on  $x = 0$  are constant, the solution is just the steady state solution (1.81). In particular, the characteristics are  $e^{-x} = 1 - (t - \tau)$ , and the dividing characteristic is that with  $\tau = 0$ , thus

$$t_d = 1 - e^{-x}, \quad x_d = -\ln(1 - t). \quad (1.88)$$

The solution in  $t < t_d$  is thus

$$x = -\ln(1 - t) + \int_0^\xi \frac{h_0(s) ds}{h_0(s) - t}, \quad (1.89)$$

but the transient is of little interest since it disappears after finite time,  $t = 1$ . As a check, notice that if  $h_0 = e^{-\xi}$ , the steady state solution is regained everywhere.

The steady solution can be extended to positive Reynolds number. In steady flow we then find

$$u_x = Ku + \frac{1}{4}Re u^2 \quad (1.90)$$

for some constant  $K$ , and we see that there is no solution in which the filament can be drawn to  $\infty$ , as pinch-off always occurs. This is in keeping with experience.

### 1.3.2 Capillary effects

As for the shear-driven droplet flows, one can add gravity to the model, and this is done in question 1.4. In this section we consider the modification to the equations which occurs when capillary effects are included. The normal stress conditions are modified to

$$\begin{aligned} -\sigma_{nn} &= -\frac{\gamma s_{xx}}{(1+s_x^2)^{3/2}} \quad \text{on } z = s, \\ \sigma_{nn} &= -\frac{\gamma b_{xx}}{(1+b_x^2)^{3/2}} \quad \text{on } z = b. \end{aligned} \quad (1.91)$$

The definition of  $\sigma_{nn}$  is in (1.19), and with the basic scaling (all lengths scaled with  $l$ , etc.) this leads to

$$-p - \frac{2\tau_3 s_x}{1+s_x^2} - \frac{\tau_1(1-s_x^2)}{1+s_x^2} = \frac{1}{Ca} \frac{\gamma s_{xx}}{(1+s_x^2)^{3/2}} \quad \text{on } z = s, \quad (1.92)$$

where

$$Ca = \frac{\mu U}{\gamma} \quad (1.93)$$

is the capillary number; a similar expression applies on  $z = b$ , with the opposite sign on the right hand side. When the equations are re-scaled ( $z \sim \varepsilon$ , etc.), then these take the approximate form

$$\begin{aligned} p + \tau_1 &\approx -\frac{1}{C} s_{xx} \quad \text{on } z = s, \\ p + \tau_1 &\approx \frac{1}{C} b_{xx} \quad \text{on } z = b, \end{aligned} \quad (1.94)$$

where we write

$$Ca = \varepsilon C. \quad (1.95)$$

Now the normal stress is constant across the filament, thus

$$p + \tau_1 \approx -\frac{1}{C} s_{xx} \quad (1.96)$$

everywhere, and this forces symmetry of the filament,  $s_{xx} = -b_{xx}$ . The rest of the derivation proceeds as before, except that (1.76) gains an extra term  $-s_{xxx}/C$  on the right hand side; integrating this and applying the boundary conditions leads to the modification of (1.77) as (bearing in mind that  $h = s - b$  and thus  $h_{xx} = 2s_{xx}$ )

$$\begin{aligned} h_t + (hu)_x &= 0, \\ Re h(u_t + uu_x) &= \frac{1}{2C} h h_{xxx} + 4(hu_x)_x. \end{aligned} \quad (1.97)$$

## Steady flow

The extra derivatives for  $h$  require, apparently, two extra boundary conditions. If we suppose the pressure becomes atmospheric at  $\infty$ , then we might apply

$$h_{xx} \rightarrow 0 \quad \text{as} \quad x \rightarrow \infty. \quad (1.98)$$

Since this also implies  $h_x \rightarrow 0$ , it may be sufficient. On the other hand, if  $h \rightarrow 0$  at  $\infty$ , the multiplication of the third derivative term by  $h$  may render an extra boundary condition unnecessary.

Again we can consider the steady state. Then  $hu = 1$ , and (1.97) has a first integral

$$K + \frac{Re}{h} = \frac{1}{2C} [hh_{xx} - \frac{1}{2}h_x^2] - \frac{4h_x}{h}, \quad (1.99)$$

where  $K$  is constant. Evidently there is no solution if  $Re > 0$ , as pinch-off must again occur. For the case of slow flow, taking  $Re = 0$ , we have  $K = 4$  due to the far field stress condition, and

$$h^2h_{xx} - \frac{1}{2}hh_x^2 - 8C(h_x + h) = 0. \quad (1.100)$$

We seek a solution of this with  $h(0) = 1$  and  $h(\infty) = 0$ . Phase plane analysis shows that there is a unique such solution: see question 1.8.

## Gravity

While we chose to model a thin filament pulled downwards by a tension, equally we might consider a filament descending under its own weight. In this case, the model can be derived much as before, but now the tension at infinity can be taken to be zero, and the length scale is then chosen to normalise the gravity term to equal one. The modification of (1.77) is then

$$\begin{aligned} h_t + (hu)_x &= 0, \\ h[Re(u_t + uu_x) - 1] &= 4(hu_x)_x. \end{aligned} \quad (1.101)$$

In this case, steady solutions extending to infinity exist, even if  $Re > 0$ , but if any non-zero tension is applied at infinity, the solution breaks down as before and pinch-out occurs. See also question 1.4.

## Exercises

- 1.1 A thin incompressible liquid film flows in two dimensions  $(x, z)$  between a solid base  $z = 0$  where the horizontal  $(x)$  component of the velocity is  $U(t)$ , and may depend on time, and a stationary upper solid surface  $z = h(x)$ , where a no slip condition applies. The upper surface is of horizontal length  $l$ , and is open to the atmosphere at the ends. Write down the equations and boundary conditions

describing the flow, and non-dimensionalise them assuming that  $U(t) \sim U_0$ . (You may neglect gravity.)

Assuming  $\varepsilon = d/l$  is sufficiently small, where  $d$  is a measure of the gap width, rescale the variables suitably, and derive an approximate equation for the pressure  $p$ . Hence derive a formal solution if the block is of finite length  $l$ , and the pressure is atmospheric at each end, and obtain an expression involving integrals of powers of  $h$  for the horizontal fluid flux,  $q(t) = \int_0^h u dz$ .

- 1.2 A two-dimensional incompressible fluid flow is contained between two surfaces  $z = b(x, t)$  and  $z = s(x, t)$ , on which kinematic conditions hold:

$$w = s_t + us_x \quad \text{at} \quad z = s,$$

$$w = b_t + ub_x \quad \text{at} \quad z = b.$$

By integrating the equation of conservation of mass, show that the fluid thickness  $h = s - b$  satisfies the conservation law

$$\frac{\partial h}{\partial t} + \frac{\partial}{\partial x} \int_b^s u dx = 0.$$

Extend the result to three dimensions to show that

$$h_t + \nabla_H \cdot \left[ \int_b^s \mathbf{u}_H dz \right] = 0,$$

where  $\mathbf{u}_H = (u, v)$  is the horizontal velocity, and  $\nabla_H = \left( \frac{\partial}{\partial x}, \frac{\partial}{\partial y} \right)$  is the horizontal gradient operator.

- 1.3 A two-dimensional droplet has thickness  $h(x, t)$  and satisfies the dimensionless equation

$$h_t = \left[ \frac{1}{3} h^3 (h_x - h_{xxx}) \right]_x,$$

with conditions that  $|h_x| = S$  when  $h = 0$ . Show that for a steady solution  $h_0(x)$ ,

$$h_0 = \frac{S(\cosh \lambda - \cosh x)}{\sinh \lambda},$$

where  $\lambda$  is an arbitrary (positive) parameter. If the (dimensionless) ‘volume’ of the drop  $V$  is prescribed, show that  $\lambda$  is uniquely determined, and that it increases monotonically with  $V$ . Find approximate expressions for  $\lambda$  as  $V \rightarrow 0$  and  $V \rightarrow \infty$ .

By writing  $h = h_0 + h_1$ , linearising, and then putting  $h_1 = H(x)e^{\sigma t}$ , derive a linear equation for  $H$ , and give the boundary conditions for  $H$ , assuming the margins of the drop do not move. By writing  $\sigma$  as a functional  $[H]$  in terms of integrals of  $H$  and its derivatives, show that  $\sigma < 0$  for any solution of this, and thus that the drop is stable.

Suppose that  $H$  is a solution of its governing differential equation with corresponding eigenvalue  $\sigma[H]$ . By considering variations  $\delta H$  to  $H$  such that  $\int_{-\lambda}^{\lambda} (H^2 + H_x^2) dx$  remains constant, show that the first variation  $\sigma[H + \delta H] - \sigma[H]$  is zero.

Now let  $X = x + \lambda$  so that  $h_0 \approx SX$ . By considering limiting forms of the resulting approximate equation for  $H$ , show that either  $H \propto X^2 + cX^3 + \dots$  or  $H \propto 1 + bX \ln X + \dots$ , and find the values of  $b$  and  $c$ .

- 1.4 An incompressible two-dimensional flow from a slit of width  $d$  falls vertically under gravity. Define *vertical* and *horizontal* coordinates  $x$  and  $z$ , with corresponding velocity components  $u$  and  $w$ . The stream is symmetric with free interfaces at  $z = \pm s$ , on which no stress conditions apply. Write down the equations and boundary conditions in terms of the deviatoric stress components  $\tau_1 = \tau_{11} = -\tau_{33}$  and  $\tau_3 = \tau_{13} = \tau_{31}$ , and by scaling lengths with  $l$ , velocities with the inlet velocity  $U$ , and choosing suitable scales for time  $t$  and the pressure and stresses, show that the equations take the form

$$u_x + w_z = 0,$$

$$Re \dot{u} = -p_x + \tau_{1x} + \tau_{3z} + 1,$$

$$Re \dot{w} = -p_z + \tau_{3x} - \tau_{1z},$$

where you should define  $\dot{u}$ , the Reynolds number  $Re$ , and write down expressions for  $\tau_1$  and  $\tau_3$ .

Now define  $\varepsilon = \frac{d}{l}$ , and assume it is small. Find a suitable rescaling of the equations, and show that the vertical momentum equation takes the approximate form

$$h[Re \dot{u} - 1] = 4(hu_x)_x,$$

where  $u = u(x, t)$  and  $h$  is the stream width.

Show also that

$$h_t + (hu)_x = 0.$$

Explain why suitable boundary conditions are

$$h = u = 1 \quad \text{at} \quad x = 0, \quad hu_x \rightarrow 0 \quad \text{as} \quad x \rightarrow \infty.$$

Write down a single second order equation for  $u$  in steady flow. If  $Re = 0$ , find the solution.

If  $Re > 0$ , find a pair of first order equations for  $v = \ln u$  and  $w = v_x$ . (*Note:  $w$  here is no longer the horizontal velocity.*) Show that  $(\infty, 0)$  is a saddle point, and that a unique solution satisfying the boundary conditions exists. If  $Re \gg 1$

(but still  $\varepsilon^2 Re \ll 1$ ), show (by rescaling  $w = W/Re$  and  $x = Re X$ ) that the required trajectory hugs the  $W$ -nullcline, and thus show that in this case

$$u \approx \left(1 + \frac{2x}{Re}\right)^{1/2}.$$

- 1.5 A (two-dimensional) droplet rests on a rough surface  $z = b$  and is subject to gravity  $g$  and surface tension  $\gamma$ . Write down the equations and boundary conditions which govern its motion, non-dimensionalise them, and assuming the depth at the summit  $d$  is much less than the half-width  $l$ , derive an approximate equation for the evolution in time of the depth  $h$ . Show that the horizontal velocity scale is

$$U = \frac{\rho g d^3}{\mu l},$$

and derive an approximate set of equations assuming

$$\varepsilon = \frac{d}{l} \ll 1, \quad F = \frac{U}{\sqrt{gd}} \ll 1.$$

Hence show that

$$h_t = \frac{\partial}{\partial x} \left[ \frac{1}{3} h^3 \left( s_x - \frac{1}{B} s_{xxx} \right) \right],$$

where you should define the Bond number  $B$ .

Find a steady state solution of this equation for the case of a flat base, assuming that the droplet area  $A$  and a contact angle  $\theta = \varepsilon\phi$  are prescribed, with  $\phi \sim O(1)$ , and show that it is unique. Explain how the solution chooses the unknowns  $d$  and  $l$ .

- 1.6 A droplet of thickness  $h$  satisfies the equation

$$h_t = \frac{\partial}{\partial x} \left[ \frac{1}{3} h^3 h_x \right].$$

Find a similarity solution of this equation which describes the spread of a drop of area one which is initially concentrated at the origin (i. e.,  $h(x, 0) = \delta(x)$ ).

- 1.7 A three-dimensional droplet, subject to gravity and resting on a flat horizontal surface  $z = 0$ , has surface  $z = h(x, y, t)$ , on which the pressure is given by  $p = \gamma \nabla \cdot \mathbf{n}$ , where  $\mathbf{n}$  is the unit upward normal to the surface. Show that this condition can be written in the form

$$p = -\gamma \nabla \cdot \left[ \frac{\nabla h}{\{1 + |\nabla h|^2\}^{1/2}} \right],$$

where now (and below)  $\nabla$  is the horizontal gradient  $\left( \frac{\partial}{\partial x}, \frac{\partial}{\partial y} \right)$ .

Use the assumptions of lubrication theory to derive the dimensionless droplet equation

$$h_t = \frac{1}{3} \nabla \cdot \left[ h^3 \nabla \left\{ h - \frac{1}{Bo} \nabla^2 h \right\} \right],$$

and define the Bond number  $Bo$ .

Suppose that  $Bo = \infty$  (what does this mean in terms of the surface tension?), and that a concentrated dollop of fluid of dimensionless volume  $2\pi$  is released at  $r = 0$  at  $t = 0$ . By seeking a similarity solution of the form

$$h = \frac{1}{t^\alpha} f(\eta), \quad \eta = \frac{r}{t^\beta},$$

derive and solve an equation for  $f$ , and hence show that the droplet is bounded by a moving front at

$$r \approx 1.55 t^{1/8}.$$

[Hint:  $\left(\frac{8192}{343}\right)^{1/8} \approx 1.55$ .]

Now suppose that  $Bo < \infty$ . Explain why we may take  $Bo = 1$ . Assuming this, and a boundary condition that  $h_r = -S$  where  $h = 0$ , show that the steady solution satisfies

$$h_{rr} + \frac{1}{r} h_r - h = -K,$$

where  $K$  is constant, and deduce that

$$h = \frac{S[I_0(\lambda) - I_0(r)]}{I_0'(\lambda)},$$

where  $I_0(r)$  is the modified Bessel function of the first kind, and  $r = \lambda$  is the drop margin.

Suppose that the dimensionless volume  $V$  of the drop is prescribed, so that

$$\int_0^\lambda r h(r) dr = \frac{V}{2\pi}.$$

We want to show that this determines  $\lambda$  uniquely. By consideration of the equation for  $h$ , show that

$$L(\lambda) \equiv \lambda \left[ \frac{\lambda I_0(\lambda)}{2I_0'(\lambda)} - 1 \right] = \frac{V}{2\pi S};$$

$\lambda$  will thus be unique if  $L(\lambda)$  is monotonically increasing.

Define

$$\eta(\lambda) = \frac{I_0'(\lambda)}{I_0(\lambda)},$$

and show that

$$\eta' = 1 - \frac{\eta}{\lambda} - \eta^2.$$

Assuming that  $I_0(\lambda) \sim 1 + \frac{1}{4}\lambda^2 + \frac{1}{64}\lambda^4 + \dots$  as  $\lambda \rightarrow 0$ , find the limiting behaviour of  $\eta$  as  $\lambda \rightarrow 0$ , and by consideration of trajectory directions in the semi-phase plane  $(\lambda, \eta)$ , show that  $\eta(\lambda)$  is a monotonically increasing function of  $\lambda$ , with  $\eta(\infty) = 1$ . Derive a differential equation for  $g(\lambda) = 2\eta/\lambda$ , and by the same device (but now using the  $(\lambda, g)$  semi-phase plane), show that  $g$  is a monotonically decreasing function of  $\lambda$ . Hence show that  $L(\lambda)$  is a strictly increasing function, as required.

Denoting this steady state as  $h_0(r)$ , perturb  $h$  as  $h = h_0 + h_1$ , and linearise the equation. Now put  $h_1 = H(x, y)e^{\sigma t}$  (do not assume that  $H$  is cylindrically symmetric) and write down the resulting eigenvalue problem for  $\sigma$ . Assuming that the drop margin is not perturbed, show that  $\sigma$  is real and negative for any solution of this eigenvalue problem, and hence that the drop is stable.

- 1.8 A film of fluid is drawn downwards under the action of a tensile force. A model for the dimensionless thickness  $h$  and dimensionless downwards velocity  $u$  of the film is

$$\begin{aligned} h_t + (hu)_x &= 0, \\ Re h(u_t + uu_x) &= \frac{1}{2C}hh_{xxx} + 4(hu_x)_x, \end{aligned}$$

with

$$h = u = 1 \quad \text{on} \quad x = 0, \quad hu_x \rightarrow 1 \quad \text{as} \quad x \rightarrow \infty.$$

Show that a steady state solution in which  $h \rightarrow 0$  as  $x \rightarrow \infty$  can only occur if  $Re = 0$ . In that case, determine a second order differential equation satisfied by  $h$ , and by writing  $h = \frac{1}{2}U^2$  and  $V = U' = U_x$ , write the equation as a pair of first order equations for  $U$  and  $V$ . Show that the origin is a (degenerate) saddle, and therefore show that a solution exists which satisfies the boundary conditions.

# Chapter 2

## Porous media

Groundwater is water which is stored in the soil and rock beneath the surface of the Earth. It forms a fundamental constituent reservoir of the hydrological system, and it is important because of its massive and long lived storage capacity. It is the resource which provides drinking and irrigation water for crops, and increasingly in recent decades it has become an unwilling recipient of toxic industrial and agricultural waste. For all these reasons, the movement of groundwater is an important subject of study.

Soil consists of very small grains of organic and inorganic matter, ranging in size from millimetres to microns. Differently sized (inorganic) particles have different names. Particularly, we distinguish clay particles (size  $< 2$  microns) from silt particles (2–60 microns) and sand (60 microns to 1 mm). Coarser particles still are termed gravel.

Viewed at the large scale, soil thus forms a continuum which is granular at the small scale, and which contains a certain fraction of pore space, as shown in figure 2.1. The volume fraction of the soil (or sediment, or rock) which is occupied by the pore space (or void space, or voidage) is called the *porosity*, and is commonly denoted by the symbol  $\phi$ ; sometimes other symbols are used, for example  $n$ .

Soils are formed by the weathering of rocks, and are specifically referred to as soils when they contain organic matter formed by the rotting of plants and animals. There are two main types of rock: igneous, formed by the crystallisation of molten lava, and sedimentary, formed by the cementation of sediments under conditions of great temperature and pressure as they are buried at depth.<sup>1</sup> Sedimentary rocks, such as sandstone, chalk, shale, thus have their porosity built in, because of the pre-existing granular structure. With increasing pressure, the grains are compacted, thus reducing their porosity, and eventually intergranular cements bond the grains into a rock.

Igneous rock tends to be porous also, for a different reason. It is typically the case for any rock that it is fractured. Most simply, rock at the surface of the Earth

---

<sup>1</sup>There are also *metamorphic* rocks, which form from pre-existing rocks through chemical changes induced by burial at high temperatures and pressures; for example, marble is a metamorphic form of limestone.

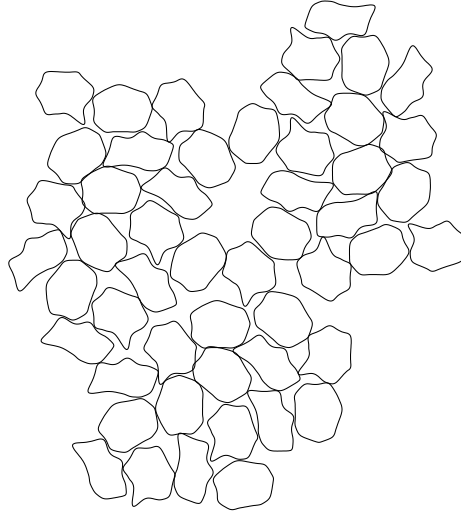


Figure 2.1: A granular porous medium.

is subjected to enormous tectonic stresses, which cause it to fold and fracture. Thus, even if the rock *matrix* itself is not porous, there are commonly faults and fractures within the rock which act as channels through which fluids may flow, and which act on the large scale as an effective porosity. If the matrix is porous at the grain scale also, then one refers to the rock as having a dual porosity, and the corresponding flow models are called double porosity models.

In the subsurface, whether it be soil, underlying regolith, a sedimentary basin, or oceanic lithosphere, the pore space contains liquid. At sufficient depth, the pore space will be saturated with fluid, normally water. At greater depths, other fluids may be present. For example, oil may be found in the pore space of the rocks of sedimentary basins. In the near surface, both air and water will be present in the pore space, and this (unsaturated) region is called the unsaturated zone, or the vadose zone. The surface separating the two is called the piezometric surface, the phreatic surface, or more simply the water table. Commonly it lies several metres below the ground surface, and more in arid regions.

## 2.1 Darcy's law

Groundwater is fed by surface rainfall, and as with surface water it moves under a pressure gradient driven by the slope of the piezometric surface. In order to characterise the flow of a liquid in a porous medium, we must therefore relate the flow rate to the pressure gradient. An idealised case is to consider that the pores consist of uniform cylindrical tubes of radius  $a$ ; initially we will suppose that these are all aligned in one direction. If  $a$  is small enough that the flow in the tubes is laminar (this will be the case if the associated Reynolds number is  $\lesssim 1000$ ), then Poiseuille

flow in each tube leads to a volume flux in each tube of  $q = \frac{\pi a^4}{8\mu} |\nabla p|$ , where  $\mu$  is the liquid viscosity, and  $\nabla p$  is the pressure gradient along the tube. A more realistic porous medium is *isotropic*, which is to say that if the pores have this tubular shape, the tubules will be arranged randomly, and form an interconnected network. However, between nodes of this network, Poiseuille flow will still be appropriate, and an appropriate generalisation is to suppose that the volume flux vector is given by

$$\mathbf{q} \approx -\frac{a^4}{\mu X} \nabla p, \quad (2.1)$$

where the approximation takes account of small interactions at the nodes; the numerical tortuosity factor  $X \gtrsim 1$  takes some account of the arrangement of the pipes.

To relate this to macroscopic variables, and in particular the porosity  $\phi$ , we observe that  $\phi \sim a^2/d_p^2$ , where  $d_p$  is a representative particle or grain size so that  $\mathbf{q}/d_p^2 \sim -\left(\frac{\phi^2 d_p^2}{\mu X}\right) \nabla p$ . We define the volume flux per unit area (having units of velocity) as the discharge  $\mathbf{u}$ . Darcy's law then relates this to an applied pressure gradient by the relation

$$\mathbf{u} = -\frac{k}{\mu} [\nabla p + \rho g \hat{\mathbf{k}}], \quad (2.2)$$

where  $\rho$  is fluid density,  $g$  is the acceleration due to gravity,  $\hat{\mathbf{k}}$  is a unit vector in the vertical (upwards) direction, and  $k$  is an empirically determined parameter called the *permeability*, having units of length squared. The discussion above suggests that we can write

$$k = \frac{d_p^2 \phi^2}{X}; \quad (2.3)$$

the numerical factor  $X$  may typically be of the order of  $10^3$ , but other assumptions can be made instead.

To check whether the pore flow is indeed laminar, we calculate the (particle) Reynolds number for the porous flow. If  $\mathbf{v}$  is the (average) fluid velocity in the pore space (what we will call the *phase-averaged* velocity), then

$$\mathbf{v} = \frac{\mathbf{u}}{\phi}; \quad (2.4)$$

If  $a$  is the pore radius, then we define a particle Reynolds number based on grain size as

$$Re_p = \frac{2\rho v a}{\mu} \sim \frac{\rho |\mathbf{u}| d_p}{\mu \sqrt{\phi}}, \quad (2.5)$$

since  $\phi \sim a/d_p$ . Suppose (2.3) gives the permeability, and we use the gravitational pressure gradient  $\rho g$  to define (via Darcy's law) a velocity scale<sup>2</sup>; then

$$Re_p \sim \frac{\phi^{3/2}}{X} \left( \frac{\rho \sqrt{g d_p} d_p}{\mu} \right)^2 \sim 10 [d_p]^3, \quad (2.6)$$

---

<sup>2</sup>This scale is thus the hydraulic conductivity, defined below in (2.9).

where  $d_p = [d_p]$  mm, and we have used  $\phi^{3/2}/X = 10^{-3}$ ,  $g = 10 \text{ m s}^{-2}$ ,  $\mu/\rho = 10^{-6} \text{ m}^2 \text{ s}^{-2}$ . Thus the flow is laminar for  $d < 5$  mm, corresponding to a gravel. Only for free flow through very coarse gravel could the flow become turbulent, but for water percolation in rocks and soils, we invariably have slow, laminar flow.

In other situations, and notably for forced gas stream flow in fluidised beds or in packed catalyst reactor beds, the flow can be rapid and turbulent. In this case, the Poiseuille flow balance  $-\nabla p = \mu \mathbf{u}/k$  can be replaced by the *Ergun equation*

$$-\nabla p = \frac{\rho |\mathbf{u}| \mathbf{u}}{k'}; \quad (2.7)$$

more generally, the right hand side will be a sum of the two (laminar and turbulent) interfacial resistances. The Ergun equation reflects the fact that turbulent flow in a pipe is resisted by *Reynolds stresses*, which are generated by the fluctuation of the inertial terms in the momentum equation. Just as for the laminar case, the parameter  $k'$ , having units of length, depends both on the grain size  $d_p$  and on  $\phi$ . Evidently, we will have

$$k' = d_p E(\phi), \quad (2.8)$$

with the numerical factor  $E \rightarrow 0$  as  $\phi \rightarrow 0$ .

## Hydraulic conductivity

Another measure of flow rate in porous soil or rock relates specifically to the passage of water through a porous medium under gravity. For free flow, the pressure gradient downwards due to gravity is just  $\rho g$ , where  $\rho$  is the density of water and  $g$  is the gravitational acceleration; thus the water flux per unit area in this case is just

$$K = \frac{k \rho g}{\mu}, \quad (2.9)$$

and this quantity is called the *hydraulic conductivity*. It has units of velocity. A hydraulic conductivity of  $K = 10^{-5} \text{ m s}^{-1}$  (about  $300 \text{ m y}^{-1}$ ) corresponds to a permeability of  $k = 10^{-12} \text{ m}^2$ , this latter unit also being called the *darcy*.

### 2.1.1 Homogenisation

The ‘derivation’ of Darcy’s law can be carried out in a more formal way using the method of homogenisation. This is essentially an application of the method of multiple (space) scales to problems with microstructure. Usually (for analytic reasons) one assumes that the microstructure is periodic, although this is probably not strictly necessary (so long as local averages can be defined).

Consider the Stokes flow equations for a viscous fluid in a medium of macroscopic length  $l$ , subject to a pressure gradient of order  $\Delta p/l$ . For simplicity we will ignore gravity. If the microscopic (e. g., grain size) length scale is  $d_p$ , and  $\varepsilon = d_p/l$ , then if we scale velocity with  $d_p^2 \Delta p / l \mu$  (appropriate for local Poiseuille-type flow), length

with  $l$ , and pressure with  $\Delta p$ , the Navier-Stokes equations can be written in the dimensionless form

$$\begin{aligned}\nabla \cdot \mathbf{u} &= 0, \\ 0 &= -\nabla p + \varepsilon^2 \nabla^2 \mathbf{u},\end{aligned}\tag{2.10}$$

together with the no-slip boundary condition,

$$\mathbf{u} = 0 \text{ on } S : f(\mathbf{x}/\varepsilon) = 0,\tag{2.11}$$

where  $S$  is the interfacial surface. We put  $\mathbf{x} = \varepsilon \boldsymbol{\xi}$  and seek solutions in the form

$$\begin{aligned}\mathbf{u} &= \mathbf{u}^{(0)}(\mathbf{x}, \boldsymbol{\xi}) + \varepsilon \mathbf{u}^{(1)}(\mathbf{x}, \boldsymbol{\xi}) \dots \\ p &= p^{(0)}(\mathbf{x}, \boldsymbol{\xi}) + \varepsilon p^{(1)}(\mathbf{x}, \boldsymbol{\xi}) \dots\end{aligned}\tag{2.12}$$

Expanding the equations in powers of  $\varepsilon$  and equating terms leads to  $p^{(0)} = p^{(0)}(\mathbf{x})$ , and  $\mathbf{u}^{(0)}$  satisfies

$$\begin{aligned}\nabla_{\boldsymbol{\xi}} \cdot \mathbf{u}^{(0)} &= 0, \\ 0 &= -\nabla_{\boldsymbol{\xi}} p^{(1)} + \nabla_{\boldsymbol{\xi}}^2 \mathbf{u}^{(0)} - \nabla_x p^{(0)},\end{aligned}\tag{2.13}$$

equivalent to Stokes' equations for  $\mathbf{u}^{(0)}$  with a forcing term  $-\nabla_x p^{(0)}$ . If  $\mathbf{w}^j$  is the velocity field which (uniquely) solves

$$\begin{aligned}\nabla_{\boldsymbol{\xi}} \cdot \mathbf{w}^j &= 0, \\ 0 &= -\nabla_{\boldsymbol{\xi}} P + \nabla_{\boldsymbol{\xi}}^2 \mathbf{w}^j + \mathbf{e}_j,\end{aligned}\tag{2.14}$$

with periodic (in  $\boldsymbol{\xi}$ ) boundary conditions and  $\mathbf{u} = 0$  on  $f(\boldsymbol{\xi}) = 0$ , where  $\mathbf{e}_j$  is the unit-vector in the  $\xi_j$  direction, then (since the equation is linear) we have (summing over  $j$ )<sup>3</sup>

$$\mathbf{u}^{(0)} = -\frac{\partial p^{(0)}}{\partial x_j} \mathbf{w}^j.\tag{2.15}$$

We define the average flux

$$\langle \mathbf{u} \rangle = \frac{1}{V} \int_V \mathbf{u}^{(0)} dV,\tag{2.16}$$

where  $V$  is the volume over which  $S$  is periodic.<sup>4</sup> Averaging (2.15) then gives

$$\langle \mathbf{u} \rangle = -\mathbf{k}^* \cdot \nabla p,\tag{2.17}$$

---

<sup>3</sup>In other words, we employ the summation convention which states that summation is implied over repeated suffixes, see for example Jeffreys and Jeffreys (1953).

<sup>4</sup>Specifically, we take  $V$  to be the soil volume, but the integral is only over the pore space volume, where  $\mathbf{u}$  is defined. In that case, the average  $\langle \mathbf{u} \rangle$  is in fact the Darcy flux (i. e., volume fluid flux per unit area).

where the (dimensionless) permeability tensor is defined by

$$k_{ij}^* = \langle w_i^j \rangle. \quad (2.18)$$

Recollecting the scales for velocity, length and pressure, we find that the dimensional version of (2.17) is

$$\langle \mathbf{u} \rangle = -\frac{\mathbf{k}}{\mu} \cdot \nabla p, \quad (2.19)$$

where

$$\mathbf{k} = \mathbf{k}^* d_p^2, \quad (2.20)$$

so that  $\mathbf{k}^*$  is the equivalent in homogenisation theory of the quantity  $\phi^2/X$  in (2.3).

### 2.1.2 Empirical measures

While the validity of Darcy's law can be motivated theoretically, it ultimately relies on experimental measurements for its accuracy. The permeability  $k$  has dimensions of (length)<sup>2</sup>, which as we have seen is related to the mean 'grain size'. If we write  $k = d_p^2 C$ , then the number  $C$  depends on the pore configuration. For a tubular network (in three dimensions), one finds  $C \approx \phi^2/72\pi$  (as long as  $\phi$  is relatively small). A different and often used relation is that of Carman and Kozeny, which applies to pseudo-spherical grains (for example sand grains); this is

$$C \approx \frac{\phi^3}{180(1-\phi)^2}. \quad (2.21)$$

The factor  $(1-\phi)^2$  takes some account of the fact that as  $\phi$  increases towards one, the resistance to motion becomes negligible. In fact, for media consisting of uncemented (i. e., separate) grains, there is a critical value of  $\phi$  beyond which the medium as a whole will deform like a fluid. Depending on the grain size distribution, this value is about 0.5 to 0.6. When the medium deforms in this way, the description of the intergranular fluid flow can still be taken to be given by Darcy's law, but this now constitutes a particular choice of the interactive drag term in a two-phase flow model. At lower porosities, deformation can still occur, but it is elastic not viscous (on short time scales), and given by the theory of consolidation or compaction, which we discuss later.

In the case of soils or sediments, empirical power laws of the form

$$C \sim \phi^m \quad (2.22)$$

are often used, with much higher values of the exponent (e.g.  $m = 8$ ). Such behaviour reflects the (chemically-derived) ability of clay-rich soils to retain a high fraction of water, thus making flow difficult. Table 2.1 gives typical values of the permeability of several common rock and soil types, ranging from coarse gravel and sand to finer silt and clay.

$k$ (m <sup>2</sup> )	material
10 <sup>-8</sup>	gravel
10 <sup>-10</sup>	sand
10 <sup>-12</sup>	fractured igneous rock
10 <sup>-13</sup>	sandstone
10 <sup>-14</sup>	silt
10 <sup>-18</sup>	clay
10 <sup>-20</sup>	granite

Table 2.1: Different grain size materials and their typical permeabilities.

An explicit formula of Carman-Kozeny type for the turbulent Ergun equation expresses the ‘turbulent’ permeability  $k'$ , defined in (2.7), as

$$k' = \frac{\phi^3 d_p}{175(1 - \phi)}. \quad (2.23)$$

## 2.2 Basic groundwater flow

Darcy’s equation is supplemented by an equation for the conservation of the fluid phase (or phases, for example in oil recovery, where these may be oil and water). For a single phase, this equation is of the simple conservation form

$$\frac{\partial}{\partial t}(\rho\phi) + \nabla \cdot (\rho\mathbf{u}) = 0, \quad (2.24)$$

supposing there are no sources or sinks within the medium. In this equation,  $\rho$  is the material density, that is, mass per unit volume *of the fluid*. A term  $\phi$  is not present in the divergence term, since  $\mathbf{u}$  has already been written as a volume flux (i.e., the  $\phi$  has already been included in it: *cf.* (2.4)).

Eliminating  $\mathbf{u}$ , we have the parabolic equation

$$\frac{\partial}{\partial t}(\rho\phi) = \nabla \cdot \left[ \frac{k}{\mu} \rho \{ \nabla p + \rho g \hat{\mathbf{k}} \} \right], \quad (2.25)$$

and we need a further equation of state (or two) to complete the model. The simplest assumption corresponds to incompressible groundwater flowing through a rigid porous medium. In this case,  $\rho$  and  $\phi$  are constant, and the governing equation reduces (if also  $k$  is constant) to Laplace’s equation

$$\nabla^2 p = 0. \quad (2.26)$$

This simple equation forms the basis for the following development. Before pursuing this, we briefly mention one variant, and that is when there is a compressible

pore fluid (e. g., a gas) in a non-deformable medium. Then  $\phi$  is constant (so  $k$  is constant), but  $\rho$  is determined by pressure and temperature. If we can ignore the effects of temperature, then we can assume  $p = p(\rho)$  with  $p'(\rho) > 0$ , and (also neglecting gravity whose effect for gases is commonly small)

$$\rho_t = \frac{k}{\mu\phi} \nabla \cdot [\rho p'(\rho) \nabla \rho], \quad (2.27)$$

which is a nonlinear diffusion equation for  $\rho$ , sometimes called the *porous medium equation*. If  $p \propto \rho^\gamma$ ,  $\gamma > 0$ , this is degenerate when  $\rho = 0$ , and the solutions display the typical feature of finite spreading rate of compactly supported initial data.

### 2.2.1 Boundary conditions

The Laplace equation (2.26) in a domain  $D$  requires boundary data to be prescribed on the boundary  $\partial D$  of the spatial domain. Typical conditions which apply are a no flow through condition at an impermeable boundary,  $\mathbf{u} \cdot \mathbf{n} = 0$ , whence

$$\frac{\partial p}{\partial n} + \rho g \mathbf{n} \cdot \hat{\mathbf{k}} = 0 \quad \text{on} \quad \partial D, \quad (2.28)$$

or a permeable surface condition

$$p = p_a \quad \text{on} \quad \partial D, \quad (2.29)$$

where for example  $p_a$  would be atmospheric pressure at the ground surface. Another example of such a condition would be the prescription of oceanic pressure at the interface with the oceanic crust.

A more common application of the condition (2.29) is in the consideration of flow in the saturated zone below the water table (which demarcates the upper limit of the saturated zone). At the water table, the pressure is in equilibrium with the air in the unsaturated zone, and (2.29) applies. The water table is a free surface, and an extra kinematic condition is prescribed to locate it. This condition says that the phreatic surface is also a material surface for the underlying groundwater flow, so that its velocity is equal to the average fluid velocity (*not* the flux): bearing in mind (2.4), we have

$$\frac{\partial F}{\partial t} + \frac{\mathbf{u}}{\phi} \cdot \nabla F = 0 \quad \text{on} \quad \partial D, \quad (2.30)$$

if the free surface  $\partial D$  is defined by  $F(\mathbf{x}, t) = 0$ .

### 2.2.2 Dupuit approximation

One of the principally obvious features of mature topography is that it is relatively flat. A slope of 0.1 is very steep, for example. As a consequence of this, it is typically also the case that gradients of the free groundwater (phreatic) surface are also small, and a consequence of this is that we can make an approximation to the equations of

groundwater flow which is analogous to that used in shallow water theory or the lubrication approximation, i. e., we can take advantage of the large aspect ratio of the flow. This approximation is called the Dupuit, or Dupuit–Forchheimer, approximation.

To be specific, suppose that we have to solve

$$\nabla^2 p = 0 \quad \text{in} \quad 0 < z < h(x, y, t), \quad (2.31)$$

where  $z$  is the vertical coordinate,  $z = h$  is the phreatic surface, and  $z = 0$  is an impermeable basement. We let  $\mathbf{u}$  denote the horizontal (vector) component of the Darcy flux, and  $w$  the vertical component. In addition, we now denote by  $\nabla = \left( \frac{\partial}{\partial x}, \frac{\partial}{\partial y} \right)$  the horizontal component of the gradient vector. The boundary conditions are then

$$\begin{aligned} p = 0, \quad \phi h_t + \mathbf{u} \cdot \nabla h = w \quad \text{on} \quad z = h, \\ \frac{\partial p}{\partial z} + \rho g = 0 \quad \text{on} \quad z = 0; \end{aligned} \quad (2.32)$$

here we take (gauge) pressure measured relative to atmospheric pressure. The condition at  $z = 0$  is that of no normal flux, allowing for gravity.

Let us suppose that a horizontal length scale of relevance is  $l$ , and that the corresponding variation in  $h$  is of order  $d$ , thus

$$\varepsilon = \frac{d}{l} \quad (2.33)$$

is the size of the phreatic gradient, and is small. We non-dimensionalise the variables by scaling as follows:

$$\begin{aligned} x, y \sim l, \quad z \sim d, \quad p \sim \rho g d, \\ \mathbf{u} \sim \frac{k \rho g d}{\mu l}, \quad w \sim \frac{k \rho g d^2}{\mu l^2}, \quad t \sim \frac{\phi \mu l^2}{k \rho g d}. \end{aligned} \quad (2.34)$$

The choice of scales is motivated by the same ideas as lubrication theory. The pressure is nearly hydrostatic, and the flow is nearly horizontal.

The dimensionless equations are

$$\begin{aligned} \mathbf{u} = -\nabla p, \quad \varepsilon^2 w = -(p_z + 1), \\ \nabla \cdot \mathbf{u} + w_z = 0, \end{aligned} \quad (2.35)$$

with

$$\begin{aligned} p_z = -1 \quad \text{on} \quad z = 0, \\ p = 0, \quad h_t = w + \nabla p \cdot \nabla h \quad \text{on} \quad z = h. \end{aligned} \quad (2.36)$$

At leading order as  $\varepsilon \rightarrow 0$ , the pressure is hydrostatic:

$$p = h - z + O(\varepsilon^2). \quad (2.37)$$

More precisely, if we put

$$p = h - z + \varepsilon^2 p_1 + \dots, \quad (2.38)$$

then (2.35) implies

$$p_{1zz} = -\nabla^2 h, \quad (2.39)$$

with boundary conditions, from (2.36),

$$p_{1z} = 0 \quad \text{on} \quad z = 0,$$

$$p_{1z} = -h_t + |\nabla h|^2 \quad \text{on} \quad z = h. \quad (2.40)$$

Integrating (2.39) from  $z = 0$  to  $z = h$  thus yields the evolution equation for  $h$  in the form

$$h_t = \nabla \cdot [h \nabla h], \quad (2.41)$$

which is a nonlinear diffusion equation of degenerate type when  $h = 0$ .

This is easily solved numerically, and there are various exact solutions which are indicated in the exercises. In particular, steady solutions are found by solving Laplace's equation for  $\frac{1}{2}h^2$ , and there are various kinds of similarity solution. (2.41) is a second order equation requiring two boundary conditions. A typical situation in a river catchment is where there is drainage from a watershed to a river. A suitable problem in two dimensions is

$$h_t = (hh_x)_x + r, \quad (2.42)$$

where the source term  $r$  represents recharge due to rainfall. It is given by

$$r = \frac{r_D}{\varepsilon^2 K}, \quad (2.43)$$

where  $r_D$  is the rainfall rate and  $K = k\rho g/\mu$  is the hydraulic conductivity. At the divide (say,  $x = 0$ ), we have  $h_x = 0$ , whereas at the river (say,  $x = 1$ ), the elevation is prescribed,  $h = 1$  for example. The steady solution is

$$h = [1 + r - rx^2]^{1/2}, \quad (2.44)$$

and perturbations to this decay exponentially. If this value of the elevation of the water table exceeds that of the land surface, then a seepage face occurs, where water seeps from below and flows over the surface. This can sometimes be seen in steep mountainous terrain, or on beaches, when the tide is going out.

The Dupuit approximation is not uniformly valid at  $x = 1$ , where conditions of symmetry at the base of a valley would imply that  $u = 0$  (below the river), and thus  $p_x = 0$ . There is therefore a boundary layer near  $x = 1$ , where we rescale the variables by writing

$$x = 1 - \varepsilon X, \quad w = \frac{W}{\varepsilon}, \quad h = 1 + \varepsilon H, \quad p = 1 - z + \varepsilon P. \quad (2.45)$$

Substituting these into the two-dimensional version of (2.35) and (2.36), we find

$$u = P_X, \quad W = -P_z, \quad \nabla^2 P = 0 \quad \text{in} \quad 0 < z < 1 + \varepsilon H, \quad 0 < X < \infty, \quad (2.46)$$

with boundary conditions

$$\begin{aligned}
P &= H, \quad \varepsilon H_t + P_X H_X = \frac{W}{\varepsilon} + r \quad \text{on} \quad z = 1 + \varepsilon H, \\
P_X &= 0 \quad \text{on} \quad X = 0, \\
P_z &= 0 \quad \text{on} \quad z = 0, \\
P &\sim H \sim rX \quad \text{as} \quad X \rightarrow \infty.
\end{aligned} \tag{2.47}$$

At leading order in  $\varepsilon$ , this is simply

$$\begin{aligned}
\nabla^2 P &= 0 \quad \text{in} \quad 0 < z < 1, \quad 0 < X < \infty, \\
P_z &= 0 \quad \text{on} \quad z = 0, 1, \\
P_X &= 0 \quad \text{on} \quad X = 0, \\
P &\sim rX \quad \text{as} \quad X \rightarrow \infty.
\end{aligned} \tag{2.48}$$

Evidently, this has no solution unless we allow the incoming groundwater flux  $r$  from infinity to drain to the river at  $X = 0, z = 1$ . We do this by having a singularity in the form of a sink at the river,

$$P \sim \frac{r}{\pi} \ln \{X^2 + (1 - z)^2\} \quad \text{near} \quad X = 0, \quad z = 1. \tag{2.49}$$

The solution to (2.48) can be obtained by using complex variables and the method of images, by placing sinks at  $z = \pm(2n + 1)$ , for integral values of  $n$ . Making use of the infinite product formula (Jeffrey 2004, p. 72)

$$\prod_1^{\infty} \left(1 + \frac{\zeta^2}{(2n + 1)^2}\right) = \cosh \frac{\pi\zeta}{2}, \tag{2.50}$$

where  $\zeta = X + iz$ , we find the solution to be

$$P = \frac{r}{\pi} \ln \left[ \cosh^2 \frac{\pi X}{2} \cos^2 \frac{\pi z}{2} + \sinh^2 \frac{\pi X}{2} \sin^2 \frac{\pi z}{2} \right]. \tag{2.51}$$

The complex variable form of the solution is

$$\phi = P + i\psi = \frac{2r}{\pi} \ln \cosh \frac{\pi\zeta}{2}, \tag{2.52}$$

which is convenient for plotting. The streamlines of the flow are the lines  $\psi = \text{constant}$ , and these are shown in figure 2.2.

This figure illustrates an important point, which is that although the flow towards a drainage point may be more or less horizontal, near the river the groundwater seeps upwards from depth. Drainage is not simply a matter of near surface recharge and drainage. This means that contaminants which enter the deep groundwater may reside there for a very long time.

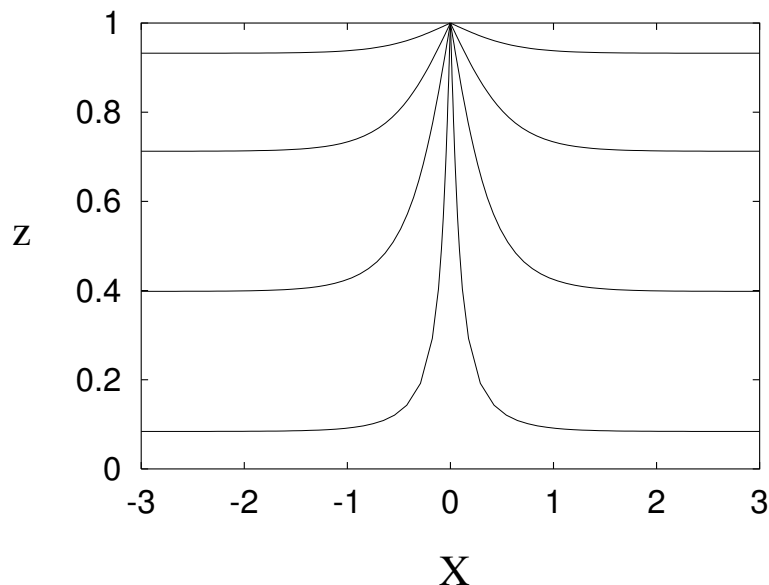


Figure 2.2: Groundwater flow lines towards a river at  $X = 0$ ,  $z = 1$ .

A related point concerns the recharge parameter  $r$  defined in (2.43). According to table 2.1, a typical permeability for sand is  $10^{-10} \text{ m}^2$ , corresponding to a hydraulic conductivity of  $K = 10^{-3} \text{ m s}^{-1}$ , or  $3 \times 10^4 \text{ m y}^{-1}$ . Even for phreatic slopes as low as  $\varepsilon = 10^{-2}$ , the recharge parameter  $r \lesssim O(1)$ , and shallow aquifer drainage is feasible.

However, finer-grained sediments are less permeable, and the calculation of  $r$  for a silt with permeability of  $10^{-14} \text{ m}^2$  ( $K = 10^{-7} \text{ m s}^{-1} = 3 \text{ m y}^{-1}$ ) suggests that  $r \sim 1/\varepsilon^2 \gg 1$ , so that if the Dupuit approximation applied, the groundwater surface would lie above the Earth's surface everywhere. This simply points out the obvious fact that if the groundmass is insufficiently permeable, drainage cannot occur through it but water will accumulate at the surface and drain by overland flow. The fact that usually the water table is below but quite near the surface suggests that the long term response of landscape to recharge is to form topographic gradients and sufficiently deep sedimentary basins so that this *status quo* can be maintained.

## 2.3 Unsaturated soils

Let us now consider flow in the unsaturated zone. Above the water table, water and air occupy the pore space. If the porosity is  $\phi$  and the water volume fraction per unit volume of soil is  $W$ , then the ratio  $S = W/\phi$  is called the *relative saturation*. If  $S = 1$ , the soil is saturated, and if  $S < 1$  it is unsaturated. The pore space of an unsaturated soil is configured as shown in figure 2.3. In particular, the air/water interface is curved, and in an equilibrium configuration the curvature of this interface will be constant throughout the pore space. The value of the curvature depends on

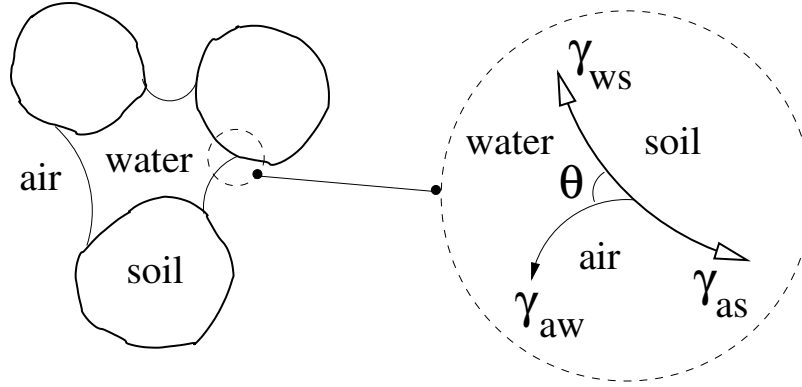


Figure 2.3: Configuration of air and water in pore space. The contact angle  $\theta$  measured through the water is acute, so that water is the *wetting* phase.  $\gamma_{ws}$ ,  $\gamma_{as}$  and  $\gamma_{aw}$  are the surface energies of the three interfaces.

the amount of liquid present. The less liquid there is (i. e., the smaller the value of  $S$ ), then the smaller the pores where the liquid is found, and thus the higher the curvature. Associated with the curvature is a suction effect due to surface tension across the air/water interface. The upshot of all this is that the air and water pressures are related by a *capillary suction characteristic* function which expresses the difference between the pressures as a function of mean curvature, and hence, directly,  $S$ . Elementary geometry in a cylindrical pore of diameter  $d_p$  implies

$$p_a - p = \frac{2\gamma \cos \theta}{d_p}, \quad (2.53)$$

where  $\theta$  is the contact angle. More generally, we can take

$$p_a - p = f(S). \quad (2.54)$$

The suction characteristic  $f(S)$  is equal to  $2\gamma\kappa$ , where  $\kappa$  is the mean interfacial curvature:  $\gamma$  is the surface tension. For air and water in soil,  $f$  is positive as water is the *wetting phase*, that is, the *contact angle* at the contact line between air, water and soil grain is acute, measured through the water (see figure 2.3). The resulting form of  $f(S)$  displays hysteresis as indicated in figure 2.4, with different curves depending on whether drying or wetting is taking place.

### 2.3.1 The Richards equation

To model the flow, we have the conservation of mass equation in the form

$$\frac{\partial(\phi S)}{\partial t} + \nabla \cdot \mathbf{u} = 0, \quad (2.55)$$

where we take  $\phi$  as constant. Darcy's law for an unsaturated flow has the form

$$\mathbf{u} = -\frac{k(S)}{\mu} [\nabla p + \rho g \hat{\mathbf{k}}], \quad (2.56)$$

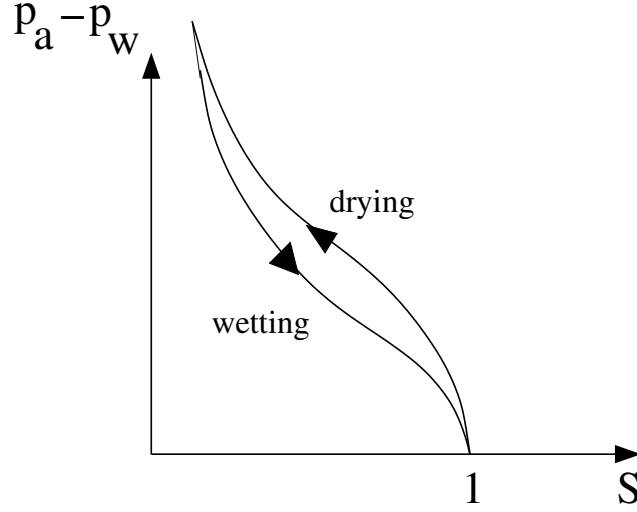


Figure 2.4: Capillary suction characteristic. It displays hysteresis in wetting and drying.

where the permeability  $k$  depends on  $S$ . If  $k(1) = k_0$  (the saturated permeability), then one commonly writes  $k = k_0 k_r(S)$ , where  $k_r$  is the *relative permeability*. The most obvious assumption would be  $k_r = S$ , but this is rarely appropriate, and a better representation is a convex function, such as  $k_r = S^3$ . An even better representation is a function such as  $k_r = \left(\frac{S - S_0}{1 - S_0}\right)_+^3$ , where  $S_0$  is known as the residual saturation.

It represents the fact that in fine-grained soils, there is usually some minimal water fraction which cannot be removed. It is naturally associated with a capillary suction characteristic function  $p_a - p = f(S)$  which tends to infinity as  $S \rightarrow S_0+$ , also appropriate for fine-grained soils.

In one dimension, and if we take the vertical coordinate (upwards) to be  $z$ , we obtain the *Richards equation*

$$\phi \frac{\partial S}{\partial t} - \frac{\partial V(S)}{\partial z} = \frac{\partial}{\partial z} \left[ D(S) \frac{\partial S}{\partial z} \right], \quad (2.57)$$

where

$$V(S) = K_0 k_r(S), \quad D(S) = -\frac{K_0}{\rho g} k_r(S) f'(S), \quad K_0 = \frac{k_0 \rho g}{\mu}; \quad (2.58)$$

$K_0$  is the saturated hydraulic conductivity. We are assuming  $p_a = \text{constant}$  (and also that the soil matrix is incompressible).

### 2.3.2 Non-dimensionalisation

We choose scales for the variables as follows:

$$f = \Pi \psi, \quad z \sim l, \quad t \sim \frac{\phi l}{K_0}, \quad (2.59)$$

where we have defined the suction pressure scale to be

$$\Pi = \frac{\gamma}{d_p}; \quad (2.60)$$

here  $d_p$  is the (mean) pore diameter and  $\gamma$  is the surface tension, assumed constant. The Richards equation then becomes, in dimensionless variables,

$$S_t - k'_r(S)S_z = \varepsilon [D^*(S)S_z]_z, \quad (2.61)$$

where

$$D^*(S) = -k_r(S)\psi'(S). \quad (2.62)$$

Note that  $\psi$  is a decreasing function, so that the diffusion coefficient  $D^* > 0$ , as is indeed necessary. The single dimensionless parameter is

$$\varepsilon = \frac{\Pi}{\rho gl}, \quad (2.63)$$

and is small for coarse soils, and  $O(1)$  for fine-grained soils. As a specific example, we take  $l = 1$  m, so that  $\rho gl \sim 10^4$  Pa. If we take  $\gamma = 70$  mN m<sup>-1</sup> for water/air, and  $d_p \sim 0.1$  mm, then  $\Pi \sim 700$  Pa, and  $\varepsilon \sim 0.07$ ; this may be appropriate for sandy soils. For silty soils, we might have  $d_p \sim 10$   $\mu$ m, and then  $\varepsilon \sim 0.7$ .

As a specific example, we consider the case of soil wetting due to surface infiltration: of rainfall, for example. Suppose that there is a constant downwards flux of (dimensional) rainfall  $q$  at the surface. It is convenient to define the depth  $\zeta = -z$ , and take the vadose zone to be in  $0 < \zeta < 1$ . The Richards equation is then

$$S_t + k'_r(S)S_\zeta = \varepsilon [D^*(S)S_\zeta]_\zeta, \quad (2.64)$$

and suitable boundary conditions for the saturation are

$$\begin{aligned} k_r(S) - \varepsilon D^*(S)S_\zeta &= q^* \quad \text{at} \quad \zeta = 0, & q^* &= \frac{q}{K_0}, \\ S &= 1 \quad \text{at} \quad \zeta = 1. \end{aligned} \quad (2.65)$$

In the steady state, the first condition in (2.65) applies everywhere, and the solution is a quadrature,

$$\int_S^1 \frac{\varepsilon D^*(S) dS}{k_r(S) - q^*} = 1 - \zeta. \quad (2.66)$$

Obviously  $S$  must be an increasing function of  $\zeta$ , and this requires  $q^* < k_r(1) = 1$ , in other words  $q < K_0$ : the supplied rainfall must be less than the saturated hydraulic conductivity.

What if it is not? It is easy to see from the solution (2.66) that as  $q^* \rightarrow 1-$ , the saturation approaches one. If  $q > K_0$ , the supplied flux at the surface is greater than the soil's maximum drainage capacity (which is the saturated hydraulic conductivity). So in this case, water must pond at the surface, and the boundary condition is replaced

by  $S = 1$  at  $\zeta = 0$ ; clearly in this case, the soil is waterlogged and the water table is pushed up to the soil surface. Such ponding is commonly observed during periods of heavy rainfall. For silt with  $k_0 = 10^{-14} \text{ m}^2$ , the hydraulic conductivity  $K_0 \sim 10^{-7} \text{ m s}^{-1}$  or  $3 \text{ m y}^{-1}$ , while average rainfall in England, for example, is  $\leq 1 \text{ m y}^{-1}$ . Thus *on average*  $q^* \leq 1$  for such soils, but during storms we can expect  $q^* \gg 1$ . When ponding does occur, the pond depth is determined by the balance between precipitation, infiltration, and surface run-off.

### 2.3.3 Snow melting

An application of the unsaturated flow model occurs in the study of melting snow. In particular, it is found that pollutants which may be uniformly distributed in snow (e. g. sulphate  $\text{SO}_4^{2-}$  from sulphur emissions via acid rain) can be concentrated in melt water run-off, with a consequent enhanced detrimental effect on stream pollution. The question then arises, why this should be so? We shall find that uniform surface melting of a dry snowpack can lead to a meltwater spike at depth.

Suppose we have a snow pack of depth  $l$ . Snow is a porous aggregate of ice crystals, and meltwater formed at the surface can percolate through the snow pack to the base, where run-off occurs. (We ignore effects of re-freezing of meltwater.) The model (2.64) is appropriate, and to be specific, we will also take

$$k_r = S^3, \quad \psi(S) = \frac{1}{S} - S, \quad (2.67)$$

based on typical experimental results.

Suitable boundary conditions in a melting event might be to prescribe the melt flux  $q_0$  at the surface, thus

$$k_r \left( \varepsilon \frac{\partial \psi}{\partial \zeta} + 1 \right) = q^* = \frac{q_0}{K_0} \quad \text{at} \quad \zeta = 0. \quad (2.68)$$

If the base is impermeable, then

$$k_r \left( \varepsilon \frac{\partial \psi}{\partial \zeta} + 1 \right) = 0 \quad \text{at} \quad \zeta = 1. \quad (2.69)$$

This is certainly not realistic if  $S$  reaches 1 at the base, since then ponding must occur and presumably melt drainage will occur via a sub-horizontal flow under the snowpack, but we will examine the initial stages of the flow using (2.69) before that happens. Finally, we suppose  $S = 0$  at  $t = 0$ . Again, this is not realistic in the model (it implies infinite capillary suction) but it is a feasible approximation to make.

Simplification of this model now leads to the dimensionless Richards equation in the form

$$\frac{\partial S}{\partial t} + 3S^2 \frac{\partial S}{\partial \zeta} = \varepsilon \frac{\partial}{\partial \zeta} \left[ S(1 + S^2) \frac{\partial S}{\partial \zeta} \right]. \quad (2.70)$$

If we choose  $\gamma = 70 \text{ mN m}^{-1}$ ,  $d_p = 0.1 \text{ mm}$ ,  $\rho = 10^3 \text{ kg m}^{-3}$ ,  $g = 10 \text{ m s}^{-2}$ ,  $l = 1 \text{ m}$  as before, then again  $\varepsilon = 0.07$ . It follows that (2.70) has a propensity to form shocks,

these being diffused by the term in  $\varepsilon$  over a distance  $O(\varepsilon)$  (by analogy with the shock structure for the Burgers equation).

We want to solve (2.70) with the initial condition

$$S = 0 \quad \text{at} \quad t = 0, \quad (2.71)$$

and the boundary conditions

$$S^3 - \varepsilon S(1 + S^2) \frac{\partial S}{\partial \zeta} = q^* \quad \text{on} \quad \zeta = 0, \quad (2.72)$$

and

$$S^3 - \varepsilon S(1 + S^2) \frac{\partial S}{\partial \zeta} = 0 \quad \text{at} \quad \zeta = 1. \quad (2.73)$$

Roughly, for  $\varepsilon \ll 1$ , these are

$$\begin{aligned} S &= S_0 \quad \text{at} \quad \zeta = 0, \\ S &= 0 \quad \text{at} \quad \zeta = 1, \end{aligned} \quad (2.74)$$

where  $S_0 = q^{*1/3}$ , which we initially take to be  $O(1)$  (and  $< 1$ , so that surface ponding does not occur).

Neglecting  $\varepsilon$ , the solution is the step function

$$\begin{aligned} S &= S_0, & \zeta < \zeta_f, \\ S &= 0, & \zeta > \zeta_f, \end{aligned} \quad (2.75)$$

and the shock front at  $\zeta_f$  advances at a rate  $\dot{\zeta}_f$  given by the jump condition

$$\dot{\zeta}_f = \frac{[S^3]_{-}^{+}}{[S]_{-}^{+}} = S_0^2. \quad (2.76)$$

In dimensional terms, the shock front moves at speed  $q_0/\phi S_0$ , which is in fact obvious (given that it has constant  $S$  behind it).

The shock structure is similar to that of Burgers' equation. We put

$$\zeta = \zeta_f + \varepsilon Z, \quad (2.77)$$

and  $S$  rapidly approaches the quasi-steady solution  $S(Z)$  of

$$-cS' + 3S^2S' = [S(1 + S^2)S']', \quad (2.78)$$

where  $c = \dot{\zeta}_f$ ; hence

$$S(1 + S^2)S' = -S(S_0^2 - S^2), \quad (2.79)$$

in order that  $S \rightarrow S_0$  as  $Z \rightarrow -\infty$ , and where we have chosen

$$c = S_0^2, \quad (2.80)$$

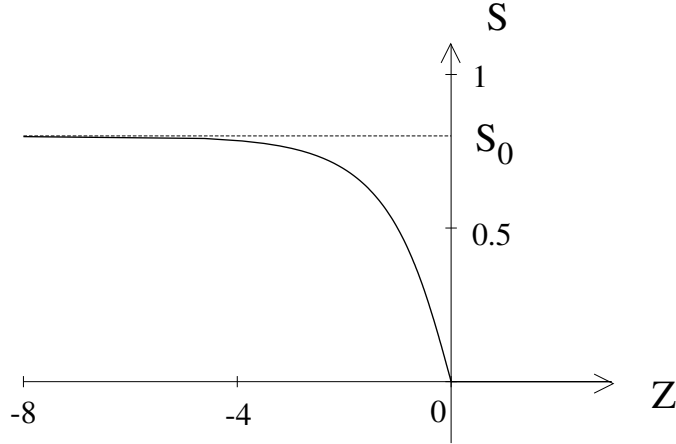


Figure 2.5:  $S(Z)$  given by (2.82); the shock front terminates at the origin.

(as  $S_+ = 0$ ), thus reproducing (2.76). The solution is a quadrature,

$$\int^S \frac{(1 + S^2) dS}{(S_0^2 - S^2)} = -Z, \quad (2.81)$$

with an arbitrary added constant (amounting to an origin shift for  $Z$ ). Hence

$$S - \frac{(1 + S_0^2)}{2S_0} \ln \left[ \frac{S_0 + S}{S_0 - S} \right] = Z. \quad (2.82)$$

The shock structure is shown in figure 2.5; the profile terminates where  $S = 0$  at  $Z = 0$ . In fact, (2.79) implies that  $S = 0$  or (2.82) applies. Thus when  $S$  given by (2.82) reaches zero, the solution switches to  $S = 0$ . The fact that  $\partial S/\partial Z$  is discontinuous is not a problem because the diffusivity  $S(1 + S^2)$  goes to zero when  $S = 0$ . This degeneracy of the equation is a signpost for fronts with discontinuous derivatives: essentially, the profile can maintain discontinuous gradients at  $S = 0$  because the diffusivity is zero there, and there is no mechanism to smooth the jump away.

Suppose now that  $k_0 = 10^{-10} \text{ m}^2$  and  $\mu/\rho = 10^{-6} \text{ m}^2 \text{ s}^{-1}$ ; then the saturated hydraulic conductivity  $K_0 = k_0 \rho g / \mu = 10^{-3} \text{ m s}^{-1}$ . On the other hand, if a metre thick snow pack melts in ten days, this implies  $q_0 \sim 10^{-6} \text{ m s}^{-1}$ . Thus  $S_0^3 = q_0 / K_0 \sim 10^{-3}$ , and the approximation  $S \approx S_0$  looks less realistic. With

$$S^3 - \varepsilon S(1 + S^2) \frac{\partial S}{\partial \zeta} = S_0^3, \quad (2.83)$$

and  $S_0 \sim 10^{-1}$  and  $\varepsilon \sim 10^{-1}$ , it seems that one should assume  $S \ll 1$ . We define

$$S = \left( \frac{S_0^3}{\varepsilon} \right)^{1/2} s; \quad (2.84)$$

(2.83) becomes

$$\beta s^3 - s \left[ 1 + \frac{S_0^3}{\varepsilon} s^2 \right] \frac{\partial s}{\partial \zeta} = 1 \quad \text{on } \zeta = 0, \quad (2.85)$$

and we have  $S_0^3/\varepsilon \sim 10^{-2}$ ,  $\beta = (S_0/\varepsilon)^{3/2} \sim 1$ .

We neglect the term in  $S_0^3/\varepsilon$ , so that

$$\beta s^3 - s \frac{\partial s}{\partial \zeta} \approx 1 \quad \text{on } \zeta = 0, \quad (2.86)$$

and substituting (2.84) into (2.70) leads to

$$\frac{\partial s}{\partial \tau} + 3\beta s^2 \frac{\partial s}{\partial \zeta} \approx \frac{\partial}{\partial \zeta} \left[ s \frac{\partial s}{\partial \zeta} \right], \quad (2.87)$$

if we define  $t = \tau / (\varepsilon S_0^3)^{1/2}$ . A simple analytic solution is no longer possible, but the development of the solution will be similar. The flux condition (2.86) at  $\zeta = 0$  allows the surface saturation to build up gradually, and a shock will only form if  $\beta \gg 1$  (when the preceding solution becomes valid).

### 2.3.4 Similarity solutions

If, on the other hand,  $\beta \ll 1$ , then the saturation profile approximately satisfies

$$\begin{aligned} \frac{\partial s}{\partial \tau} &= \frac{\partial}{\partial \zeta} \left[ s \frac{\partial s}{\partial \zeta} \right], \\ -s \frac{\partial s}{\partial \zeta} &= \begin{cases} 1 & \text{on } \zeta = 0, \\ 0 & \text{on } \zeta = 1. \end{cases} \end{aligned} \quad (2.88)$$

At least for small times, the model admits a similarity solution of the form

$$s = \tau^\alpha f(\eta), \quad \eta = \zeta / \tau^\beta, \quad (2.89)$$

where satisfaction of the equations and boundary conditions requires  $2\alpha = \beta$  and  $2\beta = 1 = \alpha$ , whence  $\alpha = \frac{1}{3}$ ,  $\beta = \frac{2}{3}$ , and  $f$  satisfies

$$(ff')' - \frac{1}{3}(f - 2\eta f') = 0, \quad (2.90)$$

with the condition at  $\zeta = 0$  becoming

$$-ff' = 1 \quad \text{at } \eta = 0. \quad (2.91)$$

The condition at  $\zeta = 1$  can be satisfied for small enough  $\tau$ , as we shall see, because the equation (2.90) is degenerate, and  $f$  reaches zero in a finite distance,  $\eta_0$ , say, and  $f = 0$  for  $\eta > \eta_0$ . As  $\eta = 1/\tau^{2/3}$  at  $\zeta = 1$ , then this solution will satisfy the no flux condition at  $\zeta = 1$  as long as  $\tau < \eta_0^{-3/2}$ , when the advancing front will reach  $\zeta = 1$ .

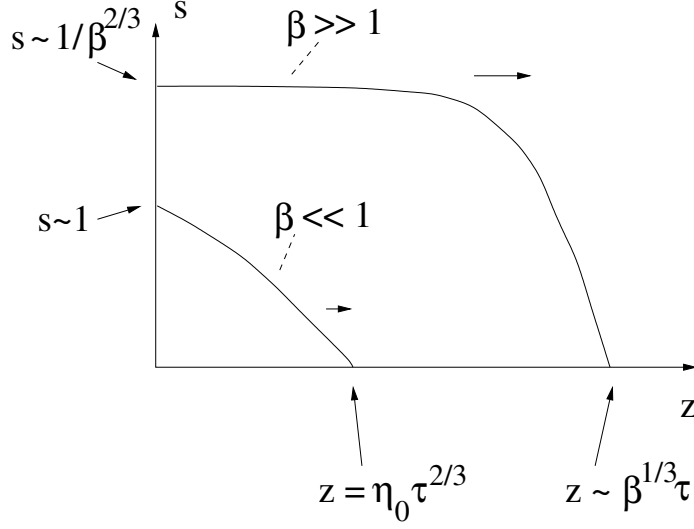


Figure 2.6: Schematic representation of the evolution of  $s$  in (2.87) for both large and small  $\beta$ .

To see why  $f$  behaves in this way, integrate once to find

$$f(f' + \frac{2}{3}\eta) = -1 + \int_0^\eta f d\eta. \quad (2.92)$$

For small  $\eta$ , the right hand side is negative, and  $f$  is positive (to make physical sense), so  $f$  decreases (and in fact  $f' < -\frac{2}{3}\eta$ ). For sufficiently small  $f(0) = f_0$ ,  $f$  will reach zero at a finite distance  $\eta = \eta_0$ , and the solution must terminate. On the other hand, for sufficiently large  $f_0$ ,  $\int_0^\eta f d\eta$  reaches 1 at  $\eta = \eta_1$  while  $f$  is still positive (and  $f' = -\frac{2}{3}\eta_1$  there). For  $\eta > \eta_1$ , then  $f$  remains positive and  $f' > -\frac{2}{3}\eta$  ( $f$  cannot reach zero for  $\eta > \eta_1$  since  $\int_0^\eta f d\eta > 1$  for  $\eta > \eta_1$ ). Eventually  $f$  must have a minimum and thereafter increase with  $\eta$ . This is also unphysical, so we require  $f$  to reach zero at  $\eta = \eta_0$ . This will occur for a range of  $f_0$ , and we have to select  $f_0$  in order that

$$\int_0^{\eta_0} f d\eta = 1, \quad (2.93)$$

which in fact represents global conservation of mass. Figure 2.6 shows the schematic form of solution both for  $\beta \gg 1$  and  $\beta \ll 1$ . Evidently the solution for  $\beta \sim 1$  will have a profile with a travelling front between these two end cases.

## 2.4 Immiscible two-phase flows: the Buckley-Leverett equation

In some circumstances, the flow of more than one phase in a porous medium is important. The type example is the flow of oil and gas, or oil and water (or all three!) in a sedimentary basin, such as that beneath the North Sea. Suppose there are two phases; denote the phases by subscripts 1 and 2, with fluid 2 being the *wetting fluid*, and  $S$  is its saturation. Then the capillary suction characteristic is

$$p_1 - p_2 = p_c(S), \quad (2.94)$$

with the capillary suction  $p_c$  being a positive, monotonically decreasing function of saturation  $S$ ; mass conservation takes the form

$$\begin{aligned} -\phi \frac{\partial S}{\partial t} + \nabla \cdot \mathbf{u}_1 &= 0, \\ \phi \frac{\partial S}{\partial t} + \nabla \cdot \mathbf{u}_2 &= 0, \end{aligned} \quad (2.95)$$

where  $\phi$  is (constant) porosity, and Darcy's law for each phase is

$$\begin{aligned} \mathbf{u}_1 &= -\frac{k_0}{\mu_1} k_{r1} \left[ \nabla p_1 + \rho_1 g \hat{\mathbf{k}} \right], \\ \mathbf{u}_2 &= -\frac{k_0}{\mu_2} k_{r2} \left[ \nabla p_2 + \rho_2 g \hat{\mathbf{k}} \right], \end{aligned} \quad (2.96)$$

with  $k_{ri}$  being the relative permeability of fluid  $i$ .

For example, if we consider a one-dimensional flow, with  $z$  pointing upwards, then we can integrate (2.95) to yield the total flux

$$u_1 + u_2 = q(t). \quad (2.97)$$

If we define the mobilities of each fluid as

$$M_i = \frac{k_0}{\mu_i} k_{ri}, \quad (2.98)$$

then it is straightforward to derive the equation for  $S$ ,

$$\phi \frac{\partial S}{\partial t} = -\frac{\partial}{\partial z} \left[ M_{\text{eff}} \left\{ \frac{q}{M_1} + \frac{\partial p_c}{\partial z} + (\rho_1 - \rho_2)g \right\} \right], \quad (2.99)$$

where the effective mobility is given by

$$M_{\text{eff}} = \left( \frac{1}{M_1} + \frac{1}{M_2} \right)^{-1}. \quad (2.100)$$

This is a convective-diffusion equation for  $S$ . If suction is very small, we obtain the *Buckley-Leverett equation*

$$\phi \frac{\partial S}{\partial t} + \frac{\partial}{\partial z} \left[ M_{\text{eff}} \left\{ \frac{q}{M_1} + (\rho_1 - \rho_2)g \right\} \right] = 0, \quad (2.101)$$

which is a nonlinear hyperbolic wave equation. As a typical situation, suppose  $q = 0$ , and  $k_{r2} = S^3$ ,  $k_{r1} = (1 - S)^3$ . Then

$$M_{\text{eff}} = \frac{k_0 S^3 (1 - S)^3}{\mu_1 S^3 + \mu_2 (1 - S)^3}, \quad (2.102)$$

and the wave speed  $v(S)$  is given by

$$v = -(\rho_2 - \rho_1)g M'_{\text{eff}}(S) = v_0 V(S), \quad (2.103)$$

where

$$\begin{aligned} v_0 &= \frac{(\rho_2 - \rho_1)g k_0}{\mu_2}, & V(S) &= \frac{\chi'(S)}{\chi(S)^2}, \\ \chi(S) &= \frac{\mu_r}{(1 - S)^3} + \frac{1}{S^3}, & \mu_r &= \frac{\mu_1}{\mu_2}. \end{aligned} \quad (2.104)$$

The variation of  $V$  with  $S$  is shown in figure 2.7. For  $\rho_2 > \rho_1$  (as for oil and water, where water is the wetting phase), waves move upwards at low water saturation and downwards at high saturation.

Shocks will form, but these are smoothed by the diffusion term  $-\frac{\partial}{\partial z} \left[ M_{\text{eff}} p'_c \frac{\partial S}{\partial z} \right]$ , in which the diffusion coefficient is

$$D = -M_{\text{eff}} p'_c. \quad (2.105)$$

As a typical example, take

$$p_c = \frac{p_0 (1 - S)^{\lambda_1}}{S^{\lambda_2}} \quad (2.106)$$

with  $\lambda_i > 0$ . Then we find

$$D = k_0 p_0 S^{2-\lambda_2} (1 - S)^{2+\lambda_1} \left[ \frac{\lambda_1 S + \lambda_2 (1 - S)}{\mu_1 S^3 + \mu_2 (1 - S)^3} \right], \quad (2.107)$$

and we see that  $D$  is typically degenerate at  $S = 0$ . In particular, if  $\lambda_2 < 2$ , then infiltration of the wetting phase into the non-wetting phase proceeds at a finite rate, and this always occurs for infiltration of the non-wetting phase into the wetting phase.

A particular limiting case is when one phase is much less dense than the other, the usual situation being that of gas and liquid. This is exemplified by the problem of snow-melt run-off considered earlier. In that case, water is the wetting phase, thus

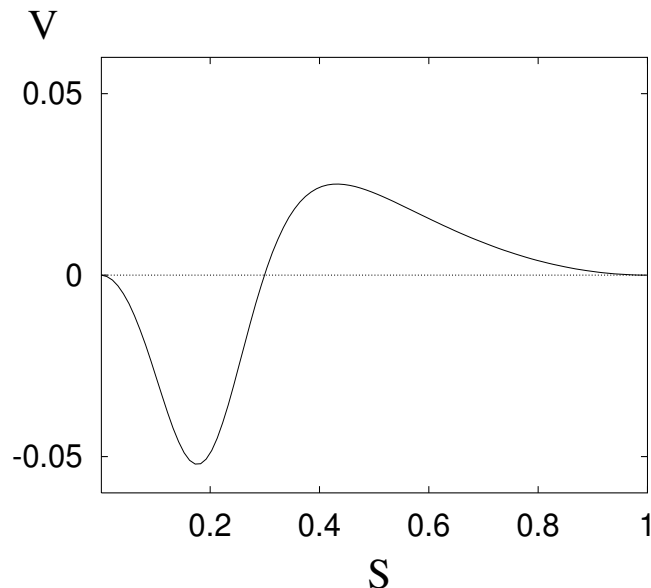


Figure 2.7: Graph of dimensionless wave speed  $V(S)$  as a function of wetting fluid saturation, indicating the speed and direction of wave motion ( $V > 0$  means waves move upwards) if the wetting fluid is more dense. The viscosity ratio  $\mu_r$  (see (2.104)) is taken to be 30.

$\rho_2 - \rho_1 = \rho_w - \rho_a$  is positive, and also  $\mu_w \approx 10^{-3}$  Pa s,  $\mu_a \approx 10^{-5}$  Pa s, whence  $\mu_a \ll \mu_w$  ( $\mu_r \ll 1$ ), so that, from (2.102),

$$M_{\text{eff}} \approx \frac{k_0 S^3}{\mu_w}, \quad (2.108)$$

at least for saturations not close to unity. Shocks form and propagate downwards (since  $\rho_2 > \rho_1$ ). The presence of non-zero flux  $q < 0$  does not affect this statement. Interestingly, the approximation (2.108) will always break down at sufficiently high saturation. Inspection of  $V(S)$  for  $\mu_r = 0.01$  (as for air and water) indicates that (2.108) is an excellent approximation for  $S \lesssim 0.5$ , but not for  $S \gtrsim 0.6$ ; for  $S \gtrsim 0.76$ ,  $V$  is positive and waves move upwards. As  $\mu_r \rightarrow 0$ , the right hand hump in figure 2.7 moves towards  $S = 1$ , but does not disappear; indeed the value of the maximum increases, and is  $V \sim \mu_r^{-1/3}$ . Thus the single phase approximation for unsaturated flow is a singular approximation when  $\mu_r \ll 1$  and  $1 - S \ll 1$ .

## 2.5 Consolidation

Consolidation refers to the ability of a granular porous medium such as a soil to compact under its own weight, or by the imposition of an overburden pressure. The grains of the medium rearrange themselves under the pressure, thus reducing the porosity and in the process pore fluid is expelled. Since the porosity is no longer

constant, we have to postulate a relation between the porosity  $\phi$  and the pore pressure  $p$ . In practice, it is found that soils, when compressed, obey a (non-reversible) relation between  $\phi$  and the *effective pressure*

$$p_e = P - p, \quad (2.109)$$

where  $P$  is the overburden pressure.

The concept of effective pressure, or more generally effective stress, is an extremely important one. The idea is that the total imposed pressure (e.g., the overburden pressure due to the weight of the rock or soil) is borne by both the pore fluid and the porous medium. The pore fluid is typically at a lower pressure than the overburden, and the extra stress (the effective stress) is that which is applied through grain to grain contacts. Thus the effective pressure is that which is transmitted through the porous medium, and it is in consequence of this that the medium responds to the effective stress; in particular, the characteristic relation between  $\phi$  and  $p_e$  represents the nonlinear pseudo-elastic effect of compression.

The dependence of the effective pressure on porosity is non-trivial and involves hysteresis, as indicated in figure 2.8. Specifically, a soil follows the *normal consolidation line* providing consolidation is occurring, i.e.  $\dot{p}_e > 0$ . However, if at some point the effective pressure is reduced, only a partial recovery of  $\phi$  takes place. When  $p_e$  is increased again,  $\phi$  more or less retraces its (overconsolidated) path to the normal consolidation line, and then resumes its normal consolidation path. Here we will ignore effects of hysteresis, as in (3.105).

When modelling groundwater flow in a consolidating medium, we must take account also of deformation of the medium itself. In turn, this requires prescription of

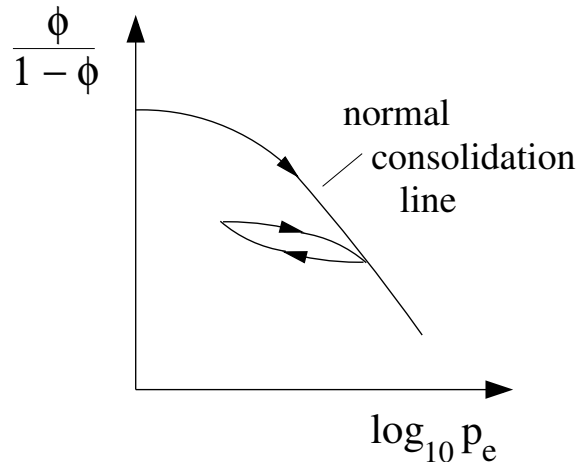


Figure 2.8: Form of the relationship between porosity and effective pressure. A hysteretic decompression-reconsolidation loop is indicated. In soil mechanics this relationship is often written in terms of the *void ratio*  $e = \phi/(1 - \phi)$ , and specifically  $e = e_0 - C_c \log_{10} p_e$ , where  $C_c$  is the *compression index*.

a constitutive rheology for the deformable matrix. This is often a complex matter, but luckily in one dimension, the issue does not arise, and a one-dimensional model is often what is of practical interest. We take  $z$  to point vertically upwards, and let  $v$  and  $w$  be the linear (or *phase-averaged*) velocities of liquid and solid, respectively. Then  $\phi v$  and  $(1 - \phi)w$  are the respective fluxes, and conservation of mass of each phase requires

$$\begin{aligned}\frac{\partial \phi}{\partial t} + \frac{\partial(\phi v)}{\partial z} &= 0, \\ -\frac{\partial \phi}{\partial t} + \frac{\partial}{\partial z}\{(1 - \phi)w\} &= 0;\end{aligned}\tag{2.110}$$

Darcy's law is then

$$\phi(v - w) = -\frac{k}{\mu} \left[ \frac{\partial p}{\partial z} + \rho_l g \right],\tag{2.111}$$

while the overburden pressure satisfies

$$\frac{\partial P}{\partial z} = -[\rho_s(1 - \phi) + \rho_l \phi]g, \quad P = P_0 \quad \text{on} \quad z = h;\tag{2.112}$$

here  $z = h$  represents the ground surface and  $P_0$  is the applied load. The effective pressure is just  $p_e = P - p$ .

Note that by adding the two mass conservation equations and integrating, we have

$$\phi v + (1 - \phi)w = q(t),\tag{2.113}$$

which can be determined from the boundary conditions. In particular, if we assume an impermeable basement where  $v = w = 0$ , then  $q = 0$  and

$$w = -\frac{\phi v}{1 - \phi}, \quad \phi(v - w) = -w.\tag{2.114}$$

We use the definition of the effective pressure in (2.109), together with (2.112) and (2.113), to derive the equation

$$\frac{\partial \phi}{\partial t} = -\frac{\partial}{\partial z} \left[ \frac{k}{\mu} (1 - \phi) \left\{ \frac{\partial p_e}{\partial z} + \Delta \rho (1 - \phi) g \right\} \right],\tag{2.115}$$

where  $\Delta \rho = \rho_s - \rho_l$ , and since  $p_e(\phi)$  is a monotonically decreasing function, this brings us back to the Richards equation (2.57). Specifically, we can write (2.115) in the form

$$\phi_t + V_z = [D\phi_z]_z,\tag{2.116}$$

where

$$V(\phi) = \frac{k(\phi)\Delta \rho g}{\mu} (1 - \phi)^2, \quad D = -\frac{k(\phi)}{\mu} (1 - \phi) p'_e(\phi),\tag{2.117}$$

and this can be compared to (2.57).

A commonly used expression in soil mechanics for the relationship between effective pressure and porosity is a logarithmic dependence of the *void ratio*  $\phi/(1 - \phi)$  on  $p_e$ , as mentioned in figure 2.8. The *normal consolidation line* for a soil is that part of the yield surface on which the shear stress vanishes, and we may take

$$\frac{\phi}{1 - \phi} = e_0 - C_c \log_{10} \left( \frac{p_e}{p_e^0} \right); \quad (2.118)$$

the quantity  $C_c$  is called the *compression index*. Note that this prescription will not be valid at small effective pressure, since as  $p_e \rightarrow 0$ , the porosity will tend to its value at loose packing, which we denote as  $\phi_0$ . This gives  $p_e$  as a monotonically decreasing function of  $\phi$  for  $0 < \phi < 1$ , and in particular,

$$p_e'(\phi) = -\frac{0.43 p_e}{C_c(1 - \phi)^2}, \quad (2.119)$$

where  $0.43 \approx \ln 10$ . In this case,

$$D = \frac{0.43 k(\phi) p_e}{\mu C_c(1 - \phi)}. \quad (2.120)$$

The diffusion coefficient  $D$  is sometimes written as  $c_v$ , and is known as the *coefficient of consolidation*. If we use values  $\mu = 10^{-3}$  Pa s,  $p_e = 10^4$  Pa,  $k = 10^{-14}$  m<sup>2</sup> (for silt),  $C_c = 0.1$  and  $\phi = 0.4$ , then  $D \sim 10^{-6}$  m<sup>2</sup> s<sup>-1</sup>. Of course this value depends strongly on the permeability, or equivalently the hydraulic conductivity  $K = \frac{k\rho g}{\mu}$ . For the silt permeability,  $K \sim 3$  m y<sup>-1</sup>, whereas actual soils (with organic matter, worm burrows, etc.), typically have hydraulic conductivities  $\sim 1$  m d<sup>-1</sup>, which is about a hundred times larger, and would give a corresponding diffusion coefficient of  $D \sim 10^{-4}$  m<sup>2</sup> s<sup>-1</sup>.

We suppose these equations apply in a vertical column  $0 < z < h$ , for which suitable boundary conditions are (with an impermeable basement and no surface load)

$$\begin{aligned} v = w = 0 & \quad \text{at} \quad z = 0, \\ \phi = \phi_0, \dot{h} = w & \quad \text{at} \quad z = h, \end{aligned} \quad (2.121)$$

and with an initial condition for  $\phi$ . Note that by comparing (2.110)<sub>1</sub> and (2.116), and using (2.114),

$$w = -\frac{(V - D\phi_z)}{1 - \phi}. \quad (2.122)$$

Therefore the boundary conditions in (2.121) collapse to

$$\begin{aligned} V - D\phi_z = 0 & \quad \text{at} \quad z = 0, \\ \phi = \phi_0, \dot{h} = -\frac{(V - D\phi_z)}{1 - \phi} & \quad \text{at} \quad z = h. \end{aligned} \quad (2.123)$$

In the steady state, it follows that  $V - D\phi_z = 0$ , and thus

$$\int_{\phi}^{\phi_0} \frac{D(\phi) d\phi}{V(\phi)} = h - z. \quad (2.124)$$

If  $C_c$  is small (and typical values are in the range  $C_c \leq 0.1$ ) then  $\phi$  varies little, and we can suppose  $V$  and  $D$  are approximately constant. In this case, the consolidation equation takes the simpler form

$$\phi_t = D\phi_{zz}, \quad (2.125)$$

together with (2.123), and the steady solution (2.124) is just

$$\phi = \phi_0 - \frac{V}{D}(h_0 - z). \quad (2.126)$$

We now consider settlement of the ground after imposition of a surface load pressure  $\Delta P$ . We suppose the final steady state has depth  $h_\infty$ , so that the final steady solution (with  $D$  and  $V$  being constant) is

$$\phi^* = \phi_\infty - \frac{V}{D}(h_\infty - z), \quad (2.127)$$

and  $\phi_\infty = \phi(p_e^\infty)$ , where  $p_e^\infty$  is the applied surface effective pressure. With no initial surface load,  $p_e^\infty = \Delta P$ , the prescribed surface load, and so (for small changes in  $\phi$ )

$$\phi_\infty \approx \phi_0 - |\phi'(0)|\Delta P. \quad (2.128)$$

We perturb the system by writing

$$\phi = \phi^*(z) + \Phi, \quad h = h_\infty + \eta, \quad (2.129)$$

and then linearising the equation and boundary conditions. This leads to

$$\begin{aligned} \Phi_t &= D\Phi_{zz}, \\ \Phi_z &= 0 \quad \text{on} \quad z = 0, \\ \frac{V}{D}\eta + \Phi &= 0, \quad \eta_t = \frac{D\Phi_z}{1 - \phi_\infty} \quad \text{on} \quad z = h_\infty. \end{aligned} \quad (2.130)$$

Eliminating  $\eta$  from the surface boundary condition gives

$$\Phi_t + \frac{V\Phi_z}{1 - \phi_\infty} = 0 \quad \text{on} \quad z = h_\infty. \quad (2.131)$$

Subtracting the initial condition from the final condition, we find

$$\Phi = \phi_0 - \phi_\infty - \frac{V}{D}(h_0 - h_\infty), \quad \eta = h_0 - h_\infty \quad \text{at} \quad t = 0. \quad (2.132)$$

At this point we realise that the initial depth  $h$  is unconstrained. It is in fact determined by the volume of solids in the domain (which, unlike the volume of water which is squeezed out the top, is conserved). Thus we require

$$\int_0^{h_\infty+\eta} [1 - (\phi^* + \Phi)] dz = \int_0^{h_\infty} (1 - \phi^*) dz, \quad (2.133)$$

and linearising this leads to the normalising condition

$$\int_0^{h_\infty} \Phi dz = (1 - \phi_\infty)\eta. \quad (2.134)$$

This is consistent with (2.130) (as it must be), and it provides the necessary relation between  $h_0$  and  $h_\infty$ , which is, using (2.128),

$$\frac{h_0 - h_\infty}{h_\infty} = \frac{|\phi'(0)|\Delta P}{1 - \phi_\infty + \frac{Vh_\infty}{D}}, \quad (2.135)$$

and this is the (relative) settlement due to a given load.

The other quantity of interest is the settlement time. The normal mode solutions of (2.130) are

$$\Phi = e^{-Ds^2t} \cos sz, \quad (2.136)$$

where

$$\tan \kappa = -\frac{\kappa}{Pe}, \quad \kappa = sh_\infty, \quad Pe = \frac{h_\infty V}{D(1 - \phi_\infty)}; \quad (2.137)$$

here  $Pe$  is a suitable Péclet number for the flow, and  $s$  is the wavenumber (normally one uses  $k$ , but that is already taken for the permeability). It is graphically straightforward to see that there is an infinite number of values of  $\kappa_1, \kappa_2, \dots$  (positive, without loss of generality) satisfying (2.137), with  $(n - \frac{1}{2})\pi < \kappa_n < n\pi$ . The settlement or consolidation time scale  $t_c$  is essentially determined by  $\kappa_1$ , and is thus

$$t_c \sim \frac{h_\infty^2}{D\kappa_1^2}, \quad (2.138)$$

where  $\kappa_1$  lies between  $\frac{1}{2}\pi$  and  $\pi$ . It depends primarily on the permeability  $k$ . If we use (2.120), and take  $k \sim 10^{-14} \text{ m}^2$  (silt),  $C_c = 0.1$ ,  $\phi = 0.3$ ,  $\mu = 10^{-3} \text{ Pa s}$ ,  $P_0 = 10^5 \text{ Pa}$  (a small house), then  $D \sim 0.6 \times 10^{-5} \text{ m}^2 \text{ s}^{-1}$ . Similarly, with  $\Delta\rho = 2 \times 10^3 \text{ kg m}^{-3}$ , we find  $V \sim 10^{-7} \text{ m s}^{-1}$ , and so, if we take  $h_\infty = 10 \text{ m}$ , the Péclet number is  $Pe \sim 0.23$ ; not extremely small, but small enough to use the approximation of small  $Pe$  in (2.137). When  $Pe$  is small,  $\kappa \approx \frac{1}{2}\pi$ , and so 14.82

$$t_c \sim \frac{4h_\infty^2}{\pi^2 D}, \quad (2.139)$$

which gives  $t_c \sim 3$  months.

## Exercises

- 2.1 Show that for a porous medium idealised as a cubical network of tubes, the permeability is given (approximately) by  $k = d_p^2 \phi^2 / 72\pi$ , where  $d_p$  is the grain size. How is the result modified if the pore space is taken to consist of planar sheets between identical cubical blocks? (The volume flux per unit width between two parallel plates a distance  $h$  apart is  $-h^3 p' / 12\mu$ , where  $p'$  is the pressure gradient.)
- 2.2 A sedimentary rock sequence consists of two type of rock with permeabilities  $k_1$  and  $k_2$ . Show that in a unit with two horizontal layers of thickness  $d_1$  and  $d_2$ , the effective horizontal permeability (parallel to the bedding plane) is

$$k_{\parallel} = k_1 f_1 + k_2 f_2,$$

where  $f_i = d_i / (d_1 + d_2)$ , whereas the effective vertical permeability is given by

$$k_{\perp}^{-1} = f_1 k_1^{-1} + f_2 k_2^{-1}.$$

Show how to generalise this result to a sequence of  $n$  layers of thickness  $d_1, \dots, d_n$ .

Hence show that the effective permeabilities of a thick stratigraphic sequence containing a distribution of (thin) layers, with the proportion of layers having permeabilities in  $(k, k + dk)$  being  $f(k)dk$ , are given by

$$k_{\parallel} = \int_0^{\infty} k f(k) dk, \quad k_{\perp}^{-1} = \int_0^{\infty} \frac{f(k) dk}{k}.$$

- 2.3 Groundwater flows between an impermeable basement at  $z = h_b(x, y, t)$  and a phreatic surface at  $z = z_p(x, y, t)$ . Write down the equations governing the flow, and by using the Dupuit approximation, show that the saturated depth  $h$  satisfies

$$\phi h_t = \frac{k \rho g}{\mu} \nabla \cdot [h \nabla z_p],$$

where  $\nabla = (\partial/\partial x, \partial/\partial y)$ . Deduce that a suitable time scale for flows in an aquifer of typical depth  $h_0$  and extent  $l$  is  $t_{gw} = \phi \mu l^2 / k \rho g h_0$ .

I live a kilometer from the river, on top of a layer of sediments 100 m thick (below which is impermeable basement). What sort of sediments would those need to be if the river responds to rainfall at my house within a day; within a year?

- 2.4 A two-dimensional earth dam with vertical sides at  $x = 0$  and  $x = l$  has a reservoir on one side ( $x < 0$ ) where the water depth is  $h_0$ , and horizontal dry land on the other side, in  $x > l$ . The dam is underlain by an impermeable basement at  $z = 0$ .

Write down the equations describing the saturated groundwater flow, and show that they can be written in the dimensionless form

$$u = -p_x, \quad \varepsilon^2 w = -(p_z + 1),$$

$$p_{zz} + \varepsilon^2 p_{xx} = 0,$$

and define the parameter  $\varepsilon$ . Write down suitable boundary conditions on the impermeable basement, and on the phreatic surface  $z = h(x, t)$ .

Assuming  $\varepsilon \ll 1$ , derive the Dupuit-Forchheimer approximation for  $h$ ,

$$h_t = (hh_x)_x \quad \text{in } 0 < x < 1.$$

Show that a suitable boundary condition for  $h$  at  $x = 0$  (the dam end) is

$$h = 1 \quad \text{at } x = 0.$$

Now define the quantity

$$U = \int_0^h p \, dz,$$

and show that the horizontal flux

$$q = \int_0^h u \, dz = -\frac{\partial U}{\partial x}.$$

Hence show that the conditions of hydrostatic pressure at  $x = 0$  and constant (atmospheric) pressure at  $x = 1$  (the seepage face) imply that

$$\int_0^1 q \, dx = \frac{1}{2}.$$

Deduce that, if the Dupuit approximation for the flux is valid all the way to the toe of the dam at  $x = 1$ , then  $h = 0$  at  $x = 1$ , and show that in the steady state, the (dimensional) discharge at the seepage face is

$$q_D = \frac{k\rho gh_0^2}{2\mu l}.$$

Supposing the above description of the solution away from the toe to be valid, show that a possible boundary layer structure near  $x = 1$  can be described by writing

$$x = 1 - \varepsilon^2 X, \quad h = \varepsilon H, \quad z = \varepsilon Z, \quad p = \varepsilon P,$$

and write down the resulting leading order boundary value problem for  $P$ .

2.5 I get my water supply from a well in my garden. The well is of depth  $h_0$  (relative to the height of the water table a large distance away) and radius  $r_0$ . Show that the Dupuit approximation for the water table height  $h$  is

$$\phi \frac{\partial h}{\partial t} = \frac{k\rho g}{\mu} \frac{1}{r} \frac{\partial}{\partial r} \left( rh \frac{\partial h}{\partial r} \right).$$

If my well is supplied from a reservoir at  $r = l$ , where  $h = h_0$ , and I withdraw a constant water flux  $q_0$ , find a steady solution for  $h$ , and deduce that my well will run dry if

$$q_0 > \frac{\pi k \rho g h_0^2}{\mu \ln[l/r_0]}.$$

Use plausible values to estimate the maximum yield (gallons per day) I can use if my well is drilled through sand, silt or clay, respectively.

2.6 A volume  $V$  of effluent is released into the ground at a point ( $r = 0$ ) at time  $t$ . Use the Dupuit approximation to motivate the model

$$\phi \frac{\partial h}{\partial t} = \frac{k\rho g}{\mu} \frac{1}{r} \frac{\partial}{\partial r} \left( rh \frac{\partial h}{\partial r} \right),$$

$$h = h_0 \quad \text{at } t = 0, \quad r > 0,$$

$$\int_0^\infty r(h - h_0) dr = V/2\pi, \quad t > 0,$$

where  $h_0$  is the initial height of the water table above an impermeable basement. Find suitable similarity solutions in the two cases (i)  $h_0 = 0$  (ii)  $h_0 > 0$ ,  $h - h_0 \ll h_0$ , and comment on the differences you find.

2.7 Rain falls steadily at a rate  $q$  (volume per unit area per unit time) on a soil of saturated hydraulic conductivity  $K_0$  ( $= k_0 \rho_w g / \mu$ , where  $k_0$  is the saturated permeability). By plotting the relative permeability  $k_r$  and suction characteristic  $\sigma\psi/d$  as functions of  $S$  (assuming a residual liquid saturation  $S_0$ ), show that a reasonable form to choose for  $k_r(\psi)$  is  $k_r = e^{-c\psi}$ . If the water table is at depth  $h$ , show that, in a steady state,  $\psi$  is given as a function of the dimensionless depth  $z^* = z/z_c$ , where  $z_c = \sigma/\rho_w g d$  ( $\sigma$  is the surface tension,  $d$  the grain size) by

$$h^* - z^* = \frac{1}{2}\psi - \frac{1}{c} \ln \left[ \frac{\sinh\{\frac{1}{2}(\ln \frac{1}{q^*} - c\psi)\}}{\sinh\{\frac{1}{2} \ln \frac{1}{q^*}\}} \right],$$

where  $h^* = h/z_c$ , providing  $q^* = q/K_0 < 1$ . Deduce that if  $h \gg z_c$ , then  $\psi \approx \frac{1}{c} \ln \frac{1}{q^*}$  near the surface. What happens if  $q > K_0$ ?

2.8 Derive the Richards equation

$$\phi \frac{\partial S}{\partial t} = - \frac{\partial}{\partial z} \left[ \frac{k_0}{\mu} k_r(S) \left\{ \frac{\partial p_c}{\partial z} + \rho_w g \right\} \right]$$

for one-dimensional infiltration of water into a dry soil, explaining the meaning of the terms, and giving suitable boundary conditions when the surface flux  $q$  is prescribed. Show that if the surface flux is large compared with  $k_0\rho_w g/\mu$ , where  $k_0$  is the saturated permeability, then the Richards equation can be approximated, in suitable non-dimensional form, by a nonlinear diffusion equation of the form

$$\frac{\partial S}{\partial t} = \frac{\partial}{\partial z} \left[ D \frac{\partial S}{\partial z} \right].$$

Show that, if  $D = S^m$ , a similarity solution exists in the form

$$S = t^\alpha F(\eta), \quad \eta = z/t^\beta,$$

where  $\alpha = \frac{1}{m+2}$ ,  $\beta = \frac{m+1}{m+2}$ , and  $F$  satisfies

$$(F^m F')' = \alpha F - \beta \eta F', \quad F^m F' = -1 \text{ at } \eta = 0, \quad F \rightarrow 0 \text{ as } \eta \rightarrow \infty.$$

Deduce that

$$F^m F' = -(\alpha + \beta) \int_\eta^{\eta_0} F d\eta - \beta \eta F,$$

where  $\eta_0$  (which may be  $\infty$ ) is where  $F$  first reaches zero. Deduce that  $F' < 0$ , and hence that  $\eta_0$  must be finite, and is determined by

$$\int_0^{\eta_0} F d\eta = \frac{1}{\alpha + \beta}.$$

What happens for  $t > F(0)^{-1/\alpha}$ ?

2.9 Write down the equations describing one-dimensional consolidation of wet sediments in terms of the variables  $\phi, v, w, p, p_e$ , these being the porosity, solid and liquid (linear) velocities, and the pore and effective pressures. Neglect the effect of gravity.

Saturated sediments of depth  $h$  lie on a rigid but permeable (to water) basement, through which a water flux  $W$  is removed. Show that

$$w = \frac{k}{\mu} \frac{\partial p}{\partial z} - W,$$

and deduce that  $\phi$  satisfies the equation

$$\frac{\partial \phi}{\partial t} = \frac{\partial}{\partial z} \left[ (1 - \phi) \left\{ \frac{k}{\mu} \frac{\partial p}{\partial z} - W \right\} \right].$$

If the sediments are overlain by water, so that  $p = \text{constant}$  (take  $p = 0$ ) at  $z = h$ , and if  $\phi = \phi_0 + p/K$ , where the compressibility  $K$  is large (so  $\phi \approx \phi_0$ ), show that a suitable reduction of the model is

$$\frac{\partial p}{\partial t} - W \frac{\partial p}{\partial z} = c \frac{\partial^2 p}{\partial z^2},$$

where  $c = K(1 - \phi_0)k/\mu$ , and  $p = 0$  on  $z = h$ ,  $p_z = \mu W/k$ . Non-dimensionalise the model using the length scale  $h$ , time scale  $h^2/c$ , and pressure scale  $\mu Wh/k$ . Hence describe the solution if the parameter  $\varepsilon = \mu Wh/k$  is small, and find the rate of surface subsidence. What has this to do with Venice?

- 2.10 Write down a model for vertical flow of two immiscible fluids in a porous medium. Deduce that the saturation  $S$  of the wetting phase satisfies the equation

$$\phi \frac{\partial S}{\partial t} + \frac{\partial}{\partial z} \left[ M_{\text{eff}} \left\{ \frac{q}{M_{nw}} + g\Delta\rho \right\} \right] = -\frac{\partial}{\partial z} \left[ M_{\text{eff}} \frac{\partial p_c}{\partial z} \right],$$

where  $z$  is a coordinate pointing *downwards*,

$$p_c = p_{nw} - p_w, \quad \Delta\rho = \rho_w - \rho_{nw}, \quad M_{\text{eff}}^{-1} = (M_w^{-1} + M_{nw}^{-1}),$$

$q$  is the total downward flux, and the suffixes  $w$  and  $nw$  refer to the wetting and non-wetting fluid respectively. Define the phase mobilities  $M_i$ . Give a criterion on the capillary suction  $p_c$  which allows the Buckley-Leverett approximation to be made, and show that for  $q = 0$  and  $\mu_w \gg \mu_{nw}$ , waves typically propagate downwards and form shocks. What happens if  $q \neq 0$ ? Is the Buckley-Leverett approximation realistic — e.g. for air and water in soil? (Assume  $p_c \sim 2\gamma/r_p$ , where  $\gamma = 70 \text{ mN m}^{-1}$ , and  $r_p$  is the pore radius: for clay, silt and sand, take  $r_p = 1 \mu, 10 \mu, 100 \mu$ , respectively.)

- 2.11 A model for snow melt run-off is given by the following equations:

$$\begin{aligned} u &= \frac{k}{\mu} \left[ \frac{\partial p_c}{\partial z} + \rho_l g \right], \\ k &= k_0 S^3, \\ \phi \frac{\partial S}{\partial t} + \frac{\partial u}{\partial z} &= 0, \\ p_c &= p_0 \left( \frac{1}{S} - S \right). \end{aligned}$$

Explain the meaning of the terms in these equations, and describe the assumptions of the model.

The intrinsic permeability  $k_0$  is given by

$$k_0 = 0.077 d^2 \exp[-7.8 \rho_s/\rho_l],$$

where  $\rho_s$  and  $\rho_l$  are snow and water densities, and  $d$  is grain size. Take  $d = 1 \text{ mm}$ ,  $\rho_s = 300 \text{ kg m}^{-3}$ ,  $\rho_l = 10^3 \text{ kg m}^{-3}$ ,  $p_0 = 1 \text{ kPa}$ ,  $\phi = 0.4$ ,  $\mu = 1.8 \times 10^{-3} \text{ Pa s}$ ,  $g = 10 \text{ m s}^{-2}$ , and derive a non-dimensional model for melting of a one metre thick snow pack at a rate (i.e.  $u$  at the top surface  $z = 0$ ) of  $10^{-6} \text{ m s}^{-1}$ . Determine whether capillary effects are small; describe the nature of the model equation, and find an approximate solution for the melting of an initially dry snowpack. What is the (meltwater flux) run-off curve?

2.12 Consider the following model, which represents the release of a unit quantity of groundwater at  $t = 0$  in an aquifer  $-\infty < x < \infty$ , when the Dupuit approximation is used:

$$\begin{aligned} h_t &= (hh_x)_x, \\ h &= 0 \text{ at } t = 0, x \neq 0, \\ \int_{-\infty}^{\infty} h dx &= 1 \end{aligned}$$

(i. e.,  $h = \delta(x)$  at  $t = 0$ ). Show that a similarity solution to this problem exists in the form

$$h = t^{-1/3}g(\xi), \quad \xi = x/t^{1/3},$$

and find the equation and boundary conditions satisfied by  $g$ . Show that the water body spreads at a finite rate, and calculate what this is.

Formulate the equivalent problem in three dimensions, and write down the equation satisfied by the similarity form of the solution, assuming cylindrical symmetry. Does this solution have the same properties as the one-dimensional solution?

# Chapter 3

## Convection

Convection is the fluid motion induced by buoyancy; buoyancy is the property of a fluid whereby its density depends on external properties. The most common form of convection is *thermal convection*, which occurs due to the dependence of density on temperature: warm fluid is light, and therefore rises. Everyday examples of this are the circulation induced by a convector heater, or the motion which can be seen in a saucepan of oil when it is heated. (In the latter case, one can see convection rolls in the fluid, regular but time-dependent.) Another common form of convection is *compositional convection*, which is induced by density changes dependent on composition. An example of this occurs during the formation of sea ice in the polar regions. As salty sea water freezes, it rejects the salt (the ice is almost pure water substance), and the resulting salty water is denser than the sea water from which it forms, and thus induces a convective motion below the ice. Below, we discuss three geophysical examples from convection, but convection is everywhere: it drives the oceanic circulation, it drives the atmospheric circulation, it causes thunderstorms, it occurs in glass manufacture, in a settling pint of Guinness, in back boilers, in solar panels. And, it has formed the thematic core of the subject of geophysical fluid dynamics for almost a century.

### 3.1 Mantle convection

Most people have heard of continental drift, the process whereby the Earth's continents drift apart relative to each other. The Atlantic Ocean is widening at the rate of several centimetres a year, the crashing of India into Asia over the last 50 My (fifty million years) has caused the continuing uplift of the Himalayas, Scotland used to be joined to Newfoundland. The continents ride, like rafts of debris, on the tectonic plates of the Earth, which separate at mid-ocean ridges and converge at subduction zones. The theory of plate tectonics, which originated with the work of Wegener and Holmes in the early part of the twentieth century, and which was finally accepted by geophysicists in the 'plate tectonics revolution' of the 1960's, describes the surface of the Earth as being split up into some thirteen major tectonic plates: see figure

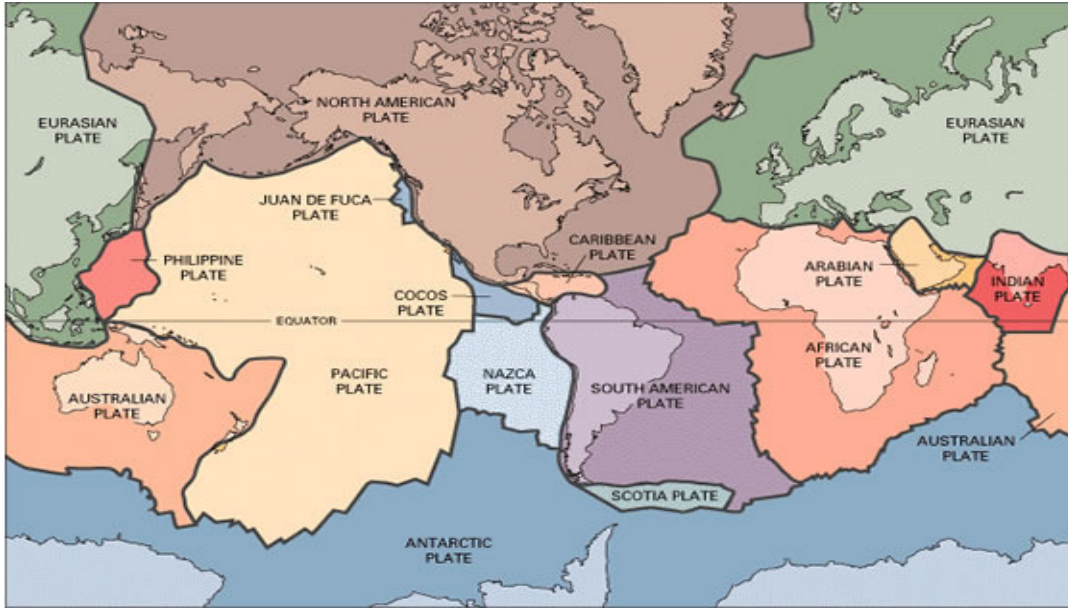


Figure 3.1: The tectonic plates of the Earth.

3.1. These plates move relative to each other across the surface, and this motion is the surface manifestation of a convective motion in the Earth's *mantle*, which is the part of the Earth from the surface to a depth of about 3,000 kilometres, and which consists of an assemblage of polycrystalline silicate rocks. Upwelling occurs at mid-ocean ridges, for example the mid-Atlantic ridge which passes through Iceland, and the East Pacific Rise off the coast of South America, which passes through the Galapagos Islands. The plates sink into the mantle at subduction zones, which adjoin continental boundaries, and which are associated with the presence of oceanic trenches.

The plates are so called because they are conceived of as moving quasi-rigidly. They are in fact the cold upper thermal boundary layers of the convective motion, in-

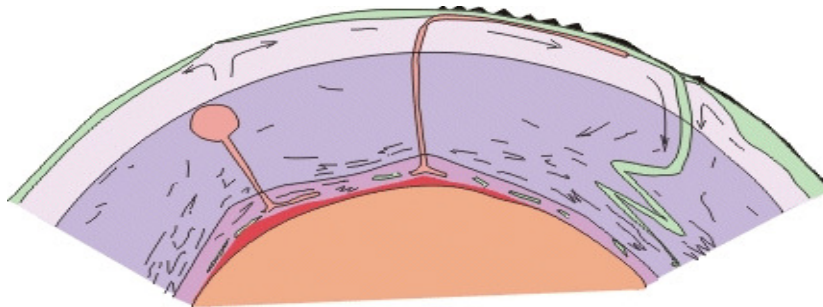


Figure 3.2: A cartoon of mantle convection. We see plumes, mid-ocean ridges, subducting slabs.

licated schematically in figure 3.2, and are plate-like because the strong temperature dependence of mantle viscosity renders these relatively cold rocks extremely viscous. One may wonder how the mantle moves at all, consisting as it does of mostly solid polycrystalline rocks. In fact, solids will deform just as fluids do when subjected to stress. The deformation is enabled by the migration of dislocations within the crystalline lattice of the solid grains of the rock. The effective viscosity of the Earth's mantle is a whopping  $10^{21}$  Pa s; this is about eight orders of magnitude greater than the viscosity of ice, and twenty-four orders greater than the viscosity of water.

The reason that the mantle convects is that the Earth is cooling. The primordial heat of formation has gradually been lost over the Earth's history, but the central core of the planet is still very hot; some six thousand degrees Celsius at the centre of the Earth. This heat from the core is instrumental in heating the mantle from below, and driving the convective flow. Radioactive heating also contributes to an extent which is not certain, but which is thought to be significant.

## 3.2 The Earth's core

Part of the heat which drives mantle convection is derived from cooling the Earth's core. The core is the part of the Earth which lies between its centre and the mantle. Like the mantle, it is also some three thousand kilometres deep, and consists of a molten outer core of iron, alloyed with some lighter element, usually thought to be sulphur or oxygen, in a concentration of some 10%. The inner core is solid (pure) iron, of radius 1,000 km. It is generally thought that the core was initially molten throughout, and that the inner core has gradually solidified from the outer core over the course of geological time. It is the consequent release of latent heat which, at least partly, powers mantle convection.

One may wonder how the outer core can be liquid, and the inner core solid, if the inner core is hotter (as it must be). The reason for this is that the solidification temperature (actually the liquidus temperature, see below) depends on pressure, through the Clapeyron effect. This is the effect whereby a pressure cooker works: the boiling temperature increases with pressure, and similarly, the solidification temperature of the outer core iron alloy increases with pressure, and thus also depth. Thus, the inner core can be below the solidification temperature because of the greater pressure there.

The convection in the outer core is partly due to the dependence of density on temperature, but the primary dependence is, as often the case when composition varies, due to the dependence of density on the concentration of sulphur (or oxygen). In order to understand how the solidification of the inner core leads to convection, we need to understand the general thermodynamic way in which melting and solidification occur in multi-component materials. This is illustrated in figure 3.3, which indicates how the solidification temperatures vary with composition in a two-component melt. At a given temperature, there are two curves which describe the concentrations of the solid and liquid, when these are in thermodynamic equilibrium with each other. These two curves are called the solidus and liquidus, respectively. Often there are two sets of

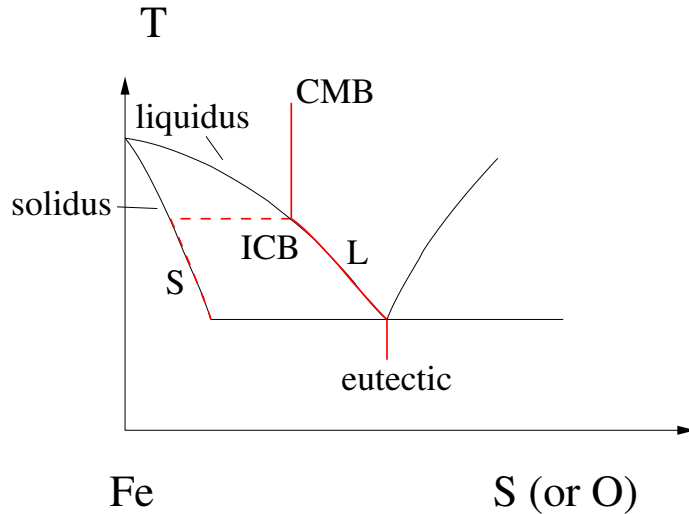


Figure 3.3: Typical phase diagram for a two-component alloy with a eutectic point. When the liquid reaches the liquidus (L), the resulting solid has the concentration of the solidus (S). When the liquid reaches the eutectic point, two solids, iron-rich and sulphur-rich respectively, will be formed.

solidus and liquidus curves, and they meet at a point called the eutectic point. The way in which a liquid alloy solidifies is then indicated by the red line in figure 3.3. In the outer core, the composition is relatively constant, but the temperature decreases (relative to the liquidus) from the core-mantle boundary (CMB) to the inner core boundary (ICB), where solidification occurs. (The phase diagram is indicated as if at constant pressure; in reality, the curves will also vary with pressure.)

At this temperature, the solid which crystallises has the solidus concentration, which is richer in iron than the liquid, and so as the temperature cools during freezing, the liquid concentration of sulphur or oxygen increases because of its rejection at the freezing interface. It is this source of buoyancy which provides the driving force for compositional convection.

Actually, it is typically the case that when alloys solidify, they do not form a solid with a clear interface. Rather, such a situation is typically *morphologically unstable*, and a dendritic mush consisting of a solid-liquid mixture is formed, as shown in figure 3.4. The convection caused by the release of light fluid now occurs throughout the mush, and leads to the formation of narrow ‘chimneys’, from which plumes emerge.

In the Earth’s core, it is this convection which forms the magnetic field. Convection in an electrically conducting fluid causes a magnetic field to grow, providing the magnetic diffusivity is sufficiently small, through the action of the Lorentz force. The study of such instabilities is a central part of the subject of magnetohydrodynamics.

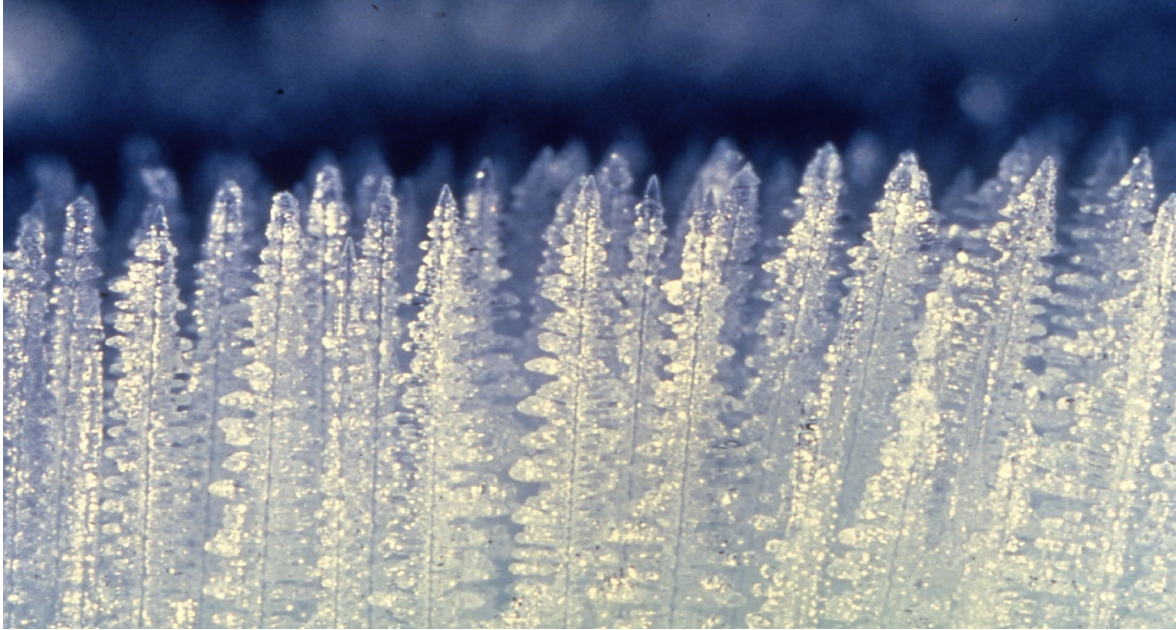


Figure 3.4: A dendritic mush in the solidification of ammonium chloride in the laboratory. Convection occurs within the mush, leading to the formation of ‘chimneys’ which act as sources of plumes in the residual melt. Photo courtesy of Grae Worster.

### 3.3 Magma chambers

Our final example of convection arises in the formation and cooling of magma chambers. When mantle rock upwells, either at mid-ocean ridges, or in isolated thermal plumes such as that below Hawaii, the slight excess temperature causes the rock to partially melt. It is thought that the melt fraction can then ascend through the residual porous matrix, forming rivulets and channels which allow the escape of the magma through the lithosphere to the crust.<sup>1</sup> As the magma ascends into the crust, it can typically encounter unconformities, where the rock types alter, and where the density may be less than that of the magma. In that case, the magma will stop rising, but will spread laterally, simultaneously uplifting the overlying strata. Thus forms the *laccolith*, a magmatic intrusion, and over the course of time such intrusions, or magma chambers, will solidify, forming huge cauldrons of rock which may later be exposed at the Earth’s surface.

Convection undoubtedly occurs in such chambers, which may be tens of kilometres in extent. The hot magma is continuously chilled at the roof and sides of the chamber, and this leads to convective currents continually draining towards the floor of the chamber. There they will accumulate, leading to a cold, crystal-rich layer ly-

---

<sup>1</sup>The *lithosphere* is the cold surface boundary layer of the convecting mantle, of depth some 100 km in the oceanic mantle, somewhat greater beneath continents; the crust is a relatively thin layer of rocks near the surface, formed through partial melting of the mantle and the resulting volcanism.



Figure 3.5: Graded layering in the Skaergaard intrusion. Photograph courtesy of Kurt Hollocher.

ing stagnant below the convecting upper portion. This is essentially the filling box mechanism which is discussed further below.

Magmas are multi-component alloys, and their convective solidification can lead to various exotic phenomena. The phase diagram of the type in figure 3.3 causes chemical differentiation on the large scale (in metal alloy castings this is called macrosegregation). For example, in an olivine–plagioclase magma, the heavy olivine will crystallise out first, and the crystals may settle to the base of the chamber. The residual liquid is then plagioclase-rich and lighter. So the end result would be a chamber having two distinct layers. Successive injections of magma may then lead to a sequence of such layers, as is seen in the Scottish island of Rum, and this has been suggested as an explanation for these particular layers.

Other magma chambers show layering at a much finer scale, and the origin of these layers is a mystery. An example is shown in figure 3.5. The layers are reminiscent of double-diffusive layering, which we discuss in section 3.6.2, but efforts to build a theory round this idea, or indeed any other, have so far not met with success.

### 3.4 Rayleigh–Bénard convection

The simplest model of convection is the classical Rayleigh–Bénard model in which a layer of fluid is heated from below, by application of a prescribed temperature

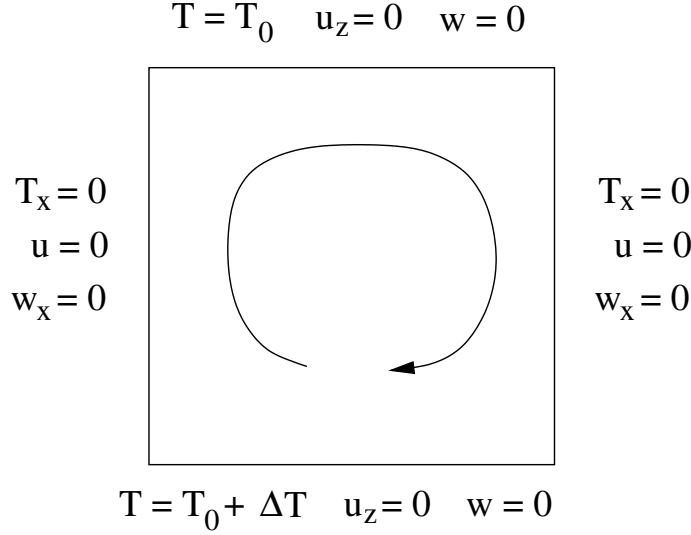


Figure 3.6: Geometry of a convection cell.

difference across the layer. Depending on the nature of the boundaries, one may have a no slip condition or a no shear stress condition applied at the bounding surfaces. For the case of mantle convection, one conceives of both the oceans (or atmosphere) and the underlying fluid outer core as exerting no stress on the extremely viscous mantle, so that no stress conditions are appropriate, and in fact it turns out that this is the simplest case to consider. The geometry of the flow we consider is shown in figure 3.6. It is convenient to assume lateral boundaries, although in a wide layer, these simply represent the convection cell walls, and can be an arbitrary distance apart.

The equations describing the flow are the Navier-Stokes equations, allied with the energy equation and an equation of state, and can be written in the form

$$\begin{aligned}
 \rho_t + \nabla \cdot (\rho \mathbf{u}) &= 0, \\
 \rho[\mathbf{u}_t + (\mathbf{u} \cdot \nabla) \mathbf{u}] &= -\nabla p - \rho g \mathbf{k} + \mu \nabla^2 \mathbf{u}, \\
 \rho c_p [T_t + \mathbf{u} \cdot \nabla T] &= k \nabla^2 T, \\
 \rho &= \rho_0 [1 - \alpha(T - T_0)];
 \end{aligned} \tag{3.1}$$

in these equations,  $\rho$  is the density,  $\mathbf{u}$  is the velocity,  $p$  is the pressure,  $g$  is the acceleration due to gravity,  $\mathbf{k}$  is the unit upwards vector,  $\mu$  is viscosity,  $c_p$  is the specific heat,  $T$  is temperature,  $k$  is thermal conductivity,  $\rho_0$  is the density at the reference temperature  $T_0$  at the surface of the fluid layer, and  $\alpha$  is the thermal expansion coefficient. The boundary conditions for the flow are indicated in figure 3.6, and correspond to prescribed temperature at top and bottom, no flow through the boundaries, and no shear stress at the boundaries. The lateral boundaries represent stress free ‘walls’, but as mentioned above, these simply indicate the boundaries of the convection cells

(across which there is no heat transport, hence the no flux condition for temperature).

To proceed, we non-dimensionalise the variables as follows. We use the convective time scale, and a thermally related velocity scale, and use the depth of the box  $d$  as the length scale:

$$\begin{aligned} \mathbf{u} &\sim \frac{\kappa}{d}, & \kappa &= \frac{k}{\rho_0 c_p}, & t &\sim \frac{d^2}{\kappa}, & \mathbf{x} &\sim d, \\ p - [p_0 + \rho_0 g(d - z)] &\sim \frac{\mu \kappa}{d^2}, & T - T_0 &\sim \Delta T. \end{aligned} \quad (3.2)$$

Here  $p_0$  is the (prescribed) pressure at the surface, which we take as constant. We would also scale  $\rho \sim \rho_0$ , but in the scaled equations below, the density has been algebraically eliminated. The scaled equations take the form

$$\begin{aligned} -BT_t + \nabla \cdot [(1 - BT)\mathbf{u}] &= 0, \\ \frac{1}{Pr}[1 - BT][\mathbf{u}_t + (\mathbf{u} \cdot \nabla)\mathbf{u}] &= -\nabla p + Ra T \hat{\mathbf{k}} + \nabla^2 \mathbf{u}, \\ (1 - BT)(T_t + \mathbf{u} \cdot \nabla T) &= \nabla^2 T, \end{aligned} \quad (3.3)$$

and the dimensionless parameters are defined as

$$B = \alpha \Delta T, \quad Pr = \frac{\mu}{\rho_0 \kappa}, \quad Ra = \frac{\alpha \rho_0 \Delta T g d^3}{\mu \kappa}; \quad (3.4)$$

the parameters  $Ra$  and  $Pr$  are known as the Rayleigh and Prandtl numbers, respectively. The Prandtl number is a property of the fluid; for air it is 0.7, and for water it is 7. The Rayleigh number is a measure of the strength of the heating. As we shall see, convective motion occurs if the Rayleigh number is large enough, and it becomes vigorous if the Rayleigh number is large. The parameter  $B$  might be termed a Boussinesq number, although this is not common usage.

Suppose we think of values typical for a layer of water in a saucepan. We take  $d = 0.1$  m,  $\mu = 2 \times 10^{-3}$  Pa s,  $\Delta T = 100$  K,  $\alpha = 3 \times 10^{-5}$  K<sup>-1</sup>,  $\rho_0 = 10^3$  kg m<sup>-3</sup>,  $\kappa = 0.3 \times 10^{-6}$  m<sup>2</sup> s<sup>-1</sup>,  $g = 9.8$  m s<sup>-2</sup>. Then we have  $Pr \approx 7$ ,  $B \approx 3 \times 10^{-3}$ , and  $Ra \approx 5 \times 10^7$ . In this case, we have that  $B \ll 1$  and  $Ra \gg 1$ . This is typically the case. We now make the Boussinesq approximation, which says that  $B \ll 1$ , and we ignore the terms in  $B$  in (3.3). In words, we assume that the density is constant, except in the buoyancy term. The mathematical reason for this exception is that, although  $Ra \propto B$  (and so  $Ra \rightarrow 0$  as  $B \rightarrow 0$ ), the actual numerical sizes of the two parameters are typically very different. The adoption of the Boussinesq approximation leads to what are called the Boussinesq equations of thermal convection:

$$\begin{aligned} \nabla \cdot \mathbf{u} &= 0, \\ \frac{1}{Pr}[\mathbf{u}_t + (\mathbf{u} \cdot \nabla)\mathbf{u}] &= -\nabla p + \nabla^2 \mathbf{u} + Ra T \hat{\mathbf{k}}, \\ T_t + \mathbf{u} \cdot \nabla T &= \nabla^2 T, \end{aligned} \quad (3.5)$$

with associated boundary conditions for free slip:

$$\begin{aligned} T = 1, \quad \mathbf{u} \cdot \mathbf{n} = \tau_{nt} = 0 \quad \text{on } z = 0, \\ T = 0, \quad \mathbf{u} \cdot \mathbf{n} = \tau_{nt} = 0 \quad \text{on } z = 1, \end{aligned} \quad (3.6)$$

where  $\tau_{nt}$  represents the shear stress.

### 3.4.1 Linear stability

It is convenient to study the problem of the onset of convection in two dimensions  $(x, z)$ . In this case we can define a stream function  $\psi$  which satisfies

$$u = -\psi_z, \quad w = \psi_x. \quad (3.7)$$

(The sign is opposite to the usual convention; for  $\psi > 0$  this describes a clockwise circulation.) We eliminate the pressure by taking the curl of the momentum equation (3.5)<sub>2</sub>, which leads, after some algebra (see also question 3.2), to the pair of equations for  $\psi$  and  $T$ :

$$\begin{aligned} \frac{1}{Pr} [\nabla^2 \psi_t + \psi_x \nabla^2 \psi_z - \psi_z \nabla^2 \psi_x] &= Ra T_x + \nabla^4 \psi, \\ T_t + \psi_x T_z - \psi_z T_x &= \nabla^2 T, \end{aligned} \quad (3.8)$$

with the associated boundary conditions

$$\begin{aligned} \psi = \nabla^2 \psi = 0 \quad \text{at } z = 0, 1, \\ T = 0 \quad \text{at } z = 1, \\ T = 1 \quad \text{at } z = 0. \end{aligned} \quad (3.9)$$

In the absence of motion,  $\mathbf{u} = \mathbf{0}$ , the steady state temperature profile is linear,

$$T = 1 - z, \quad (3.10)$$

and the lithostatic pressure is modified by the addition of

$$p = -\frac{Ra}{2}(1 - z)^2. \quad (3.11)$$

(Even if  $Ra$  is large, this represents a small correction to the lithostatic pressure, of relative size  $O(B)$ .) The stream function is just

$$\psi = 0. \quad (3.12)$$

We define the temperature perturbation  $\theta$  by

$$T = 1 - z + \theta. \quad (3.13)$$

This yields

$$\begin{aligned} \frac{1}{Pr} [\nabla^2 \psi_t + \psi_x \nabla^2 \psi_z - \psi_z \nabla^2 \psi_x] &= \nabla^4 \psi + Ra \theta_x, \\ \theta_t - \psi_x + \psi_x \theta_z - \psi_z \theta_x &= \nabla^2 \theta, \end{aligned} \quad (3.14)$$

and the boundary conditions are

$$\psi_{zz} = \psi = \theta = 0 \quad \text{on } z = 0, 1. \quad (3.15)$$

In the Earth's mantle, the Prandtl number is large, and we will now simplify the algebra by putting  $Pr = \infty$ . This assumption does not in fact affect the result which is obtained for the critical Rayleigh number at the onset of convection. The linear stability of the basic state is determined by neglecting the nonlinear advective terms in the heat equation. We then seek normal modes of wave number  $k$  in the form

$$\begin{aligned} \psi &= f(z)e^{\sigma t + ikx}, \\ \theta &= g(z)e^{\sigma t + ikx}, \end{aligned} \quad (3.16)$$

whence  $f$  and  $g$  satisfy (putting  $Pr = \infty$ )

$$\begin{aligned} (D^2 - k^2)^2 f + ikRa g &= 0, \\ \sigma g - ikf &= (D^2 - k^2)g, \end{aligned} \quad (3.17)$$

where  $D = d/dz$ , and

$$f = f'' = g = 0 \quad \text{on } z = 0, 1. \quad (3.18)$$

By inspection, solutions are

$$f = \sin m\pi z, \quad g = b \sin m\pi z, \quad (3.19)$$

( $n = 1, 2, \dots$ ) providing

$$\sigma = \frac{k^2 Ra}{(m^2 \pi^2 + k^2)^2} - (m^2 \pi^2 + k^2), \quad (3.20)$$

which determines the growth rate for the  $m$ -th mode of wave number  $k$ .

Since  $\sigma$  is real, instability is characterised by a positive value of  $\sigma$ . We can see that  $\sigma$  decreases as  $m$  increases; therefore the value  $m = 1$  gives the most unstable value of  $\sigma$ . Also,  $\sigma$  is negative for  $k \rightarrow 0$  or  $k \rightarrow \infty$ , and has a single maximum. Since  $\sigma$  increases with  $Ra$ , we see that  $\sigma > 0$  (for  $m = 1$ ) if  $Ra > Ra_{ck}$ , where

$$Ra_{ck} = \frac{(\pi^2 + k^2)^3}{k^2}. \quad (3.21)$$

In turn, this value of the Rayleigh number depends on the selected wave number  $k$ . Since an arbitrary disturbance will excite all wave numbers, it is the minimum

value of  $Ra_{ck}$  which determines the absolute threshold for stability. The minimum is obtained when

$$k = \frac{\pi}{\sqrt{2}}, \quad (3.22)$$

and the resulting critical value of the Rayleigh number is

$$Ra_c = \frac{27\pi^4}{4} \approx 657.5; \quad (3.23)$$

That is, the steady state is linearly unstable if  $Ra > Ra_c$ .

For other boundary conditions, the solutions are still exponentials, but the coefficients, and hence also the growth rate, must be found numerically. The resultant critical value of the Rayleigh number is higher for no slip boundary conditions, for example, (it is about 1707), and in general, thermal convection is initiated at values of  $Ra \gtrsim O(10^3)$ .

### 3.5 High Rayleigh number convection

We have seen that convection occurs if the Rayleigh number is larger than  $O(10^3)$  in general, depending on the precise boundary conditions which apply. In the Earth's mantle, suitable values of the constituent parameters are  $\alpha = 3 \times 10^{-5} \text{ K}^{-1}$ ,  $\Delta T = 3000 \text{ K}$ ,  $\rho_0 = 3 \times 10^3 \text{ kg m}^{-3}$ ,  $g = 10 \text{ m s}^{-2}$ ,  $d = 3000 \text{ km}$ ,  $\eta_0 = 10^{21} \text{ Pa s}$ ,  $\kappa_0 = 10^{-6} \text{ m}^2 \text{ s}^{-1}$ , and for these values, the Rayleigh number is slightly less than  $10^8$ . Thus the Rayleigh number is much larger than the critical value, and as a consequence we can expect the convection to be vigorous (if velocities of centimetres per year can be said to be vigorous).

There are various intuitive ways in which we can get a sense of the likely behaviour of the convective solutions of the Boussinesq equations when  $Ra \gg 1$ . Since  $Ra$  multiplies the buoyancy term, any  $O(1)$  lateral temperature gradient will cause enormous velocities. One might thus expect the flow to organise itself so that either horizontal temperature gradients are small, or they are confined to thin regions, or both. Since  $O(1)$  temperature variations are enforced by the boundary conditions, the latter is more plausible, and thus we have the idea of the *thermal plume*, a localised upwelling of hot fluid which will be instantly familiar to glider pilots and seabirds.

A mathematically intuitive way of inferring the same behaviour follows from the expectation that increasing  $Ra$  drives increasing velocities; then large  $Ra$  should imply large velocity, and the conduction term in the heat equation  $\mathbf{u} \cdot \nabla T = \nabla^2 T$  is correspondingly small. Since the conduction term represents the highest derivative in the equation, its neglect would imply a reduction of order, and correspondingly we would expect *thermal boundary layers* to exist at the boundaries of the convecting cell. This is in fact what we will find: a hot thermal boundary layer adjoins the lower boundary, and a cold one adjoins the upper boundary, and a rapid circulation in the interior of the cell detaches these as upwelling and downwelling plumes. The general structure of the resulting flow is shown in figure 3.7. We analyse this structure in the following sections.

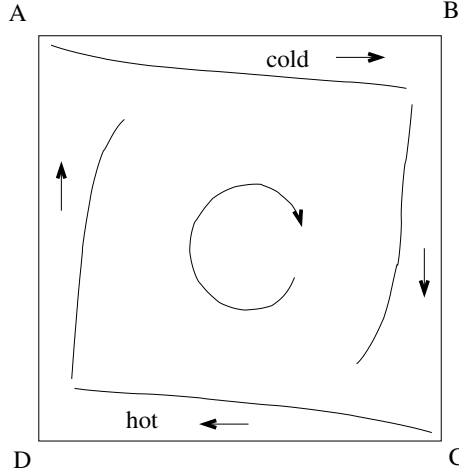


Figure 3.7: Schematic representation of boundary layer convection

### 3.5.1 Boundary layer theory

We now consider a convection cell in a finite box, as shown in figure 3.7, with (dimensionless) top and bottom boundaries at  $z = 0, 1$ , and side walls at  $x = 0, a$ . The Boussinesq equations describing thermal convection are written in the following dimensionless form:

$$\begin{aligned}\nabla \cdot \mathbf{u} &= 0, \\ \frac{1}{Pr} \frac{d\mathbf{u}}{dt} &= -\nabla p + \nabla^2 \mathbf{u} + Ra T \mathbf{k}, \\ \frac{dT}{dt} &= \nabla^2 T,\end{aligned}\tag{3.24}$$

where  $\mathbf{u}$  is velocity,  $p$  is pressure,  $T$  is temperature, and the Rayleigh and Prandtl numbers are defined in (3.4).

By considering only two-dimensional motion in the  $(x, z)$  plane, we define the stream function  $\psi$  by

$$u = -\psi_z, \quad w = \psi_x;\tag{3.25}$$

the vorticity is then  $(0, \omega, 0)$ , where  $\omega = -\nabla^2 \psi$ . Taking the curl of the momentum equation, we derive the set

$$\begin{aligned}\omega &= -\nabla^2 \psi, \\ \frac{dT}{dt} &= T_t + \psi_x T_z - \psi_z T_x = \nabla^2 T, \\ \frac{1}{Pr} \frac{d\omega}{dt} &= -Ra T_x + \nabla^2 \omega,\end{aligned}\tag{3.26}$$

which are supplemented by the boundary conditions

$$\begin{aligned}
\psi, \omega &= 0 \quad \text{on } x = 0, a, z = 0, 1, \\
T &= \frac{1}{2} \quad \text{on } z = 0, \\
T &= -\frac{1}{2} \quad \text{on } z = 1, \\
T_x &= 0 \quad \text{on } x = 0, a;
\end{aligned} \tag{3.27}$$

here  $a$  is the aspect ratio, and we have chosen free slip (no stress) conditions at the cell boundaries. Note that we have chosen that we have changed the reference temperature for the scaled temperature from  $T_0$  to  $T_0 - \frac{1}{2}\Delta T$ ; this is purely a matter of convenience, as the resultant symmetry of the thermal boundary conditions is more natural.

### Rescaling

The idea is that when  $Ra \gg 1$ , thermal boundary layers of thickness  $\delta \ll 1$  will form at the edges of the flow, and both  $\psi$  and  $\omega$  will be  $\gg 1$  in the flow. To scale the equations properly, we rescale the variables as

$$\psi, \omega \sim \frac{1}{\delta^2}, \tag{3.28}$$

and define

$$\delta = Ra^{-1/3}. \tag{3.29}$$

Rescaled, the equations are thus, in the steady state,

$$\begin{aligned}
\omega &= -\nabla^2 \psi, \\
\psi_x T_z - \psi_z T_x &= \delta^2 \nabla^2 T, \\
\nabla^2 \omega &= \frac{1}{\delta} T_x + \frac{1}{Pr \delta^2} \frac{d\omega}{dt}.
\end{aligned} \tag{3.30}$$

In order that the inertia terms be unimportant, we require  $Pr \delta^2 \gg 1$ , i. e.,  $Pr \gg Ra^{2/3}$ . This assumption is easily satisfied in the Earth's mantle, but is difficult to achieve in the laboratory. Nevertheless, we assume this henceforth.

As in any singular perturbation procedure, we now examine the flow region by region, introducing special rescalings in regions where boundary conditions cannot be satisfied. Before doing so, note that the statement of the flow problem is symmetric, and we will therefore take the solution to be symmetric also.

### Core flow

The temperature equation is linear in  $T$ , and implies  $T = T_0(\psi) + O(\delta^2)$ . For a flow with closed streamlines, the Prandtl-Batchelor theorem then implies  $T_0 = \text{constant}$

(this follows from the exact integral  $\oint_C \frac{\partial T}{\partial n} ds = 0$ , where the integral is around a streamline, whence  $T'_0(\psi) \oint_C \frac{\partial \psi}{\partial n} ds = 0$ ); it then follows that  $T$  is constant to all (algebraic) orders of  $\delta$ , and is in fact zero by the symmetry of the flow. Thus

$$\begin{aligned} T &= 0, \\ \nabla^4 \psi &= 0, \end{aligned} \tag{3.31}$$

and clearly the core flow cannot have  $\psi = \omega = 0$  at the boundaries, for non-zero  $\psi$ . In fact,  $\omega$  jumps at the side-walls where the plume buoyancy generates a non-zero vorticity. We examine the plumes next.

### Plumes

Near  $x = 0$ , for example, we rescale the variables as

$$x = \delta X, \quad \psi = \delta \Psi, \tag{3.32}$$

so that to leading order, we have

$$\Psi_{XX} \approx 0, \tag{3.33}$$

whence  $\Psi \approx w_p(z)X$ , and to match to the core flow, we define  $w_p = \psi_x|_{x=0}$  as the core velocity at  $x = 0$ . Also

$$\begin{aligned} \Psi_X T_z - \Psi_z T_X &\approx T_{XX}, \\ \omega_{XX} &\approx T_X, \end{aligned} \tag{3.34}$$

the latter of which integrates to give

$$\omega = \int_0^X T dX, \quad \omega_p = \int_0^\infty T dX, \tag{3.35}$$

where matching requires  $\omega_p$  to be the core vorticity at  $x = 0$ . Integration of (3.34)<sub>1</sub> gives

$$\int_0^\infty T d\Psi = C, \tag{3.36}$$

where  $C$  is constant, and it follows that the core flow must satisfy the boundary condition  $\omega \psi_x = C$  on  $x = 0$  (and therefore, by symmetry,  $-C$  at  $x = a$ ). In summary, the effective boundary conditions for the core flow are

$$\begin{aligned} \psi &= 0 \quad \text{on} \quad x = 0, a, \quad z = 0, 1, \\ \psi_{zz} &= 0 \quad \text{on} \quad z = 0, 1, \\ \psi_x \psi_{xx} &= -C \quad \text{on} \quad x = 0, \quad \psi_x \psi_{xx} = C \quad \text{on} \quad x = a, \end{aligned} \tag{3.37}$$

and the solution can be found as the *canonical solution*

$$\psi = C^{1/2} \hat{\psi}(x, z), \quad (3.38)$$

where  $\hat{\psi}$  must be determined numerically. It thus remains to determine  $C$ . This requires consideration of the thermal boundary layers. Thermal boundary layers are necessary at the top and bottom because the core temperature ( $T = 0$ ) does not satisfy the boundary conditions there.

### Thermal boundary layers

Near the top surface, for example, we rescale the variables by writing

$$z = 1 - \delta Z, \quad \psi = \delta \Psi, \quad \omega = \delta \Omega, \quad (3.39)$$

to find the leading order rescaled equation for  $\Psi$  to be simply

$$\Psi_{ZZ} \approx 0, \quad (3.40)$$

whence  $\Psi \sim u_s(x)Z$ , and  $u_s$  is the core value of the surface velocity  $-\psi_z|_{z=1}$ . Then  $\Omega_{ZZ} \approx T_x$  determines  $\Omega$  (with  $\Omega = 0$  on  $Z = 0$ , and  $\Omega \sim \omega_s(x)Z$  as  $Z \rightarrow \infty$ , where  $\omega_s$  is the core value of the surface vorticity), and  $T$  satisfies

$$\Psi_Z T_x - \Psi_x T_Z \approx T_{ZZ}. \quad (3.41)$$

In Von Mises coordinates  $x, \Psi$ , the equation is

$$T_x \sim \frac{\partial}{\partial \Psi} \left[ \Psi_Z \frac{\partial T}{\partial \Psi} \right], \quad (3.42)$$

and putting  $\xi = \int_0^x u_s(x) dx$ , this is just the diffusion equation

$$T_\xi = T_{\Psi\Psi}, \quad (3.43)$$

with

$$T = -\frac{1}{2} \quad \text{on} \quad \Psi = 0, \quad T \rightarrow 0 \quad \text{as} \quad \Psi \rightarrow \infty. \quad (3.44)$$

Note that the same Von Mises transformation (but from  $(z, X)$  to  $(z, \Psi)$ ) can be used in the plume equation (3.34)<sub>1</sub>, which can thus also be written in the diffusion equation form (3.43), where  $\xi$  is extended as  $\int^z w_p(z) dz$ .

A quantity of interest is the Nusselt number, defined as

$$Nu = - \int_0^1 \frac{\partial T}{\partial z}(x, 1) dx, \quad (3.45)$$

and from the above, this can be written as

$$Nu \approx \left[ \int_0^\infty -T d\Psi \right]_{x=0}^{x=a} Ra^{1/3}. \quad (3.46)$$

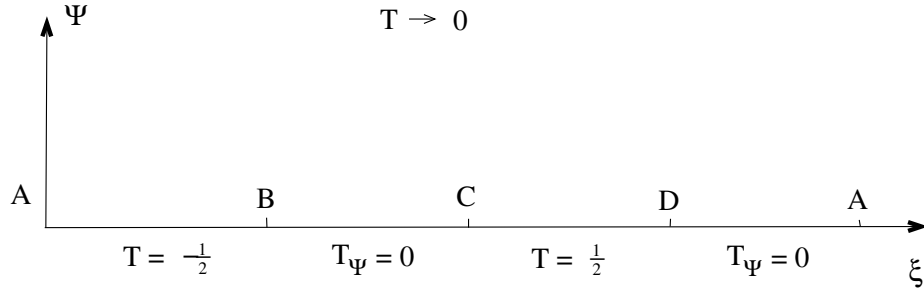


Figure 3.8: Boundary conditions for the thermal boundary layer solution of (3.49).

### Corner flow

The core flow has a singularity in each corner, where (if  $r$  is distance from the corner), then  $\psi \sim r^{3/2}$ ,  $\omega \sim r^{-1/2}$ , and (for the corner at  $x = 0$ ,  $z = 0$ , for example)  $x, z \sim r$ . There must be a region where this singularity is alleviated by the incorporation of the buoyancy term. This requires  $\omega/r^2 \sim 1/\delta r$ , whence  $r \sim \delta^{2/3}$ . Rescaling the variables as indicated ( $x, z \sim \delta^{2/3}$ ,  $\psi \sim \delta$ ,  $\omega \sim \delta^{-1/3}$ ) then gives the temperature equation as

$$\Psi_X T_Z - \Psi_Z T_X \sim \delta \nabla^2 T, \quad (3.47)$$

which shows that (since the  $\psi$  scale,  $\delta$ , is the same as that of the boundary layers adjoining the corner) the boundary layer temperature field is carried through the corner region without change (to leading order). The corner flow thus has  $T \approx T(\Psi)$ , so that

$$\nabla^4 \Psi + T'(\Psi) \Psi_X = 0, \quad (3.48)$$

with appropriate matching conditions. The main point of this is to show that in solving the thermal boundary layer equations round the perimeter of the box, the transverse profile (in  $\Psi$ ) can be taken to be continuous when the boundary conditions change at the corners.

### Solution strategy

The Von Mises transformation shows that the temperature in the thermal boundary layers and the thermal plumes satisfies the diffusion equation

$$T_\xi = T_{\Psi\Psi}, \quad (3.49)$$

where we define

$$\xi = \int_0^s U(s) ds, \quad (3.50)$$

and we define  $s$  to be arc length around the perimeter of the box (starting for example at the point  $A$  in figure 3.7, and  $U(s)$  is the (core-determined) tangential velocity on the perimeter. The temperature equation must be solved in the four regions

corresponding to the boundary layer at  $z = 1$ , plume at  $x = a$ , boundary layer at  $z = 0$ , and plume at  $x = 0$ , representing the four edges  $AB$ ,  $BC$ ,  $CD$ ,  $DA$  indicated in figure 3.7, with  $T$  being continuous at each junction point (corner), and

$$\begin{aligned}
T &\rightarrow 0 \quad \text{as} \quad \Psi \rightarrow \infty, \\
T &= -\frac{1}{2} \quad \text{on} \quad \Psi = 0 \quad [z = 1, \text{ top } AB], \\
T_\Psi &= 0 \quad \text{on} \quad \Psi = 0 \quad [x = a, \text{ right } BC], \\
T &= \frac{1}{2} \quad \text{on} \quad \Psi = 0 \quad [z = 0, \text{ bottom } CD], \\
T_\Psi &= 0 \quad \text{on} \quad \Psi = 0 \quad [x = 0, \text{ left } DA],
\end{aligned} \tag{3.51}$$

as indicated in figure 3.8.

What of the initial condition? The novelty here is that prescription of an initial condition is supplanted by the necessary requirement that the solution be periodic in  $\xi$ . Beginning from  $x = 0$ ,  $z = 1$ , we may denote the values of  $\xi$  at the corners as  $\xi_A$  ( $x = 0$ ,  $z = 1$ ),  $\xi_B$  ( $x = a$ ,  $z = 1$ ),  $\xi_C$  ( $x = a$ ,  $z = 0$ ),  $\xi_D$  ( $x = 0$ ,  $z = 0$ ). Now from the definition of  $\xi$ , we have  $\xi_k = C^{1/2}\hat{\xi}_k$ , where the values of  $\hat{\xi}_k$  are independent of  $C$  (because they are determined by the canonical solution in (3.38)). Putting

$$\xi = C^{1/2}\hat{\xi}, \quad \Psi = C^{1/4}\hat{\Psi}, \quad T(\xi, \Psi) = \hat{T}(\hat{\xi}, \hat{\Psi}), \tag{3.52}$$

we see that the problem for  $\hat{T}(\hat{\xi}, \hat{\Psi})$  is independent of  $C$ .

Just as for the flow in the core, this problem must be solved numerically for  $\hat{T}(\hat{\xi}, \hat{\Psi})$ . Assuming this is done, then

$$\int_0^\infty T(\xi, \Psi) d\Psi = C^{1/4} \int_0^\infty \hat{T}(\hat{\xi}, \hat{\Psi}) d\hat{\Psi}. \tag{3.53}$$

If, for example, we evaluate both quantities at  $\xi = 0$  (i. e., the point  $A$ ), then it follows from (3.36) that

$$C = \int_0^\infty T(0, \Psi) d\Psi = C^{1/4} \int_0^\infty \hat{T}(0, \hat{\Psi}) d\hat{\Psi}, \tag{3.54}$$

and this determines  $C$  as

$$C = \left[ \int_0^\infty \hat{T}(0, \hat{\Psi}) d\hat{\Psi} \right]^{4/3}. \tag{3.55}$$

Given this, the Nusselt number is then given from (3.46) as

$$Nu \approx C^{1/4} \left[ - \int_0^\infty \hat{T} d\hat{\Psi} \right]_0^{\hat{\xi}_A} Ra^{1/3}. \tag{3.56}$$

### No-slip boundary conditions

For no slip boundary conditions, the necessary preliminary rescaling is  $\psi \sim 1/\delta^3$ ,  $\omega \sim 1/\delta^3$ , where  $\delta = Ra^{-1/5}$ . Thus the Nusselt number  $Nu \sim Ra^{1/5}$ . There is no longer parity between the thermal boundary layers and plumes, as the former are slowed down by the no slip conditions. The rescaled equations are

$$\begin{aligned}\omega &= -\nabla^2\psi, \\ \psi_x T_z - \psi_z T_x &= \delta^3 \nabla^2 T, \\ \nabla^2 \omega &= \frac{1}{\delta^2} T_x.\end{aligned}\tag{3.57}$$

The core flow is as before; the thermal boundary layers have  $\psi \sim \delta^2$ ,  $\omega \sim 1$ ,  $z \sim \delta$ , so that vorticity balances buoyancy), and all three equations are necessary to solve for  $T$ ; it is still the case that  $\int T d\psi$  is conserved at corners, but now in the plume,  $x \sim \delta^{3/2}$ ,  $\psi \sim \delta^{3/2}$ , and  $T \sim \delta^{1/2}$ . The initial plume profile is effectively a delta function, and the plume temperature is just the resultant similarity solution. The remainder of the structure must be computed numerically.

## 3.6 Double-diffusive convection

Double-diffusive convection refers to the motion which is generated by buoyancy, when the density depends on two diffusible substances or quantities. The simplest examples occur when salt solutions are heated; then the two diffusing quantities are heat and salt. Double-diffusive processes occur in sea water and in lakes, for example. Other simple examples occur in multi-component fluids containing more than one dissolved species; convection in magma chambers is one such.

The guiding principle behind double-diffusive convection is still that light fluid rises, and convection occurs in the normal way (the direct mode) when the steady state is statically unstable (i. e., when the density increases with height), but confounding factors arise when, as normally the case, the two substances diffuse at different rates. Particularly when we are concerned with temperature and salt, the ratio of thermal to solutal diffusivity is large, and in this case different modes of convection occur near the statically neutral buoyancy state: the cells can take the form of long thin ‘fingers’, or the onset of convection can be oscillatory. In practice, fingers are seen, but oscillations are not.

A further variant on Rayleigh-Bénard convection arises in the form of convective layering. This is a long-lived transient form of convection, in which separately convecting layers form, and is associated partly with the high diffusivity ratio, and partly with the usual occurrence of no flux boundary conditions for diffusing chemical species.

We pose a model for double-diffusive convection based on a density which is related linearly to temperature  $T$  and salt composition  $c$  in the form

$$\rho = \rho_0[1 - \alpha(T - T_0) + \beta(c - c_0)],\tag{3.58}$$

where we take  $\alpha$  and  $\beta$  to be positive constants; thus the presence of salt makes the fluid heavier. The equation that then needs to be added to (3.1) is that for convective diffusion of salt:

$$c_t + \mathbf{u} \cdot \nabla c = D \nabla^2 c, \quad (3.59)$$

where  $D$  is the solutal diffusion coefficient, assuming a dilute solution. We adopt the same scaling of the variables as before, with the extra choice

$$c - c_0 \sim \Delta c, \quad (3.60)$$

where  $\Delta c$  is a relevant salinity scale (in our stability analysis, it will be the prescribed salinity difference between the lower and upper surfaces of the fluid layer). The Boussinesq form of the scaled equations, based on the assumptions that  $\alpha \Delta T \ll 1$  and  $\beta \Delta c \ll 1$ , are then

$$\begin{aligned} \nabla \cdot \mathbf{u} &= 0, \\ \frac{1}{Pr} [\mathbf{u}_t + (\mathbf{u} \cdot \nabla) \mathbf{u}] &= -\nabla p + \nabla^2 \mathbf{u} + Ra T \hat{\mathbf{k}} - Rs c \hat{\mathbf{k}}, \\ T_t + \mathbf{u} \cdot \nabla T &= \nabla^2 T, \\ c_t + \mathbf{u} \cdot \nabla c &= \frac{1}{Le} \nabla^2 c. \end{aligned} \quad (3.61)$$

The Rayleigh number  $Ra$  and the Prandtl number  $Pr$  are defined as before, and the solutal Rayleigh number  $Rs$  and the Lewis number  $Le$  are defined by

$$Rs = \frac{\beta \rho_0 \Delta c g d^3}{\mu \kappa}, \quad Le = \frac{\kappa}{D}. \quad (3.62)$$

Note that in the absence of temperature gradients, the quantity  $-Rs Le$  would be the effective Rayleigh number determining convection.

### 3.6.1 Linear stability

Now we study the linear stability of a steady state maintained by prescribed temperature and salinity differences  $\Delta T$  and  $\Delta c$  across a stress-free fluid layer. In dimensionless terms, we pose the boundary conditions

$$\begin{aligned} \psi = \nabla^2 \psi = 0 &\quad \text{at } z = 0, 1, \\ T = c = 0 &\quad \text{at } z = 1, \\ T = c = 1 &\quad \text{at } z = 0, \end{aligned} \quad (3.63)$$

where as before, we restrict attention to two dimensions, and adopt a stream function  $\psi$ . The steady state is

$$c = 1 - z, \quad T = 1 - z, \quad \psi = 0, \quad (3.64)$$

and we perturb it by writing

$$c = 1 - z + C, \quad T = 1 - z + \theta, \quad (3.65)$$

and then linearising the equations on the basis that  $C, \theta, \psi \ll 1$ . This leads to

$$\begin{aligned} \frac{1}{Pr} \nabla^2 \psi_t &\approx Ra \theta_x - Rs C_x + \nabla^4 \psi, \\ \theta_t - \psi_x &\approx \nabla^2 \theta, \\ C_t - \psi_x &\approx \frac{1}{Le} \nabla^2 C, \end{aligned} \quad (3.66)$$

with

$$C = \psi = \psi_{zz} = \theta = 0 \quad \text{on} \quad z = 0, 1. \quad (3.67)$$

By inspection, solutions satisfying the temperature and salinity equations are

$$\begin{aligned} \psi &= \exp(ikx + \sigma t) \sin m\pi z, \\ \theta &= \frac{ik}{\sigma + K^2} \exp(ikx + \sigma t) \sin m\pi z, \\ C &= \frac{ik}{\sigma + \frac{K^2}{Le}} \exp(ikx + \sigma t) \sin m\pi z, \end{aligned} \quad (3.68)$$

where we have written

$$K^2 = k^2 + m^2\pi^2. \quad (3.69)$$

Substituting these into the momentum equation leads to the dispersion relation determining  $\sigma$  in terms of  $k$ :

$$(\sigma + K^2 Pr)(\sigma + K^2) \left( \sigma + \frac{K^2}{Le} \right) + k^2 Pr \left[ \frac{(Rs - Ra)\sigma}{K^2} + Rs - \frac{Ra}{Le} \right] = 0. \quad (3.70)$$

This is a cubic in  $\sigma$ , which can be written in the form

$$\sigma^3 + a\sigma^2 + b\sigma + c = 0, \quad (3.71)$$

where

$$\begin{aligned} a &= K^2 \left( Pr + 1 + \frac{1}{Le} \right), \\ b &= K^4 \left( Pr + \frac{1}{Le} + \frac{Pr}{Le} \right) + \frac{k^2}{K^2} Pr (Rs - Ra), \\ c &= \frac{K^6}{Le} Pr + k^2 Pr \left( Rs - \frac{Ra}{Le} \right). \end{aligned} \quad (3.72)$$

Instability occurs if any one of the three roots of (3.71) has positive real part. Since  $Le$  and  $Pr$  are properties of the fluid, we take them as fixed, and study the

effect of varying  $Ra$  and  $Rs$  on the stability boundaries where  $\text{Re } \sigma = 0$ . Firstly, if  $Ra < 0$  and  $Rs > 0$ , then  $a$ ,  $b$  and  $c$  are all positive. We can then show (see question 3.3) that  $\text{Re } \sigma < 0$  for all three roots providing  $ab > c$ , and this is certainly the case if  $Le > 1$ , which is always true for heat and salt diffusion. Thus when both temperature and salinity fields are stabilising, the state of no motion is linearly stable.

To find regions of instability in the  $(Rs, Ra)$  plane, it thus suffices to locate the curves where  $\text{Re } \sigma = 0$ . There are two possibilities. The first is referred to as exchange of stability, or the direct mode, and occurs when  $\sigma = 0$ . From (3.71), this is when  $c = 0$ , or  $Rs = \frac{Ra}{Le} - \frac{K^6}{k^2 Le}$ . This is a single curve (for each  $k$ ), and since we know that  $\text{Re } \sigma < 0$  in  $Ra < 0$  and  $Rs > 0$ , this immediately tells us that a direct instability occurs if

$$Ra - Le Rs > R_c = \min_k \frac{K^6}{k^2} = \frac{27\pi^4}{4}. \quad (3.73)$$

This direct transition is the counterpart of the onset of Rayleigh-Bénard convection, and shows that  $Ra - Le Rs$  is the effective Rayleigh number. This is consistent with the remark just after (3.62).

The other possibility is that there is a Hopf bifurcation, i. e., a pair of complex conjugate values of  $\sigma$  cross the imaginary axis at  $\pm i\Omega$ , say. The condition for this is  $ab = c$ , which is again a single curve, and one can show (see question 3.4) that oscillatory instability occurs for

$$Ra > \frac{\left(Pr + \frac{1}{Le}\right) Rs}{1 + Pr} + \frac{\left(1 + \frac{1}{Le}\right) \left(Pr + \frac{1}{Le}\right)}{Pr} R_c. \quad (3.74)$$

Direct instability occurs along the line  $XZ$  in figure 3.9, while oscillatory instability occurs at the line  $XW$ . Between  $XW$  and the continuation  $XU$  of  $XZ$ , there are two roots with positive real part and one with negative real part. As  $Ra$  increases above  $XW$ , it is possible that the two complex roots coalesce on the real axis, so that the oscillatory instability is converted to a direct mode. One can show (see question 3.5) that the criterion for this is that  $b < 0$  and

$$c = \frac{1}{9} \left[ ab + \frac{(a^2 - 6b)}{3} \{-a + (a^2 - 3b)^{1/2}\} \right]. \quad (3.75)$$

For large  $Rs$ , this becomes (for  $k^2 = \frac{\pi^2}{2}$ )

$$Ra \approx Rs + \frac{3R_c^{1/3} Rs^{2/3}}{2^{2/3} Pr^{1/3}}, \quad (3.76)$$

and is shown as the line  $XW$  in figure 3.9. Thus the onset of convection is oscillatory only between the lines  $XW$  and  $XV$ , and beyond (above)  $XV$  it is direct. In practice, oscillations are rarely seen.

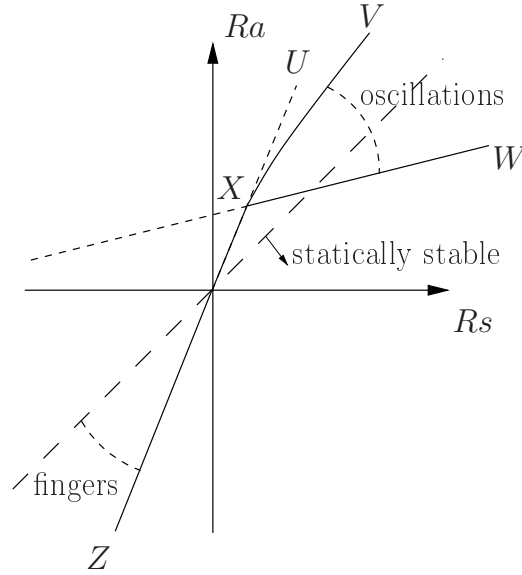


Figure 3.9: Stability diagram for double-diffusive convection.

### Fingers

If we return to the cubic in the form (3.70), and consider the behaviour of the roots in the third quadrant as  $Ra, Rs \rightarrow -\infty$ , it is easy to see that one root is

$$\sigma \approx \frac{K^2 \left[ \frac{Ra}{Le} - Rs \right]}{Rs - Ra}, \quad (3.77)$$

while the other two are oscillatorily stable (see question 3.6). Thus this growth rate is positive when  $Le Rs < Ra < Rs$  and grows unboundedly with the wave number  $k$  (since  $K^2 = k^2 + \pi^2$  when  $m = 1$ ). This is an indication of ill-posedness, and in fact we anticipate that  $\sigma$  will become negative at large  $k$ . To see when this occurs, inspection of (3.70) shows that the neglected terms in the approximation (3.77) become important when  $k \sim |Ra|^{1/4}$ , where  $\sigma$  is maximum (of  $O|Ra|^{1/4}$ ), and then  $\sigma \sim -k^2$  for larger  $k$ . Thus in the ‘finger’ régime sector indicated in figure 3.9, the most rapidly growing wavelengths are short, and the resulting waveforms are tall and thin. This is what is seen in practice, and the narrow cells are known as fingers. An example is shown in figure 3.10.

### 3.6.2 Layered convection

The linear stability analysis we have given above is only partially relevant to double diffusive convection. It is helpful in the understanding of the finger régime, but the oscillatory mode of convection is not particularly relevant. The other principal phenomenon which double diffusive systems exhibit is that of layering. This is a



Figure 3.10: Finger convection (Turner 1974).

transient, but long-term, phenomenon associated often with the heating of a stable salinity gradient, and arises because in normal circumstances, more appropriate boundary conditions for salt concentration are to suppose that there is no flux at the bounding surfaces.

In pure thermal convection, the heating of an initially stably thermally stratified fluid will lead to the formation of a layer of convecting fluid below the stable region. This (single) convecting layer will grow in thickness until it fills the entire layer. This is essentially the ‘filling box’. Suppose now we have a stable salinity gradient which is heated from below. Again a convecting layer forms, which mixes the temperature and concentration fields so that they are uniform within the layer. At the top of the convecting layer, there will be a step down  $\Delta T$  in temperature, and a step down  $\Delta c$  in salinity. It is found experimentally that  $\alpha\Delta T = \beta\Delta c$ , that is, the *boundary layer*<sup>2</sup> is neutrally stable. However, the disparity in diffusivities (typically  $Le \gg 1$ ) means that there is a thicker thermal conductive layer ahead of the interface. In effect, the stable salinity gradient above the convecting layer is heated by the layer itself, and a second, and then a third, layer forms. In this way, the entire fluid depth can fill up with a sequence of long-lived, separately convecting layers. The layers will eventually merge and form a single convecting layer over a time scale controlled by the very slow transport of salinity between the convecting layers. Such layers are very suggestive of some of the fossilised layering seen in magma chambers, as for example in figure 3.5, but the association may be a dangerous one. An experimental realisation of this

---

<sup>2</sup>For discussion of boundary layers, see section 3.5.1.

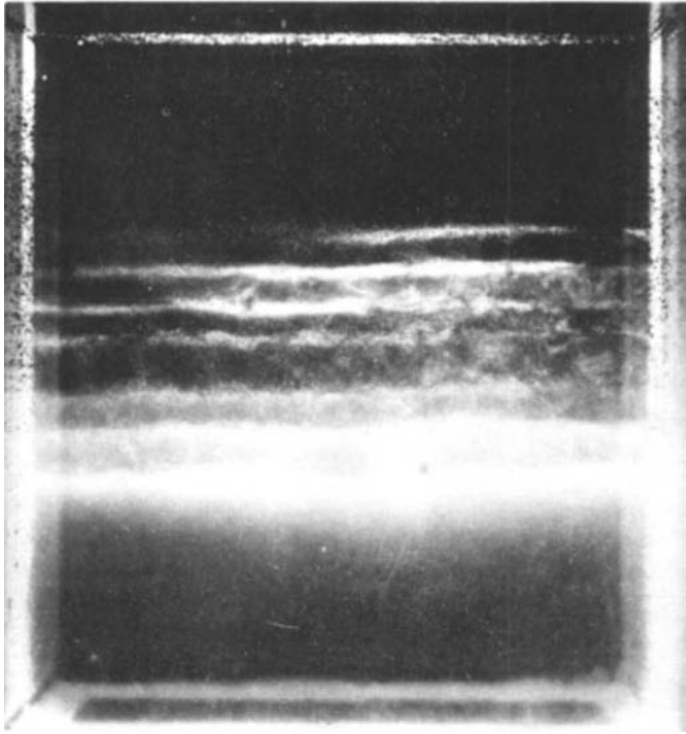


Figure 3.11: Layered convection (Turner 1974). A stable salt solution has been heated from below.

form of layered convection is shown in figure 3.11.

A further example of some of the exotic behaviour which double diffusion can lead to is shown in figure 3.12, again taken from the review article by Turner (1974). In this experiment, the two diffusing substances were sugar and salt, and the fluid was initially set up with a top-heavy gradient of salt (which plays the rôle of temperature here as its diffusivity is larger) and a bottom-heavy gradient of sugar, such that the overall density gradient was statically stable. This is the analogue of cold/fresh above hot/salty, so in the ‘diffusive’ régime of the first quadrant in figure 3.9. The rôle of the Prandtl number is taken by the Schmidt number defined by

$$Sc = \frac{\nu}{D_l}, \quad (3.78)$$

where  $D_l$  is the diffusivity of salt and  $\nu$  is the kinematic viscosity. (The ‘Lewis’ number is the ratio  $D_l/D_g$ , where  $D_g$  is the diffusivity of sugar. For salt and sugar,  $Le \approx 3$ .)<sup>3</sup> Now the Schmidt number for salt is around  $10^6$ , so the ‘Prandtl’ number is large, and the static stability limit in the diffusive régime is essentially the same as the dynamic stability limit: so nothing should happen. However, if a sloping boundary

<sup>3</sup>Specifically,  $D_l \approx 1.5 \times 10^{-9} \text{ m}^2 \text{ s}^{-1}$  (Vitagliano and Lyons 1956) and  $D_g \approx 0.5 \times 10^{-9} \text{ m}^2 \text{ s}^{-1}$  (Ziegler *et al.* 1987).

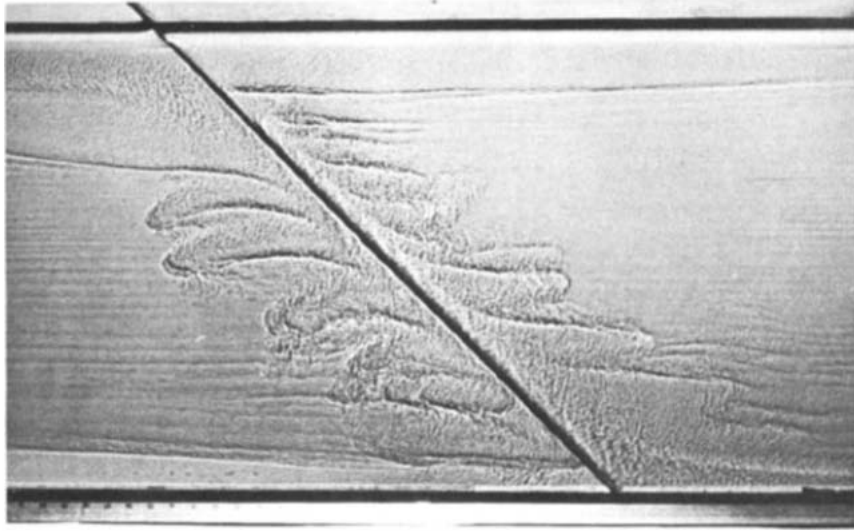


Figure 3.12: Sloping layered convection (Turner 1974).

exists as shown, convection is initiated, and takes the layered form shown. We leave it as an exercise to explain why.

## 3.7 Parameterised convection

The boundary layer theory described in section 3.5 applies to steady state solutions at high Rayleigh number, but in fact real convection becomes time-varying at such parameter values. The behaviour becomes first oscillatory, and then becomes increasingly irregular, so that at very high Rayleigh numbers, the cellular structure of convection in a fluid layer breaks down. The upwelling and downwelling plumes of the boundary layer theory still exist, but their detachment is sporadic and irregular. In these circumstances, the theoretical description of convection may become, paradoxically, easier. Just as for turbulent shear flows at high Reynolds numbers, one uses empirically-based measures of the fluxes at boundaries to describe the flow. Turbulence mixes the fluid, so that, as in the boundary layer theory, the interior of a convecting cell is taken to be isothermal. In this section, we describe one particular example of turbulent convection to illustrate these ideas. The example is that of the turbulent convective plume.

### 3.7.1 Plumes

A plume is an isolated convective upwelling. Examples are the rise of smoke from an industrial chimney, the formation of cumulus clouds over oceans, ‘black smokers’ at mid-ocean rise vents, and explosive volcanic eruptions. In these examples, a source of buoyancy at (essentially) a point drives a convective flow in the fluid above. As



Figure 3.13: On the left, a sub-oceanic black smoker issuing from a vent at the ocean floor; on the right, an industrial chimney. Images from <http://oceanexplorer.noaa.gov>.

suggested in figure 3.13, the plume forms a turbulent, approximately conical region, with a fairly sharp (but time-varying) boundary. The turbulence causes rapid convective mixing, and allows us to conceptualise the plume as a relatively homogeneous cloud of density  $\rho = \rho_0 - \Delta\rho$  rising through an ambient medium of density  $\rho_0$ . If  $\rho_0$  depends on height  $z$ , then the medium is called a stratified medium, and it is stably stratified if  $\rho'_0(z) < 0$ .

### Mathematical model

The simplest mathematical model is of a steady<sup>4</sup> cylindrically symmetric plume of radius  $r = b(z)$ , in which we use cylindrical coordinates  $(r, z)$ , with corresponding velocity components  $(u, w)$  (thus the upwards fluid velocity is  $w$ ). The plume rises through a medium of density  $\rho_0(z)$ . We will make the Boussinesq approximation, which is that variations in density are neglected, except in the buoyancy term of the momentum equation, and in the ‘buoyancy’ equation itself. This requires variations of the density from that of the ambient density to be small, and also that the variation

---

<sup>4</sup>The turbulent time variation is averaged out.

of  $\rho_0$  with height (if any) is small. The basic model is then given by

$$\begin{aligned}
\frac{1}{r}(ru)_r + w_z &= 0, \\
uu_r + ww_z &= -\frac{1}{\rho_0}p_r + \frac{1}{r}\frac{\partial}{\partial r}\left[\nu_T r \frac{\partial u}{\partial r}\right], \\
uw_r + ww_z &= -\frac{1}{\rho_0}p_z - \frac{\rho}{\rho_0}g + \frac{1}{r}\frac{\partial}{\partial r}\left[\nu_T r \frac{\partial w}{\partial r}\right], \\
u\rho_r + w\rho_z &= +\frac{1}{r}\frac{\partial}{\partial r}\left[\nu_T r \frac{\partial \rho}{\partial r}\right].
\end{aligned} \tag{3.79}$$

These equations represent respectively conservation of mass, momentum (horizontal and vertical), and buoyancy;  $p$  is the pressure,  $\rho$  the density,  $\rho_0$  the reference density, and  $g$  is the acceleration due to gravity. We have included radial diffusion terms which represent the effects of turbulent mixing:  $\nu_T$  is a turbulent eddy diffusivity. We define the density deficit  $\Delta\rho$  in the plume to be

$$\Delta\rho = \rho_0 - \rho. \tag{3.80}$$

The Boussinesq approximation is based on the assumption that  $\Delta\rho$  is small,  $\Delta\rho \ll \rho_0$ . The laminar viscous terms are neglected on the basis that the flow is turbulent (so the Reynolds number is large). In fact, turbulent flows are better modelled (by Reynolds averaging) through the use of *Reynolds stresses*, which arise through the time-averaged effect of interacting velocity fluctuations,<sup>5</sup> but in fact such Reynolds stresses are themselves relatively small (a fact that is not commonly noted); however in the present case we include them, at least temporarily, to allow for radial mixing (longitudinal mixing can be neglected on the basis of our imminent assumption that the plume is thin).

The rather odd-looking final equation requires some comment. It caters for the fact that the density deficit in plumes may arise because of temperature, dissolved concentrations or particulate load, or a combination. But in all such cases, the turbulent conservation field for the relevant variable is simply that advection is zero; for example we would have  $T_t + \mathbf{u} \cdot \nabla T = \nabla \cdot [\nu_T \nabla T]$  for temperature, and similarly for particulate or solute concentrations. Thus the buoyancy conservation equation simply represents this fact, together with the assumption that the density is an algebraic function of the conserved quantities. In certain circumstance, the veracity of this assumption may need to be examined further. For example, in a volcanic ash-laden plume, the eruption column has a density which is dependent on both temperature and ash concentration, and it rises through a surrounding stratified atmosphere whose

---

<sup>5</sup>In more detail, if we write the (three-dimensional) velocity components as  $u_i = \bar{u}_i + u'_i$ , where the overbar denotes a suitable average (for example a local time average), then the (deviatoric) Reynolds stress tensor which appears in the Navier-Stokes equation for the *averaged* velocity is given by  $\tau_{ij}^{Re} = -\rho \overline{u'_i u'_j}$ . Commonly the Reynolds stress tensor is prescribed by use of an *eddy viscosity* in terms of the strain rate of the averaged velocity field, which then allows the prescription of a turbulent Reynolds number, commonly of  $O(10^2)$ .

stratification is itself determined by the relation of density to temperature and pressure. In such circumstance, (3.79)<sub>4</sub> may warrant further consideration, but such issues will be ignored here.

The principal approximation that we make is that the plume is *thin*, and this allows the well-worn use of the lubrication approximation (and also explains why we omitted the vertical diffusion terms), which implies that the radial pressure variation is small, and thus the pressure is that of the surrounding ambient fluid,

$$p_z \approx -\rho_0 g. \quad (3.81)$$

This allows us to write the remaining three equations in terms of the *reduced gravity*, which is defined to be

$$g' = \frac{g\Delta\rho}{\rho_0}. \quad (3.82)$$

The equations (3.79) then take the simple form

$$\begin{aligned} (ru)_r + rw_z &= 0, \\ uw_r + ww_z &= g' + \frac{1}{r} \frac{\partial}{\partial r} \left[ \nu_T r \frac{\partial w}{\partial r} \right], \\ N^2 w + ug'_r + wg'_z &= \frac{1}{r} \frac{\partial}{\partial r} \left[ \nu_T r \frac{\partial g'}{\partial r} \right], \end{aligned} \quad (3.83)$$

where  $N$  is the Brunt-Väisälä frequency, defined as

$$N = \left( -\frac{g\rho'_0}{\rho_0} \right)^{1/2}, \quad (3.84)$$

and we have put a pre-factor of  $1 - \frac{\Delta\rho}{\rho_0}$  equal to one in the  $N^2$  term.

It is fairly evident in figure 3.13 that the plume has a fairly well-defined edge, and we will assume this. The boundary of the plume is taken to be at  $r = b(z)$ . The question then arises as to what, if any, boundary conditions should be applied there. Since the ambient fluid outside the plume has  $w = g' = 0$ , these are natural conditions to apply, at least when the diffusion terms are included. We therefore pose the conditions

$$w = g' = 0 \quad \text{at} \quad r = b(z). \quad (3.85)$$

One might suppose that also  $u = 0$  would be appropriate, but in fact this is found not to be the case. The turbulent eddies of the plume incorporate the ambient fluid, and dramatically increase the plume volume flux. If the entrainment velocity (inwards) at the edge of the plume is  $u_e$ , then we have that

$$u = -u_e \quad \text{at} \quad r = b. \quad (3.86)$$

The entrainment velocity needs to be constituted, and a common assumption is to suppose that

$$u_e = \alpha \bar{w}, \quad (3.87)$$

where  $\bar{w}$  is the cross-sectionally averaged vertical velocity, and the value of  $\alpha$  is found experimentally to be approximately 0.1. We note that the plume boundary  $r = b(z)$  is indeterminate, so that an extra condition to determine it is apparently necessary. If  $b = \infty$ , this issue does not arise.

**The case  $\nu_T = 0$**

We now ignore the radial diffusion terms in (3.83) by putting  $\nu_T = 0$ . The resulting equations are given by

$$\begin{aligned} (ru)_r + rw_z &= 0, \\ uw_r + ww_z &= g', \\ ug'_r + wg'_z &= -N^2w, \end{aligned} \tag{3.88}$$

and are hyperbolic, and suitable boundary conditions to consider are (3.85) and (3.86) at the plume boundary; in addition, for a plume emanating from a vent of radius  $a$  at  $z = 0$ , we might pose

$$w = w_0, \quad u = 0, \quad g' = g'_0 \quad \text{at} \quad z = 0, \quad 0 < r < a. \tag{3.89}$$

Whether all these conditions can be applied depends on the characteristic directions of the hyperbolic set (3.88). This is examined in question 3.8. If we define the Stokes stream function by  $ru = \psi_z$ ,  $rw = -\psi_r$ , then the characteristics are just the streamlines, and follow the direction of flow. Therefore the characteristics point inwards from all parts of the boundary, and all the boundary conditions can be applied.

Without writing an analytical solution for the flow, what happens is fairly clear (we assume positive vent buoyancy,  $g'_0 > 0$ ). On the streamlines from the vent which form the central part of the plume,  $g' \equiv g'_0$ , and  $w$  increases upwards, thus the vent streamlines shrink radially. Equally, the prescription of  $g' = 0$  on the plume boundary  $r = b$  ensures that  $g' = w = 0$  on all characteristics that begin there, so that  $g' = 0$  everywhere outside the vent characteristics; the characteristics are horizontal. In fact, there is no reason to define the plume outside the central core, since there is no buoyancy there.

It is fairly clear what the matter is: the diffusion terms in (3.83) can not be ignored. Their effect is precisely to broaden the spike of buoyancy which emerges from the vent. We can go further. A typical prescription for the eddy diffusivity is to take (in the present situation)

$$\nu_T = \varepsilon_T b w, \tag{3.90}$$

where  $\varepsilon_T$  is relatively small, perhaps  $\sim 10^{-2}$ . The point is that with this assumption, the diffusivity tends to zero at the plume edge, which suggests as with other examples of such degenerate diffusion that no extra condition is necessary to determine it (and that its location is at a finite distance).

## Moment equations

In order to progress with the solution of the equations (3.83), we integrate them from the centre to the edge of the plume, the second and third after multiplying by  $r$ . With our assumption that  $\nu_T = 0$  when  $w = 0$ , the two diffusion integrals vanish, and we are left with three evolution equations for the three quantities

$$\begin{aligned} Q &= 2\pi \int_0^b r w \, dr, \\ M &= 2\pi \int_0^b r w^2 \, dr, \\ B &= 2\pi \int_0^b r w g' \, dr, \end{aligned} \tag{3.91}$$

which are the volume flux, the momentum flux and the buoyancy flux, respectively. Bearing in mind that  $w = g' = 0$  at  $r = b$ , we find, noting also (3.86) and (3.87),

$$\begin{aligned} \frac{dQ}{dz} &= 2\pi\alpha b\bar{w}, \\ \frac{dM}{dz} &= 2\pi \int_0^b r g' \, dr, \\ \frac{dB}{dz} &= -N^2 Q. \end{aligned} \tag{3.92}$$

We note also that

$$Q = \pi b^2 \bar{w}, \tag{3.93}$$

so that these are almost self-contained. In order to proceed, some further simplifications must be made. We consider first the case of an unstratified environment.

## Unstratified environment

In the case that the ambient fluid is unstratified, the Brunt-Väisälä frequency  $N$  is zero, and the buoyancy flux  $B$  is constant. In practice it is sufficient to consider the release of buoyant material from a point source, as this effectively is the common situation of interest. If in addition we suppose that the volume flux (and hence also the momentum flux) is zero at the source, then there is no intrinsic length scale in the problem, and a similarity solution is suggested. Indeed, the only dimensional quantities in the problem are the buoyancy flux  $B$  with units of  $\text{m}^4 \text{s}^{-3}$  and the lengths  $r$  and  $z$ . So the similarity variable must be

$$\eta = \frac{r}{z}, \tag{3.94}$$

and the solution must have the form, by dimensional reasoning,

$$b = \beta z, \quad w = B^{1/3} z^{-1/3} W(\eta), \quad g' = B^{2/3} z^{-5/3} G(\eta), \tag{3.95}$$

with  $u$  being determined by quadrature. It seems that these expressions fit well to experiments, with the functions  $W$  and  $G$  being approximately Gaussians.

The question then arises, can we actually find the functions  $W$  and  $G$  by solving the model (3.83)? As we might expect, the equations without the diffusion terms admit a similarity form of solution, although as discussed above this is of little use. What is (perhaps) surprising is that the equations (3.83) *including* the diffusion terms, have a similarity solution of the form

$$w = z^\nu W(\eta), \quad u = z^\nu U(\eta), \quad g' = z^{2\nu-1} G(\eta), \quad \eta = \frac{r}{z}, \quad b = \beta z, \quad \nu = -\frac{1}{3}, \quad (3.96)$$

providing we choose the eddy diffusivity to be given by (3.90), and then  $U$ ,  $W$  and  $G$  satisfy the equations

$$\begin{aligned} (\eta U)' + \eta(\nu W - \eta W') &= 0, \\ UW' + W(\nu W - \eta W') &= G + \frac{\varepsilon_T \beta}{\eta} (\eta W W')', \\ UG' + W\{(2\nu - 1)G - \eta G'\} &= \frac{\varepsilon_T \beta}{\eta} (\eta W G')', \end{aligned} \quad (3.97)$$

with such boundary conditions as we can muster:

$$W = G = 0, \quad U = -\frac{2\alpha}{\beta^2} \int_0^\beta \eta W d\eta \quad \text{at} \quad \eta = \beta. \quad (3.98)$$

There will be symmetry conditions at  $\eta = 0$ , but since the equations in (3.97) are degenerate at both end points (and  $\beta$  is not known), it is unclear just how many conditions are necessary. In addition we have the prescribed buoyancy flux  $B$ , which gives another condition via the presumed first integral

$$B = 2\pi \int_0^\beta \eta W G d\eta. \quad (3.99)$$

It remains to be seen whether the numerical solution of (3.97) gives solutions similar to observations.

### Plumes in a stratified environment

If, as for example in the atmosphere, the ambient density decreases with height, then a similarity solution is no longer feasible because the stratification introduces a natural scale height. To derive a model for such a plume, we must assume some form for the cross-section profiles, which will allow closure expressions for the average fluxes  $B$ ,  $Q$  and  $M$  in terms of the plume (average) velocity  $w$  and radius  $b$ . The simplest assumption to make is that the profiles of buoyancy and vertical velocity have ‘top hat’ profiles, that is to say they are uniform and then drop rapidly at the plume



Figure 3.14: An umbrella cloud resulting from the eruption of Mount Redoubt, Alaska, in 1991. Image from Huppert (2000).

edges. Such profiles might be motivated by a particular choice of expression for the eddy diffusivity in (3.83), for example. With this assumption, we find

$$B = \pi b^2 w g', \quad Q = \pi b^2 w, \quad M = \pi b^2 w^2; \quad (3.100)$$

in addition we have

$$2\pi \int_0^b r g' dr = \pi b^2 g'. \quad (3.101)$$

Eliminating  $w$  and  $b$  finally yields the equations

$$\begin{aligned} \frac{dB}{dz} &= -N^2 Q, \\ \frac{dM}{dz} &= \frac{BQ}{M}, \\ \frac{dQ}{dz} &= 2\pi^{1/2} \alpha M^{1/2}. \end{aligned} \quad (3.102)$$

We can see from this that the buoyancy flux continually decreases with height, while the volume flux increases. When  $B = 0$ , the plume reaches its level of neutral buoyancy, but continues to rise because of its momentum. With  $B < 0$ ,  $M$  decreases, and will not rise any further when  $M$  reaches 0. According to the equations, the volume flux is still positive, but in fact the plume spreads out laterally, forming an *umbrella cloud* as shown in figure 3.14, and the one-dimensional description becomes irrelevant. Thus a plume in a stratified medium will level out at a height  $z_s$  which can be determined from (3.102) in the form (see question 3.11)

$$z_s = c B_0^{1/4} N^{-3/4}, \quad (3.103)$$

where  $B_0$  is the buoyancy flux at  $z = 0$ , and  $N$  is assumed constant.

### 3.8 Turbulent convection

As the Rayleigh number increases in Rayleigh–Bénard convection, the convective rolls which can be seen at the onset of convection bifurcate to three-dimensional planforms, typically either square cells or hexagons. In a layer of large horizontal extent, convective rolls tend to be weakly chaotic, because the alignment in different parts of the layer is different, and thus defects or dislocations are formed in the cellular structure, and these migrate slowly, sometimes permanently. Three-dimensional cells tend to be more stable, because they are essentially confined, but at higher Rayleigh number, an oscillatory instability sets in. The thermal boundary layers which migrate across the base of the cells and detach at the cell boundaries start to prematurely thicken and then thin again before detachment, causing an oscillation which is a manifestation of budding plume development. Eventually, these budding plumes do begin to detach before reaching the cell walls, and at this point the convection becomes temporally and spatially disordered. Thermal boundary layers thicken and plumes detach irregularly, and a defined cellular structure disappears, being replaced by a host of upwelling and downwelling thermal plumes. In fact, a large scale circulation does come into existence, but this is on a much larger scale than the typical plume spacing.

A very famous but simple model of turbulent thermal convection was put forward by Lou Howard in 1964, at the International Congress of Mechanics in Munich. In his model, a quiescent thermal boundary layer grows into an isothermal core until it reaches a critical thickness, when it suddenly forms a plume and detaches, mixing the fluid and returning to isothermal conditions. The average heat flux is then determined by that during the quiescent, conductive phase. The conductive temperature in the growing boundary layer is given by the solution of

$$T_t = \kappa T_{zz}, \quad (3.104)$$

with

$$\begin{aligned} T &= \frac{1}{2}\Delta T \quad \text{on } z = 0, \\ T &\rightarrow 0 \quad \text{as } z \rightarrow \infty; \end{aligned} \quad (3.105)$$

here we imagine a convecting fluid layer of depth  $d$ , across which the prescribed temperature difference is  $\Delta T$  (and thus half across the boundary layers on each surface). Starting from an isothermal state  $T = 0$  (boundary layer of thickness zero), the solution is

$$T = \frac{1}{2}\Delta T \operatorname{erfc} \left( \frac{z}{2\sqrt{\kappa t}} \right), \quad (3.106)$$

and thus the average heat flux from the surface  $z = 0$  is

$$F = \frac{1}{t_c} \int_0^{t_c} \left( -k \frac{\partial T}{\partial z} \right) \Big|_{z=0} dt, \quad (3.107)$$

where  $t_c$  is the time of detachment of the boundary layer. Using (3.106), we then find

$$F = \frac{k\Delta T}{2\sqrt{\kappa t_c}} = \frac{k\Delta T}{2d_c}, \quad (3.108)$$

where  $d_c = \sqrt{\kappa t_c}$  is the thickness of the thermal boundary layer at detachment.

Howard hypothesised that detachment would occur when a locally defined Rayleigh number, using the boundary layer thickness as the depth scale, became critical, of order

$$Ra_c \sim 10^3; \quad (3.109)$$

thus we define the critical thickness  $d_c$  via the effective critical Rayleigh number condition

$$\frac{\alpha\rho_0gd_c^3\Delta T}{2\mu\kappa} = Ra_c, \quad (3.110)$$

where the factor 2 allows for the temperature drop of  $\frac{1}{2}\Delta T$  across the boundary layer. In terms of the Rayleigh number of the fluid layer

$$Ra = \frac{\alpha\rho_0gd^3\Delta T}{\mu\kappa}, \quad (3.111)$$

we thus have the dimensionless heat flux, called the Nusselt number  $Nu$ , given by

$$Nu = \frac{F}{(k\Delta T/d)} = \frac{d}{d_c} = cRa^{1/3}, \quad (3.112)$$

where

$$c = (2Ra_c)^{-1/3} \approx 0.08. \quad (3.113)$$

Thus the heat flux can be parameterised as

$$F = c \left( \frac{\alpha g c_p}{\mu} \right)^{1/3} (\rho_0 k)^{2/3} \Delta T^{4/3}, \quad (3.114)$$

which is the famous four-thirds law for turbulent convection. It is reasonably consistent with experimental results.

### 3.9 Notes and references

The theory of continental drift was famously published by Alfred Wegener, a German meteorologist, in 1915. An English translation of his book was published later, see Wegener (1924). His ideas were scorned by the geophysical establishment, and in particular, in Britain, by the colossal figure of Harold Jeffreys. The blind ignorance with which he and other fellow geologists refuted Wegener's ideas should serve (but have not) as a lesson for scientists against the perils of treating science as religion, and hypothesis as dogma. A notable supporter of the thesis of continental drift was

Holmes (1978), who understood that mantle convection was the driving mechanism. A more modern treatment of geodynamics is the classic book by Turcotte and Schubert (1982), while Davies (1999) gives a readable but technically undemanding account.

The layered magma chamber known as the Skaergaard intrusion was the subject of a massive memoir by Wager and Brown (1968), who gave painstaking descriptions of the series of layered rocks. They made some attempts at a theoretical description, as did McBirney and Noyes (1979), based on analogous processes in chemical reaction-diffusion theory. Neither of these, nor any subsequent attempts at a theoretical model, have been altogether successful.

Baines and Gill (1969), Turner (1979)

Balmforth *et al.* (2001)

The basic description of boundary layer theory at high Rayleigh number and infinite Prandtl number was first done successfully by Turcotte and Oxburgh (1967). A more complete theory is due to Roberts (1979), although even this is not quite watertight.. The necessary numerical results to compute  $C$  in (3.37) are given by Roberts (1979) and Jimenez and Zufria (1987). The results are slightly different, with the latter paper considering Roberts' numerical results to be wrong. For  $a = O(1)$ , then  $2C \approx 0.1$ .

Jimenez and Zufria (1987) claim that the equivalent problem to (3.48) for the case of no-slip boundary conditions has no solution, but do not adduce details. Their inference is that the boundary layer approximation fails: this seems a hazardous conclusion.

Linden (2000), Morton *et al.* (1956).

The model of turbulent thermal convection described in section 3.8 is due to Howard (1966). Baines and Turner (1969).

## Exercises

3.1 The Boussinesq equations of two-dimensional thermal convection can be written in the dimensionless form

$$\begin{aligned}\nabla \cdot \mathbf{u} &= 0, \\ \frac{1}{Pr} [\mathbf{u}_t + (\mathbf{u} \cdot \nabla) \mathbf{u}] &= -\nabla p + \nabla^2 \mathbf{u} + Ra T \hat{\mathbf{k}}, \\ T_t + \mathbf{u} \cdot \nabla T &= \nabla^2 T.\end{aligned}$$

Explain the meaning of these equations, and write down appropriate boundary conditions assuming stress-free boundaries.

By introducing a suitably defined stream function, show that these equations can be written in the form

$$\begin{aligned}\frac{1}{Pr} [\nabla^2 \psi_t + \psi_x \nabla^2 \psi_z - \psi_z \nabla^2 \psi_x] &= Ra T_x + \nabla^4 \psi, \\ T_t + \psi_x T_z - \psi_z T_x &= \nabla^2 T,\end{aligned}$$

with the associated boundary conditions

$$\begin{aligned}\psi = \nabla^2\psi = 0 & \quad \text{at } z = 0, 1, \\ T = 0 & \quad \text{at } z = 1, \\ T = 1 & \quad \text{at } z = 0,\end{aligned}$$

and write down the conductive steady state solution.

By linearising about this steady state, show that

$$\frac{1}{Pr} \left( \frac{\partial}{\partial t} - \nabla^2 \right) \nabla^2 \psi_t = \left( \frac{\partial}{\partial t} - \nabla^2 \right) \nabla^4 \psi + Ra \psi_{xx},$$

and deduce that solutions are  $\psi = e^{\sigma t} \sin kx \sin m\pi z$ , and thus that

$$(\sigma + K^2) \left( \frac{\sigma}{K^2 Pr} + 1 \right) - \frac{Ra k^2}{K^4} = 0, \quad K^2 = k^2 + m^2 \pi^2.$$

By considering the graph of this expression as a function of  $\sigma$ , show that oscillatory instabilities can not occur, and hence derive the critical Rayleigh number for the onset of convection.

- 3.2 A two-dimensional, incompressible fluid flow has velocity  $\mathbf{u} = (u, 0, w)$ , and depends only on the coordinates  $x$  and  $z$ . Show that there is a stream function  $\psi$  satisfying  $u = -\psi_z$ ,  $w = \psi_x$ , and that the vorticity

$$\boldsymbol{\omega} = \nabla \times \mathbf{u} = -\nabla^2 \psi \mathbf{j},$$

and thus that

$$\mathbf{u} \times \boldsymbol{\omega} = (\psi_x \nabla^2 \psi, 0, \psi_z \nabla^2 \psi),$$

and hence

$$\nabla \times (\mathbf{u} \times \boldsymbol{\omega}) = (\psi_x \nabla^2 \psi_z - \psi_z \nabla^2 \psi_x) \mathbf{j}.$$

Use the vector identity  $(\mathbf{u} \cdot \nabla) \mathbf{u} = \nabla(\frac{1}{2}u^2) - \mathbf{u} \times \boldsymbol{\omega}$  to show that

$$\nabla \times \frac{d\mathbf{u}}{dt} = [-\nabla^2 \psi_t - \psi_x \nabla^2 \psi_z + \psi_z \nabla^2 \psi_x] \mathbf{j}.$$

Show also that

$$\nabla \times \theta \mathbf{k} = -\theta_x \mathbf{j},$$

and use the Cartesian identity

$$\nabla^2 \equiv \text{grad div} - \text{curl curl}$$

to show that

$$\nabla \times \nabla^2 \mathbf{u} = -\nabla^4 \psi \mathbf{j},$$

and hence deduce that the momentum equation for Rayleigh–Bénard convection can be written in the form

$$\frac{1}{Pr} [\nabla^2 \psi_t + \psi_x \nabla^2 \psi_z - \psi_z \nabla^2 \psi_x] = Ra \theta_x + \nabla^4 \psi.$$

3.3 Suppose that  $\sigma$  satisfies

$$p(\sigma) \equiv \sigma^3 + a\sigma^2 + b\sigma + c = 0,$$

and that  $a$ ,  $b$  and  $c$  are positive. Suppose, firstly, that the roots are all real. Show in this case that they are all negative.

Now suppose that one root ( $\alpha$ ) is real and the other two are complex conjugates  $\beta \pm i\gamma$ . Show that  $\alpha < 0$ . Show also that  $\beta < 0$  if  $a > \alpha$ . Show that  $a > \alpha$  if  $p(-a) < 0$ , and hence show that  $\beta < 0$  if  $c < ab$ .

If

$$\begin{aligned} a &= K^2 \left( Pr + 1 + \frac{1}{Le} \right), \\ b &= K^4 \left( Pr + \frac{1}{Le} + \frac{Pr}{Le} \right) + \frac{k^2}{K^2} Pr(Rs - Ra), \\ c &= \frac{K^6}{Le} Pr + k^2 Pr \left( Rs - \frac{Ra}{Le} \right), \end{aligned}$$

show that  $a, b, c > 0$  if  $Ra < 0$ ,  $Rs > 0$ , and show that if  $Le > 1$ , then  $c < ab$ .

What does this tell you about the stability of a layer of fluid which is both thermally and salinely stably stratified?

3.4 Suppose that  $\sigma$  satisfies

$$p(\sigma) \equiv \sigma^3 + a\sigma^2 + b\sigma + c = 0,$$

and that all the roots have negative real part if  $c < ab$ . Show that the condition that there be two purely imaginary roots  $\pm i\Omega$  is that  $c = ab$ , and deduce that there are two (complex) roots with positive real part if  $c > ab$ . With

$$\begin{aligned} a &= K^2 \left( Pr + 1 + \frac{1}{Le} \right), \\ b &= K^4 \left( Pr + \frac{1}{Le} + \frac{Pr}{Le} \right) + \frac{k^2}{K^2} Pr(Rs - Ra), \\ c &= \frac{K^6}{Le} Pr + k^2 Pr \left( Rs - \frac{Ra}{Le} \right), \end{aligned}$$

show that this condition reduces to

$$Ra > \frac{\left( Pr + \frac{1}{Le} \right) Rs}{1 + Pr} + \frac{\left( 1 + \frac{1}{Le} \right) \left( Pr + \frac{1}{Le} \right) K^6}{Pr k^2}.$$

Assuming  $K^2 = k^2 + m^2\pi^2$ , where  $m$  is an integer, show that the minimum value of  $Ra$  where this condition is satisfied is when  $m = 1$ , and give the corresponding critical value  $Ra_{\text{osc}}$ .

3.5 On the line  $XV$  in figure 3.9, the cubic

$$p(\sigma) = \sigma^3 + a\sigma^2 + b\sigma + c$$

has two positive real roots  $\beta$  and one negative real root  $\alpha$ . Show that the condition for this to be the case is that

$$a = \alpha - 2\beta, \quad b = \beta^2 - 2\alpha\beta, \quad c = \alpha\beta^2,$$

and deduce that

$$a\beta^2 + 2b\beta + 3c = 0. \quad (1)$$

Show also that at the double root  $\beta$ ,

$$3\beta^2 + 2a\beta + b = 0. \quad (2)$$

Deduce from (1) and (2) that

$$\beta = \frac{9c - ab}{a^2 - 6b},$$

and hence, using (2), that

$$\beta = \frac{1}{3} [-a + \{a^2 - 3b\}^{1/2}]. \quad (3)$$

Explain why the positive root is taken in (3), and why we can assume  $b < 0$ .

Use the definitions

$$\begin{aligned} a &= K^2 \left( Pr + 1 + \frac{1}{Le} \right), \\ b &= K^4 \left( Pr + \frac{1}{Le} + \frac{Pr}{Le} \right) + \frac{k^2}{K^2} Pr (Rs - Ra), \\ c &= \frac{K^6}{Le} Pr + k^2 Pr \left( Rs - \frac{Ra}{Le} \right), \end{aligned}$$

to show that if  $Ra \sim Rs \gg 1$ ,  $Ra - Rs \gg 1$  and  $Le \gg 1$ , then  $XV$  is approximately given by

$$Ra \approx Rs + \frac{3K^2 Rs^{2/3}}{(4k^2 Pr)^{2/3}}.$$

3.6 The growth rate  $\sigma$  for finger instabilities is given by

$$(\sigma + K^2 Pr)(\sigma + K^2) \left( \sigma + \frac{K^2}{Le} \right) + k^2 Pr \left[ \frac{(Rs - Ra)\sigma}{K^2} + Rs - \frac{Ra}{Le} \right] = 0,$$

and  $Ra, Rs < 0$  with  $-Ra, -Rs \gg 1$ ;  $K$  is defined by  $K^2 = k^2 + \pi^2$ .

Define  $Rs = Rar$ , and consider the behaviour of the roots when  $Ra \rightarrow -\infty$  with  $r$  fixed. Show that when  $k$  is  $O(1)$ , one root is given by

$$\sigma = \frac{\left(r - \frac{1}{Le}\right) K^2}{1 - r} + O\left(\frac{1}{|Ra|}\right), \quad (*)$$

and that this is positive if

$$\frac{1}{Le} < r < 1.$$

Show that the other two roots are of  $O(|Ra|^{1/2})$ , and by putting

$$\sigma = |Ra|^{1/2}\Sigma_0 + \Sigma_1 + \dots,$$

show that they are given by

$$\sigma = \pm i \frac{k}{K} \{Pr(Ra - Rs)\}^{1/2} - \frac{1}{2} K^2 \left( Pr + \frac{1 - \frac{1}{Le}}{1 - r} \right) + O\left(\frac{1}{|Ra|^{1/2}}\right),$$

and thus represent stable modes.

Show further that when  $k$  is large, an appropriate scaling when  $(*)$  breaks down is given by

$$k = |Ra|^{1/4}\alpha, \quad \sigma = |Ra|^{1/4}\Sigma,$$

and write down the equation satisfied by  $\Sigma$  in this case. Show also that when  $\alpha$  is large, the three roots are all negative, with  $\Sigma \sim -\alpha^2 S$ , and  $S = Pr, 1$ , or  $\frac{1}{Le}$ .

Deduce that the maximal growth rate for finger instability occurs when  $k \sim |Ra|^{1/4}$ .

- 3.7 The scaled Boussinesq equations for two-dimensional thermal convection at infinite Prandtl number and large Rayleigh number  $R$  in  $0 < x < a$ ,  $0 < z < 1$ , can be written in the form

$$\begin{aligned} \omega &= -\nabla^2 \psi, \\ \nabla^2 \omega &= \frac{1}{\delta} T_x, \\ \psi_x T_z - \psi_z T_x &= \delta^2 \nabla^2 T, \end{aligned}$$

where  $\delta = R^{-1/3}$ . Explain what is meant by the Boussinesq approximation, and explain what the equations represent. Explain why suitable boundary conditions for these equations which represent convection in a box with stress free boundaries, as appropriate to convection in the Earth's mantle, are given by

$$\psi = 0, \quad \omega = 0, \quad \text{on } x = 0, a, \quad z = 0, 1,$$

$$T = \frac{1}{2} \quad \text{on} \quad z = 0, \quad T = -\frac{1}{2} \quad \text{on} \quad z = 1, \quad T_x = 0 \quad \text{on} \quad x = 0, \quad a.$$

Show that, if  $\delta \ll 1$ , there is an interior ‘core’ in which  $T \approx 0$ ,  $\nabla^4 \psi = 0$ .

By writing  $1 - z = \delta Z$ ,  $\psi = \delta \Psi$  and  $\omega = \delta \Omega$ , show that  $\Psi \approx u_s(x)Z$ , and deduce that the temperature in the thermal boundary layer at the surface is described by the approximate equation

$$u_s T_x - Z u_s' T_Z \approx T_{ZZ},$$

with

$$T = -\frac{1}{2} \quad \text{on} \quad Z = 0, \quad T \rightarrow 0 \quad \text{as} \quad Z \rightarrow \infty.$$

If  $u_s$  is constant, find a similarity solution, and show that the scaled surface heat flux  $q = \partial T / \partial Z|_{Z=0}$  is given by

$$q = \frac{1}{2} \sqrt{\frac{u_s}{\pi x}}.$$

3.8 The Boussinesq equations describing the rise of a cylindrical plume are, ignoring turbulent diffusivity,

$$\begin{aligned} (ru)_r + rw_z &= 0, \\ uw_r + ww_z &= g', \\ ug'_r + wg'_z &= 0, \end{aligned}$$

in which  $r$  and  $z$  are cylindrical coordinates,  $u$  and  $w$  are radial and vertical velocities, and  $g'$  is the reduced gravity. Explain the basis for the derivation of these equations, including a definition of what is meant by the ‘reduced gravity’.

Write the equations in the form

$$A\phi_r + B\phi_z = \mathbf{c},$$

and hence show that the characteristics  $\frac{dr}{dz} = \lambda$  satisfying  $\det(A - \lambda B) = 0$  are

$$\lambda = \frac{u}{w}, \frac{u}{w}, \infty.$$

What is meant by saying that the third characteristic is  $\infty$ ? What might make it finite?

Define a suitable stream function  $\psi$  for the flow, and show that the characteristics are the streamlines.

Assuming the plume emerges from a chimney of finite radius  $a$  with uniform upwards speed  $w_0$  and uniform buoyancy (reduced gravity)  $g_0 > 0$ , and that entrainment occurs at the plume edge, write down suitable boundary conditions

for the flow, and draw a sketch of the resulting characteristic diagram. (Assume that the plume boundary  $b(z) > a$ .)

By explicitly solving the characteristic equations, show that the edge of the central part of the plume is given by

$$r = \frac{a}{\left(1 + \frac{2g_0 z}{w_0^2}\right)^{1/4}}.$$

What happens if  $g_0 < 0$ ? Explain this physically.

3.9 The equations describing the steady motion of a turbulent plume in  $z > 0$  and  $0 < r < b(z)$  (using cylindrical polar coordinates) are

$$\begin{aligned} (ru)_r + rw_z &= 0, \\ uw_r + ww_z &= g' + \frac{1}{r} \frac{\partial}{\partial r} \left[ \nu_T r \frac{\partial w}{\partial r} \right], \\ N^2 w + ug'_r + wg'_z &= \frac{1}{r} \frac{\partial}{\partial r} \left[ \nu_T r \frac{\partial g'}{\partial r} \right], \end{aligned}$$

where  $u$  and  $w$  are radial and vertical velocities,  $g'$  is the reduced gravity,  $N$  is the Brunt–Väisälä frequency, and the eddy diffusivity is assumed to be

$$\nu_T = \varepsilon_T b w,$$

where  $\varepsilon_T \ll 1$ . Boundary conditions for the flow are

$$w = g' = 0, \quad u = -\alpha \bar{w} \quad \text{at} \quad r = b,$$

where  $\bar{w}$  is the cross-sectional average of  $w$  and  $\alpha$  ( $\approx 0.1$ ) is a positive constant, and

$$w = w_0, \quad g' = g_0 \equiv \frac{g \Delta \rho}{\rho_0} \quad \text{at} \quad z = 0, 0 < r < a,$$

where also  $b(0) = a$ .

Assuming a stratified atmosphere in which  $-\frac{1}{\rho_0} \frac{\partial \rho_0}{\partial z} \sim \frac{1}{H}$  ( $H$  is the scale height) and that  $w_0 \lesssim \sqrt{g_0 l}$ , show how to non-dimensionalise the equations so that all the terms in each equation balance. Hence show that the plume aspect ratio is  $\varepsilon_T$ , and that the natural length scale is  $l \sim \frac{H \Delta \rho}{\rho_0}$ .

By defining a stream function  $\psi$  with  $\psi = 0$  on  $r = 0$  and  $\psi > 0$  for  $r > 0$ , make a Von Mises transformation from variables  $z, r$  to  $z, \psi$ , and hence show that  $w$  and  $g'$  satisfy nonlinear diffusion-type equations.

3.10 An isolated turbulent cylindrical plume in a stratified medium of density  $\rho_0(z)$  is described by the inviscid Boussinesq equations

$$\begin{aligned} uu_r + ww_z &= -\frac{1}{\rho_0} p_r, \\ uw_r + ww_z &= -\frac{1}{\rho_0} p_z - \frac{\rho}{\rho_0} g, \\ u\rho_r + w\rho_z &= 0, \\ \frac{1}{r}(ru)_r + w_z &= 0, \end{aligned}$$

where  $(r, z)$  are cylindrical coordinates,  $(u, w)$  the corresponding velocity components,  $p$  the pressure,  $\rho$  the density,  $\rho_0$  the reference density, and  $g$  is the acceleration due to gravity. If  $\rho = \rho_0 - \Delta\rho$ , explain what is meant by the Boussinesq approximation.

Suppose the edge of the plume is at radius  $r = b$ , such that  $w = 0$  there. Suppose also that the plume entrains ambient fluid, such that

$$(ru)|_b = -b\alpha\bar{w},$$

where  $\bar{w}$  denotes the cross-sectional average value of  $w$ . Deduce that the plume volume flux

$$Q = 2\pi \int_0^b rw \, dr$$

satisfies

$$\frac{dQ}{dz} = 2\pi\alpha b\bar{w}.$$

The momentum flux is defined by

$$M = 2\pi \int_0^b rw^2 \, dr.$$

Show that, assuming that

$$\frac{\partial p}{\partial z} = -\rho_0 g$$

throughout the plume, that

$$\frac{dM}{dz} = 2\pi \int_0^b rg' \, dr,$$

where

$$g' = \frac{g\Delta\rho}{\rho_0}.$$

Why would the hydrostatic approximation be appropriate?

The buoyancy flux is defined by

$$B = 2\pi \int_0^b r w g' dr;$$

assuming  $g' = 0$  at  $r = b$ , show that

$$\frac{dB}{dz} = -N^2 Q,$$

where the Brunt–Väisälä frequency  $N$  is defined by

$$N = \left( -\frac{g\rho'_0(z)}{\rho_0} \right)^{1/2}.$$

3.11 The buoyancy flux  $B$ , momentum flux  $M$ , and mass flux  $Q$  of a turbulent plume in a stratified atmosphere satisfy the equations

$$\frac{dB}{dz} = -N^2 Q,$$

$$\frac{dM}{dz} = 2\pi \int_0^b r g' dr,$$

$$\frac{dQ}{dz} = 2\pi \alpha b w,$$

where  $w$  is the plume velocity,  $b$  is its radius,  $g'$  is the reduced gravity,  $N$  is the Brunt–Väisälä frequency,  $\alpha \approx 0.1$  is an entrainment coefficient, and  $r$  and  $z$  are radial and axial coordinates. Assuming that

$$2\pi \int_0^b r A dr = \pi b^2 A$$

for any plume quantity, assumed to be approximated by a top hat profile, show that

$$\frac{dB}{dz} = -N^2 Q,$$

$$\frac{dM}{dz} = \frac{BQ}{M},$$

$$\frac{dQ}{dz} = 2\pi^{1/2} \alpha M^{1/2}.$$

Now suppose that  $B = B_0$ ,  $M = Q = 0$  at  $z = 0$ . By non-dimensionalising the equations appropriately, show that the level of neutral buoyancy where  $B = 0$  is given by

$$z_s = \frac{\zeta_s}{(2\alpha\pi^{1/2})^{1/2}} \frac{B_0^{1/4}}{N^{3/4}},$$

where  $\zeta_s$  is a numerical constant (it is approximately measured to be 1.5). Write down the equations and boundary conditions necessary to determine  $\zeta_s$ , and by integrating them, show that

$$\zeta_s = \int_0^1 \frac{db}{\left[2 \int_b^1 (1 - \beta^2)^{1/4} d\beta\right]^{1/2}}.$$

If, instead,  $w = w_0$  and  $b = b_0$  at  $z = 0$ , show that the same model to determine  $z_s$  is valid provided  $w_0$  and  $b_0$  are small enough, and specifically if

$$w_0 \ll \frac{g'}{N}, \quad b_0^2 w_0 \ll \frac{g'^3}{N^5}.$$

Show that if the first inequality is satisfied, then the second is as well, provided

$$b_0 \lesssim \frac{g'}{N^2}.$$

If the scale height of the medium is  $h$  (i. e.,  $\rho'_0/\rho \sim 1/h$ ), show that these two inequalities take the form

$$w_0 \ll \frac{\Delta\rho}{\rho_0} \sqrt{gh}, \quad b_0 \lesssim \frac{\Delta\rho}{\rho_0} h.$$

# Chapter 4

## Rotating fluid flows

Fluid mechanics in a rotating environment is primarily of interest in the context of atmospheric and oceanic fluid flows, occurring as they do on the rotating Earth, and this will provide the main focus of this chapter. Oceanography and atmospheric science, together tagged with the epithet of geophysical fluid dynamics (GFD), are huge and related subjects which each can and do have whole books devoted to them. We will describe briefly some of the principal phenomena of GFD with a view to making sense of how the Earth's oceans and atmosphere behave. In his classic book on rotating fluids, Greenspan (1968) begins by recounting three examples of surprising behaviour of relatively commonplace observation (indeed he suggests setting up kitchen scale experiments to observe these), and we can do no better than repeat these here.

### Three experiments

In a rotating closed cylinder full of water with a flat bottom, secure a protuberance to the bottom (for example, half a wine bottle cork with some blutack) and add some fine particles to the liquid to visualise the flow. In equilibrium the motion will be a solid body rotation. If the rotation rate is then altered slightly, a column above the protuberance will become visible. Greenspan's illustration of this is shown in figure 4.1. The phenomenon is referred to as a Taylor column, or Taylor-Proudman column, and is due to the fact that the fluid flow above the protuberance is essentially two-dimensional, i. e., it does not vary with height.

A second experiment (less easy to do) generalises the first by placing an oscillating disc in the interior of the fluid. Strange oblique rays can be seen, if  $\omega < 2\Omega$ , where  $\omega$  is the oscillation frequency of the disc, and  $\Omega$  is the rotation rate of the apparatus. They are shown in figure 4.2. These are characteristics of an internal wave motion (despite the incompressibility of the flow). When  $\omega = 0$ , the characteristics are vertical and delineate the Taylor column; when  $\omega = 2\Omega$  they become horizontal and then disappear.

The third experiment is the easiest: when a cup of tea is stirred, the motion ceases after a minute or so, whereas the viscous diffusive time scale is much longer than this. The reason for this is that the rotation induces a secondary flow (manifested by the

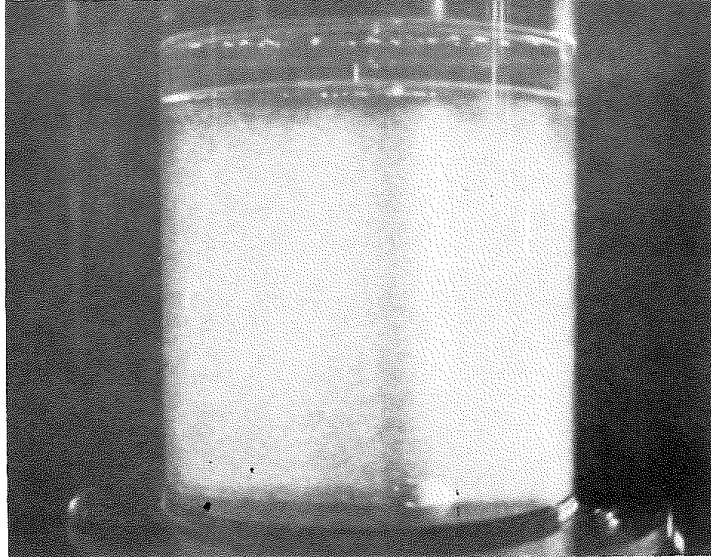


Figure 4.1: A Taylor column. Image from Greenspan (1968, figure 1.2a).

accumulation of tea leaves in the centre of the cup) caused by *Ekman suction* at the

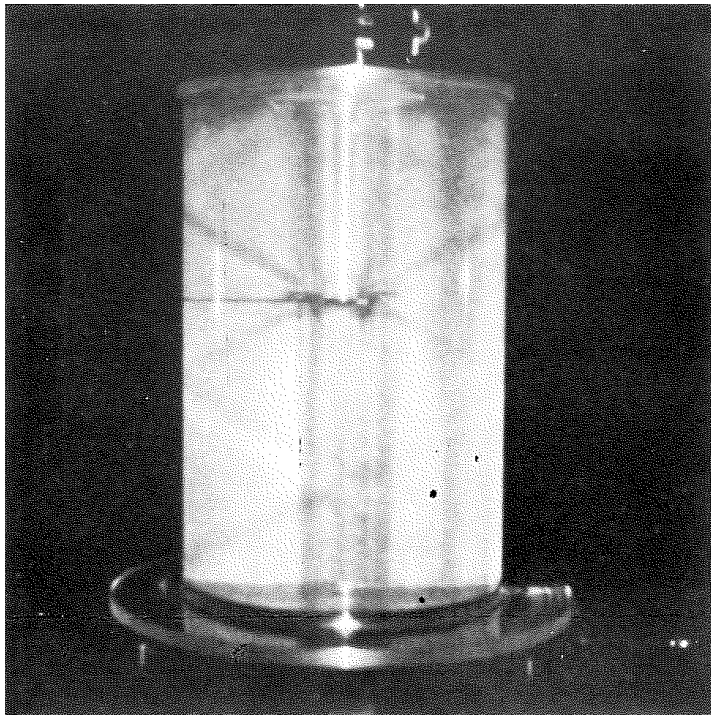


Figure 4.2: Internal waves: the strange oblique rays are (sub-)characteristics of the describing equations. Image from Greenspan (1968, figure 1.3a).

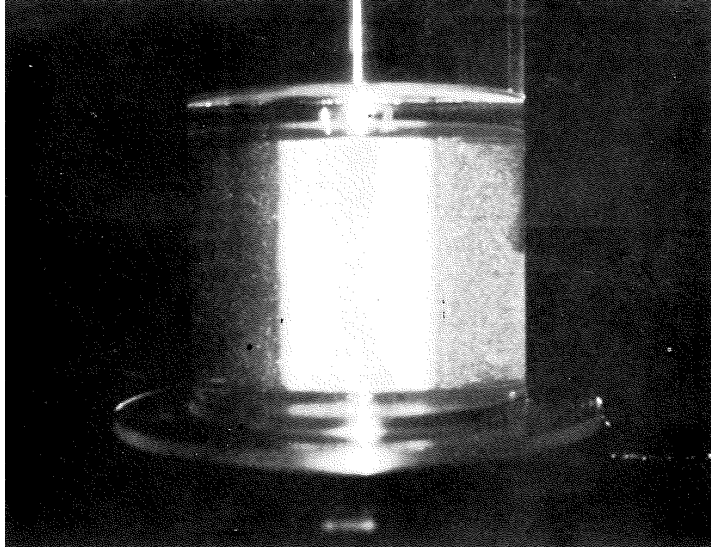


Figure 4.3: Spin-up. The rotating cylinder has been impulsively started from rest. The central white core is still stagnant (in the laboratory frame of reference) while the outer grey fluid is rotating as a solid body with the cylinder. Image from Greenspan (1968, figure 1.4).

walls. The opposing experiment, where a cylinder of stationary fluid is impulsively started to rotate, is shown in figure 4.3. The process whereby the interior fluid approaches solid body rotation is called *spin-up*. If the diameter of the cylinder is  $d$  and the kinematic viscosity of the liquid is  $\nu$ , then the viscous diffusive time scale is  $\frac{d^2}{\nu}$ , while the rotation-induced spin-up time is  $\frac{d}{(\Omega\nu)^{1/2}}$ , and typically much less.

## 4.1 Basic equations

We begin by describing the equations of motion for an incompressible fluid. Later we shall extend the discussion to compressible fluids, as is appropriate in the atmosphere. The effect of the rotating coordinate system is that time derivatives of vectors  $\mathbf{a}$  are transformed as

$$\left. \frac{d\mathbf{a}}{dt} \right|_{\text{fix}} = \left. \frac{d\mathbf{a}}{dt} \right|_{\text{rot}} + \boldsymbol{\Omega} \times \mathbf{a}, \quad (4.1)$$

because in differentiating  $\mathbf{a} = a_i \mathbf{e}_i$ , both the components  $a_i$  and the unit vectors  $\mathbf{e}_i$  change with time, and  $\dot{\mathbf{e}}_i = \boldsymbol{\Omega} \times \mathbf{e}_i$  in a rigid rotating frame. It then follows that

$$\mathbf{u}|_{\text{fix}} = \mathbf{u}|_{\text{rot}} + \boldsymbol{\Omega} \times \mathbf{r}, \quad (4.2)$$

and thus

$$\left. \frac{d\mathbf{u}}{dt} \right|_{\text{fix}} = \left. \frac{d\mathbf{u}}{dt} \right|_{\text{rot}} + 2\boldsymbol{\Omega} \times \mathbf{u}|_{\text{rot}} + \boldsymbol{\Omega} \times (\boldsymbol{\Omega} \times \mathbf{r}). \quad (4.3)$$

One can (and should) show that

$$\boldsymbol{\Omega} \times (\boldsymbol{\Omega} \times \mathbf{r}) = -\frac{1}{2} \nabla |\boldsymbol{\Omega} \times \mathbf{r}|^2, \quad (4.4)$$

and this last term (the centrifugal acceleration) is commonly absorbed into the pressure gradient. At least for atmosphere scale flows, where  $\Omega \sim 0.7 \times 10^{-4} \text{ s}^{-1}$  (check this!), it is much smaller than the gravitational acceleration, and this is also true at laboratory scale, except in such items as centrifuges or washing machines (when spinning).

It then follows that the Navier-Stokes equations in a rotating frame take the form

$$\begin{aligned} \nabla \cdot \mathbf{u} &= 0, \\ \rho \left\{ \frac{d\mathbf{u}}{dt} + 2\boldsymbol{\Omega} \times \mathbf{u} \right\} &= -\nabla p - \rho g \mathbf{k} + \mu \nabla^2 \mathbf{u}, \end{aligned} \quad (4.5)$$

where  $\mathbf{k}$  points upwards. The rotational term on the left hand side of the momentum equation is called the *Coriolis term*.

In a laboratory frame, we will take  $\boldsymbol{\Omega} = \Omega \mathbf{k}$ . It is then convenient to non-dimensionalise the equations by scaling the variables as

$$\mathbf{r} \sim l, \quad \mathbf{u} \sim U, \quad p + \rho g z \sim 2\rho U \Omega l, \quad t \sim \frac{l}{U}, \quad (4.6)$$

so that

$$\begin{aligned} \nabla \cdot \mathbf{u} &= 0, \\ \varepsilon \frac{d\mathbf{u}}{dt} + \mathbf{k} \times \mathbf{u} &= -\nabla p + E \nabla^2 \mathbf{u}, \end{aligned} \quad (4.7)$$

and the two dimensionless parameters are the Rossby number  $\varepsilon$  and the Ekman number  $E$ :

$$\varepsilon = \frac{U}{2\Omega l}, \quad E = \frac{\nu}{2\Omega l^2}, \quad (4.8)$$

where the kinematic viscosity is  $\nu = \frac{\mu}{\rho}$ . The Reynolds number appears to have vanished, but is in fact just  $\frac{\varepsilon}{E}$ .

It is useful to get some idea of the size of these numbers. In a laboratory scale, we might take  $\Omega \sim 0.5 \text{ s}^{-1}$  (a long-playing record),  $U \sim 0.01 \text{ m s}^{-1}$  (note this is the velocity in the rotating frame, i. e., relative to the rigid body motion of rotation),  $l \sim 0.1 \text{ m}$ ,  $\nu = 10^{-6} \text{ m}^2 \text{ s}^{-1}$ , and then  $\varepsilon \sim 0.1$ ,  $E \sim 10^{-4}$ . For slow (or rapidly rotating) flows such that  $\varepsilon \ll 1$ , (4.7)<sub>2</sub> becomes simply the approximate *geostrophic balance*

$$\mathbf{k} \times \mathbf{u} = -\nabla p, \quad (4.9)$$

from which it follows (take the curl) that

$$(\mathbf{k} \cdot \nabla) \mathbf{u} = 0, \quad (4.10)$$

and this explains the existence of Taylor columns. (4.10) is sometimes known as the *Taylor-Proudman theorem*.

Another consequence of (4.9) is that  $\mathbf{u} \cdot \nabla p = 0$ , and thus the streamlines of the motion are also the isobars. This is more familiar in the atmospheric context, where weather forecasts commonly plot isobars. Thus in a strongly rotational flow (small Rossby number), the fluid velocity is *orthogonal* to the pressure gradient.

The second of Greenspan's observations, on internal wave propagation, follows by consideration of the time-dependent version of (4.7) when  $\varepsilon$  and  $E$  are neglected (after first rescaling  $t \sim \varepsilon$ , thus the dimensional time scale is  $\frac{1}{2\Omega}$ ):

$$\begin{aligned}\nabla \cdot \mathbf{u} &= 0, \\ \frac{\partial \mathbf{u}}{\partial t} + \mathbf{k} \times \mathbf{u} &= -\nabla p.\end{aligned}\tag{4.11}$$

Manipulation of this (see question 4.2) shows that  $p$  satisfies the rather odd-looking equation

$$\nabla^2 p_{tt} + p_{zz} = 0,\tag{4.12}$$

with an associated homogeneous boundary condition representing no normal velocity. (4.12) possesses time-periodic solutions which represent internal waves with frequency less than twice the rotation rate.

### 4.1.1 Spin-up

The third observation (stirring a cup of tea) can be studied by the opposing problem of suddenly starting to rotate a cylinder which is initially at rest, together with its contained liquid. The resulting relaxation to a rigid body rotation is called *spin-up*. A suitable model to study this is that of (4.7), where again we neglect the Rossby number, but will retain the Ekman number, as it provides the basis for analysing the viscous boundary layers. We write (in Cartesian coordinates)  $\mathbf{u} = (u, v, w)$ , so that

$$\begin{aligned}u_x + v_y + w_z &= 0, \\ -v &= -p_x + E\nabla^2 u, \\ u &= -p_y + E\nabla^2 v, \\ 0 &= -p_z + E\nabla^2 w.\end{aligned}\tag{4.13}$$

Now (in carefully controlled conditions), what happens is that the initially stagnant core remains stagnant, and the eventual rigid body rotation creeps inwards from the outer walls. In a non-rotating fluid, this would be a purely viscous process, but the rotation makes it faster because of a process called Ekman suction. The time evolution of the flow is so slow that time derivatives can be omitted. In the core of the fluid, we neglect the viscous terms. In the rotating frame, the original stagnant flow is  $\mathbf{u} = -\mathbf{k} \times \mathbf{r}$ , thus

$$u = y, \quad v = -x;\tag{4.14}$$

note that any constant value of  $w$  is allowed in this flow. The outer value of the pressure is just  $p = p_0 - \frac{1}{2}(x^2 + y^2)$  (it should be recalled that the scaled pressure has not only removed gravity, but also the centrifugal pressure).

In order to satisfy the no-slip boundary conditions

$$u = v = 0 \quad \text{at} \quad z = 0, \quad (4.15)$$

we introduce a boundary layer scaling

$$z = \sqrt{2E}Z, \quad w = \sqrt{2E}W, \quad (4.16)$$

so that  $p \approx p(x, y) = p_0 - \frac{1}{2}(x^2 + y^2)$ , and thus

$$\begin{aligned} -v &= x + \frac{1}{2}u_{ZZ}, \\ u &= y + \frac{1}{2}v_{ZZ}; \end{aligned} \quad (4.17)$$

it is easy to solve this (define  $\phi = u + iv$ ) and the solution is

$$\begin{aligned} u &= y [1 - e^{-Z} \cos Z] + x e^{-Z} \sin Z, \\ v &= -x [1 - e^{-Z} \cos Z] + y e^{-Z} \sin Z, \end{aligned} \quad (4.18)$$

and from these we compute the vertical velocity

$$W = e^{-Z}(\cos Z + \sin Z) - 1, \quad (4.19)$$

and thus there is an *Ekman suction* velocity  $w \approx -\sqrt{2E}$  at the base of the core flow. It is this suction into the boundary layer which speeds up the spin-up time. The flux into the boundary promotes an outflow to the walls of the cylinder and (by mass conservation) a consequent shrinking of the core.

Given a core flow of dimensionless area  $A$  and a dimensionless cylinder height  $h$ , we will have

$$-2A\sqrt{2E} = h\dot{A} \quad (4.20)$$

(the factor of two because of Ekman layers at top and bottom), and thus the spin-up dimensionless time scale is  $\sim \frac{h}{2\sqrt{2E}}$ , and dimensionally

$$t_{\text{spin-up}} \sim \frac{H}{2\sqrt{\Omega\nu}}, \quad (4.21)$$

where  $H$  is the cylinder height. Try it and see!

## 4.2 Stratified flow

Doing laboratory experiments and watching your tea slow down may be diverting, but they do not explain why rotating fluid flows are of interest. For this we turn to the Earth (or indeed other planets), where two of the most interesting fluid flows are of primary concern, and being on the rotating Earth, they are of course rotating fluids. These two fluids are the atmosphere and the oceans.

### 4.2.1 Earth's atmosphere

The atmosphere is a layer of thin fluid draped around the Earth. The Earth has a radius of some 6,370 kilometres, but the bulk of the atmosphere lies in a (relatively) thin layer only ten kilometres deep. This layer is called the *troposphere*. The atmosphere extends above this, into the stratosphere and then the mesosphere, but the fluid density is very small in these upper layers (though not inconsequential), and we will simplify the discussion by conceiving of atmospheric fluid motion as being (largely) confined to the troposphere.

Atmospheric motion is described by the model described earlier. The main (and important) complication is that the atmosphere, being a gas, is compressible. It turns out this is enormously important. The oceans, being water, are more nearly incompressible, but the variation of density with temperature and salinity leads to a model of convection, as described in chapter 3, except that it is a rotating fluid. Oceanic circulation is complicated by a number of factors: there is convective motion (double-diffusive, in fact), there is wind-driven stress at the surface, and there are continents which get in the way. Particularly, the wave motion of the tides is strongly constrained by the continental margins. In the following, we will focus on the Earth's atmosphere as a specific example.

In considering the motion of the atmosphere, we need a comment on radiation balance. Atmospheric motion is driven by heating from the sun. This heating is effected by solar radiation. Radiation consists of electromagnetic waves of varying wavelengths. Matter is heated by radiation by absorbing it and then re-emitting it, and the way this works is due to the fact that the amount of energy emitted by matter depends on its absolute temperature  $T$ . The Stefan-Boltzmann law says that for a black body (a perfect emitter) the emitted energy from a surface is  $\sigma T^4$  per unit area ( $\sigma$  is a constant). The average surface temperature of the Earth is 288 K (degrees Kelvin), for example, because this is the surface temperature necessary for the emitted radiation from the top of the atmosphere to space to exactly balance the incoming solar radiation.

Now, it is more complicated than this. Firstly, the wavelength of the emitted radiation from a body depends on its temperature. The wavelength is longer at lower temperatures. Thus the Earth emits longwave radiation at 288 K, whereas the sun emits shortwave radiation at its surface temperature of 5,800 K. Secondly, not all radiation is absorbed on striking a body. Some of it may be reflected, or scattered. And, the degree of absorption or reflection depends on the wavelength. This is, for example, why we can see the sun, because the Earth's atmosphere is largely transparent to optical wavelengths.

So the sun heats the Earth by warming its surface, but it does so non-uniformly, because of the curvature of the Earth's surface: much more shortwave radiation is received at the equator. However the outgoing long wave radiation is much more uniform, although of course it is greater at the equator. Consequently, there is an energy imbalance between the equator and the poles. The equator is differentially heated, and the poles are differentially cooled. The Earth's atmospheric circulation

is a consequence of this equator-to-pole differential heating, which drives a poleward convective circulation. The effect of rapid rotation is to whip this slow poleward circulation into a rapid azimuthal circulation. At mid-latitudes this circulation is *westerly*, i. e., from the west; at the equator and poles, it is in the opposite direction.

This eastwards wind is called the *zonal wind*. And it is unstable: a phenomenon called *baroclinic instability* causes the uniform zonal wind to form north to south waves, and these meandering waves form the weather systems which can be seen on television weather forecast charts. At a smaller scale, such instabilities lead to weather fronts, essentially like shocks, and in the tropics these lead to cyclones and hurricanes. In order to begin to understand how this all works, we need a mathematical model, and this is essentially a model of shallow water theory (or shallow air theory) on a rapidly rotating sphere.

### 4.2.2 Governing equations

The basic equations describing atmospheric motion are those of mass, momentum and energy in a rotating frame, and can be written in the form

$$\begin{aligned} \frac{d\rho}{dt} + \rho \nabla \cdot \mathbf{u} &= 0, \\ \rho \left\{ \frac{d\mathbf{u}}{dt} + 2\boldsymbol{\Omega} \times \mathbf{u} \right\} &= -\nabla p - \rho \nabla \Phi + \mathbf{F}, \\ \rho c_p \frac{dT}{dt} - \frac{dp}{dt} &= Q. \end{aligned} \tag{4.22}$$

In these equations,  $p$  is the pressure,  $T$  is the absolute temperature,  $\boldsymbol{\Omega}$  is the angular velocity of the Earth, and the equations have been written with respect to a set of coordinates fixed in the (rotating) Earth. The quantity  $\mathbf{F}$  represents frictional terms, and is discussed further below.  $\Phi$  is called the geopotential; it is the gravitational potential corrected for the effect of centrifugal force, and is defined by

$$\Phi = \Phi_g - \frac{1}{2} |\boldsymbol{\Omega} \times \mathbf{r}|^2, \tag{4.23}$$

where  $\Phi_g$  is the gravitational potential. The surface  $\Phi = 0$  is called sea level; the surface of the oceans would be this geopotential surface in the absence of motion. We take  $z$  to be the coordinate normal to  $\Phi = 0$ ; essentially it is in the radial direction, and to a good approximation we can take  $\Phi = gz$ , where  $g$  is called the gravitational acceleration (although in fact it includes a small component due to centrifugal force).

The last equation in (4.22) is the energy equation:  $c_p$  is the specific heat. The second term on the left hand side is the adiabatic term, and specifically assumes a thermal expansion coefficient equal to  $1/T$ , which is a consequence of assuming, as we do, the perfect gas law as a constitutive equation for the compressible air:

$$p = \frac{\rho RT}{M_a}, \tag{4.24}$$

where  $R$  is the gas constant and  $M_a$  is the molecular weight of dry air. The term  $Q$  on the right represents a combination of effects: turbulent transport of heat, both sensible (as manifested by temperature) and latent (as manifested by moisture), radiative transport of heat, and absorption of radiation. Most of these terms are relatively small, and the dominant terms are those on the left, which means that the atmosphere is approximately *adiabatic*. Actually, the transport of moisture has a significant quantitative effect on this (the ‘wet’ adiabatic vertical temperature gradient is around  $-6 \text{ K km}^{-1}$ , whereas the ‘dry’ adiabat is about  $10 \text{ K km}^{-1}$ , but we want to avoid getting bogged down in the detail of this).

### 4.2.3 Eddy viscosity

The force  $\mathbf{F}$  represents the effects of friction. Molecular viscosity is insignificant in the atmosphere and oceans, but the flows are turbulent, and the result of this is that momentum transport by small scale eddying motion is often modelled by a diffusive frictional term of the form  $\rho\varepsilon_T\nabla^2\mathbf{u}$ , where  $\varepsilon_T$  is an ‘eddy’ (kinematic) viscosity. More generally, it varies with distance from rough boundaries.<sup>1</sup> A complication in the atmosphere and ocean is that the vertical motion is much smaller than the horizontal, and this leads to the idea that different eddy viscosities are appropriate for horizontal and vertical momentum transport. We denote these coefficients as  $\varepsilon_H$  and  $\varepsilon_V$ , and take them as constants. To be precise, we then represent the frictional terms in the form

$$\mathbf{F} = \rho\varepsilon_H\nabla_H^2\mathbf{u} + \rho\varepsilon_V\frac{\partial^2\mathbf{u}}{\partial z^2}, \quad (4.25)$$

where  $\nabla_H^2 = \frac{\partial^2}{\partial x^2} + \frac{\partial^2}{\partial y^2}$ , and  $x, y$  are ‘horizontal’ coordinates,  $z$  is the vertical coordinate. The choice of suitable coordinates is discussed below. Since the friction terms will only be important in boundary layers where the sphericity is unimportant, we need not concern ourselves with such niceties in defining  $\mathbf{F}$ . Frictional effects are generally relatively small. In the atmosphere, they are confined to a ‘boundary layer’ adjoining the surface, having a typical depth of 1000 metres, and bulk motion above this layer is effectively inviscid, and so we will largely ignore the effects of friction.

### 4.2.4 Potential temperature

The energy equation is commonly written in terms of the *potential temperature*, defined as

$$\theta = T \left( \frac{p_0}{p} \right)^{R/M_a c_p}, \quad (4.26)$$

where  $p_0$  is a reference value, which we take to be the (constant) surface pressure. The use of this variable is that

$$\rho c_p T \frac{d\theta}{\theta} = \rho c_p dT - dp, \quad (4.27)$$

---

<sup>1</sup>And then, we write  $\mathbf{F} = \nabla \cdot \boldsymbol{\tau}_T$ ,  $\boldsymbol{\tau}_T = \frac{1}{2}\varepsilon_T(\nabla\mathbf{u} + \nabla\mathbf{u}^T)$ .

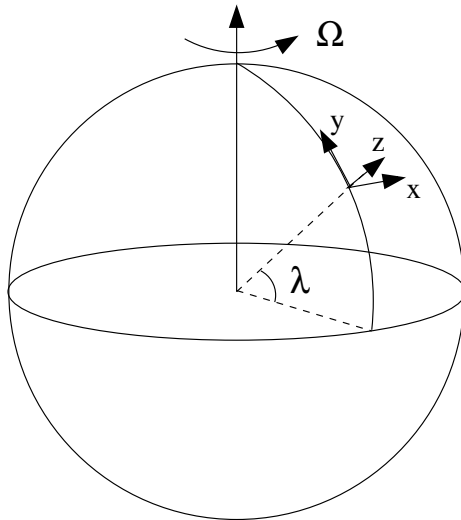


Figure 4.4: A local quasi-Cartesian coordinate system in the mid-latitudes.

so that  $\theta$  is constant for the dry adiabatic basic state of question 4.3.<sup>2</sup> in which we neglect  $Q$ . The energy equation then takes the form

$$\frac{p d\theta}{\theta dt} = \frac{RQ}{M_a c_p}. \quad (4.28)$$

### 4.2.5 Coordinates

A real complication on the Earth is the spherical geometry. On the other hand the atmosphere is shallow, so that it is quasi-Cartesian. The effect will be that most of the curvilinear terms disappear, but the cost of this is that it is necessary to place the origin somewhere specific: the problem with spherical coordinates is that they have poles.

It is common in presenting the equations of motion to use a coordinate system which is based in mid-latitudes, and we will follow that here also, for the most part. But to begin with, we write the equations in terms of spherical polar coordinates. We take  $r$  to be the radius measured from the Earth's centre,  $\lambda$  to be the angle of latitude, and  $\phi$  to be the angle of longitude. In terms of the more usual definition of spherical polar coordinates  $(r, \theta, \phi)$ ,  $r$  and  $\phi$  are the same, and  $\lambda = \frac{\pi}{2} - \theta$ . We denote velocity components in  $\phi, \lambda, r$  directions as  $u, v, w$  (because we are setting up  $\phi, \lambda, r$ , i. e., east, north, upwards, as future  $x, y, z$  cartesian variables, see figure 4.4), and we

<sup>2</sup>Thus  $s = c_p \ln \theta$ , where  $s$  is entropy.

denote the vector velocity  $\mathbf{u} = (u, v, w)$ .<sup>3</sup> The definitions of the vector derivatives are

$$\begin{aligned}\nabla \cdot \mathbf{u} &= \frac{1}{r \cos \lambda} \frac{\partial u}{\partial \phi} + \frac{1}{r \cos \lambda} \frac{\partial (v \cos \lambda)}{\partial \lambda} + \frac{1}{r^2} \frac{\partial}{\partial r} (r^2 w), \\ \nabla &= \left( \frac{1}{r \cos \lambda} \frac{\partial}{\partial \phi}, \frac{1}{r} \frac{\partial}{\partial \lambda}, \frac{\partial}{\partial r} \right),\end{aligned}\tag{4.29}$$

and the momentum equations have the form (omitting the friction terms)

$$\begin{aligned}\frac{du}{dt} + \frac{uw}{r} - \frac{uv}{r} \tan \lambda - 2\Omega v \sin \lambda + 2\Omega w \cos \lambda &= -\frac{1}{\rho r \cos \lambda} \frac{\partial p}{\partial \phi}, \\ \frac{dv}{dt} + \frac{vw}{r} + \frac{u^2}{r} \tan \lambda + 2\Omega u \sin \lambda &= -\frac{1}{\rho r} \frac{\partial p}{\partial \lambda}, \\ \frac{dw}{dt} - \frac{(u^2 + v^2)}{r} - 2\Omega u \cos \lambda &= -\frac{1}{\rho} \frac{\partial p}{\partial r} - g.\end{aligned}\tag{4.30}$$

These are awkward equations, but they can be simplified by scaling and approximation. We can immediately see that there is an issue at the poles, where  $\cos \lambda = 0$ , and we will simply ignore the polar regions. The way to deal with them would be to use the polar angle  $\theta = \frac{\pi}{2} - \lambda$  (at the north pole), and then  $(\theta, \phi, r)$  would be a local set of cylindrical polar coordinates. One of the features of the Earth's weather systems is that they have a horizontal length scale which, though large, is not global in extent. The description of such systems is facilitated by using a local, near cartesian coordinate system. To do this, we choose a particular latitude on which to put the cartesian origin, and this then limits the applicability of the resulting approximate model to phenomena appropriate to this latitude. Luckily, as we have seen, there is a natural division of the global circulation into three bands (one in each hemisphere): tropical, mid-latitude and polar. We associate these three latitudes with values of  $\lambda$  near zero, of  $O(1)$ , and near  $\pm \frac{\pi}{2}$ . We take  $\lambda = \lambda_0$  to define the  $x$ - $z$  plane.

Specifically, we define east, north and vertical coordinates  $x$ ,  $y$  and  $z$  by the relations

$$x = \phi r \cos \lambda_0, \quad y = (\lambda - \lambda_0)r, \quad z = r - r_0,\tag{4.31}$$

where  $r_0$  is the radius at sea level. We then have

$$\frac{1}{r \cos \lambda} \frac{\partial}{\partial \phi} = \mu \frac{\partial}{\partial x}, \quad \frac{1}{r} \frac{\partial}{\partial \lambda} = \frac{\partial}{\partial y}, \quad \frac{\partial}{\partial r} = \frac{\partial}{\partial z} + \frac{1}{r} \left( x \frac{\partial}{\partial x} + y \frac{\partial}{\partial y} \right),\tag{4.32}$$

---

<sup>3</sup>It should be pointed out that the Earth deviates noticeably from being a sphere; it is more nearly an oblate spheroid, whose radius varies by some 20 km between pole and equator. This is of some conceptual importance, since gravity is the most important force, and the use of a purely spherical coordinate system would yield large 'horizontal' forces in the momentum equations. The correct procedure is to define the level 'horizontal' surfaces to be geopotential surfaces, so that there are no horizontal gravitational forces. But the geometric deviation from sphericity is so small that in effect we regain the form of the equations in spherical polars, as presented here.

where

$$\mu = \frac{\cos \lambda_0}{\cos \lambda}, \quad (4.33)$$

so that

$$\begin{aligned} \nabla &= \left( \mu \frac{\partial}{\partial x}, \frac{\partial}{\partial y}, \frac{\partial}{\partial z} \right) + \frac{\mathbf{k}}{r} \left( x \frac{\partial}{\partial x} + y \frac{\partial}{\partial y} \right), \\ \nabla \cdot \mathbf{u} &= \mu \frac{\partial u}{\partial x} + \mu \frac{\partial(v/\mu)}{\partial y} + \frac{\partial w}{\partial z} + \frac{1}{r} \left\{ x \frac{\partial w}{\partial x} + y \frac{\partial w}{\partial y} + 2w \right\}. \end{aligned} \quad (4.34)$$

The momentum equations are then

$$\begin{aligned} \frac{du}{dt} - 2\Omega v \sin \lambda + 2\Omega w \cos \lambda + \frac{1}{r} [uw - uv \tan \lambda] &= -\frac{\mu}{\rho} \frac{\partial p}{\partial x}, \\ \frac{dv}{dt} + 2\Omega u \sin \lambda + \frac{1}{r} [vw + u^2 \tan \lambda] &= -\frac{1}{\rho} \frac{\partial p}{\partial y}, \\ \frac{dw}{dt} - 2\Omega u \cos \lambda - \frac{(u^2 + v^2)}{r} &= -\frac{1}{\rho} \left[ \frac{\partial p}{\partial z} + \frac{1}{r} \left( x \frac{\partial p}{\partial x} + y \frac{\partial p}{\partial y} \right) \right] - g. \end{aligned} \quad (4.35)$$

These still look horrendous, but a major simplification results from the fact that the Earth's radius is much larger than atmospheric depth. If the horizontal length scale (more specifically the poleward range) is much less than Earth's radius, it is possible to ignore the small terms in  $\frac{1}{r}$ , and take  $\lambda = \lambda_0$  except in the Coriolis term (this is a Boussinesq-like approximation; we might call it the Coriolis approximation). The result of all this is that (4.34) can be simplified to

$$\nabla = \left( \frac{\partial}{\partial x}, \frac{\partial}{\partial y}, \frac{\partial}{\partial z} \right), \quad \nabla \cdot \mathbf{u} = \frac{\partial u}{\partial x} + \frac{\partial v}{\partial y} + \frac{\partial w}{\partial z}, \quad (4.36)$$

and the equations of motion take the simpler form

$$\begin{aligned} \frac{d\rho}{dt} + \rho \nabla \cdot \mathbf{u} &= 0, \\ \frac{du}{dt} - 2\Omega v \sin \lambda + 2\Omega w \cos \lambda &= -\frac{1}{\rho} \frac{\partial p}{\partial x}, \\ \frac{dv}{dt} + 2\Omega u \sin \lambda &= -\frac{1}{\rho} \frac{\partial p}{\partial y}, \\ \frac{dw}{dt} - 2\Omega u \cos \lambda &= -\frac{1}{\rho} \frac{\partial p}{\partial z} - g, \\ \frac{p}{\theta} \frac{d\theta}{dt} = \frac{RQ}{M_a c_p}, \quad \rho &= \frac{M_a p}{R\theta} \left( \frac{p_0}{p} \right)^\alpha, \quad \alpha = \frac{R}{M_a c_p}. \end{aligned} \quad (4.37)$$

The removal of all these extra terms can be justified by non-dimensionalisation of the model, but is omitted for clarity. See, for example, Pedlosky (1987) or Fowler (2011).



Figure 4.5: Periodic gravity waves in Lapland, Northern Finland, October 2004.

### 4.3 Gravity waves

Atmospheric motions are dominated by various kinds of waves. Large scale waves are associated with weather systems and can be seen on the charts used in weather forecasts. but much smaller scale waves occur, and are made visible by the periodic formation of clouds. An example is shown in figure 4.5. In this section we study these small scale waves.

The basic state of the atmosphere is that of a stable stratified fluid in which

$$\rho = \bar{\rho}(z), \quad p = \bar{p}(z). \quad (4.38)$$

The heating term is small so that to a good approximation, the potential temperature is constant, and  $\rho$  is a function of pressure only, in which, from (4.37).

$$\frac{1}{\rho} \frac{\partial \rho}{\partial p} = \frac{1 - \alpha}{p}. \quad (4.39)$$

Two particular sorts of waves which are familiar in fluid mechanics are *sound waves* and *gravity waves*. Sound waves are associated with compressibility; they travel at a speed (the speed of sound) which depends on density but is independent of wave number: they are *monochromatic*. At sea level this speed is about  $330 \text{ m s}^{-1}$ : much faster than typical wind speeds; as a consequence, we might expect sound waves to be high frequency phenomena which are not relevant to common atmospheric motions. If we denote the sound wave speed as  $c_s$ , then the dispersion relation relating frequency

$\omega$  to wave speed and wave number  $k$  is just

$$\omega = kc_s, \quad c_s = \left( \frac{d\bar{p}}{d\bar{\rho}} \right)^{1/2} = \left\{ \frac{\bar{p}}{(1-\alpha)\bar{\rho}} \right\}^{1/2}; \quad (4.40)$$

$c_s$  is the adiabatic sound speed.

Gravity waves are familiar as the waves which propagate on the surface of the sea. The ingredients of the theory which describes them are mass conservation (where horizontal divergence is accommodated by vertical contraction and expansion), acceleration, gravity, pressure gradient, and a vertical stratification which, in the simplest form of the theory, is manifested by the interface between dense underlying fluid (e. g., water) and a lighter overlying fluid (e. g., air). Gravity waves can be seen propagating at the interface between two incompressible liquids such as oil and water, and gravity waves will similarly propagate in a continuously stratified fluid contained in a vertically confined channel; in this case the waves are less easily visualised, and they are often called internal waves, or internal gravity waves.

In the sense that the atmosphere consists of a dense troposphere beneath a light stratosphere, we can expect gravity waves to propagate as undulations in the tropopause altitude. More generally, gravity waves will propagate as internal waves in the stratified atmosphere. Gravity waves can be seen commonly in the atmosphere, because the vertical undulations of the air causes periodic cloud formation as air rises (and thus cools). Figure 4.5 shows a particular striking example from Lapland of low lying periodic gravity waves.

For the simple case of an incompressible fluid of depth  $h$ , the dispersion relation between frequency and wavenumber is  $\omega^2 = gk \tanh kh$ . In the case of a shallow fluid (such as the atmosphere), the long wave limit  $kh \ll 1$  may be appropriate, and then the wave speed is constant, and

$$\omega \approx k\sqrt{gh}. \quad (4.41)$$

This applies to waves of wavelength larger than 10 km (the waves in figure 4.5 are of smaller wavelength). Comparing (4.41) with (4.40), we see that long gravity waves in the atmosphere are essentially the same as sound waves, since in an approximately hydrostatic atmosphere,  $\bar{p} \sim \bar{\rho}gh$ . In an incompressible fluid, density is manifested as fluid column depth, and the pressure is proportional to this, so that the dimensionless ‘sound’ speed is equal to one. For internal waves, the height of the column need not change, but the common factor is that the height of geopotential surfaces propagates in both types of wave.

We can recover gravity waves from the atmospheric model of (4.37) by assuming a reference state of a stratified hydrostatic, adiabatic atmosphere in which there is no motion. In addition, the shallowness of the atmosphere implies  $w \ll u, v$  and we will ignore it. For small disturbances in which  $u$  and  $v$  are small as is  $P = p - \bar{p}$ , we

can write, using (4.40),

$$\begin{aligned}\frac{1}{c_s^2}P_t + \bar{\rho}(u_x + v_y) &= 0, \\ u_t - 2\Omega v \sin \lambda &= -\frac{1}{\bar{\rho}}P_x, \\ v_t + 2\Omega u \sin \lambda &= -\frac{1}{\bar{\rho}}P_y.\end{aligned}\tag{4.42}$$

Because we focus on short wavelengths, we take  $\lambda$  to be constant. These are linear equations, and the fact that  $\bar{\rho}$  and  $c_s$  depend on  $z$  is immaterial. We can write these equations in terms of the horizontal divergence  $\Delta = u_x + v_y$ , the vorticity  $\zeta = v_x - u_y$ , and a dimensionless pressure perturbation given by  $P = \bar{\rho}c_s^2\Pi$ . We obtain

$$\begin{aligned}\Pi_t + \Delta &= 0, \\ \Delta_t - f\zeta + c_s^2\nabla^2\Pi &= 0, \\ \zeta_t + f\Delta &= 0,\end{aligned}\tag{4.43}$$

where the Coriolis parameter is

$$f = 2\Omega \sin \lambda.\tag{4.44}$$

The solutions are of the form

$$\begin{pmatrix} \Pi \\ \Delta \\ \zeta \end{pmatrix} = \mathbf{w} \exp\{i(kx + ly + \omega t)\},\tag{4.45}$$

provided

$$\begin{pmatrix} i\omega & 1 & 0 \\ -c_s^2K^2 & i\omega & -f \\ 0 & f & i\omega \end{pmatrix} \mathbf{w} = \mathbf{0}, \quad K^2 = k^2 + l^2;\tag{4.46}$$

$K$  is the (two-dimensional) wavenumber. Solutions to this exist provided either  $\omega = 0$ , or

$$\omega^2 = f^2 + K^2c_s^2,\tag{4.47}$$

and this latter equation is the dispersion relation for gravity waves in a stratified atmosphere. These waves are called *Poincaré waves*.

### 4.3.1 Kelvin waves

Another kind of wave can be found by seeking solutions in which  $v = 0$ . Such waves are particularly relevant to propagation in a confined zonal channel (for example in the ocean), where the condition  $v = 0$  at the north and south boundaries allows  $v = 0$

everywhere. This requires  $\partial\Delta/\partial y = -\partial\zeta/\partial x$ , and substitution into (4.46) then shows that we must have  $l = -\frac{if}{c_s}$ , and thus solutions are exponential in  $y$ , and

$$\omega = kc_s; \quad (4.48)$$

these waves are called *Kelvin waves*. They are *edge waves*, because they decay exponentially away from one or other boundary. Together with the geostrophic mode  $\omega = 0$ , Poincaré and Kelvin waves form the complete spectrum of waves for the flow. The mode  $\omega = 0$  is associated with low frequency waves which emerge in the higher order quasi-geostrophic approximation (which is derived in section 4.5); these slow waves are called *Rossby waves*, or *planetary waves*, and will be discussed in section 4.6.

The constant term in (4.47) arises from rotation and the Coriolis force. In the high frequency limit, we see that  $\omega \approx Kc_s$ , and this is consistent with the long wave limit of gravity wave theory, and the acoustic wave speed given in (4.40). Gravity waves are essentially long wavelength sound waves, and Poincaré waves are their modification by the effects of rotation. The critical length scale  $\frac{c_s}{f}$  above which rotation becomes important is known as the Rossby radius of deformation. Because  $\bar{p} \sim \bar{\rho}gh$ , it can equivalently be defined as  $\frac{\sqrt{gh}}{f}$ . For atmospheric motion, it is of order 3000 km, so that rotation is unimportant for smaller scale gravity waves.

## 4.4 Non-dimensionalisation

There are three obvious length scales of immediate relevance. These are the depth  $h$  of the troposphere, the radius  $r_0$  of the Earth, and the length scale  $l$  of horizontal atmospheric motions. We have  $h = 10$  km,  $r_0 = 6370$  km, and the largest (*synoptic*) scales of mid-latitude weather systems are observed to be  $l = 1000$  km. These lengths combine to form two dimensionless parameters,

$$\delta = \frac{h}{l}, \quad \Sigma = \frac{l}{r_0}. \quad (4.49)$$

both of which are small:  $\delta \approx 0.01$ ,  $\Sigma \approx 0.16$ . The ideas of lubrication theory, using the fact that  $\delta \ll 1$ , suggest that in the vertical momentum equation,  $\frac{\partial p}{\partial z} \approx -\rho g$ , i. e., the pressure is approximately hydrostatic, as in our basic state. Lubrication theory also suggests that if  $U$  is a suitable horizontal velocity scale, then the appropriate vertical velocity scale is  $hU/l$ , in order that the material derivative retains vertical acceleration.

Sphericity in the equations is manifested by the trigonometric terms in  $\lambda$ . We scale the variables as follows:

$$\begin{aligned} x, y \sim l, \quad z \sim h, \quad u, v \sim U, \quad w \sim \delta U, \\ t \sim \frac{l}{U}, \quad \rho \sim \rho_0, \quad p \sim p_0, \quad \theta, T \sim T_0, \end{aligned} \quad (4.50)$$

where we choose

$$p_0 = \frac{\rho_0 R T_0}{M_a} = \rho_0 g h \quad (4.51)$$

(which actually defines  $h$  as the (dry) atmospheric scale height, cf. question 4.3). The length scales  $l$  and  $r_0$  are those we have described, the horizontal wind speed  $U$  is typically about  $20 \text{ m s}^{-1}$ , and the density and temperature scales  $\rho_0$  and  $T_0$  are their values at sea level. (These are determined by the mass of the atmosphere and the effective radiative temperature.) For the moment we assume they are constant. This is a reasonable approximation for  $\rho_0$  but less so for temperature.

The scaled mass conservation equation is just

$$\frac{d\rho}{dt} + \rho \nabla \cdot \mathbf{u} = 0. \quad (4.52)$$

The momentum equations take the dimensionless form

$$\begin{aligned} Ro \frac{du}{dt} - v \sin \lambda + \delta w \cos \lambda &= -\frac{Ro}{F^2} \frac{1}{\rho} \frac{\partial p}{\partial x}, \\ Ro \frac{dv}{dt} + u \sin \lambda &= -\frac{Ro}{F^2} \frac{1}{\rho} \frac{\partial p}{\partial y}, \\ \delta \left[ \delta Ro \frac{dw}{dt} - u \cos \lambda \right] &= -\frac{Ro}{F^2} \left( \frac{1}{\rho} \frac{\partial p}{\partial z} + 1 \right), \end{aligned} \quad (4.53)$$

in which

$$\lambda = \lambda_0 + \Sigma y, \quad (4.54)$$

and the extra parameters are the Rossby number and the Froude number,

$$Ro = \frac{U}{2\Omega l}, \quad F = \frac{U}{\sqrt{gh}}. \quad (4.55)$$

For  $U = 20 \text{ m s}^{-1}$ ,  $\Omega = 0.7 \times 10^{-4} \text{ s}^{-1}$ ,  $l = 10^3 \text{ km}$ ,  $g = 10 \text{ m s}^{-2}$ ,  $h = 10 \text{ km}$ , we have  $Ro \approx 0.14$ ,  $F \approx 0.06$ , and thus  $F^2/Ro \approx 0.03$ . Evidently the pressure is essentially hydrostatic, as we expect for a shallow flow.

If we scale  $\theta$  as well as  $T$  with  $T_0$ , then the dimensionless definition of  $\theta$  is

$$\theta = \frac{T}{p^\alpha}, \quad (4.56)$$

in which

$$\alpha = \frac{R}{M_a c_p}. \quad (4.57)$$

The equation of state is simply

$$\rho = \frac{p}{T} = \frac{p^{1-\alpha}}{\theta}, \quad (4.58)$$

and the dimensionless energy equation takes the form

$$\frac{p}{\theta} \frac{d\theta}{dt} = Q^*, \quad Q^* = \frac{Ql}{\rho_0 c_p T_0 U}. \quad (4.59)$$

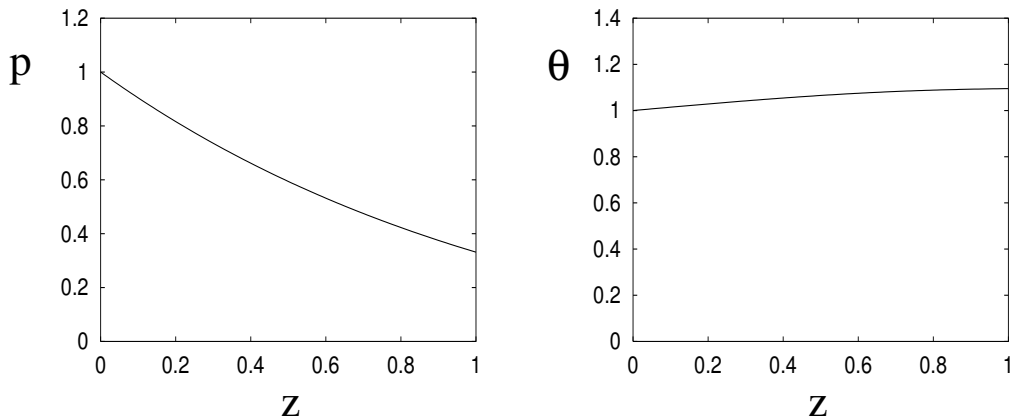


Figure 4.6: Solution of (4.61). The pressure is excellently approximated by  $p \approx e^{-1.08z}$ , and the potential temperature is excellently approximated by  $\theta \approx 1 + 0.15z - 0.05z^2$ .

#### 4.4.1 Parameter estimates

We have already estimated typical values  $\delta \approx 0.01$ ,  $Ro \approx 0.14$ ,  $F \approx 0.06$ ,  $\Sigma \approx 0.16$ ; also  $\alpha \approx 0.29$ . We need further to estimate a value of  $Q^*$ . This is quite complicated, and we will avoid details (for which, see Fowler (2011)). It is possible to estimate  $Q^*$  by consideration of the terms which contribute to it, of which the most significant is the latent heat transport due to atmospheric moisture content, and after that the radiative transport of heat. We consider these two terms in turn.

First, if we ignore both terms, then  $Q^* = 0$ , and  $\theta = 1$ : this is the *dry adiabat* of question 4.3. If instead we assume a wet, saturated atmosphere (but ignore radiative heat transport), then one can show that (4.59) is modified to

$$\frac{d\theta}{dt} = -m(\theta, p) \frac{dp}{dt}, \quad (4.60)$$

where  $m$  is a small term which describes transport of latent heat in a saturated atmosphere. Crucially it is positive, so that  $\theta$  increases with height, which means the atmosphere is stably stratified. This defines a *wet adiabat*  $\theta_w$  as a function of  $p$ , but since  $p \approx p(z)$  is hydrostatic ( $p_z \approx -\rho$  in (4.53)), we can equally well take it to be  $\theta_w(z)$ . Figure 4.6 shows a numerical solution of the (dimensionless) coupled system describing the hydrostatic pressure and corresponding wet adiabatic potential temperature  $\theta_w$ , which is

$$\frac{d\theta_w}{dz} = m(\theta_w, p)\rho, \quad \frac{dp}{dz} = -\rho, \quad \rho = \frac{p^{1-\alpha}}{\theta_w}, \quad (4.61)$$

with both being equal to one at  $z = 0$ . Note that  $\theta_z \sim 0.1$ , of similar size to the Rossby number.

It turns out that the deviation from the wet adiabat is important. A simple estimate follows from consideration of radiative transport in a grey, opaque atmosphere,

when it can be approximately represented by an effective thermal conductivity. When scaled, this leads to a modified form of the energy equation in the form

$$\frac{d\theta}{dt} = -m(\theta, p) \frac{dp}{dt} + \frac{\alpha H}{Pe}, \quad H = c^* \frac{\partial}{\partial z} \left( k^* \frac{\partial T}{\partial z} \right), \quad (4.62)$$

where  $c^*$  and  $k^*$  are  $O(1)$  functions of  $\theta$  and  $p$ , so that the heating term  $H \sim O(1)$ . The quantity

$$Pe = \frac{Uh^2}{\kappa l} \quad (4.63)$$

is a reduced Péclet number,  $\kappa$  being the effective thermal diffusivity for radiative heat transport. Estimates for this suggest it is large,  $Pe \sim 20$ .

At this point, we realise that we took  $l \sim 1,000$  km and  $U \sim 20$  m s<sup>-1</sup> based on typical observed values. But the system is self-contained, and these scales ought to be deducible from the model. And indeed they are: we now *define*  $U$  and  $l$  through the suggested distinguished balance of terms:

$$\frac{F^2 \sin \lambda_0}{Ro} = \frac{\alpha}{Pe} = \varepsilon^2, \quad (4.64)$$

where it is conventional to define the (modified) Rossby number as

$$\varepsilon = \frac{Ro}{\sin \lambda_0} = \frac{U}{fl}, \quad (4.65)$$

in which the Coriolis parameter  $f$  is defined as

$$f = 2\Omega \sin \lambda_0. \quad (4.66)$$

Note that at this point we now lose touch with the tropics, as we assume  $\sin \lambda_0 \sim O(1)$ , and not zero. It is not difficult to accommodate  $\lambda_0 = 0$  though (see question 4.4). This leads to the definitions

$$U = \left( \frac{\alpha \kappa g}{fh} \right)^{1/2}, \quad l = U \left( \frac{h^2}{\alpha \kappa f^2} \right)^{1/3}, \quad (4.67)$$

and calculation of these using values suggested previously leads to  $U \approx 26$  m s<sup>-1</sup>,  $l \approx 1290$  km. Success!

### 4.4.2 A reduced model

With these (and earlier) assumptions, the equations (4.52), (4.53), (4.62) and (4.58) become

$$\begin{aligned}
\frac{d\rho}{dt} + \rho \nabla \cdot \mathbf{u} &= 0, \\
\varepsilon \frac{du}{dt} - v \frac{\sin \lambda}{\sin \lambda_0} + \delta w \frac{\cos \lambda}{\sin \lambda_0} &= -\frac{1}{\varepsilon^2} \frac{1}{\rho} \frac{\partial p}{\partial x}, \\
\varepsilon \frac{dv}{dt} + u \frac{\sin \lambda}{\sin \lambda_0} &= -\frac{1}{\varepsilon^2} \frac{1}{\rho} \frac{\partial p}{\partial y}, \\
\delta \left[ \delta \varepsilon \frac{dw}{dt} - u \frac{\cos \lambda}{\sin \lambda_0} \right] &= -\frac{1}{\varepsilon^2} \left( \frac{1}{\rho} \frac{\partial p}{\partial z} + 1 \right), \\
\frac{d\theta}{dt} &= -m(\theta, p) \frac{dp}{dt} + \varepsilon^2 H, \\
\rho &= \frac{p^{1-\alpha}}{\theta}.
\end{aligned} \tag{4.68}$$

We now adopt the formal asymptotic limits

$$m \sim \Sigma \sim \varepsilon, \quad \delta \sim \varepsilon^2 \tag{4.69}$$

(these also justify our earlier neglect of the various curvilinear terms in (4.35)), and we define the  $O(1)$  function  $\Gamma(\theta, p)$  by

$$m = \frac{\varepsilon \Gamma}{\rho}. \tag{4.70}$$

In addition we define

$$\beta = \frac{\Sigma \cot \lambda_0}{\varepsilon} \sim O(1), \tag{4.71}$$

so that

$$\frac{\sin \lambda}{\sin \lambda_0} = 1 + \varepsilon \beta y + O(\varepsilon^2). \tag{4.72}$$

This approximation by a linear dependence on  $y$  is called the *beta-plane approximation*.

The first two components of the momentum equation momentum equation imply

$$p = \bar{p}(z) + \varepsilon^2 P, \tag{4.73}$$

and therefore, because

$$\frac{\partial p}{\partial z} \approx -\rho + O(\varepsilon^4), \tag{4.74}$$

we have

$$\rho = \bar{\rho}(z) + O(\varepsilon^2), \tag{4.75}$$

and therefore also

$$\theta = \bar{\theta}(z) + \varepsilon^2 \Theta. \tag{4.76}$$

Expanding the equations in powers of  $\varepsilon$  up to terms of  $O(\varepsilon)$  (but the energy equation to  $O(\varepsilon^2)$ ), we thus obtain the reduced approximate system

$$\begin{aligned}
\bar{\rho}u_x + \bar{\rho}v_y + (\bar{\rho}w)_z &= 0, \\
\varepsilon \frac{du}{dt} - v(1 + \varepsilon\beta y) &= -\frac{1}{\bar{\rho}}P_x, \\
\varepsilon \frac{dv}{dt} + u(1 + \varepsilon\beta y) &= -\frac{1}{\bar{\rho}}P_y, \\
\bar{p}' &= -\bar{\rho}, \quad \bar{\rho} = \frac{\bar{p}^{1-\alpha}}{\bar{\theta}}, \\
\varepsilon^2 \frac{d\Theta}{dt} + w\bar{\theta}' &= \varepsilon w\Gamma + \varepsilon^2 H.
\end{aligned} \tag{4.77}$$

Note that  $\Gamma(\theta, p) \approx \Gamma(\bar{\theta}, \bar{p})$  is a function of  $z$  only.

### 4.4.3 Geostrophic flow

We already saw that the neglect of the acceleration terms causes the existence of Taylor columns and isobaric flow in laboratory conditions. Much the same is true here. We put  $\varepsilon = 0$  in the  $x$  and  $y$  momentum equations, and this gives

$$\bar{\rho}u \approx -P_y, \quad \bar{\rho}v \approx P_x, \tag{4.78}$$

which in turn implies in the mass conservation equation that  $(\bar{\rho}w)_z = O(\varepsilon)$ . Thus we write

$$w = \varepsilon W \tag{4.79}$$

on the basis of a boundary condition that  $w = 0$  at  $z = 0$ . More generally, the no flow through condition at the ground is modified by the small friction terms (which we have ignored) in the momentum equation; these cause the existence of a boundary layer (the planetary boundary layer) to occur. The effect of rotation in this boundary layer is to cause a small vertical velocity at the top of the layer, proportional to the square root of an appropriately defined Ekman number  $E$ , and this velocity is often called Ekman pumping.

The rotation forces the vertical velocity to be even smaller than the shallowness of the flow would suggest. A consequence of (4.78) is that  $\mathbf{u} \cdot \nabla_H p \approx 0$ , which implies that horizontal winds are approximately along isobars. This odd behaviour (we normally expect fluid flow to be down pressure gradients) is entirely due to the rapid rotation of the planet. A consequence of (4.79) is that the material derivative is essentially horizontal, which is to say that in (4.77) we have

$$\frac{d}{dt} \approx \frac{D}{Dt} \equiv \frac{\partial}{\partial t} + u \frac{\partial}{\partial x} + v \frac{\partial}{\partial y}, \tag{4.80}$$

and this is used below.

This kind of flow is called *geostrophic flow*. In it the velocity is determined by the pressure field. The question then arises, how to determine the pressure field. The answer to this question lies in extending the geostrophic approximation by going to the next order in  $\varepsilon$ , and this leads to an equation called the *quasi-geostrophic potential vorticity equation*.

## 4.5 The quasi-geostrophic potential vorticity equation

With the adoption of (4.79), the energy equation in (4.77) takes the form

$$W(\bar{\theta}' - \varepsilon\Gamma) = \varepsilon \left( H - \frac{d\Theta}{dt} \right). \quad (4.81)$$

Now since, according to (4.74)  $\frac{\partial p}{\partial z} = -\rho + O(\varepsilon^4)$ , it follows, using (4.73), (4.76) and (4.68)<sub>6</sub>, that

$$P_z = -\frac{\bar{p}^{1-\alpha}}{\bar{\theta}} \left[ \frac{(1-\alpha)P}{\bar{p}} - \frac{\Theta}{\bar{\theta}} \right], \quad (4.82)$$

and this can be manipulated to the form

$$\Theta = \bar{\theta}^2 \frac{\partial}{\partial z} \left[ \frac{P}{\bar{p}^{1-\alpha}} \right]. \quad (4.83)$$

The geostrophic wind approximation (4.78) suggests that we write

$$P = \bar{\rho}\psi, \quad (4.84)$$

where  $\psi$  is the geostrophic stream function, thus

$$u = -\frac{\partial\psi}{\partial y}, \quad v = \frac{\partial\psi}{\partial x}. \quad (4.85)$$

Bearing in mind that  $\bar{\rho} = \frac{\bar{p}^{1-\alpha}}{\bar{\theta}}$ , it follows that

$$\Theta = \bar{\theta}^2 \frac{\partial}{\partial z} \left[ \frac{\psi}{\bar{\theta}} \right] = \frac{\partial\psi}{\partial z} + O(\varepsilon), \quad (4.86)$$

since  $\bar{\theta}'(z) = O(\varepsilon)$ . This relation, together with the geostrophic wind approximation, gives us the *thermal wind equations*:

$$\frac{\partial u}{\partial z} = -\frac{\partial\Theta}{\partial y}, \quad \frac{\partial v}{\partial z} = \frac{\partial\Theta}{\partial x}. \quad (4.87)$$

Next we form an equation for the (vertical) vorticity

$$\zeta = \frac{\partial v}{\partial x} - \frac{\partial u}{\partial y} = \nabla^2 \psi \quad (4.88)$$

by cross differentiating (4.77)<sub>2,3</sub> to eliminate the pressure derivatives. Using the conservation of mass equation, together with (4.79) and (4.80), we derive the quasi-geostrophic potential vorticity equation (QGPVE)

$$\frac{D\zeta}{Dt} + \beta \frac{\partial \psi}{\partial x} = \frac{1}{\bar{\rho}} \frac{\partial(\bar{\rho}W)}{\partial z}, \quad (4.89)$$

where  $D/Dt$  denotes the horizontal material derivative introduced above; note that

$$\frac{D}{Dt} = \frac{\partial}{\partial t} - \frac{\partial \psi}{\partial y} \frac{\partial}{\partial x} + \frac{\partial \psi}{\partial x} \frac{\partial}{\partial y}, \quad (4.90)$$

and that the left hand side is the material derivative of  $\zeta + \beta y$ : this quantity is the *potential vorticity*.

The unknown in the QGPVE is  $W$ . Surprisingly, its determination comes from the energy equation (4.81). Let us denote the stratification function  $S(z)$  by

$$S(z) = \frac{1}{\varepsilon} \left[ \frac{d\bar{\theta}}{dz} - \frac{d\theta_w}{dz} \right], \quad (4.91)$$

and note that by observation (and assumption) it is positive and  $O(1)$ . It is related to the Brunt-Väisälä frequency  $N$ , which is the frequency of small vertical oscillations in the atmosphere; in fact  $S \propto N^2$ . Positive  $S$  (and thus real  $N$ ) indicates a stably stratified atmosphere. If  $S$  were to become negative, the atmosphere would become unstably stratified and it would overturn. The energy equation is thus

$$\frac{D\Theta}{Dt} = H - WS. \quad (4.92)$$

In summary, we have the vorticity  $\zeta$  and potential temperature  $\Theta$  defined in terms of the stream function  $\psi$  by (4.88) and (4.86). Two separate equations for  $\zeta$  and  $\Theta$  are then (4.89) and (4.92), from which  $W$  and  $S(z)$  must also be determined, the latter by averaging the equations.

By an application of Green's theorem in the plane, we have that

$$\iint_A \frac{D\Lambda}{Dt} dS = \frac{\partial}{\partial t} \iint_A \Lambda dS - \oint_{\partial A} \Lambda d\psi, \quad (4.93)$$

where  $A$  is any horizontal area at fixed  $z$ . In particular, if  $A$  is a closed region on the boundaries of which  $\psi$  is constant in space, i. e., there is no flow through  $\partial A$ , then the boundary integral is zero.<sup>4</sup> Let an overbar denote a spatial horizontal average over

---

<sup>4</sup>We have in mind that  $A$  is the region of zonal mid-latitude flow, bounded to the north by the polar front, and to the south by the tropical front. We can allow  $A$  to be a periodic strip on the sphere also.

A. Putting  $\Lambda = \Theta$ , it follows that

$$\frac{\partial \bar{\Theta}}{\partial t} = H - \bar{W}S, \quad (4.94)$$

where  $\bar{W}(z)$  is the horizontal average of  $W$ . Applying the same procedure to (4.89), we have

$$\frac{\partial \bar{\zeta}}{\partial t} = \frac{1}{\bar{\rho}} \frac{\partial}{\partial z} [\bar{\rho} \bar{W}]. \quad (4.95)$$

It turns out that the Ekman pumping boundary condition, to which we alluded on page 123, gives a value of  $\bar{W}$  at  $z = 0$  of

$$\bar{W}_0 = E^* \bar{\zeta}_0, \quad (4.96)$$

where  $\bar{\zeta}_0$  is the spatially averaged vorticity at the surface, and

$$E^* = \sqrt{\frac{E}{2\varepsilon^2}}, \quad E = \frac{\varepsilon_V}{2\Omega h^2}, \quad (4.97)$$

where the vertical eddy diffusivity was introduced in (4.25). Integrating (4.95), we have (using  $\bar{\rho} = 1$  at  $z = 0$ )

$$\bar{\rho} \bar{W} = \int_0^z \bar{\rho} \bar{\zeta}_t dz + E^* \bar{\zeta}_0, \quad (4.98)$$

and it follows from this that the stratification parameter is defined by the relation

$$\frac{\bar{\rho}}{S} = \frac{\int_0^z \bar{\rho} \bar{\zeta}_t dz + E^* \bar{\zeta}_0}{H - \bar{\Theta}_t}. \quad (4.99)$$

We can go further if we assume that the solutions are stationary (not necessarily steady), i. e., a well-defined time average exists.<sup>5</sup> The time averages of the time derivative terms are zero, and thus it simply follows (since  $H$ ,  $S$  and  $\bar{\rho}$  are functions only of  $z$ ) that

$$H = \widehat{W}S, \quad \bar{\rho} \widehat{W} = \widehat{W}_0, \quad (4.100)$$

where  $\widehat{W}$  is the time average of  $\bar{W}$ , and the constant  $\widehat{W}_0$  is the value of the surface boundary value of  $\widehat{W}$  at  $z = 0$ . The Ekman pumping boundary condition (4.96) implies that

$$\widehat{W}_0 = E^* \widehat{\zeta}_0, \quad (4.101)$$

where  $\widehat{\zeta}_0$  is the space averaged vorticity at the surface.

The two equations in (4.100) define  $S$  and  $\widehat{W}$ , and in particular we find that

$$\frac{\bar{\rho}}{S} = \frac{E^* \widehat{\zeta}_0}{H}. \quad (4.102)$$

---

<sup>5</sup>This is what we would generally expect. Unbounded drift of  $\psi$  would indicate breakdown of the perturbation expansion because of the presence of secular terms.

This equation thus defines the stratification function  $S(z)$  for a stationary (but not necessarily steady) atmosphere.<sup>6</sup> Evidently, the wet adiabatic profile ( $S = 0$ ) is obtained (in stationary conditions) only if the heating rate  $H$  is zero.

We can now use the identity

$$\frac{\partial}{\partial z} \left[ K(z) \frac{D\Theta}{Dt} \right] = \frac{D}{Dt} \left[ \frac{\partial}{\partial z} \left( K(z) \frac{\partial \psi}{\partial z} \right) \right] \quad (4.103)$$

to show, using (4.92), that

$$\frac{1}{\bar{\rho}} \frac{\partial}{\partial z} [\bar{\rho} W] = \frac{1}{\bar{\rho}} \frac{\partial}{\partial z} \left[ \frac{\bar{\rho} H}{S} \right] - \frac{D}{Dt} \left[ \frac{1}{\bar{\rho}} \frac{\partial}{\partial z} \left( \frac{\bar{\rho}}{S} \frac{\partial \psi}{\partial z} \right) \right], \quad (4.104)$$

and therefore (4.89) can be written

$$\frac{D}{Dt} \left[ \nabla^2 \psi + \beta y + \frac{1}{\bar{\rho}} \frac{\partial}{\partial z} \left( \frac{\bar{\rho}}{S} \frac{\partial \psi}{\partial z} \right) \right] = \frac{1}{\bar{\rho}} \frac{\partial}{\partial z} \left[ \frac{\bar{\rho} H}{S} \right] = 0, \quad (4.105)$$

using (4.102). This is one form of the quasi-geostrophic potential vorticity equation. It is precisely that given by Pedlosky (1987, equation(6.5.21)). It is a single equation for the geostrophic stream function  $\psi$ , providing the stratification  $S$  is known. In most treatments of its solutions, the stratification parameter  $S$  is assumed known (from measurements for example), and then the equation (4.105) can be considered on its own. However, in reality  $S$  must be determined from (4.102), which indicates that the stratification is determined in terms of the solution of the equation (4.105) itself, which is thus an integro-differential equation for the stream function  $\psi$ . This equation is apparently only well-posed if  $S > 0$ , i. e., if the time mean surface value of the vorticity  $\hat{\zeta}_0$  is positive (assuming also that  $H > 0$ ), but there seems to be no obvious reason why this should necessarily be the case. Actually, the situation is reminiscent of the internal waves we discussed on page 103 (see figure 4.2). If the stratification became negative, it seems the atmosphere would become inherently unstable. It would start to ‘boil’, with severe convective storms shrouding the planet. The mild, quasi-geostrophic description of the weather would no longer be apt, and climate change would be a sudden, dramatic reality. The day after tomorrow, indeed. The possibility of such a catastrophic scenario appears to have entirely bypassed climate scientists.

## 4.6 Rossby waves

We now return to our earlier discussion of atmospheric waves in section 4.3. There we described gravity waves, known as Poincaré waves. These are the rotational equivalent of high frequency sound waves. However, one possible mode had zero frequency,

---

<sup>6</sup>This derivation is somewhat similar to that of Pedlosky (1987); however, he did not provide an explicit recipe for  $S(z)$ . See also question 4.5.

and we postponed discussion of it. In reality, the zero frequency was essentially a consequence of geostrophic approximation, but in the quasi-geostrophic approximation these waves are found to have non-zero frequency; they are called *Rossby waves*.

We seek a wave motion corresponding to the zero frequency geostrophic gravity wave mode satisfying (4.46) with  $\omega = 0$ . This is the Rossby wave, and it is most simply examined by studying (4.105) in the absence of heating, and assuming that the stratification parameter  $S$  is prescribed. (Such simplifications are in fact commonly made in studying the properties of (4.105).) We define a vertical eigenfunction  $\Psi(z)$  satisfying the ordinary differential equation

$$\frac{1}{\bar{\rho}} \left[ \frac{\bar{\rho}}{S} \Psi' \right]' = -m^2 \Psi, \quad (4.106)$$

where for suitable homogeneous boundary conditions on  $\Psi$ ,  $m^2$  will be positive. With  $H = 0$ ,  $\psi = 0$  is a solution of (4.105), and small amplitude solutions of the equation will satisfy the linearised equation

$$\frac{\partial}{\partial t} \left[ \nabla^2 \psi + \frac{1}{\bar{\rho}} \frac{\partial}{\partial z} \left( \frac{\bar{\rho}}{S} \frac{\partial \psi}{\partial z} \right) \right] + \beta \frac{\partial \psi}{\partial x} = 0. \quad (4.107)$$

This has solutions

$$\psi = \Psi(z) \exp[i(kx + ly + \omega t)], \quad (4.108)$$

providing

$$\omega = \frac{k\beta}{k^2 + l^2 + m^2}. \quad (4.109)$$

These are Rossby waves. The wave speed  $-\omega/k$  is negative, so that the waves move westwards (relative to the mean flow, which is here zero). The sphericity of the Earth (i. e.,  $\beta > 0$ ) is essential in causing the waves to move.

## 4.7 Baroclinic instability

Gravity waves are the sound of the atmosphere. Like a bell which reverberates when struck, gravity waves are excited externally. For example, when the atmosphere flows over mountains, the waves are visualised by the periodic rows of clouds which form in the lee. However, they do not play a prominent part in large scale weather flows, because they are damped fairly rapidly by friction, and they are generated by external effects such as topographic forcing, not by internal dynamics.

Rossby waves, on the other hand, do play an important part in the day to day weather, and this is because they are continually generated by an instability in the underlying basic zonal flow. This instability is called *baroclinic instability*, and it is responsible for the basic wave-like nature of the circulation in mid-latitudes.

We consider the stability of a basic state which is taken to be a purely zonal flow. Because the quasi-geostrophic model is essentially inviscid (and conductionless), there is no unique such state. In the absence of the heating term  $H$  on the right hand side of

(4.105), *any* zonal stream function  $\psi(y, z)$  satisfies the QG equation (4.105). However, we would expect that over sufficiently long time scales, the potential temperature  $\Theta$  of a zonal flow would become equal to the underlying surface temperature  $\Theta_0(y)$ , which ultimately is what drives the flow. A local expansion on the mid-latitude length scale of the global  $O(\varepsilon)$  variation in  $\theta$  suggests the prescription of  $\Theta_0 = -y$  at  $z = 0$ . The choice  $\Theta = -y$  implies the zonal flow

$$\psi = k - yz; \quad (4.110)$$

generally,  $k = k(z)$  but we will take it as constant,  $k = 1$ . We will use (4.110) as the basic state whose stability we wish to study.

### 4.7.1 The Eady model

The simplest model in which baroclinic instability is manifested is the Eady (1949) model. In this model, the tropopause is considered to be a rigid lid, so that we impose

$$W = 0 \quad \text{at} \quad z = 1. \quad (4.111)$$

Basal friction is ignored, corresponding to  $E^* = 0$  in (4.96), so that

$$W = 0 \quad \text{at} \quad z = 0. \quad (4.112)$$

The Earth's sphericity is ignored by putting  $\beta = 0$  in (4.105), the heating term  $H = 0$  (consistent with the basic state (4.110), and both the density  $\bar{\rho}$  and the stratification  $S$  are taken as constant. The equation to be solved is thus the QG equation in the form

$$\frac{D}{Dt} \left[ \nabla^2 \psi + \frac{1}{S} \frac{\partial^2 \psi}{\partial z^2} \right] = 0, \quad (4.113)$$

with boundary conditions which derive from (4.92):

$$\frac{D}{Dt} \left( \frac{\partial \psi}{\partial z} \right) = 0 \quad \text{at} \quad z = 0, 1, \quad (4.114)$$

together with the no flow conditions  $\partial \psi / \partial x = 0$  on  $y = \pm 1$ . In addition, (4.89) implies that

$$\frac{D}{Dt} \int_0^1 \zeta \, dz = 0. \quad (4.115)$$

This is automatically satisfied when  $\psi$  satisfies (4.113) and (4.114).

We write

$$\psi = 1 - yz + \Psi, \quad (4.116)$$

and linearise for small  $\Psi$  to find

$$\left( \frac{\partial}{\partial t} + z \frac{\partial}{\partial x} \right) \left[ \nabla^2 \Psi + \frac{1}{S} \frac{\partial^2 \Psi}{\partial z^2} \right] = 0, \quad (4.117)$$

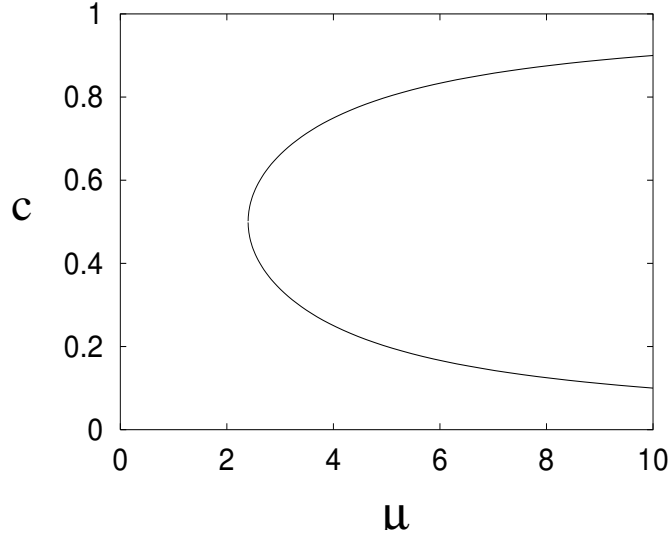


Figure 4.7: Wave speed of perturbations in the Eady model. Instability occurs where the wave speeds are complex conjugates, for  $\mu \lesssim 2.4$ .

subject to

$$\begin{aligned} \left( \frac{\partial}{\partial t} + z \frac{\partial}{\partial x} \right) \frac{\partial \Psi}{\partial z} - \frac{\partial \Psi}{\partial x} &= 0 \quad \text{on } z = 0, 1, \\ \Psi &= 0 \quad \text{on } y = \pm 1. \end{aligned} \quad (4.118)$$

We seek solutions as linear combinations of the form

$$\Psi = A(z)e^{\sigma t + ikx + il_n y}, \quad (4.119)$$

where  $l_n = \frac{1}{2}n\pi$ , and  $n$  is an integer. The appropriate linear combination of the  $y$ -dependent part is  $\sin l_n y$  for  $n$  even, and  $\cos l_n y$  for  $n$  odd. Then

$$(ikz + \sigma) [A'' - \mu^2 A] = 0, \quad (4.120)$$

where

$$\mu^2 = (k^2 + l^2)S, \quad (4.121)$$

and

$$(ikz + \sigma)A' - ikA = 0 \quad \text{on } z = 0, 1. \quad (4.122)$$

Smooth solutions of (4.120) are linear combinations of  $\cosh \mu z$  and  $\sinh \mu z$ , and the dispersion relation which results from satisfaction of the boundary conditions in (4.120) is

$$c = -\frac{\sigma}{ik} = \frac{1}{2} \pm \frac{1}{\mu} \left[ \left( \frac{\mu}{2} - \coth \frac{\mu}{2} \right) \left( \frac{\mu}{2} - \tanh \frac{\mu}{2} \right) \right]^{1/2}, \quad (4.123)$$

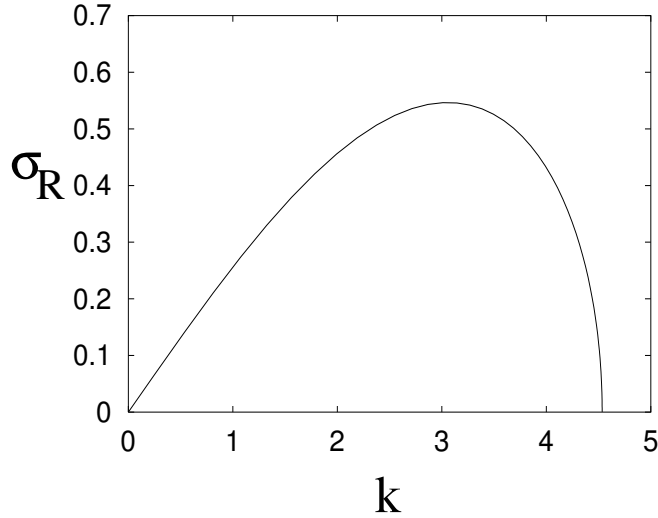


Figure 4.8: Growth rate  $\sigma_R$  of perturbations in the Eady model as a function of wavenumber  $k$  when the stratification  $S = 0.25$ . The growth rate is well approximated by  $\sigma_R \approx 0.145k(k_c - k)^{1/2}$ , where  $k_c = \sqrt{\frac{\mu_c^2}{S} - \frac{\pi^2}{4}}$  is the maximum wavenumber for instability.

where  $c$  is the wave speed. Figure 4.7 shows the (real) value of  $c$  as a function of (positive)  $\mu$ . Since  $\mu/2 > \tanh(\mu/2)$ , it is clear that  $c$  is complex for  $\mu < \mu_c$ , where

$$\frac{\mu_c}{2} = \coth \frac{\mu_c}{2}, \quad \mu_c \approx 2.399. \quad (4.124)$$

Complex conjugate values of  $c$  indicate instability, and this occurs for  $\mu < \mu_c$ . Instability occurs if  $k^2 + l^2 < \mu_c^2/S$ , and thus is effected by the minimum values  $k = 0$ ,  $l = \frac{1}{2}\pi$ , and the Eady instability criterion is

$$S < \frac{4\mu_c^2}{\pi^2} \approx 2.218; \quad (4.125)$$

this is readily satisfied in the Earth's atmosphere.

Evidently, the waves (stable or unstable) move to the east in the northern hemisphere, as is observed. The wave speed of unstable waves is 0.5, and the growth rate is

$$\sigma_R = \frac{k}{\mu} \left[ \left( \coth \frac{\mu}{2} - \frac{\mu}{2} \right) \left( \frac{\mu}{2} - \tanh \frac{\mu}{2} \right) \right]^{1/2}. \quad (4.126)$$

The growth rate goes to zero as  $k \rightarrow 0$ , and also as  $\mu \rightarrow \mu_c$ . Since, for the fundamental mode ( $n = 1$ )  $\mu^2 = \left( k^2 + \frac{\pi^2}{2} \right) S$  increases with  $k$ , it appears that the growth rate is maximum for an intermediate value of  $k$ . Indeed, figure 4.8 shows a typical graph of the growth rate plotted as a function of wave number  $k$ . Although linear stability

gives us no information about the eventual form of the growing waves, it is plausible that the maximum growth rate at wavenumber  $k_m$  selects the preferred wavelength of disturbances as  $2\pi/k_m$ . This appears to be consistent with actual synoptic scale waves in mid-latitudes.

## 4.7.2 The Charney model

A slightly more complicated model of baroclinic instability is the Charney (1947) model. It is similar to the Eady model, but assumes a stratification of the form  $\bar{\rho} = e^{-\lambda z}$ , and also  $\beta \neq 0$ . It retains the assumption of constant  $S$  and that the basic flow is a simple shear flow,  $\psi = -yz$ . If, as before, we put

$$\psi = -yz + \Psi, \quad \psi = \Phi(z)e^{ik(x-ct)+l_n y}, \quad (4.127)$$

then the linearised equation for  $\Phi$  becomes

$$(z - c)(\Phi'' - \lambda\Phi' - K^2 S\Phi) + (\lambda + \beta S)\Phi = 0, \quad (4.128)$$

where  $K^2 = k^2 + l_n^2$ , and the boundary conditions are still given by (4.122):

$$(z - c)\Phi' - \Phi = 0 \quad \text{on} \quad z = 0, 1. \quad (4.129)$$

The analysis of this is still possible, but is more complicated (see Pedlosky 1987, pp. 532 ff.). In particular, at the point of instability where  $c$  is real, there is a *critical layer* at  $z = c$  if  $0 < c < 1$ . This is similar to the Rayleigh equation in hydrodynamic stability theory.

## 4.8 Frontogenesis

What has all this to do with the weather? If we look at a weather map, or listen to a weather forecaster on a mid-latitude television station, we will hear about fronts and depressions, low pressure systems, cyclones and anti-cyclones. These are indeed the standard bearers of the atmosphere, bringing their associated good and bad weather, storms, rainfall and snow. We are now in a position at least to describe how these features occur.

The weather is described, at least in essence, by some form of the geostrophic or quasi-geostrophic equations. Dissipative effects due to eddy viscosity and eddy thermal conductivity have a short term (days) effect in the planetary boundary layer within a kilometre or so of the surface, but only control the mean temperature of the troposphere over much longer time scales. As a consequence, weather is effectively described by a conservative system, indeed certain approximate models can be written as a Hamiltonian system, and as a consequence it is subject to the same sort of large amplitude fluctuations as those which characterise instability in such systems.

The basic poleward gradient of surface temperature attempts to drive a zonal flow, which is linearly unstable in the presence of a sufficiently small stratification

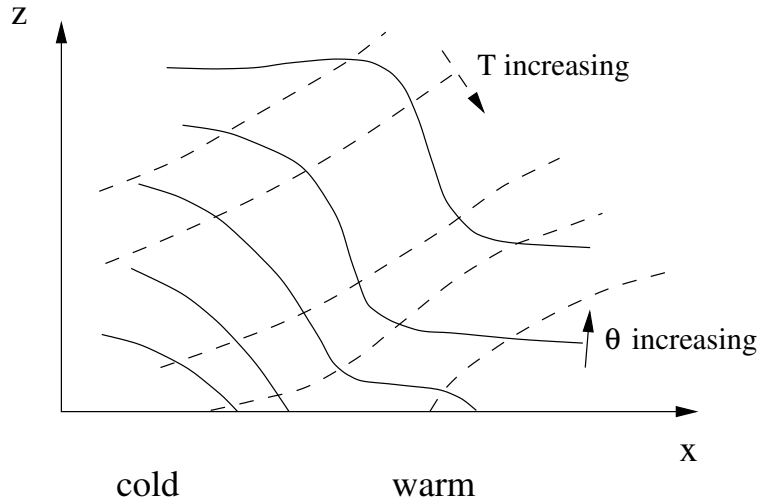


Figure 4.9: Contours of temperature (dashed lines) and potential temperature (solid lines) in a forming front.

parameter  $S$ . The very simplest representation of this instability is found in the Eady model (4.113) and (4.114), which is a nonlinear hyperbolic equation for the potential vorticity. The consequence of the instability is that the steady, parallel characteristics of the zonal flow are distorted and intersect, forming a shock, as illustrated in figure 4.9. This is a front. It consists of a tongue of cold air intruded under warmer air, and the width of the front is typically of order 100 km.

As the front develops, the baroclinic instability also distorts the flow in a wave like pattern. The effect of this is to bend the front round, as illustrated in figure 4.10, forming a series of vortex-like rings. In the atmosphere, these are the cyclonic disturbances which form the mid-latitude low pressure storm systems, with typical dimensions of 2000 km. They also occur in the ocean, forming coherent rings of some 50 km diameter.

The description above is a little idealistic. On the Earth, fronts are an intrinsic consequence of the difference in properties between different air masses. The mid-latitude cells, for example, are bounded north and south by fronts across which the wind direction and the temperature changes. The warm mid-latitude westerlies are bounded polewards by the cold polar easterlies. The situation is complicated by continents and oceans. Continental air is dry, whereas oceanic air is moist. As a consequence of these geographic variations there are a number of different types of air masses, and the boundaries between these provide the seeds for frontal development. The fronts move and distort as shown in figure 4.10, but it is more sensible to think of the roll-up of a planar front and the formation of storm systems as a result of (Kelvin-Helmholtz like) instability of a linear vortex sheet, rather than as a consequence of shock formation in the nonlinear wave evolution of the quasi-geostrophic potential vorticity equation (QGPVE). In fact, the QGPVE does not do a very good job of

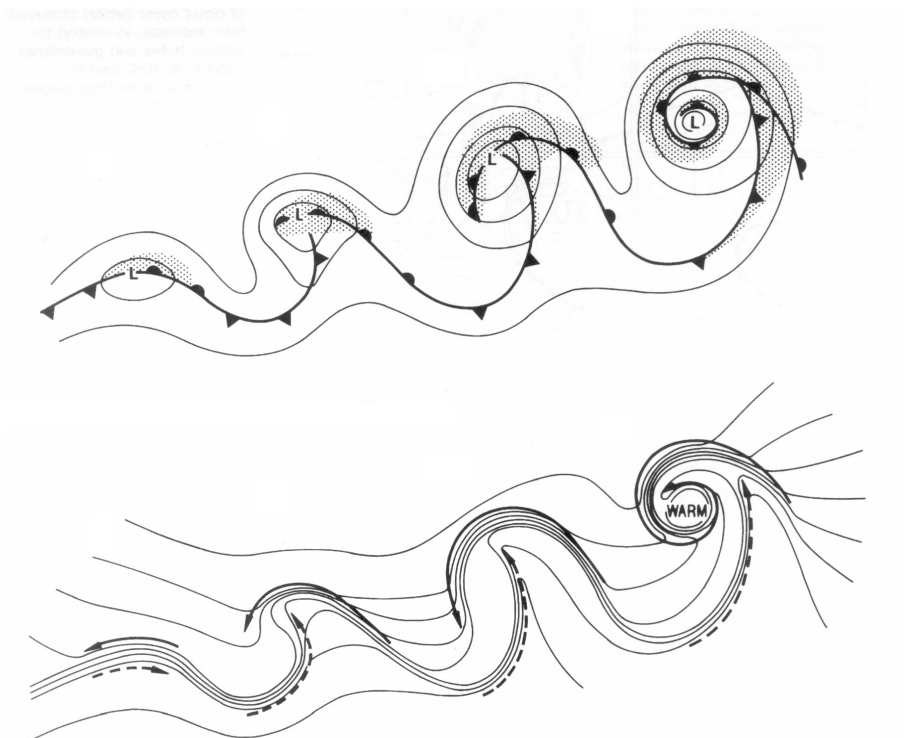


Figure 4.10: Two views of the formation of cyclonic depressions from a baroclinically unstable front. The illustration resembles the Kármán vortex street which forms at moderate Reynolds number in the flow past a cylinder. The upper diagram shows isobars, the front, and cloud cover (stippled); the lower diagram shows isotherms, and flow of cold air (solid arrows) and warm air (dashed arrows). From Barry and Chorley (1998), page 162.

numerical weather front prediction.<sup>7</sup>

## 4.9 Depressions and hurricanes

The storm systems which develop as shown in figure 4.10 are called cyclones. They are like vortices which rotate anti-clockwise, and are associated with low pressure at their centres (thus they are also called depressions). Conversely, a high pressure vortex rotating clockwise is called an anti-cyclone. A severe storm with central pressure of 960 millibars represents a dimensionless amplitude of  $0.04 \sim \varepsilon^2$ , and is thus within the remit of the quasi-geostrophic scaling.

In the tropics, tropical cyclones occur, and the most severe of these is the hurricane, or typhoon. In essence, the hurricane is very similar to the mid-latitude depression, consisting of an anti-clockwise rotating vortex, with wind convergence at

<sup>7</sup>This comment is due to Peter Lynch.

the surface, and divergence at the tropopause. It is, however, fuelled by convection, and can be thought of as the result of a strong convective plume interacting with the Coriolis force, which causes the rotation, and in fact organises it into a spiral wave structure, as can be seen in satellite images by the spiral cloud formations.

The hurricane is distinguished by its high winds, high rainfall and relatively small size (hundreds rather than the thousands of kilometres of a mid-latitude cyclone). The strongest hurricane on record was hurricane Gilbert in 1988, where the central pressure fell to 888 mbar, and maximum windspeeds were in excess of  $55 \text{ m s}^{-1}$  ( $200 \text{ km hr}^{-1}$ ). The strong convection is a consequence of evaporation from a warm ocean, and it is generally thought that hurricane formation requires a sea surface temperature above  $27^\circ$  centigrade, or 300 K. Relative to a mean surface temperature of 288 K, this is an amplitude of 12 K, and dimensionlessly  $12/288 \approx 0.04$ , of  $O(\varepsilon^2)$ . In the tropics, the Rossby number  $\varepsilon$  is higher, and near the equator the quasi-geostrophic approximation breaks down, but hurricanes do not form in a band near the equator.

Hurricanes typically move westwards in the prevailing tropospheric winds, and dissipate as they move over land, where the fuelling warm oceanic water is not present, and surface friction is greater. They develop a central eye, which is relatively calm and cloud free, and in which air flow is downwards. In hurricanes, this eye is warm.

## 4.10 Notes and references

### Exercises

4.1 It will be helpful in the following to use the summation convention, in which summation over repeated suffixes is understood. The Kronecker delta is  $\delta_{ij}$ , and equals 1 if  $i = j$ , and 0 otherwise. The alternating tensor  $\varepsilon_{ijk}$  is 1 if  $\{i, j, k\}$  is an even permutation of  $\{1, 2, 3\}$ ,  $-1$  if it is an odd permutation, and 0 otherwise.

Show that

$$\varepsilon_{ijk}\varepsilon_{ipq} = \delta_{jp}\delta_{kq} - \delta_{jq}\delta_{kp}.$$

Show that the determinant of a matrix  $A = (a_{ij})$  is

$$\det A = \varepsilon_{ijk}a_{1i}a_{2j}a_{3k}.$$

Show that

$$\boldsymbol{\Omega} \times (\boldsymbol{\Omega} \times \mathbf{r}) = (\boldsymbol{\Omega} \cdot \mathbf{r})\mathbf{r} - \Omega^2 \mathbf{r}.$$

Show that

$$\nabla \times \mathbf{a} = \varepsilon_{ijk} \mathbf{e}_i \frac{\partial a_k}{\partial x_j}.$$

finally, show that

$$\boldsymbol{\Omega} \times (\boldsymbol{\Omega} \times \mathbf{r}) = -\frac{1}{2} \nabla |\boldsymbol{\Omega} \times \mathbf{r}|^2.$$

4.2 A fluid flows in a rapidly rotating container  $D$  such that its velocity is given by the system

$$\begin{aligned}\nabla \cdot \mathbf{u} &= 0, \\ \mathbf{u}_t + \mathbf{k} \times \mathbf{u} &= -\nabla p.\end{aligned}$$

Assuming  $\mathbf{k}$  is in the  $z$  direction, show that

$$\begin{aligned}\nabla \times (\mathbf{k} \times \mathbf{u}) &= -\mathbf{u}_z, \\ \nabla \cdot (\mathbf{k} \times \mathbf{u}) &= -\mathbf{k} \cdot \boldsymbol{\omega}, \quad \boldsymbol{\omega} = \nabla \times \mathbf{u}.\end{aligned}$$

Hence show that  $p$  satisfies

$$\nabla^2 p_{tt} + p_{zz} = 0 \quad \text{in } D.$$

Next, show that

$$\mathbf{u}_{ttt} + \mathbf{u}_t + \mathbf{k}(\mathbf{k} \cdot \nabla)p - \mathbf{k} \times \nabla p_t = -\nabla p_{tt},$$

and deduce that if  $\mathbf{u} \cdot \mathbf{n} = 0$  on the boundary  $\partial D$ , then

$$(\mathbf{n} \cdot \mathbf{k})p_z - \mathbf{n} \times \mathbf{k} \cdot \nabla p_t + \mathbf{n} \cdot \nabla p_{tt} = 0 \quad \text{on } \partial D.$$

Oscillatory solutions of the form  $p = \phi(\mathbf{r})e^{i\lambda t}$  are sought. Write down the equation satisfied by  $\phi$ , and show that it is hyperbolic (with  $z$  being the time-like variable) if  $|\lambda| < 1$ , and that the ‘wave speed’ is  $\frac{\lambda}{\sqrt{1 - \lambda^2}}$ .

Write down the equation and boundary conditions for  $\phi$  in the two-dimensional  $(x, z)$  unit square  $[0, 1] \times [0, 1]$ , and deduce that normal mode solutions  $\cos m\pi x \cos n\pi z$  exist, and find the corresponding values of  $\lambda$ .

4.3 Derive a reference state for a dry atmosphere (no condensation) by using the equation of state

$$p = \frac{\rho RT}{M_a},$$

the hydrostatic pressure

$$\frac{\partial p}{\partial z} = -\rho g,$$

and the dry adiabatic temperature equation

$$\rho c_p \frac{dT}{dt} - \frac{dp}{dt} = 0.$$

Show that

$$\bar{T} = T_0 - \frac{gz}{c_p}, \quad \bar{p} = p_0 p^*(z),$$

where

$$p^*(z) = \left(1 - \frac{gz}{c_p T_0}\right)^{M_a c_p / R}.$$

Use the typical values  $c_p T_0 / g \approx 29$  km,  $M_a c_p / R \approx 3.4$ , to show that the pressure can be adequately represented by

$$\bar{p} = p_0 \exp(-z/H),$$

where here the scale height is defined as

$$H = \frac{RT_0}{M_a g} \approx 8.4 \text{ km.}$$

(A slightly better numerical approximation near the tropopause is obtained if the scale height is chosen as 7 km.)

4.4 A dimensionless model of atmospheric motion is given by

$$\begin{aligned} \frac{d\rho}{dt} + \rho \nabla \cdot \mathbf{u} &= 0, \\ \varepsilon \frac{du}{dt} - v \sin \lambda &= -\frac{1}{\varepsilon^2} \frac{1}{\rho} \frac{\partial p}{\partial x}, \\ \varepsilon \frac{dv}{dt} + u \sin \lambda &= -\frac{1}{\varepsilon^2} \frac{1}{\rho} \frac{\partial p}{\partial y}, \\ O(\varepsilon^2) &= -\frac{1}{\varepsilon^2} \left( \frac{1}{\rho} \frac{\partial p}{\partial z} + 1 \right), \\ \frac{d\theta}{dt} &= -\frac{\varepsilon \Gamma}{\rho} \frac{dp}{dt} + \varepsilon^2 H, \\ \rho &= \frac{p^{1-\alpha}}{\theta}, \end{aligned}$$

where  $\Gamma(\theta, p)$  is a positive  $O(1)$  function, and  $\varepsilon \ll 1$ . (Note the distinction to (4.68).)

In the tropics, it is appropriate to take  $\lambda = \varepsilon \beta y$ ,  $\beta = O(1)$ .

4.5 Suppose that  $\theta$  satisfies the equation

$$\frac{D\theta}{Dt} + \varepsilon W \frac{\partial \theta}{\partial z} = \varepsilon^2 \Gamma W + \varepsilon^2 H, \quad (*)$$

where  $\Gamma$  and  $H$  are constants,  $W = W(x, y)$  and the horizontal material derivative is given by

$$\frac{D}{Dt} = \frac{\partial}{\partial t} - \frac{\partial \psi}{\partial y} \frac{\partial}{\partial x} + \frac{\partial \psi}{\partial x} \frac{\partial}{\partial y},$$

where  $\psi$  is the geostrophic stream function.

The equation is to be solved in the region  $V$ :  $-L < x < L$ ,  $-1 < y < 1$ ,  $0 < z < 1$ , with the boundary condition  $\theta = 1 + \varepsilon^2 \Theta_0(y)$  on  $z = 0$ , and an initial condition for  $\theta$ . We can assume without loss of generality that the average of  $\Theta_0$  over  $y$  is zero. (Why?) Assume that  $\psi = \pm 1$  on  $y = \pm 1$ , and that it is periodic in  $x$  (with period  $2L$ ). Comment on the suitability of the initial and boundary conditions. Does it matter whether  $W$  is positive or negative??

If  $A$  is any horizontal section of  $V$ , show that

$$\int_A \frac{D\theta}{Dt} dS = \frac{\partial}{\partial t} \int_A \theta dS,$$

and deduce that the equation

$$\frac{D\theta}{Dt} = g$$

only has a bounded solution if  $\bar{g}(z) = 0$ , where  $\bar{g}$  is the time average of  $\int_A g dS$ .

By expanding  $\theta$  as  $\theta_0 + \varepsilon\theta_1 + \varepsilon^2\theta_2 + \dots$  and assuming that the solution remains regular, find the equations satisfied by  $\theta_i$ ,  $i = 1, 2, 3$ , and show that a solution exists in which  $\theta_0 = \theta_0(z)$ ; whence also

$$\theta_0 = 1$$

and  $\theta_1 = \theta_1(z)$ , and  $\theta_1$  is given by

$$\theta_1 = \left( \Gamma + \frac{H}{W} \right) z;$$

whence

$$\frac{D\theta_2}{Dt} = H \left( 1 - \frac{W}{\bar{W}} \right). \quad (\dagger)$$

Suppose now that  $\theta_2 = \frac{\partial\psi}{\partial z}$ ; show that  $\frac{D}{Dt} \left[ \frac{\partial\theta_2}{\partial z} \right] = \frac{\partial}{\partial z} \left( \frac{D\theta_2}{Dt} \right)$ , and deduce that a solution for  $\theta_2$  can be found in the form  $\theta_2 = \bar{\theta}_2(z) + \Theta(x, y)$ , where  $\Theta(x, y)$  is a particular solution of  $(\dagger)$ , and show that the secularity constraint at  $O(\varepsilon^3)$  implies that we can take  $\bar{\theta}_2 = 0$ . Deduce that  $\psi = z\Theta(x, y)$ .

Suppose now that a diffusion term  $\varepsilon^2 \frac{\partial^2 \theta}{\partial z^2}$  is added to the right hand side of  $(*)$ . Show that the preceding discussion still applies, but now  $\Theta$  represents an outer solution for  $\theta_2$  away from the boundary  $z = 0$ . By writing  $\theta_2 = \Theta + \chi$  and  $z = \varepsilon Z$ , show that  $\chi$  satisfies the approximate boundary layer equation

$$\frac{D\chi}{Dt} + W \frac{\partial\chi}{\partial Z} = \frac{\partial^2 \chi}{\partial Z^2},$$

with boundary conditions

$$\begin{aligned}\chi &\rightarrow 0 \quad \text{as } Z \rightarrow \infty, \\ \chi &= \chi_0(x, y) = \Theta_0 - \Theta \quad \text{on } Z = 0.\end{aligned}$$

For the particular case of a steady zonal flow in which  $\frac{D}{Dt} = u \frac{\partial}{\partial x}$ ,  $u = u(y)$ ,  $W = W(y)$  and  $\chi_0 = \sum_k \hat{\chi}_k(y) e^{ikx}$ , show that

$$\chi = \sum_k \hat{\chi}_k(y) e^{ikx - \alpha Z},$$

where

$$\alpha = \left( \frac{W^2}{4} + iku \right)^{1/2} - \frac{W}{2}. \quad (\ddagger)$$

By writing  $\frac{W^2}{4} + iku = (p + iq)^2$ ,  $p > 0$ , and defining the square root in  $(\ddagger)$  as having  $p > 0$ , show that  $\text{Re } \alpha > 0$  irrespective of the sign of  $W$ . How would you expect  $\Theta$  to behave over long time scales in this case?

4.6 The mass and momentum equations for atmospheric motion in the rotating frame of the Earth can be written in the form

$$\begin{aligned}\rho_t + \nabla \cdot [\rho \mathbf{u}] &= 0, \\ \rho \left[ \frac{d\mathbf{u}}{dt} + 2\boldsymbol{\Omega} \times \mathbf{u} \right] &= -\nabla p - \rho g \hat{\mathbf{k}},\end{aligned}$$

where  $(x, y, z)$  are local Cartesian coordinates at latitude  $\lambda = \lambda_0$ . What is the magnitude of  $\Omega$ ?

Scale the variables by writing

$$\begin{aligned}x, y \sim l, \quad z \sim h, \quad u, v \sim U, \quad w \sim \delta U, \quad t \sim \frac{l}{U}, \\ \rho \sim \rho_0, \quad T \sim T_0, \quad p = p_0 \bar{p}(z) + \rho_0 \Omega l \sin \lambda_0 P,\end{aligned}$$

where

$$\delta = \frac{h}{l}, \quad p_0 = \rho_0 g h = \frac{\rho_0 R T_0}{M},$$

and show that the horizontal components take the form

$$\begin{aligned}\varepsilon \frac{du}{dt} - f v &= -\frac{1}{\rho} P_x, \\ \varepsilon \frac{dv}{dt} + f u &= -\frac{1}{\rho} P_y,\end{aligned}$$

where

$$f = \frac{\sin \lambda}{\sin \lambda_0},$$

and give the definition of the Rossby number  $\varepsilon$ . Show that in a linear approximation,

$$f \approx 1 + \varepsilon \beta y,$$

where

$$\beta = \frac{l}{R_E} \frac{\cot \lambda_0}{\varepsilon} = O(1),$$

and  $R_E$  is Earth's radius.

The dimensionless pressure  $\Pi = p/p_0$ , density  $\rho$ , temperature  $T$  and potential temperature  $\theta$  in the atmosphere satisfy the relations

$$\rho = \frac{\Pi}{T}, \quad T = \theta \Pi^\alpha, \quad -\frac{\partial \Pi}{\partial z} = \rho,$$

where  $\alpha = \frac{R}{M_a c_p}$  is constant. Assuming that

$$\Pi = \bar{p} + \varepsilon^2 P, \quad \theta = \bar{\theta} + \varepsilon^2 \Theta,$$

and that  $\varepsilon \ll 1$ , deduce that  $\rho \approx \bar{\rho}(z)$ , and thence that

$$w = O(\varepsilon), \quad \bar{\rho}u \approx -P_y, \quad \bar{\rho}v \approx P_x.$$

Show also that consistency between the two forms of scaled pressure requires the definition of the velocity scale to be

$$U = \frac{4(\Omega l \sin \lambda_0)^3}{gh},$$

and determine this value, if  $l = 1,500$  m,  $\lambda_0 = 45^\circ$ ,  $g = 9.8$  m s<sup>-2</sup>,  $h = 8$  km.

Show that

$$\Theta \approx \bar{\theta}^2 \frac{\partial}{\partial z} \left[ \frac{P}{\bar{p}^{1-\alpha}} \right],$$

and by defining a stream function via  $P = \bar{\rho}\psi$  and assuming that  $\bar{\theta} \approx 1$ , deduce that  $\Theta \approx \psi_z$ , and hence deduce the *thermal wind equations*:

$$\frac{\partial u}{\partial z} = -\frac{\partial \Theta}{\partial y}, \quad \frac{\partial v}{\partial z} = \frac{\partial \Theta}{\partial x}.$$

4.7

4.8

4.9 The quasi-geostrophic potential vorticity equation is

$$\frac{d}{dt} \left[ \nabla^2 \psi + \frac{1}{\bar{\rho}} \frac{\partial}{\partial z} \left( \frac{\bar{\rho}}{S} \frac{\partial \psi}{\partial z} \right) \right] + \beta \psi_x = \frac{1}{\bar{\rho}} \frac{\partial}{\partial z} \left( \frac{\bar{\rho} H}{S} \right),$$

where  $\nabla^2 = \frac{\partial^2}{\partial x^2} + \frac{\partial^2}{\partial y^2}$ , and  $\bar{\rho}$ ,  $S$  and  $H$  are functions of  $z$ , the first two being positive. The horizontal material derivative is

$$\frac{d}{dt} = \frac{\partial}{\partial t} + u \frac{\partial}{\partial x} + v \frac{\partial}{\partial y}, \quad u = -\psi_y, \quad v = \psi_x.$$

In the Eady model of baroclinic instability, solutions to the QGPVE are sought in a channel  $0 < y < 1$ ,  $0 < z < 1$ , with boundary conditions

$$\frac{d}{dt} \psi_z = 0 \quad \text{at} \quad z = 0, 1, \quad \psi_x = 0 \quad \text{at} \quad y = 0, 1,$$

and it is supposed that  $\bar{\rho}$  and  $S$  are constant, and  $\beta = H = 0$ . Show that a particular solution is the zonal flow  $\psi = -yz$ , and describe its velocity field. By considering the thermal wind equations, explain why this is a meaningful solution.

By writing  $\psi = -yz + \Psi$  and linearising the equations, derive an equation for  $\Psi$ , and show that it has solutions

$$\Psi = A(z) e^{ik(x-ct)} \sin n\pi y,$$

providing

$$(z - c)(A'' - \mu^2 A) = 0, \\ (z - c)A' = A \quad \text{on} \quad z = 0, 1,$$

where you should define  $\mu$ .

Using the fact that  $x\delta(x) = 0$ , show that if  $0 < c < 1$ , the solution can be found as a Green's function for the equation  $A'' - \mu^2 A = 0$ .

Give a criterion for instability, and show that for the normal mode solutions in which  $A$  is analytic,

$$c = \frac{1}{2} \pm \frac{1}{\mu} \left\{ \left( \frac{\mu}{2} - \coth \frac{\mu}{2} \right) \left( \frac{\mu}{2} - \tanh \frac{\mu}{2} \right) \right\}^{1/2},$$

and hence show that the zonal flow is unstable if  $\mu < \mu_c$ , where

$$\frac{\mu}{2} = \coth \frac{\mu}{2},$$

and calculate this value. Deduce that the flow is unstable for  $S < S_c$ , and calculate  $S_c$ .

4.10

# Chapter 5

## Two-phase flows

Two-phase flow occurs in numerous situations in industry, as well as in nature. Two-phase flow refers to the coexistence of two phases of a substance in a flow. By a phase, we typically refer to the state of matter: gas, liquid or solid. And indeed typically (though not always) the phases are liquid and gas, as for example in the common occurrence of steam-water flows, or liquid and solid, as in flows of coal slurries or sediment-laden rivers, or gas and solid, as in fluidised bed reactors or explosive volcanic eruptions. But more generally we refer to two-phase flows as occurring in the flow of two different *substances*: for example, the flow of oil and water in an oil well is a two-phase flow. Actually, in that case there may also be gas, so that one has a *three-phase flow*.

In some of these examples, *phase change* is important. For example in boilers, water is heated as it flows through a bank of channels, until it starts to boil. This leads to a two-phase flow region until (possibly) *dryout* occurs, and the flow is of superheated steam. The boundaries which physically divide the various régimes are called the *boiling boundary* and the *superheat boundary*.

A similar situation occurs in nuclear reactors where liquid sodium is commonly used as a coolant. Here it is important that dryout does not occur, since the insulating properties of vapour reduce the cooling efficiency of the flow. Two-phase flow also occurs in condensers, where superheated steam is cooled through the reverse sequence of two-phase and then sub-cooled regions.

Natural examples of two-phase flows include volcanic eruptions, where a variety of such flows can occur, for example ash flows (gas/solid), and Strombolian eruptions, where dissolved gases are exsolved as the magma rises (and loses pressure), so that the erupting flow is of a gas/liquid mixture.

Examples such as those above commonly involve turbulent flow, which brings its own complications, but already dictates the use of some form of averaging, and we shall see that averaging is essential to a useful description of two-phase flow. But there are also examples of slow two-phase flows in which inertia is not important, but averaging in some fashion still occurs. The simplest, slightly trivial example is that of unsaturated flow in groundwater (see chapter 2); trivial, because one commonly ignores the motion of the second phase (air). But the use of Darcy's law for the pore

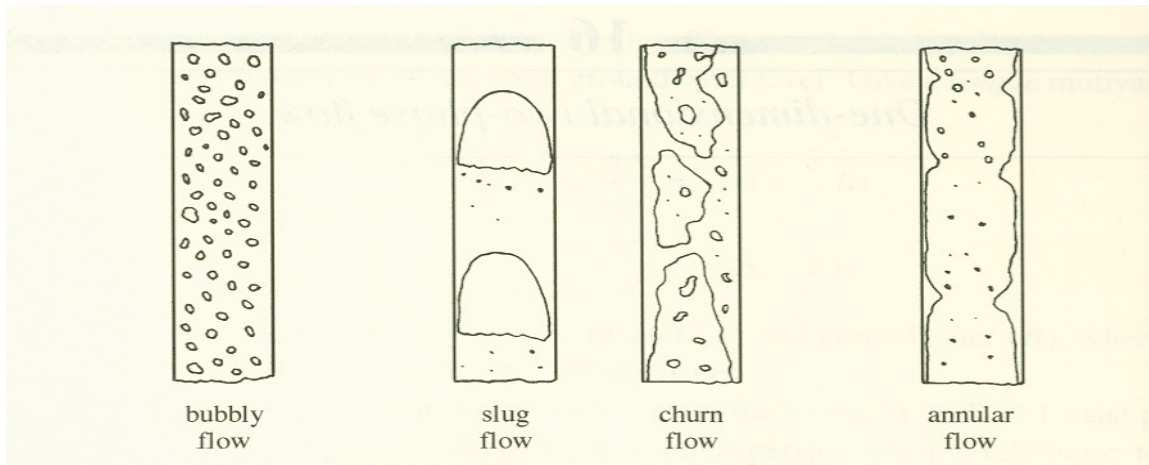


Figure 5.1: Flow patterns in vertical flow.

fluid momentum is already an example of the use of averaging; indeed, one can *derive* Darcy’s law by the use of homogenisation, which is a form of spatial averaging (see section 2.1.1 on page 28).

Important slow two-phase flows occur in the ubiquitous formation of ‘mushy zones’ in solidification processing of alloys; but the same process occurs during the formation of sea ice. Another such example is in the formation and transport of magma deep within the Earth. Both these examples involve phase change (as do steam/water flows), and their modelling consequently involves the use of the energy equation in quite unexpected ways.

## 5.1 Flow régimes

Modelling two-phase flow is complicated by a variety of factors. For a start, the distribution of phases means that averaging must be done so that average variables such as void fraction can be defined. (This is analogous to the definition of variables such as porosity in permeable media.)

A further complication is that confined turbulent two-phase flows can exist in a variety of régimes, all of which will generally occur in a boiling flow, for example. For the flow of an externally heated liquid in a tube (a common industrial example), boiling commences when small bubbles are nucleated at the wall, detach and are taken up by the fluid. Initially, the liquid away from the walls may still be *sub-cooled* (below boiling point), so that heat transfer to the vapour is predominantly at the wall. When the liquid reaches saturation (and in fact becomes slightly superheated), then this régime of *bubbly flow* evolves, by virtue of bubble coalescence and evaporation at the bubble interfaces, to the régime known as *slug flow*, in which plugs of gas filling the tube alternate with slugs of bubbly fluid. As the evaporation proceeds, the gas plugs become irregular, and one gets *churn flow*, which leads finally to *annular flow*,

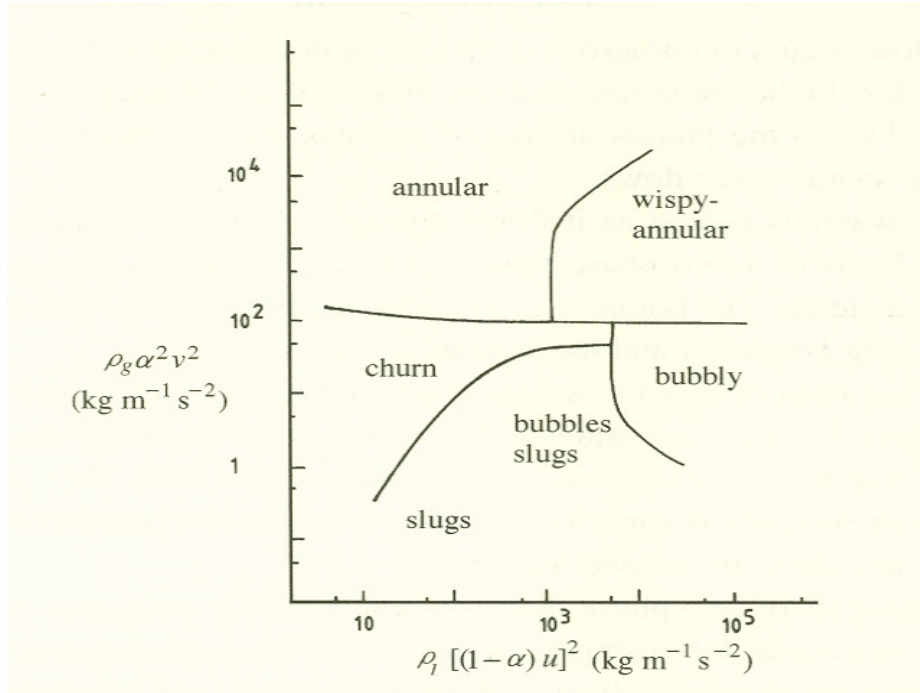


Figure 5.2: Flow régime map due to Hewitt and Roberts (1969).

in which the liquid is confined to a film at the tube wall, and the gas flows in the core. Shearing between the gas and the liquid causes droplets to be eroded and entrained in the gas. The sequence of flows is portrayed in figure 5.1. Various experimentally based laws to determine parametric criteria for which type of régime a particular flow will adopt lead to the construction of *flow régime maps*, an example of which is shown in figure 5.2. Such figures are entirely based on experiment, and there is little understanding of what causes the transition between the phases.

## 5.2 A simple two-phase flow model

Two-phase flow equations are averaged in various ways: in time, cross-sectionally, in space. Another method of averaging is the *ensemble average*, which is a conceptual average over different realisations of the flow. This in fact is the method of choice, as it avoids awkwardness (for example in time-averaging) of trying to separate what is rapidly fluctuating behaviour from the slower secular variation; ensemble averaging essentially appeals to the *ergodic hypothesis*<sup>1</sup> of chaotic behaviour in Hamiltonian

<sup>1</sup>The ergodic hypothesis is most easily framed in the context of the motion of a large number of perfectly elastic particles in a box (the hard-sphere gas) which interact via collision but otherwise move at constant velocity between collisions. It asserts that the time average of position and velocity of a single particle trajectory is equal to the instantaneous average of these quantities over all particles.

systems.

Let us begin by considering the simplest model for one-dimensional flow of gas and liquid in a tube. We seek relations for cross-sectionally averaged variables representing the two fluids. In keeping with the ergodic hypothesis, we might suppose that the cross-sectional average in itself incorporates a time or ensemble average. The variables of concern are the void fraction  $\alpha$ , which is the gas volume fraction;  $u$  and  $v$ , which are the liquid and gas velocities; and averaged pressures  $p_l$  and  $p_g$  for each phase. We take  $z$  to be the axial coordinate along the tube. As an example, we concentrate on air-water flow, for example, for which the viscous stresses are manifested through the wall friction, while the internal friction is largely due to *Reynolds stresses*; both of these terms must in general be constituted. In writing the simplest model (in order to examine its structure), we will in fact omit frictional terms for the moment. We also ignore gravity.

Ignoring surface tension, it superficially seems reasonable to take  $p_g = p_l = p$ , and then equations conserving mass and momentum of each phase are

$$\begin{aligned}
 (\alpha\rho_g)_t + (\alpha\rho_g v)_z &= 0, \\
 \{\rho_l(1-\alpha)\}_t + \{\rho_l(1-\alpha)u\}_z &= 0, \\
 \{\rho_l(1-\alpha)u\}_t + \{\rho_l(1-\alpha)u^2\}_z &= -(1-\alpha)p_z, \\
 (\alpha\rho_g v)_t + (\alpha\rho_g v^2)_z &= -\alpha p_z.
 \end{aligned} \tag{5.1}$$

Here,  $\rho_g$  and  $\rho_l$  are the gas and liquid densities, which themselves must be prescribed by equations of state. In keeping with our aim to keep things simple, we will take them as constant. These equations can be derived from first principles in the usual way. But there are hidden assumptions involved; in particular, we have made the assumption (in the acceleration terms) that the average of the square is equal to the square of the average. If the (ensemble) average velocity is cross-sectionally uniform, this is fine, but in practice it is inaccurate. One way to modify the equations is to introduce *profile coefficients*: we come back to these later. Another apparent oddity is the weighting of the pressure gradient, for example in the gas momentum equation, where instead of the term  $-\alpha p_z$ , we might expect to see  $-(\alpha p)_z$ . We return to this later when considering averaging.

The equations (5.1) represent four equations for the variables  $\alpha, u, v, p$ . These are simple generalisations of Euler's equations to the case of two-fluid motion. As commonly done, we can use the conservation of mass equations to simplify the momentum equations, and the model then takes the form (with the densities constant)

$$\begin{aligned}
 \alpha_t + (\alpha v)_z &= 0, \\
 -\alpha_t + \{(1-\alpha)u\}_z &= 0, \\
 \rho_l(u_t + uu_z) &= -p_z, \\
 \rho_g(v_t + vv_z) &= -p_z.
 \end{aligned} \tag{5.2}$$

## 5.2.1 Boundary conditions

In the absence of viscous terms, this system of four first order equations will have characteristics which we expect to be real, and we expect to apply initial conditions for  $\alpha, u, v$  at  $t = 0$ , and four boundary conditions. Thinking of how one might do an experiment, we might prescribe an outlet pressure, and then, if we imagine the two phases being supplied at the inlet from separate streams, we could apply  $\alpha, u$  and  $v$  there. In fact, the determination of  $p$  can obviously be uncoupled from the system, so that effectively it is a third order system, with  $p$  being determined by a quadrature. Actually, we can go further, since addition of the two mass conservation equations show that there is a first integral, so that in fact the system reduces to a second order system. On account of this, two of the characteristic speeds are infinite, corresponding to the instantaneous transmission of information which is implicit in a quadrature. Let us now calculate these.

## 5.2.2 Characteristics

The equations (5.2) can be written in the form

$$A\boldsymbol{\psi}_t + B\boldsymbol{\psi}_z = \mathbf{0}, \quad (5.3)$$

where  $\boldsymbol{\psi} = (\alpha, u, v, p)^T$  and, if  $\rho_g$  and  $\rho_l$  are constant,

$$A = \begin{pmatrix} 1 & 0 & 0 & 0 \\ -1 & 0 & 0 & 0 \\ 0 & \rho_l & 0 & 0 \\ 0 & 0 & \rho_g & 0 \end{pmatrix}, \quad B = \begin{pmatrix} v & 0 & \alpha & 0 \\ -u & 1 - \alpha & 0 & 0 \\ 0 & \rho_l u & 0 & 1 \\ 0 & 0 & \rho_g v & 1 \end{pmatrix}. \quad (5.4)$$

The characteristics  $\frac{dz}{dt} = \lambda$  are defined by the solutions of

$$\det(\lambda A - B) = 0. \quad (5.5)$$

The reason for this in general is as follows. We assume  $B^{-1}A$  is diagonalisable, as is generally the case. If  $P$  is the matrix of column eigenvectors of  $B^{-1}A$  satisfying

$$B^{-1}AP = PD^{-1}, \quad (5.6)$$

where  $D = \text{diag}(\lambda_i)$  ( $\lambda_i^{-1}$  are the eigenvalues of  $B^{-1}A$ ), then the substitution  $\boldsymbol{\psi} = P\mathbf{u}$  transforms (5.3) to

$$\mathbf{u}_t + D\mathbf{u}_z = -(P^{-1}P_t + DP^{-1}P_z)\mathbf{u}, \quad (5.7)$$

and thus each component satisfies an ordinary differential equation

$$\frac{du_i}{dt} = -[(P^{-1}P_t + DP^{-1}P_z)\mathbf{u}]_i \quad (5.8)$$

on the characteristic  $\frac{dz}{dt} = \lambda_i$ . This is all very well if the matrix multiplying  $\mathbf{u}$  on the right hand side does not involve derivatives of  $\mathbf{u}$ , but in general it will, since  $A$  and

$B$  and therefore  $P$  will generally depend on  $\mathbf{u}$ . The most familiar example is that of the shallow water equations, where it turns out (see question 5.2) that the matrix  $P$  is actually constant, so that in that case  $u_i$  is constant on its characteristic and is a Riemann invariant.

Even in that case, it does not help to solve the system except in simple cases, since the different characteristics have different directions, and generally  $\lambda_i$  is a function of all the  $u_j$ . But in general, the right hand side will depend also on derivatives of  $\mathbf{u}$ , so the equation (5.7) is even less useful. The problem is that the linear transformation from  $\boldsymbol{\psi}$  to  $\mathbf{u}$  is not the most appropriate one. Suppose more generally, that we define a transformation

$$\boldsymbol{\psi} = \mathbf{g}(\mathbf{u}) \quad (5.9)$$

for some vector function  $\mathbf{g}$ . If we define the Jacobian matrix  $G$  via

$$G_{ij} = \frac{\partial g_i}{\partial u_j}, \quad (5.10)$$

then  $\boldsymbol{\psi}_t = G\mathbf{u}_t$ ,  $\boldsymbol{\psi}_z = G\mathbf{u}_z$ , and thus applying (5.6) to (5.3) yields

$$P^{-1}G\mathbf{u}_t + DP^{-1}G\mathbf{u}_z = \mathbf{0}, \quad (5.11)$$

and thus we should choose the transformation  $\mathbf{g}(\mathbf{u})$  by solving  $G = P$ ; this gives a set of differential equations for each  $g_i$ . Specifically, we want

$$\frac{\partial g_i}{\partial u_j} = P_{ij}, \quad (5.12)$$

of which the solution is just

$$g_i = \int^{\mathbf{u}} P_{ij} du_j, \quad (5.13)$$

provided

$$\oint P_{ij} du_j = 0 \quad (5.14)$$

for each  $i$  and any closed loop in  $\mathbf{u}$  space. This can be effected by appropriate normalisation of the columns of  $P$ .

We do not pursue this further here, but simply take (5.5) as the recipe for the characteristics. Using (5.4), we then find that the eigenvalues  $\lambda$  must satisfy

$$\rho_g(1 - \alpha)(\lambda - v)^2 + \rho_l\alpha(\lambda - u)^2 = 0, \quad (5.15)$$

with the other two being infinite, as already mentioned. Hence

$$\lambda = \frac{u \pm isv}{1 \pm is}, \quad s = \left[ \frac{\rho_g(1 - \alpha)}{\rho_l\alpha} \right]^{1/2}. \quad (5.16)$$

It follows that there are two *complex* characteristics unless  $u = v$ . Consequently, the model is *ill-posed* as it stands. To see the practical effect of complex characteristics,

consider a uniform state  $\psi = \psi_0$ , subject to small perturbations proportional to  $\exp(\sigma t + ikz)$ . Such solutions exist if  $\sigma = ik\lambda = \mp k\lambda_I + ik\lambda_R$ , where  $\lambda = \lambda_R \pm i\lambda_I$  represents (5.16). Thus if  $\lambda_I \neq 0$ , there are unstable solutions, moreover these grow arbitrarily fast at very short wavelengths. These grid scale instabilities are a practical sign of an ill-posed problem.

So, this model is *wrong*, although it seems to be based on sound physical principles. What is the matter? Well, there are various simple fixes. Inserting profile coefficients in the momentum flux terms is one. But there is something more fundamental than this. In the present formulation, the two phases exert no influence on each other, they are not aware of each other, and this is not right. If one phase moves relative to the other, there will be an interfacial drag, and there will be acceleration terms between the phases. The interfacial drag does not affect ill-posedness, but the interphasic acceleration terms (called virtual mass terms) may do, as they involve derivatives of the variables.

The other important issue is the assumption of constant pressures. We have already seen in chapter 2 that in unsaturated groundwater flow, the air and water pressures differ by a suction which depends on the water volume fraction, or in that in consolidation theory, that the effective pressure (which is the difference between the overburden pressure and the pore pressure) is a function of porosity; moreover, these descriptions are essential to the integrity of the model. A similar concept is likely to be generally the case.

### 5.2.3 Modifications

One possible resolution of the issue of ill-posedness lies in the inclusion of a number of terms which have been neglected in (5.1), and which should be included in more realistic models. We now introduce some of these, although where they come from must wait till we consider the formal process of averaging in section 5.3. We will continue to focus on gas-liquid mixtures, and will assume the liquid density  $\rho_l$  is constant, but allow the possibility of variable gas density  $\rho_g$ . We now present an elaboration of (5.1), and will then discuss the added terms in sequence. The model is

$$\begin{aligned}
(\rho_g \alpha)_t + (\rho_g \alpha v)_z &= \Gamma, \\
\rho_l [-\alpha_t + \{(1 - \alpha)u\}_z] &= -\Gamma, \\
\rho_l \{(1 - \alpha)u\}_t + \rho_l \{D_l(1 - \alpha)u^2\}_z &= -(1 - \alpha) \frac{\partial p_l}{\partial z} - (1 - \alpha) \rho_l g + M - F, \\
(\rho_g \alpha v)_t + (\rho_g \alpha v^2)_z &= -\alpha \frac{\partial p_g}{\partial z} - \alpha \rho_g g - M.
\end{aligned} \tag{5.17}$$

There are in fact other terms one can include, but these are the most important in practice. We now consider them in turn.

## Phase change

The first extra term in the two conservation of mass equations is the source term  $\Gamma$ ; this represents change of phase, and is of importance in a number of practical situations, such as steam-water flows, where due to external heating, the water boils. This, evidently, is what happens in a boiler. Phase change is of importance in other two-phase systems, such as the convective motion of clouds, solidification of alloys (section ?? and the degassing flow in volcanic vents (section ??). The question in a boiling flow is then, what determines  $\Gamma$ ? As one might expect, this involves an appropriate form of the energy equations, and this is discussed in section 5.2.5.

## Profile coefficients

We have already mentioned profile coefficients. These arise in averaging, because the formulation in (5.1) assumes implicitly that the velocity profiles are *plug flow*, i. e., constant across the cross section. This is generally not the case, particularly for the liquid (continuous) phase, and the quantity  $D_l$  in (5.17)<sub>3</sub> indicates this. It is naturally greater than one in practice.

## Gravity

Obviously, (5.1) had no gravitational acceleration, and equally obviously, this should be included. Although the equations of the model can equally apply to flow in an inclined channel, in which case  $g$  would be the downstream component of gravity, we will focus here on a vertical channel. Sub-horizontal two-phase flow is important in oil pipelines, for example, and the corresponding régime diagrams are different, but the same general precepts apply.

## Interfacial drag

The most obvious apparent feature of a two-phase flow is that there is a drag between the phases. Generally this is manifested in two ways: viscous friction at the interface generates an interfacial drag, and this is denoted by the term  $M$  in the model. Particularly for gas bubbles in liquid, one would suppose that this term is small, but in practice it is commonly assumed that the flow is turbulent, so that the frictional effects are manifested by Reynolds stresses. One particular constitutive assumption which embodies this is to take

$$M = \frac{3C_D\alpha\rho_l|v-u|(v-u)}{4d_B} \quad (5.18)$$

for bubbly flow, where  $C_D$  is a drag coefficient and  $d_B$  is bubble diameter, and other such prescriptions are available for other flow régimes.

The other effect of obstruction of each phase by the other is a purely inviscid one. If a bubble moves through a fluid, the fluid must be displaced, and this requires work to be done. In the averaged equations, this effect is manifested by various terms, and

in particular *virtual mass* terms. They are not shown in (5.17) but will be included in later versions of the model.

### Wall friction

The final added term in (5.17) is the wall friction term  $F$ . For flow in a tube, this represents the effect of turbulent friction at the wall. Most flow régimes have liquid at the wall, and so this term is present only in the liquid momentum equation. A common prescription is to take

$$F = \frac{4f\rho_l u^2}{d}, \quad (5.19)$$

where  $d$  is the tube diameter and  $f$  is a friction factor, usually small (it is dimensionless). The form of  $F$  arises for the following reason: the original form of the liquid momentum equation as a cross-sectional average is

$$\{\rho_l A(1 - \alpha)u\}_t + \dots = \dots - C\tau, \quad (5.20)$$

where  $A$  is the cross-sectional area,  $C$  is the circumferential length, and  $\tau$  is the wall stress. The choice  $\tau = f\rho_l u^2$  is a common assumption in turbulent flows, and the factor  $\frac{4}{d}$  is just  $\frac{C}{A}$ .

### 5.2.4 Constitution of the pressures

In some circumstances, it is essential to take differing values of the two phasic pressures, to represent the idea that even in the absence of relative motion, a differential pressure will be related to a change of volume fraction. We will illustrate this for a bubbly flow using a description in Batchelor's (1967) book, not because it is particularly significant in that case, but because it is in other situations such as magma transport (see section ??). It is also the only example I know of where a form of *bulk viscosity* can be *derived*, as opposed to postulated.

As is commonly the case in prescribing such constitutive relations, its form follows from a local description of the dynamics. We consider the motion of an incompressible fluid of viscosity  $\mu$  containing spherical bubbles of a compressible gas. If we consider one such bubble of radius  $a$ , with far-field pressure being  $p_l$  and the liquid being at rest there, and we suppose that the gas pressure  $p_g$  inside the bubble is uniform, then mass and momentum equations for the liquid are

$$\begin{aligned} \frac{\partial}{\partial r}(r^2 u) &= 0, \\ \rho_l(u_t + uu_r) &= -p_r + \mu \left( u_{rr} + \frac{2}{r}u_r - \frac{2}{r^2}u \right), \end{aligned} \quad (5.21)$$

where  $r$  is the spherical polar radius (measured from the centre of the bubble). It

follows that

$$\begin{aligned} u &= \frac{a^2 \dot{a}}{r^2}, \\ p_l - p &= \rho_l \left[ \frac{1}{2} u^2 - \frac{a^2 \dot{a}}{r} \right], \end{aligned} \quad (5.22)$$

and that the normal stress  $\sigma_{rr} = -p + 2\mu \frac{\partial u}{\partial r}$  is given by

$$p_l + \sigma_{rr} = \rho_l \left[ \frac{1}{2} u^2 - \frac{a^2 \dot{a}}{r} \right] - \frac{4\mu a^2 \dot{a}}{r^3}. \quad (5.23)$$

At the bubble wall, we require the normal stress  $\sigma_{rr} = -p_g - \frac{2\gamma}{a}$ , if we allow for a surface tension  $\gamma$ . It follows that

$$p_l - p_g = -\rho_l \left[ \frac{3}{2} \dot{a}^2 + a \ddot{a} \right] - \frac{4\mu \dot{a}}{a} - \frac{2\gamma}{a}. \quad (5.24)$$

If a fluid contains  $n$  bubbles of small diameter  $a$  per unit volume (which move with the fluid), so that the void fraction  $\alpha = \frac{4\pi n a^3}{3}$ , then since

$$\frac{d\alpha}{dt} = \nabla \cdot \mathbf{u} \quad (5.25)$$

(following the fluid), it follows that

$$\nabla \cdot \mathbf{u} = \frac{3\alpha \dot{a}}{a}, \quad (5.26)$$

and thus (5.24) provides a constitutive law giving  $p_l - p_g$  in terms of  $\alpha$  and  $\nabla \cdot \mathbf{u}$ . In the particular case that bubble size is sufficiently small and that surface tension can be ignored, this is just

$$p_l - p_g = -\kappa \nabla \cdot \mathbf{u}, \quad (5.27)$$

where

$$\kappa = \frac{4\mu}{3\alpha}. \quad (5.28)$$

This has the form of a bulk viscosity relation ( $\kappa$  is the bulk viscosity), and has the same interpretation as given by Batchelor, because the local thermodynamic equilibrium pressure is that at the interface,  $p_g$ , while the dynamic pressure is that in the far field,  $p_l$ . It is an appropriate choice when the liquid is very viscous (in the case of magma transport, the ‘liquid’ is actually a solid!).

For industrial scale flows, where we might take a tube height of 10 m, and thus a gravitational head of  $10^5$  Pa, assuming bubble sizes of 1 cm and a time scale of 1 s, the inertial and viscous terms in (5.24) are negligible, and the surface tension term is small, but becomes significant for smaller millimetre-sized bubbles.

When there is relative motion between bubbles and liquid, a potential flow calculation suggests

$$p_l - p_g = \xi \rho_l (v - u)^2, \quad (5.29)$$

where  $\xi \sim \frac{1}{4}$ . This relation is due to Stuhmiller (1977), and it can be added to the other terms in (5.24). It scales the pressure difference with the liquid acceleration, and is thus important in rapid flows.

### 5.2.5 Phase change and the energy equation

The phase change term in (5.17) is determined through consideration of energy conservation. Just as for mass and momentum, there will be two energy equations, one for each phase; and just as in the mass and momentum equations there will be an interfacial transport term which transports heat between the phases. This transport occurs if there is a difference between the local phasic average temperatures, and it is generally assumed that the corresponding heat transfer coefficient is so large that the two averaged temperatures are approximately equal. This being the case, it suffices to write a single energy equation for the whole mixture. It is a little awkward to do this. The form of energy conservation for a single phase fluid is

$$\frac{\partial}{\partial t} \left[ \frac{1}{2} \rho u^2 + \rho e + \rho \Phi \right] + \nabla \cdot \left[ \left\{ \frac{1}{2} \rho u^2 + \rho e + \rho \Phi \right\} \mathbf{u} \right] = \nabla \cdot (\boldsymbol{\sigma} \cdot \mathbf{u}) - \nabla \cdot \mathbf{q}, \quad (5.30)$$

Here  $e$  is the internal energy,  $\Phi$  is the potential energy, and  $\mathbf{q}$  is the heat flux. In the usual way (Fowler 2011, p. 819), the mass and momentum single-phase conservation laws can be used to simplify this to the form

$$\rho \frac{de}{dt} = \sigma_{ij} \dot{\epsilon}_{ij} - \nabla \cdot \mathbf{q}, \quad (5.31)$$

and thus also

$$\rho \left[ \frac{de}{dt} + p \frac{dv}{dt} \right] = \tau_{ij} \dot{\epsilon}_{ij} - \nabla \cdot \mathbf{q}, \quad (5.32)$$

where the specific volume is  $v = \frac{1}{\rho}$ . The viscous dissipation term  $\tau_{ij} \dot{\epsilon}_{ij}$  can generally be ignored, and if we introduce the enthalpy

$$h = e + pv, \quad (5.33)$$

this takes the approximate form (cf. (4.22))

$$\rho \frac{dh}{dt} - \frac{dp}{dt} = -\nabla \cdot \mathbf{q}. \quad (5.34)$$

The equation is useful in this form because the latent heat  $L$  is just defined as

$$L = h_g - h_l, \quad (5.35)$$

evaluated at the saturation temperature (boiling point, for example).

Averaging of the energy equation or, as we can now call it, the enthalpy equation, is awkward because of the adiabatic term  $\frac{dp}{dt}$ . Luckily, this term is commonly small. For example, for steam and water at around atmospheric pressure,  $L \sim 2.2 \times 10^6$  J kg<sup>-1</sup> and  $\rho_g \sim 0.6$  kg m<sup>-3</sup>, and thus  $\rho_g L \sim 1.3 \times 10^6$  Pa, and this is usually much larger than any applied pressure drop. If we then drop the adiabatic term and write (5.34) in the form

$$(\rho h)_t + \nabla \cdot (\rho h \mathbf{u}) = -\nabla \cdot \mathbf{q}, \quad (5.36)$$

it becomes amenable to averaging, as described in section 5.3. If we are simply concerned with the mixture energy equation, on the basis that the phase temperatures are the same, then we simply add weighted versions of (5.36), so that

$$\{\alpha \rho_g h_g + (1 - \alpha) \rho_l h_l\}_t + \nabla \cdot \{\alpha \rho_g h_g \mathbf{v} + (1 - \alpha) \rho_l h_l \mathbf{u}\} \approx Q, \quad (5.37)$$

where averaging of the heat transport over both phases simply gives the externally applied heat flux  $Q$  at the wall. The temperature is simply given by its saturation value, and although this will vary somewhat with pressure, the variation is usually small and can be ignored.<sup>2</sup> In this case we can take

$$h_l = h_{\text{sat}}, \quad h_g = h_{\text{sat}} + L, \quad (5.38)$$

and (5.37) reduces to the simple form

$$L [(\alpha \rho_g)_t + \nabla \cdot (\alpha \rho_g \mathbf{v})] = Q, \quad (5.39)$$

and thus simply

$$\Gamma = \frac{Q}{L}. \quad (5.40)$$

This simply says that all external heat supply is used in adding latent heat.

### 5.3 Averaging: two-fluid models

The formal process by which we derive equations for two-phase flow is by an appropriate method of averaging. Let us examine this process in greater detail. There are many different ways of approaching averaging, and here we follow that outlined by Drew and Wood (1985), or Drew (1983). The idea is to use indicator functions  $X_k$  for each phase (labelled by  $k$ ) such that  $X_k(\mathbf{x}, t) = 1$  if  $\mathbf{x}$  is in phase  $k$  at time  $t$ , and  $X_k = 0$  otherwise.  $X_k$  is an example of a *generalised function*, whose derivatives must be defined in a roundabout way, as discussed below. Averaged equations can be obtained by multiplying the pointwise conservation laws for phase  $k$  by  $X_k$ , and

---

<sup>2</sup>In fact, the Clapeyron equation gives the variation of the saturation temperature  $T_{\text{sat}}$  as  $\frac{\Delta T}{T_{\text{sat}}} = \frac{\Delta v \Delta p}{L} \approx \frac{v_g \Delta p}{L}$ , which is small when the adiabatic term is, as already assumed.

averaging. The question arises, what average is used? One naturally thinks of a spatial average, or a time average, but these have disadvantages as follows. Since we wish to define averages which are functions of space and time, averages must be local. For example, we could define the void fraction as

$$\alpha(\mathbf{x}, t) = \bar{X}_g \equiv \frac{1}{T} \int_{t-T}^t X_g(\mathbf{x}, t') dt', \quad (5.41)$$

which is a local time average. We could define a local space average similarly. The problem then is that time variation on scales less than  $T$  is suppressed, so there is an implicit assumption that there is an asymptotic separation between fluctuation time scales and macroscopic time scales, but how to determine this separation is unclear. So the preferred method is to in effect use the averaging which is used in statistical mechanics, which is an *ensemble average*. We mentioned this earlier. In a sense it is subject to the same criticism. In order to obtain an ensemble average (of a deterministic system), one assumes chaotic solutions (and thus the ergodic hypothesis) which seems reasonable, and then the averaging is done over the initial conditions. It is simplest to think of this in the absence of phase transition. Then a fluid element in each phase remains in that phase, and the element has a location  $\mathbf{x}(t, \boldsymbol{\xi})$  such that  $\mathbf{x}(0, \boldsymbol{\xi}) = \boldsymbol{\xi}$ . If the initial phase distribution is given by  $X_k = X_k^0(\boldsymbol{\xi})$ , then

$$X_k(\boldsymbol{\xi}, 0) = X_k^0(\boldsymbol{\xi}), \quad (5.42)$$

and the average is defined rather messily as

$$\alpha[\mathbf{x}(\boldsymbol{\xi}, t), t] = \bar{X}_g = \frac{1}{|N(\boldsymbol{\xi})|} \int_{N(\boldsymbol{\xi})} X_g[\mathbf{x}(\boldsymbol{\xi}', t), t] d\boldsymbol{\xi}', \quad (5.43)$$

where  $N(\boldsymbol{\xi})$  is some local neighbourhood of  $\boldsymbol{\xi}$ . The same issue arises, how large should this neighbourhood be, but the ergodic hypothesis suggests it can be indefinitely small, provided  $t$  is large enough. In practice, the details of averaging do not overtly appear in the description.

A typical conservation law has the form

$$\frac{\partial}{\partial t}(\rho\psi) + \nabla \cdot (\rho\psi\mathbf{v}) = -\nabla \cdot \mathbf{J} + \rho f. \quad (5.44)$$

Multiplying by  $X_k$  and averaging yields (the overbar denotes the average)

$$\begin{aligned} \frac{\partial}{\partial t}(\overline{X_k \rho \psi}) + \nabla \cdot [\overline{X_k \rho \psi \mathbf{v}}] &= -\nabla \cdot [\overline{X_k \mathbf{J}}] + \overline{X_k \rho f} \\ &+ \overline{\rho \psi \left\{ \frac{\partial X_k}{\partial t} + \mathbf{v}_i \cdot \nabla X_k \right\}} + \overline{\{\rho \psi (\mathbf{v} - \mathbf{v}_i) + \mathbf{J}\} \cdot \nabla X_k}, \end{aligned} \quad (5.45)$$

where we assume that  $\overline{\nabla f} = \nabla \bar{f}$ ,  $\frac{\partial \bar{f}}{\partial t} = \bar{\frac{\partial f}{\partial t}}$ , which will be the case for sufficiently well-behaved  $f$ . In (5.45),  $\mathbf{v}_i$  is the average interfacial velocity of the boundary of phase  $k$ , and derivatives of  $X_k$  are interpreted as generalised functions.

The type example of a generalised function  $\delta(x)$ , which is *defined* by the recipe

$$\int_{-\infty}^{\infty} \phi(x)\delta(x) dx = \phi(0) \quad (5.46)$$

for any smooth *test function* satisfying  $\phi(\pm\infty) = 0$ . More generally, such functions are defined in a similar way, by integration using test functions. As a particular example

$$\frac{\partial X_k}{\partial t} + \mathbf{v}_i \cdot \nabla X_k = 0, \quad (5.47)$$

since if  $\phi$  is any smooth test function vanishing at large values of  $\mathbf{x}$  and  $t$ , then

$$\begin{aligned} \iint \phi \left[ \frac{\partial X_k}{\partial t} + \mathbf{v}_i \cdot \nabla X_k \right] dV dt &= - \iint X_k \left[ \frac{\partial \phi}{\partial t} + \mathbf{v}_i \cdot \nabla \phi \right] dV dt \\ &= - \int_{-\infty}^{\infty} \int_{V_k(t)} \left[ \frac{\partial \phi}{\partial t} + \mathbf{v}_i \cdot \nabla \phi \right] dV dt \\ &= - \int_{-\infty}^{\infty} \frac{d}{dt} \int_{V_k(t)} \phi dV dt = - \left[ \int_{V_k(t)} \phi dV \right]_{-\infty}^{\infty} = 0. \end{aligned} \quad (5.48)$$

The last term in (5.45) is related to the interfacial surface average, since  $\nabla X_k$  picks out interfacial values. If  $\mathbf{w}$  is a function of  $\mathbf{x}$  and  $t$ ,  $\mathbf{w} \cdot \nabla X_k$  is defined via a test function  $\phi(\mathbf{x}, t)$  by

$$\int_V \phi \mathbf{w} \cdot \nabla X_k dV = - \int_V X_k \nabla \cdot (\phi \mathbf{w}) dV = - \int_{V_k} \nabla \cdot (\phi \mathbf{w}) dV = - \int_{S_k} \phi w_n dS, \quad (5.49)$$

where  $w_n$  is the normal component of  $\mathbf{w}$  at the interface, pointing *away* from phase  $k$ . This suggests that  $\overline{\mathbf{w} \cdot \nabla X_k}$  can be identified with the *surface* average of  $-\mathbf{w} \cdot \mathbf{n}$ .

Now put  $\psi = 1$ ,  $\mathbf{J} = \mathbf{0}$ ,  $f = 0$  in (5.44), corresponding to mass conservation. Then equations of conservation of mass of each phase are, from (5.45),

$$\frac{\partial}{\partial t} (\overline{X_k \rho}) + \nabla \cdot [\overline{X_k \rho \mathbf{v}}] = \overline{\rho(\mathbf{v} - \mathbf{v}_i) \cdot \nabla X_k}. \quad (5.50)$$

The form of (5.50) suggests that we define the average phase volume, density and velocity as follows:

$$\alpha_k = \overline{X_k}, \quad \rho_k = \frac{\overline{X_k \rho}}{\alpha_k}, \quad \mathbf{v}_k = \frac{\overline{X_k \rho \mathbf{v}}}{\alpha_k \rho_k}, \quad (5.51)$$

so that (5.50) gives

$$\frac{\partial}{\partial t} (\alpha_k \rho_k) + \nabla \cdot [\alpha_k \rho_k \mathbf{v}_k] = \Gamma_k, \quad (5.52)$$

where  $\Gamma_k = \overline{\rho(\mathbf{v} - \mathbf{v}_i) \cdot \nabla X_k}$ , and represents a mass source due to phase change (without which  $\mathbf{v} = \mathbf{v}_i$  at the interface).

Next, consider momentum conservation. With appropriate interpretation of tensor notation,<sup>3</sup> we put

$$\psi = \mathbf{v}, \quad \mathbf{J} = p\mathbf{I} - \boldsymbol{\tau}, \quad f = \mathbf{g}, \quad (5.53)$$

where  $\boldsymbol{\tau}$  is the deviatoric stress tensor,  $\mathbf{g}$  is gravity. Then

$$\begin{aligned} \frac{\partial}{\partial t}(\overline{X_k \rho \mathbf{v}}) + \nabla \cdot [\overline{X_k \rho \mathbf{v} \mathbf{v}}] = \\ \nabla \cdot [\overline{X_k (-p\mathbf{I} + \boldsymbol{\tau})}] + \overline{X_k \rho \mathbf{g}} + \overline{\{\rho \mathbf{v}(\mathbf{v} - \mathbf{v}_i) + (p\mathbf{I} - \boldsymbol{\tau})\} \cdot \nabla X_k}. \end{aligned} \quad (5.54)$$

Now  $\overline{X_k \rho \mathbf{v}} = \alpha_k \rho_k \mathbf{v}_k$ , and we would like to have  $\overline{X_k \rho \mathbf{v} \mathbf{v}} = \alpha_k \rho_k \mathbf{v}_k \mathbf{v}_k$ ; but evidently the latter is not the case. Since the flow is normally turbulent, this can be circumvented by separating  $\mathbf{v}$  (and, more generally  $\psi$ ) into mean and fluctuating parts, thus  $\mathbf{v} = \mathbf{v}_k + \mathbf{v}'_k$ , so that

$$\overline{X_k \rho \mathbf{v} \mathbf{v}} = \alpha_k \rho_k \mathbf{v}_k \mathbf{v}_k + \overline{X_k \rho \mathbf{v}'_k \mathbf{v}'_k}; \quad (5.55)$$

The second term can be interpreted as the averaged Reynolds stress. The momentum equation can thus be written as

$$\begin{aligned} \frac{\partial}{\partial t}(\alpha_k \rho_k \mathbf{v}_k) + \nabla \cdot [\alpha_k \rho_k \mathbf{v}_k \mathbf{v}_k] = \\ \nabla \cdot [\alpha_k (\mathbf{T}_k + \mathbf{T}'_k)] + \alpha_k \rho_k \mathbf{g} + \mathbf{M}_k + \mathbf{v}_{ki}^m \Gamma_k, \end{aligned} \quad (5.56)$$

where

$$\begin{aligned} \alpha_k \mathbf{T}_k &= \overline{X_k (-p\mathbf{I} + \boldsymbol{\tau})}, \\ \alpha_k \mathbf{T}'_k &= \overline{X_k \rho \mathbf{v}'_k \mathbf{v}'_k}, \\ \mathbf{M}_k &= \overline{(p\mathbf{I} - \boldsymbol{\tau}) \cdot \nabla X_k}, \\ \mathbf{v}_{ki}^m &= \frac{\overline{[\rho \mathbf{v}(\mathbf{v} - \mathbf{v}_i) \cdot \nabla X_k]}}{\overline{[\rho(\mathbf{v} - \mathbf{v}_i) \cdot \nabla X_k]}}. \end{aligned} \quad (5.57)$$

Evidently, the average pressure in phase  $k$  is  $p_k = \frac{\overline{X_k p}}{\alpha_k}$ . If we neglect viscous stresses, we can write the interfacial momentum source as

$$\mathbf{M}_k = \overline{p \nabla X_k} = p_{ki} \nabla \alpha_k + \mathbf{M}'_k, \quad (5.58)$$

where

$$\mathbf{M}'_k = \overline{(p - p_{ki}) \nabla X_k}, \quad (5.59)$$

$p_{ki}$  is the average interfacial pressure on phase  $k$ , and we use  $\overline{\nabla X_k} = \nabla \alpha_k$ . Thus the momentum equation can be written as

$$\begin{aligned} \frac{\partial}{\partial t}(\alpha_k \rho_k \mathbf{v}_k) + \nabla \cdot [\alpha_k \rho_k \mathbf{v}_k \mathbf{v}_k] = \\ -\alpha_k \nabla p_k - (p_k - p_{ki}) \nabla \alpha_k \\ + \nabla \cdot [\alpha_k \mathbf{T}'_k] + \alpha_k \rho_k \mathbf{g} + \mathbf{M}'_k + \mathbf{v}_{ki}^m \Gamma_k. \end{aligned} \quad (5.60)$$

---

<sup>3</sup>In particular, the tensor  $\mathbf{v} \mathbf{v}$  has components  $v_i v_j$ , and the divergence of a second rank tensor  $\boldsymbol{\sigma}$  with components  $\sigma_{ij}$  is the vector  $\mathbf{e}_i \frac{\partial \sigma_{ij}}{\partial x_j}$ .

Commonly, we might assume  $p_k = p_{ki}$  and the pressure term is explicitly  $-\alpha_k \nabla p_k$ . This explains why we took the pressure gradient terms in (5.1) in the form that we did.

### 5.3.1 Jump conditions

Before we consider particular forms for some of these interfacial average terms, we note that at the interface between the phases, the conservation laws imply jump conditions, and these too must be averaged. The averaged jump conditions provide some constraints on the interfacial averages. For the general purpose conservation law (5.44), the corresponding jump condition is

$$[\{\rho\psi(\mathbf{v} - \mathbf{v}_i) + \mathbf{J}\} \cdot \mathbf{n}_{12}]_1^2 = -m, \quad (5.61)$$

where  $m$  is the interfacial source of  $\psi$  and the unit normal  $\mathbf{n}_{12}$  points from phase 1 to phase 2. In mass conservation this will be zero, but for momentum it corresponds to surface tension. Since  $\mathbf{n}_{12} = -\frac{\nabla X_1}{|\nabla X_1|}$ , (5.61) takes the form, when averaged,

$$\left[ \overline{\{\rho\psi(\mathbf{v} - \mathbf{v}_i) + \mathbf{J}\} \cdot \nabla X_1} \right]_1^2 = \bar{m} \equiv \overline{m |\nabla X_1|}, \quad (5.62)$$

Applying this to the interfacial average terms in (5.52) and (5.56), it follows that

$$\begin{aligned} \sum \Gamma_k &= 0, \\ \sum \mathbf{M}_k + \mathbf{v}_{ki}^m \Gamma_k &= \bar{\mathbf{m}}, \end{aligned} \quad (5.63)$$

since of course  $\nabla X_2 = -\nabla X_1$  (and for the momentum equation,  $\mathbf{m}$  is a vector).

### 5.3.2 Constitutive laws

We have already indicated that the mass source term  $\Gamma_g = -\Gamma_l$  is determined, often quite simply, by the energy equation. It remains to constitute the various pressures in the momentum equations, along with the interfacial source terms. To provide a focus, we consider a gas-liquid bubbly flow as an example.

Commonly the phase change momentum velocity  $\mathbf{v}_{ki}$  is ignored on the basis that it is small, and we shall follow this assumption. Drew and Wood (1985) provide a parameterisation based on the work of Ishii (1975).

A natural assumption is to take

$$p_g = p_{gi} = p_{li} + \frac{2\gamma}{r_b}, \quad (5.64)$$

where  $\gamma$  is surface tension, and  $r_b$  is a suitable mean bubble radius. As mentioned earlier in (5.29), a representative prescription for the continuous phase pressure difference is

$$p_l - p_{li} = \xi \rho_l (v - u)^2. \quad (5.65)$$

It remains to constitute the interfacial drag terms  $\mathbf{M}'_k$ . We define

$$\bar{\mathbf{m}} = \frac{2\gamma \nabla \alpha}{r_b}, \quad (5.66)$$

and then with the above assumptions, (5.63) implies that the interfacial drag terms are equal and opposite,

$$\mathbf{M}'_g + \mathbf{M}'_l = \mathbf{0}. \quad (5.67)$$

The dispersed phase drag term  $\mathbf{M}'_g$  consists of several different parts, each of them a force per unit volume. Most straightforward is the actual interfacial drag, which at low bubble Reynolds number would be due to viscous stresses, but at higher relative velocities is due to Reynolds stresses at the bubble scale. In any event, we prescribe

$$\mathbf{M}'_g{}^D = \frac{3\alpha\rho_l C_D |\mathbf{v} - \mathbf{u}| (\mathbf{v} - \mathbf{u})}{8r_b}, \quad (5.68)$$

as we did earlier:  $C_D$  is the drag coefficient. Other flow régimes have different such prescriptions. There are other terms as well. The virtual mass force is

$$\mathbf{M}'_g{}^{VM} = C_{VM} \alpha \rho_l \left[ \left\{ \frac{\partial \mathbf{v}}{\partial t} + (\mathbf{v} \cdot \nabla) \mathbf{v} \right\} - \left\{ \frac{\partial \mathbf{u}}{\partial t} + (\mathbf{u} \cdot \nabla) \mathbf{u} \right\} \right]. \quad (5.69)$$

Other terms are the Faxén force, the lift force and the Basset force, but will not be discussed here. The interfacial drag term is then the sum of these forces, for example

$$\mathbf{M}_g = \mathbf{M}'_g{}^D + \mathbf{M}'_g{}^{VM}. \quad (5.70)$$

### 5.3.3 One-dimensional flows: cross-sectional averaging

For flow in a tube, with  $z$  being the axial coordinate. One can integrate the equations (5.52) and (5.56) over the cross-sectional area, and we end up with the one-dimensional model provided earlier. The additional integration provides a couple of extra features in the momentum equations. With  $\mathbf{k}$  being a unit vector in the  $z$ -direction, integration over a penny-shaped volume of cross-sectional area  $A$  and height  $\delta z$ , followed by taking the limit  $\delta z \rightarrow 0$ , leads to

$$\frac{\partial}{\partial t} \int_A \alpha_k \rho_k \mathbf{v}_k dA + \frac{\partial}{\partial z} \int_A \alpha_k \rho_k v_k \mathbf{v}_k dA = \int_{\partial A} \alpha_k (\mathbf{T}_k + \mathbf{T}'_k) \cdot \mathbf{n} ds + \dots, \quad (5.71)$$

where rather awkwardly we define the average upwards velocity to be  $v_k = \mathbf{v}_k \cdot \mathbf{k}$ . If we now take the axial component of this vector equation, we have the one-dimensional equation in the form

$$\frac{\partial}{\partial t} \int_A \alpha_k \rho_k v_k dA + \frac{\partial}{\partial z} \int_A \alpha_k \rho_k v_k^2 dA = \int_{\partial A} \alpha_k \mathbf{k} \cdot (\mathbf{T}_k + \mathbf{T}'_k) \cdot \mathbf{n} ds + \dots \quad (5.72)$$

The expression on the right is the wall stress, which we introduced in (5.19).

The other distinguishing feature in a wall-bounded one-dimensional flow is that there may be systematic cross-flow variation of the local mean velocity. We naturally define cross-sectional averages (with an overbar) as

$$\bar{\alpha}_k = \frac{1}{A} \int_A \alpha_k dA, \quad \bar{\alpha}_k \bar{\rho}_k = \frac{1}{A} \int_A \alpha_k \rho_k dA, \quad \bar{\alpha}_k \bar{\rho}_k \bar{v}_k = \frac{1}{A} \int_A \alpha_k \rho_k v_k dA, \quad (5.73)$$

but in general the advective term in (5.72) is not equal to  $A \bar{\alpha}_k \bar{\rho}_k \bar{v}_k^2$  as we would wish, unless  $v_k$  is uniform across the tube. For example, suppose that

$$v_k = 2\bar{v}_k(1 - r^2) \quad (5.74)$$

in a tube of unit radius; then  $\overline{v^2} = \frac{4}{3}\bar{v}^2$ . In general, we close the system by assuming that

$$\frac{1}{A} \int_A \alpha_k \rho_k v_k^2 dA = D_k \bar{\alpha}_k \bar{\rho}_k \bar{v}_k^2, \quad (5.75)$$

where  $D_k$  is known as a *profile coefficient*.

### Profile coefficients and well-posedness

Profile coefficients are one cosmetic way in which the ill-posedness of (5.2) can be removed. Let us adjust that model by writing

$$\begin{aligned} \alpha_t + (\alpha v)_z &= 0, \\ -\alpha_t + [(1 - \alpha)u]_z &= 0, \\ \rho_g(\alpha v)_t + \rho_g(D_g \alpha v^2)_z &= -\alpha p_z, \\ \rho_l[(1 - \alpha)u]_t + \rho_l[D_l(1 - \alpha)u^2]_z &= -(1 - \alpha)p_z. \end{aligned} \quad (5.76)$$

It will usually be appropriate to choose  $D_g = 1$ , but we allow  $D_l \neq 1$ . Then the last two of (5.76) can be written as

$$\begin{aligned} \rho_g[v_t + vv_z] &= -p_z, \\ \rho_l \left[ u_t + (2D_l - 1)uu_z - (D_l - 1) \left[ \frac{u^2}{1 - \alpha} \right] \alpha_z \right] &= -p_z, \end{aligned} \quad (5.77)$$

and the system can be written as (5.3) for  $\boldsymbol{\psi} = (\alpha, u, v, p)^T$ , with

$$A = \begin{pmatrix} 1 & 0 & 0 & 0 \\ -1 & 0 & 0 & 0 \\ 0 & \rho_l & 0 & 0 \\ 0 & 0 & \rho_g & 0 \end{pmatrix}, \quad B = \begin{pmatrix} v & 0 & \alpha & 0 \\ -u & (1 - \alpha) & 0 & 0 \\ -\frac{\rho_l(D_l - 1)u^2}{(1 - \alpha)} & \rho_l(2D_l - 1)u & 0 & 1 \\ 0 & 0 & \rho_g v & 1 \end{pmatrix}. \quad (5.78)$$

The characteristics  $\frac{dz}{dt} = \lambda$  satisfy  $\det(\lambda A - B) = 0$ , hence with  $s$  defined in (5.16),

$$(\lambda - u)^2 = \nu[u^2 + 2u(\lambda - u)] - s^2(\lambda - v)^2, \quad (5.79)$$

where  $\nu = D_l - 1$ . For small values of  $s$  and  $\nu$ , we see that  $\lambda$  is real provided

$$\nu > s^2(u - v)^2/u^2, \quad (5.80)$$

so that practically, a profile coefficient above one is sufficient to make the basic system have real characteristics, and hence be well-posed. Other possibilities to render the system well-posed can be chosen. In practice, any realistic model will (and *should*) be well-posed, otherwise it will be physically meaningless. This needs to be borne in mind when attempting numerical solution of the model.

### 5.3.4 Scaling the model

We return to the one-dimensional model (5.17):

$$\begin{aligned} (\rho_g \alpha)_t + (\rho_g \alpha v)_z &= \Gamma, \\ \rho_l[-\alpha_t + \{(1 - \alpha)u\}_z] &= -\Gamma, \\ \rho_l\{(1 - \alpha)u\}_t + \rho_l\{D_l(1 - \alpha)u^2\}_z &= -(1 - \alpha)\frac{\partial p_l}{\partial z} - (1 - \alpha)\rho_l g + M - F, \\ (\rho_g \alpha v)_t + (\rho_g \alpha v^2)_z &= -\alpha\frac{\partial p_g}{\partial z} - \alpha\rho_g g - M, \end{aligned} \quad (5.81)$$

where we take (cf. (5.70))

$$M = \frac{3C_D \alpha \rho_l |v - u|(v - u)}{4d_B} + C_{VM} \alpha \rho_l (\dot{v} - \dot{u}), \quad (5.82)$$

and we have written

$$\dot{v} = v_t + vv_z, \quad \dot{u} = u_t + uu_z. \quad (5.83)$$

The wall friction is

$$F = \frac{4f\rho_l|u|u}{d}, \quad (5.84)$$

and we suppose the pressure relations

$$p_l - p_{li} = \xi\rho_l(v - u)^2, \quad (5.85)$$

and

$$p_g = p_{gi} = p_{li} + \frac{2\gamma}{r_b^* \alpha^{1/3}}, \quad (5.86)$$

where  $r_b^*$  is a maximal bubble radius and  $\gamma$  is the surface tension.

Now we scale the equations (for bubbly flow) as follows:

$$u, v \sim U, \quad z \sim l, \quad t \sim \frac{l}{U}, \quad p - p_a \sim \rho_l g l, \quad \Gamma \sim \frac{\rho_g U}{l}, \quad (5.87)$$

We take  $\rho_l$  and  $\rho_g$  to be constant, and define their ratio to be

$$\delta = \frac{\rho_g}{\rho_l}, \quad (5.88)$$

and this is normally small. Since  $\Gamma = \frac{Q}{L}$  is prescribed, we could sensibly use the  $\Gamma$ -scaling to define  $U$ ; here, however, we suppose  $U$  is determined from the inlet boundary condition, for example. The resulting dimensionless model can be written in the form

$$\begin{aligned} \alpha_t + (\alpha v)_z &= \Gamma, \\ -\alpha_t + \{(1 - \alpha)u\}_z &= -\delta\Gamma, \\ F^2 [\{(1 - \alpha)u\}_t + \{D_l(1 - \alpha)u^2\}_z] &= -(1 - \alpha) \left[ p_z + 1 - \sigma \left( \frac{1}{\alpha^{1/3}} \right)_z + \xi F^2 \{(v - u)^2\}_z \right] \\ &\quad + \frac{\Lambda |v - u|(v - u)}{\alpha^{1/3}} - \kappa |u|u + C_{VM} F^2 \alpha (\dot{v} - \dot{u}), \\ \delta F^2 \{(\alpha v)_t + (\alpha v^2)_z\} &= -\alpha p_z - \delta \alpha - \frac{\Lambda |v - u|(v - u)}{\alpha^{1/3}} - C_{VM} F^2 \alpha (\dot{v} - \dot{u}), \end{aligned} \quad (5.89)$$

where

$$F^2 = \frac{U^2}{gl}, \quad \Lambda = \frac{3C_D l}{8r_b^*} F^2, \quad \kappa = \frac{4fl}{d} F^2, \quad \sigma = \frac{2\gamma}{\rho_g g l r_b^*}. \quad (5.90)$$

To get some idea of the size of these parameters, we use laboratory scale values  $U \sim 1 \text{ m s}^{-1}$ ,  $l \sim 10 \text{ m}$ ,  $g \sim 10 \text{ m s}^{-2}$ ,  $d \sim 0.1 \text{ m}$ ,  $r_b^* \sim 0.01 \text{ m}$ ,  $\rho_l \sim 10^3 \text{ kg m}^{-3}$ ,  $\rho_g \sim 1 \text{ kg m}^{-3}$ ,  $C_{VM}, C_D, \xi \sim 1$ ,  $\gamma \sim 70 \text{ mN m}^{-1}$ ,  $f \sim 0.01$ , and then

$$\delta \sim 10^{-3}, \quad F^2 \sim 10^{-2}, \quad \Lambda \sim 10, \quad \kappa \sim 4 \times 10^{-2}, \quad \sigma \sim 10^{-4}. \quad (5.91)$$

These are all small, apart from  $\Lambda$ , and neglecting the small terms leads to the simplified system

$$\begin{aligned} \alpha_t + (\alpha v)_z &= \Gamma, \\ -\alpha_t + \{(1 - \alpha)u\}_z &= 0, \\ 0 &= -(1 - \alpha)(p_z + 1) + \frac{\Lambda |v - u|(v - u)}{\alpha^{1/3}}, \\ 0 &= -\alpha p_z - \frac{\Lambda |v - u|(v - u)}{\alpha^{1/3}}. \end{aligned} \quad (5.92)$$

This is now easily solved. We find

$$p_z = -(1 - \alpha), \quad v - u = \alpha^{2/3} \left( \frac{1 - \alpha}{\Lambda} \right)^{1/2},$$

$$u = u_0 + \Gamma(z - r) - \alpha^{5/3} \left( \frac{1 - \alpha}{\Lambda} \right)^{1/2}, \quad (5.93)$$

where  $r$  and  $u_0$  are suitable functions of  $t$ , and then  $\alpha$  satisfies the first order equation

$$\alpha_t + q_z = \Gamma, \quad q = \alpha \{u_0 + \Gamma(z - r)\} + \frac{\alpha^{5/3}(1 - \alpha)^{3/2}}{\sqrt{\Lambda}}, \quad (5.94)$$

which can be examined using the method of characteristics.

One issue in the above reduction is that the pressure drop is bounded; in fact it is hydrostatic, in terms of the mixture density. This precludes applying a pressure drop to the system which is larger than hydrostatic, which seems wrong. A possible resolution is that for such large applied pressure drops, the wall friction becomes significant, and in fact such an assumption then determines the velocity scale.

### 5.3.5 Homogeneous and drift-flux models

There are two commonly used two phase flow models other than the two-fluid model. The homogeneous model is motivated by the observation that the interfacial friction parameter

$$\Lambda = \frac{3C_D U^2}{8gr_b^*} \quad (5.95)$$

is relatively large if the bubble size is small. In this case (5.93) implies that  $v \approx u$  and it suffices to consider equations of total mass and momentum of the mixture, thus

$$\rho_t + (\rho u)_z = 0,$$

$$\rho[u_t + uu_z] = -p_z - \rho g - \frac{4f\rho_l|u|u}{d}, \quad (5.96)$$

in which the mixture density is

$$\rho = \alpha\rho_g + (1 - \alpha)\rho_l. \quad (5.97)$$

The ‘equation of state’ for this model follows from the enthalpy equation, which we take to be

$$\rho \frac{dh}{dt} = Q, \quad (5.98)$$

again neglecting the adiabatic term. Here the mixture enthalpy is defined by

$$\rho h = \alpha\rho_g h_g + (1 - \alpha)\rho_l h_l, \quad (5.99)$$

bearing in mind that also  $h_g - h_l = L$ , the latent heat.

## Drift-flux model

The *drift-flux model* allows a relative motion, but rather than have separate momentum equations, it considers total momentum conservation in the form

$$[\alpha\rho_g v + (1 - \alpha)\rho_l u]_t + [\alpha\rho_g v^2 + (1 - \alpha)\rho_l u^2]_z = -p_z - \rho g - \frac{f\rho_l|u|u}{d}, \quad (5.100)$$

and similarly the total enthalpy equation is (ignoring the adiabatic terms)

$$[\alpha\rho_g h_g + (1 - \alpha)\rho_l h_l]_t + [\alpha\rho_g v h_g + (1 - \alpha)\rho_l u h_l]_z = Q. \quad (5.101)$$

One could additionally add profile coefficients. There are, however, two mass conservation equations

$$\begin{aligned} (\alpha\rho_g)_t + (\alpha\rho_g v)_z &= \Gamma, \\ \rho_l [-\alpha_t + \{(1 - \alpha)u\}_z] &= -\Gamma, \end{aligned} \quad (5.102)$$

and the extra velocity is prescribed by a constitutive law for the *drift flux*

$$V = (1 - \alpha)(v - u), \quad (5.103)$$

commonly as a function of  $\alpha$ . This is essentially equivalent to the reduction in (5.93). This is rather akin to the status of Darcy's law.

### 5.3.6 A simple model for annular flow

Annular flows occur when the gas superficial velocity is large enough (see figure 5.2), and in this section we non-dimensionalise a suitable model for this régime. Because annular flows commonly occur in boilers, for example, we will include a more elaborate discussion of the enthalpy equations; in particular, we consider enthalpy equations for each phase, because the liquid must be superheated in order that boiling occur at the interface.

To do this, we return to the averaging procedure. We will, however, continue to ignore the adiabatic term in the enthalpy equation. In this case, the basic conservation law is (5.36), and putting  $\psi = h$  and  $\mathbf{J} = \mathbf{q}$  in (5.44), we are led in essentially the same way as for the momentum equation to the phase-averaged enthalpy equations

$$\frac{\partial}{\partial t}(\alpha_k \rho_k h_k) + \nabla \cdot [\alpha_k \rho_k h_k \mathbf{v}_k] = -\alpha \nabla \cdot [\alpha_k (\mathbf{q}_k + \mathbf{q}'_k)] + E_k + h_{ki} \Gamma_k, \quad (5.104)$$

where  $E_k$  is the interfacial heat transfer, and  $h_{ki} \Gamma_k$  is the interfacial enthalpy flux; these are defined by

$$E_k = \overline{\mathbf{q} \cdot \nabla X_k}, \quad h_{ki} \Gamma_k = \overline{\rho h (\mathbf{v} - \mathbf{v}_i) \cdot \nabla X_k}; \quad (5.105)$$

the turbulent energy flux is defined similarly to the Reynolds stress as

$$\mathbf{q}'_k = \overline{X_k \rho h'_k \mathbf{v}'_k}, \quad (5.106)$$

where we have written  $h = h_k + h'_k$  in phase  $k$ . Associated with (5.104) is the jump condition

$$E_g + E_l + L\Gamma = 0, \quad (5.107)$$

where the latent heat  $L = h_{gi} - h_{li}$ .

Unless we are in a geological (large scale) situation where the saturation temperature changes appreciably with pressure (for example, this may be relevant in a volcanic conduit), we may take the temperature to be almost constant, so that the heat flux terms  $\mathbf{q}_k$  and  $\mathbf{q}'_k$  will be neglected. The terms  $E_k$  represent heat transfer to the interface, and are commonly represented in the form

$$E_k = H_k(T_i - T_k), \quad (5.108)$$

where  $T$  is temperature and  $H_k$  are heat transfer coefficients. These are large, which is why one normally takes the temperature in the phases to be equal, but we retain the separate temperatures for the moment. In an annular flow, the gas velocity is much larger than that of the liquid, so we take  $E_g = 0$ ; the jump condition then simply prescribes the degree of superheat in the liquid. Specifically,

$$T_l = T_i + \frac{L\Gamma}{H_l}. \quad (5.109)$$

We will assume that this superheat is small, for which the criterion is that the excess sensible heat is small compared to the latent heat, thus  $H_l \gg c_{pl}\Gamma$ , where  $c_{pl}$  is the specific heat of the liquid. It then follows that our earlier discussion is appropriate, and the enthalpy equations simply combine to give

$$\Gamma = \frac{Q}{L}, \quad (5.110)$$

as in (5.40).

We now write  $\alpha$  and  $\beta$  as gas and liquid volume fractions (thus  $\beta = 1 - \alpha$ ), and we write a two-fluid model in the form

$$\begin{aligned} (\alpha\rho_g)_t + (\alpha\rho_g v)_z &= \Gamma, \\ (\beta\rho_l)_t + (\beta\rho_l u)_z &= -\Gamma, \\ (\beta\rho_l u)_t + (D_l\beta\rho_l u^2)_z &= -\beta p_z - \beta\rho_l g - F_{lw} + F_{li}, \\ (\alpha\rho_g v)_t + (\alpha\rho_g v^2)_z &= -\alpha p_z - \alpha\rho_g g - F_{li}, \end{aligned} \quad (5.111)$$

where we assume equal pressures, and ignore virtual mass terms.

The main distinction between this and bubbly flow is that the gas velocity is much larger than the liquid velocity, and the interfacial drag term is different. By analogy with the wall friction term we discussed earlier, we choose

$$\begin{aligned} F_{lw} &= \frac{4}{d} f_{lw} \rho_l |u| u, \\ F_{li} &= \frac{4\sqrt{\alpha}}{d} f_{li} \rho_g |v - \chi u| (v - \chi u). \end{aligned} \quad (5.112)$$

The factor  $\sqrt{\alpha}$  accounts for the smaller cross section of the gas core; the coefficient  $\chi$  ( $\approx 2$ ) accounts for the fact that interfacial waves, called *disturbance waves*, commonly occur on the interface, so that the friction exerted on the gas core is primarily due to the resistance which they offer.  $\chi u$  is the speed of these waves.

### Nondimensionalisation

In the following, we take  $\rho_g$  and  $\rho_l$  as constants for simplicity. We scale the variables by writing

$$z \sim l, \quad u \sim U, \quad v \sim V, \quad p - p_a \sim P, \quad \beta \sim B, \quad t \sim \frac{l}{U}, \quad (5.113)$$

where the scales  $U, V, P$  and  $B$  are chosen by balancing the following terms:

$$(\alpha\rho_g v)_z \sim \Gamma \sim (\beta\rho_l u)_z, \quad F_{lw} \sim F_{li} \sim \alpha p_z; \quad (5.114)$$

this leads to

$$V = \frac{\Gamma l}{\rho_g}, \quad U = \left( \frac{\delta f_{li}}{f_{lw}} \right)^{1/2} V, \quad B = \frac{\delta V}{U}, \quad P = \frac{4l f_{li} \rho_g V^2}{d}, \quad (5.115)$$

where we define

$$\delta = \frac{\rho_g}{\rho_l}. \quad (5.116)$$

For simplicity we will also take

$$f_{li} = f_{lw} = f, \quad (5.117)$$

say, which implies

$$\frac{U}{V} = \sqrt{\delta}, \quad B = \sqrt{\delta}, \quad (5.118)$$

and then we obtain the dimensionless set

$$\begin{aligned} -\delta\beta_t + \{(1 - \sqrt{\delta}\beta)v\}_z &= 1, \\ \beta_t + (\beta u)_z &= -1, \\ \delta^{3/2}\Pi[(\beta u)_t + D_l(\beta u^2)_z] &= -\sqrt{\delta}\beta p_z - \sqrt{\delta}G\beta - |u|u \\ &\quad + |v - \chi\sqrt{\delta}u|(v - \chi\sqrt{\delta}u), \\ \Pi \left[ \sqrt{\delta}\{(1 - \sqrt{\delta}\beta)v\}_t + \{(1 - \sqrt{\delta}\beta)v^2\}_z \right] &= -(1 - \sqrt{\delta}\beta)p_z - \delta G(1 - \sqrt{\delta}\beta) \\ &\quad - |v - \chi\sqrt{\delta}u|(v - \chi\sqrt{\delta}u), \end{aligned} \quad (5.119)$$

where the extra parameters are defined by

$$\Pi = \frac{d}{4fl}, \quad G = \frac{gd}{4fU^2} = \frac{\Pi}{F^2}, \quad F^2 = \frac{U^2}{gl}. \quad (5.120)$$

The aspect ratio  $\frac{d}{l}$  is small, but so also is the friction factor  $f$ , with orders of magnitude for each of  $10^{-2}$  being relevant. So the parameter  $\Pi$  could be large or small, but generally it is reasonable to take it as being  $O(1)$ . Earlier we proposed that the ‘Froude’ number  $F$  was small in the case of bubbly flow, which would suggest  $G$  is large, but in the case of annular flow this depends on the size of the liquid velocity, which in industrial contexts (at high ambient pressure) may be a good deal higher than we presumed earlier. So we will suppose that also  $G \sim O(1)$ , although relaxation of this assumption is easily made.

### Simplification

With the assumption that  $\delta \ll 1$ , we neglect all the corresponding terms in (5.119), and thus we have the reduced system

$$\begin{aligned} v_z &= 1, \\ \beta_t + (\beta u)_z &= -1, \\ 0 &= -|u|u + |v|v, \\ \Pi(v^2)_z &= -p_z - |v|v, \end{aligned} \tag{5.121}$$

and these are easily solved. If  $v = v_0$  and  $\beta = \beta_0$  at  $z = 0$ , then

$$v = u = v_0 + z, \tag{5.122}$$

so that

$$\beta_t + \{(v_0 + z)\beta\}_z = -1, \tag{5.123}$$

and the pressure drop down the tube (of dimensionless length 1) is

$$\Delta p = \Pi(1 + 2v_0) + v_0^2 + v_0 + \frac{1}{3}. \tag{5.124}$$

(5.123) is easily solved using characteristics. In the characteristic  $(z, t)$  space, there is a small time transient region in which the initial condition for  $\beta$  is used, and thereafter the inlet condition is used. If the inlet condition is constant, then this is just the steady solution

$$\beta = \frac{\beta_0 v_0 - z}{v_0 + z}, \tag{5.125}$$

and dryout occurs at  $z = \beta_0 v_0$ .

It should be noted that this approximate solution does not allow prescription of an inlet velocity condition for  $u$ ; this is because of the loss of the acceleration terms, which constitute a singular perturbation: satisfaction of an inlet condition for  $u$  requires an inlet boundary layer where the acceleration terms are important. It should also be noted that in the common situation where a pressure drop rather than an inlet velocity is prescribed, (5.124) indicates a minimum pressure drop for which the above solution is valid. For lower pressure drops, other terms must become important, or else the annular régime can not be maintained.

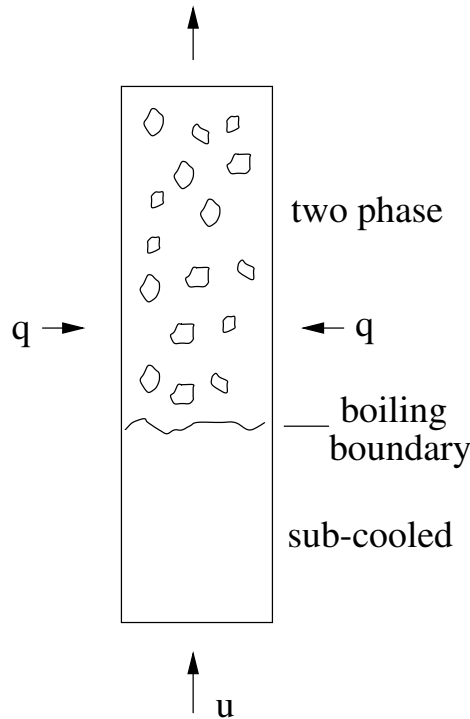


Figure 5.3: Geometry of heated flow in a boiler tube.

### 5.3.7 Disturbance waves

## 5.4 Density wave oscillations

Density wave oscillations in two phase flow have been of concern in the nuclear industry for a long time. In a steam generating boiler, water in an array of pipes is heated externally, and begins to boil as it flows along the pipes. In certain situations, the resulting two phase flow can be oscillatorily unstable, which is an undesirable feature in industrial systems. The instability mechanism is the same one that produces chugging in a domestic back boiler, if the pipework to the hot water tank is incorrectly installed (i. e., a section of pipe from fire to hot water tank is inclined downwards), and also the same that produces geysering in geothermal springs. A more direct analogy is in certain types of effusive volcanic eruptions, such as that at Villarrica volcano in Chile, where the magma flow in the vent appears to oscillate between a bubbly flow régime and a slug flow régime.

The simplest model to describe the instability was posed and analysed by Davies and Potter (1967). They studied a homogeneous two phase flow model, in which it is assumed that in the two phase region, the liquid and vapour phases move with the same velocity. This is the simplest assumption, though it is inaccurate, particularly in the annular flow régime. Nevertheless it appears to capture the essence of the instability, and serves as a useful starting point.

The geometry of the flow under consideration is shown in figure 5.3. Heat is added to the flow at a rate  $Q$  (units  $\text{W m}^{-3}$ , thus heat flux per unit length of the tube), and we suppose that the flow consists of two régimes, a sub-cooled region occupying the initial part of the tube  $0 < z < r(t)$ , and a two-phase region  $r < z < l$ , in which liquid and vapour coexist as a bubbly flow. In practice, such two phase flows pass through a succession of flow régimes, from bubbly to slug to churn to annular, as the vapour fraction increases. To model such different régimes at all requires a more sophisticated two fluid model, but it is not known with any theoretical confidence what controls the transition between the different régimes, so that the effort involved may not be appropriate.

We will study a homogeneous model of the two phase region. We suppose that the flow is driven by a pressure drop  $\Delta p$ , and that the inlet temperature and pressure (and thus also enthalpy) are prescribed. Equations describing the flow are those of conservation of mass, momentum and energy, and they take the form

$$\begin{aligned}\rho_t + (\rho u)_z &= 0, \\ \rho(u_t + uu_z) &= -p_z - \rho g - \frac{4f\rho u^2}{d}, \\ \rho \frac{dh}{dt} - \frac{dp}{dt} &= Q,\end{aligned}\tag{5.126}$$

where  $\rho$  is density (of the liquid in the single phase region, of the mixture in the two-phase region),  $u$  is velocity,  $p$  is (total) pressure, and  $h$  is enthalpy;  $\frac{d}{dt}$  is the material derivative  $\frac{\partial}{\partial t} + u\frac{\partial}{\partial x}$ ,  $f\rho u^2$  is the wall stress,  $g$  is the gravitational acceleration, and  $d$  is the tube diameter. These are to be solved subject to the conditions

$$\begin{aligned}h &= h_0 \quad \text{at } z = 0, \\ -\int_0^l p_z dz &= \Delta p.\end{aligned}\tag{5.127}$$

We may note that where previously we used  $f\rho_l u^2$  as the wall stress, here we choose  $\tau = f\rho u^2$ . The difference is largely cosmetic, since in practice the friction factor would be prescribed as a function of void fraction, Reynolds number, and so on. Since the wall stress accounts for Reynolds stresses, the use of  $\rho$  is in fact perhaps more natural. In our discussion, we will take  $f$  to be constant as a convenience.

One simplification which we immediately make is to suppose that

$$\frac{\Delta p}{\rho_g L} \ll 1,\tag{5.128}$$

where  $\rho_g$  is vapour density and  $L$  is latent heat. This is well satisfied in industrial contexts, and guarantees that the adiabatic pressure derivative term in the enthalpy equation can be ignored, which we henceforth do. For steam–water systems, this is a

good approximation. For example,  $\rho_g L \approx 270$  bars (1 bar =  $10^5$  Pa =  $10^5$  N m<sup>-2</sup>) at an operating pressure of 30 bars, and  $\rho_g L \approx 13$  bars at atmospheric pressure (where we take vapour density at the boiling point).

### 5.4.1 Sub-cooled region

In the single phase sub-cooled liquid near the inlet, we suppose the liquid is incompressible, so that  $\rho = \rho_l$  is constant, and thus  $u = U(t)$ , and

$$h_t + U h_z = \frac{Q}{\rho_l}. \quad (5.129)$$

With the inlet condition (5.127)<sub>1</sub>, this is easily solved by the method of characteristics to give

$$\begin{aligned} z &= \int_s^t U(\theta) d\theta, \\ h &= \frac{Q}{\rho_l} (t - s) + h_0. \end{aligned} \quad (5.130)$$

We assume here that  $Q$  is constant. A more realistic assumption is to have  $Q$  depend on  $u$  (via a heat transfer coefficient), and it is possible to treat this case also, though less easily. We define the saturation enthalpy of the liquid at the boiling point to be  $h_{\text{sat}}$ , and we define the inlet sub-cooling to be

$$\Delta h = h_{\text{sat}} - h_0; \quad (5.131)$$

then  $h = h_{\text{sat}}$  defines the location of the boiling boundary  $z = r(t)$ , and we find

$$r(t) = \int_{t-\tau}^t U(\theta) d\theta, \quad (5.132)$$

where

$$\tau = \frac{\rho_l \Delta h}{Q}. \quad (5.133)$$

Note that (5.132) introduces a delay  $\tau$  into the system: the boiling boundary position  $r(t)$  depends on the history of the inlet velocity  $U(t)$ .

### 5.4.2 Two-phase region

In the two phase liquid–vapour region  $z > r$ , we define the void fraction  $\alpha$  to be the volume fraction of vapour. We then have the definitions of two phase density and enthalpy:

$$\begin{aligned} \rho &= \rho_l(1 - \alpha) + \rho_g \alpha, \\ \rho h &= \rho_l h_l(1 - \alpha) + \rho_g h_g \alpha, \end{aligned} \quad (5.134)$$

where suffixes  $l$  and  $g$  indicate liquid and gas properties; note that the latent heat is

$$L = h_g - h_l, \quad (5.135)$$

and we will assume that the boiling temperature is constant, thus  $h_l = h_{\text{sat}}$ . Eliminating  $\alpha$  yields  $h$  as a function of  $\rho$ , and we substitute this into (5.126) to find that  $\rho$  and  $u$  in  $z > r$  satisfy the equations

$$\begin{aligned} \rho_t + u\rho_z &= -u_z\rho, \\ \frac{\rho_g\rho_l L}{\Delta\rho} u_z &= Q, \end{aligned} \quad (5.136)$$

where

$$\Delta\rho = \rho_l - \rho_g, \quad (5.137)$$

and the equations (5.136) are subject to the boundary conditions

$$\rho = \rho_l, \quad u = U(t) \quad \text{on} \quad z = r. \quad (5.138)$$

When this pair of equations is solved, then the inlet velocity is found by requiring that the prescribed pressure drop is

$$\Delta p = \int_0^l \left[ \rho(u_t + uu_z) + \rho g + \frac{4f\rho u^2}{d} \right] dz. \quad (5.139)$$

### 5.4.3 Non-dimensionalisation

At this point it is convenient to non-dimensionalise the model. We scale the variables as follows:

$$\rho \sim \rho_l, \quad z, r \sim l, \quad t \sim \tau, \quad u, U \sim u_0 = \frac{l}{\tau}; \quad (5.140)$$

we then find the dimensionless velocity in the two-phase region to be

$$u = U + \mu(z - r), \quad (5.141)$$

and the density there satisfies

$$\rho_t + [U + \mu(z - r)]\rho_z = -\mu\rho, \quad (5.142)$$

where

$$\mu = \frac{\rho_l \Delta h}{\rho_g L}, \quad (5.143)$$

subject to the condition that

$$\rho = 1 \quad \text{on} \quad z = r, \quad (5.144)$$

where the boiling boundary is given by

$$r = \int_{t-1}^t U(\theta) d\theta. \quad (5.145)$$

This is easily solved using the method of characteristics, and we obtain the implicit solution

$$z = r(t')e^{\mu(t-t')} + \int_{t'}^t [U(s) - \mu r(s)] e^{\mu(t-s)} ds, \quad \rho = e^{-\mu(t-t')}. \quad (5.146)$$

Eliminating  $t'$ , integrating the  $U(s)$  part of the integral by parts using (5.145), and changing the variable of integration, we can simplify the solution to the form

$$z = r(t) + \int_0^{\ln \frac{1}{\rho}} \frac{1}{\mu} U_1 \left( t - \frac{\xi}{\mu} \right) e^{\xi} d\xi, \quad (5.147)$$

in which  $U_1(\eta) = U(\eta - 1)$ .

The single phase pressure drop is

$$\Delta p_{\text{sp}} = \Delta p_i r \dot{U} + \Delta p_g r + \Delta p_f r U^2, \quad (5.148)$$

where

$$\Delta p_i = \rho_l u_0^2, \quad \Delta p_f = \frac{4fl\rho_l u_0^2}{d}, \quad \Delta p_g = \rho_l gl, \quad (5.149)$$

and the corresponding two-phase pressure drop is

$$\Delta p_{\text{tp}} = \Delta p_i \int_r^1 \rho(u_t + uu_z) dz + \Delta p_g \int_r^1 \rho dz + \Delta p_f \int_r^1 u^2 dz. \quad (5.150)$$

We define the pressure drop scale to be  $\Delta p_f$ , and then in terms of the dimensionless parameters

$$\gamma = \frac{\Delta p_g}{\Delta p_f} = \frac{gd}{4fu_0^2}, \quad \delta = \frac{\Delta p_i}{\Delta p_f} = \frac{d}{4fl} = \gamma F^2 \quad (5.151)$$

(note that  $\delta$  is distinct from its earlier usage as density ratio), the dimensionless pressure drop  $\Pi = \frac{\Delta p}{\Delta p_f}$  is given by

$$\Pi = \left[ U^2 r + \int_r^1 \rho u^2 dz \right] + \gamma \left[ \int_r^1 \rho dz + r \right] + \delta \left[ \int_r^1 \rho(u_t + uu_z) dz + \dot{U} r \right]. \quad (5.152)$$

#### 5.4.4 A reduced model

The model thus reduces to solving (5.152), subject to the definitions in (5.141), (5.145) and (5.147). The delay (scaled to be one) in this system is explicitly represented by the delayed function  $U_1(t) = U(t - 1)$ , but a second (smaller) delay corresponding to transit through the two-phase region is manifested in (5.147)

The model depends on the four parameters  $\Pi$ ,  $\mu$ ,  $\gamma$  and  $\delta$ . It is common to describe the behaviour of the system in terms of two dimensionless parameters known as the sub-cooling number  $N_{\text{sub}}$  and the phase change number  $N_{\text{pch}}$ . In terms of the parameters defined above, these are defined by

$$N_{\text{sub}} = \mu, \quad N_{\text{pch}} = \frac{\mu}{U}. \quad (5.153)$$

Stability diagrams are often given in terms of these parameters. (Obviously, assuming that  $U$  is constant, i. e., under steady state conditions.)

It is generally the case that  $\rho_g \ll \rho_l$ ; on the other hand, the enthalpy sub-cooling is  $\Delta h = c_p \Delta T$ , where  $c_p$  is the specific heat and  $\Delta T$  is the sub-cooling as a temperature deficit below the boiling temperature; at atmospheric pressure,  $\frac{L}{c_p} \approx 550$  K, so that

the relevant Stefan number  $\frac{L}{c_p \Delta T}$  can be quite large. But at least at atmospheric pressure, the density ratio dominates, and  $\mu$  is large. Boilers typically operate at high pressure, where the density ratio between steam and water is much smaller (for example a factor of 50 at 30 bars), and so  $\mu$  may not be so high. Nevertheless, we shall suppose it is sufficiently large that an approximation based on this can be developed.

To estimate the parameters  $\gamma$  and  $\delta$ , we take  $u_0 = 1$  m s<sup>-1</sup>,  $l = 10$  m,  $d = 10^{-2}$  m,  $f = 0.01$ ,  $g \sim 10$  m s<sup>-2</sup>. From these we find  $\gamma \approx 2.5$ ,  $\delta \approx 0.025$ . Thus it seems reasonable to suppose that  $\gamma \sim O(1)$ , and  $\delta \sim \frac{1}{\mu} \ll 1$ . It should be pointed out that

since  $u \sim \mu$ , then also  $\rho \sim \frac{1}{\mu}$ , which implies, since  $\rho \approx 1 - \alpha$ , that  $\alpha \approx 1$  when well into the two-phase region. This would certainly imply that régime transition occurs, and annular flow becomes appropriate at high values of  $\alpha$ . This needs to be borne in mind in practice.

Further, if  $\rho \sim \frac{1}{\mu}$ , then  $\xi \sim \ln \frac{1}{\mu}$  in the integral of (5.147), and thus  $\frac{\xi}{\mu} \ll 1$ . It then follows that we can expand the argument of  $U_1$  in (5.147), and this leads to the explicit approximation

$$\rho \approx \frac{U_1}{U_1 + \mu(z - r)}. \quad (5.154)$$

Using this together with (5.141), we find successively

$$\begin{aligned} \int_r^1 \rho u^2 dz &= U_1 \left[ \frac{\dot{r}^2}{\mu} \ln \left\{ \frac{U_1 + \mu(1-r)}{U_1} \right\} + (2U - U_1)(1-r) + \frac{1}{2}\mu(1-r)^2 \right], \\ \int_r^1 \rho dz &= \frac{U_1}{\mu} \ln \left\{ \frac{U_1 + \mu(1-r)}{U_1} \right\}, \\ \int_r^1 \rho (u_t + uu_z) dz &= \frac{\dot{U}U_1}{\mu} \ln \left\{ \frac{U_1 + \mu(1-r)}{U_1} \right\} + \mu U_1(1-r), \end{aligned} \quad (5.155)$$

and it then follows that the dimensionless pressure drop equation (5.152) takes the

approximate form

$$\Pi \approx \frac{1}{2}\mu U_1(1-r)^2 + (\gamma + U^2 + \delta\dot{U})r + U_1(2U - U_1)(1-r) + \delta\mu U_1(1-r), \quad (5.156)$$

where we have omitted on the right a small term

$$\frac{U_1 L}{\mu} \left[ (U - U_1)^2 + \gamma + \delta\dot{U} \right], \quad L = \ln \left\{ 1 + \frac{\mu(1-r)}{U_1} \right\}. \quad (5.157)$$

The terms in (5.156) are of comparable size, except that the term  $\delta r\dot{U}$  is promoted; the logarithmic term in (5.157) seems safe to neglect, as we have done.

### 5.4.5 Steady states

We begin by calculating the steady state solutions for  $U$  as a function of the prescribed pressure drop  $\Pi$ . In the steady state,  $r = U$ , and thus (5.156) takes the form (dropping the logarithmic term)

$$\Pi = \frac{1}{2}\mu U(1-U)^2 + \gamma U + U^2 + \delta\mu U(1-U). \quad (5.158)$$

We would normally expect that  $U$  would increase monotonically with  $\Pi$ , but because (5.158) is a cubic, this need not always be the case. Figure 5.4 shows steady states of  $U$  as a function of applied pressure drop. Evidently multiple steady states occur. The middle branch is unstable, this instability being known as Ledinegg instability. In the steady state  $r = U$ , so that the Ledinegg values  $0.49 \lesssim U \lesssim 0.85$  (in figure 5.4) correspond to situations where the boiling boundary approaches the outlet. Incidentally, this figure shows why it is necessary to include the apparently relatively small second, third and fourth terms in (5.158), which are of  $O(1)$ ; it is because the maximum of the ‘large’ first term is just 2.2 when  $\mu = 30$ .

### 5.4.6 Instability and ill-posedness

Oscillatory instabilities can occur as well as the direct Ledinegg instability. To study these we begin by considering only the first term in (5.156). Thus we have

$$\Pi \approx \frac{1}{2}\mu U_1(1-r)^2, \quad r = \int_{t-1}^t U(\theta) d\theta. \quad (5.159)$$

This innocuous-looking delay integral equation is ill-posed. We can see the ill-posedness as follows. If we define

$$W = \int_{t-1}^t U(\theta) d\theta, \quad (5.160)$$

then  $r = W - W_1$ , and (5.159) is

$$\dot{W}_1 = \frac{2\Pi}{\mu(1-W+W_1)^2}, \quad (5.161)$$

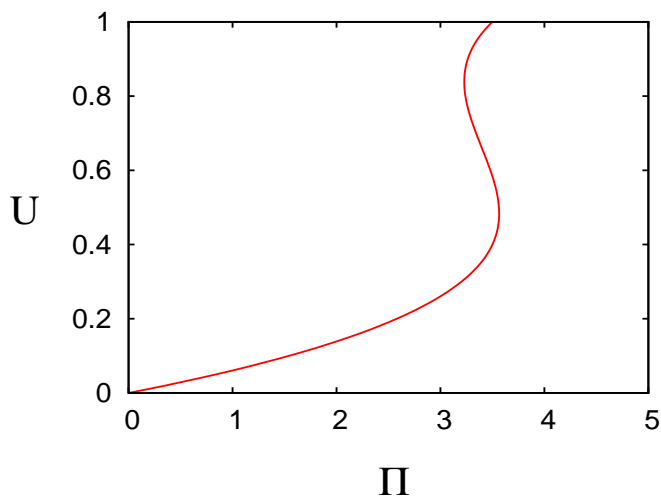


Figure 5.4: Multiple steady states of (5.156) when  $\mu = 30$ ,  $\gamma = 2.5$ ,  $\delta = 0.025$ .

which is an equation of advanced type, i. e., a delay equation with negative delay. In assessing the instability of the steady state, we then find an infinite number of unstable states, whose (complex) growth rate  $\sigma$  tends to infinity in the complex plane with  $\text{Re } \sigma > 0$ .<sup>4</sup>

To be specific, denote the steady state as  $r = U = U^*$ , and linearise the reduced model (5.159). The solutions are exponential, thus

$$U - U^* = e^{\sigma t}, \quad r - U^* = \frac{1}{\sigma} (1 - e^{-\sigma}) e^{\sigma t}, \quad (5.162)$$

and we require  $\sigma$  to satisfy the transcendental equation

$$g_0(\sigma) = \frac{1}{2} (1 - U^*)^2 e^{-\sigma} - \frac{U^* (1 - U^*)}{\sigma} (1 - e^{-\sigma}) = 0. \quad (5.163)$$

It is straightforward to show that this equation has an infinite number of roots in the complex plane, and these tend to the essential singularity at  $\infty$  in the right half plane,  $\text{Re } \sigma > 0$ . This accumulation of rapidly growing modes is the signal of an ill-posed equation of advance.

Ignoring the later terms in (5.156) is thus a singular approximation. There are a number of apparently smaller terms in (5.156) which might regularise the model. The principal suspect in this regard is the sub-cooled frictional pressure drop. Adding this yields the model

$$\Pi \approx \frac{1}{2} \mu U_1 (1 - r)^2 + U^2 r. \quad (5.164)$$

<sup>4</sup>An equation of advanced type is typified by the example  $\dot{u} = -u(t + \tau)$ , where  $\tau$  is positive. Its solution requires knowledge of the future, and so is expected to be ill-posed. Its solutions are  $e^{\sigma t}$ , where  $\sigma = -e^{\sigma \tau}$ , and clearly as  $\sigma \rightarrow \infty$ , so also  $\text{Re } \sigma \rightarrow \infty$ , and we associate this property with ill-posedness.

This gives an equation of mixed type, and regularises the model if  $\mu$  is small enough. Linear stability of the steady state yields the equation for the growth rate  $\sigma$  as

$$g_1(\sigma) = g_0(\sigma) + \frac{U^{*2}}{\mu} \left[ 2 + \frac{1 - e^{-\sigma}}{\sigma} \right] = 0. \quad (5.165)$$

Of concern is the sector where  $\sigma \rightarrow \infty$ . It is easy to show that  $\text{Re } \sigma$  cannot tend to  $+\infty$ . If  $\text{Re } \sigma$  is bounded, then we find

$$\sigma \approx \ln \left[ \frac{\mu(1 - U^*)^2}{4U^*} \right] \pm (2n + 1)i\pi \quad (5.166)$$

for large integer  $n$ , and thus the model is regularised if

$$\mu < \frac{4U^*}{(1 - U^*)^2}. \quad (5.167)$$

This conditional regularisation of the model is reminiscent of the conditional regularisation of two fluid models of bubbly flow for low enough void fraction, associated (perhaps) with flow régime transition boundaries.

The fact that the regularisation is conditional, and in particular does not apply for sufficiently large  $\mu$ , suggests that a further regularisation is necessary. The correct term to include is the derivative term, thus we replace (5.164) by

$$\Pi \approx \frac{1}{2}\mu U_1(1 - r)^2 + (U^2 + \delta\dot{U})r. \quad (5.168)$$

This unequivocally regularises the model. Linear stability of the steady state is determined by values of  $\sigma$  for which

$$g_2(\sigma) = g_1(\sigma) + \frac{\delta U^* \sigma}{\mu} = 0. \quad (5.169)$$

Now as  $\sigma \rightarrow \infty$ , we must have

$$\frac{\delta U^* \sigma}{\mu} + \frac{1}{2}(1 - U^*)^2 e^{-\sigma} \approx 0, \quad (5.170)$$

and it follows from this that

$$\sigma \approx 2ni\pi - \ln 2n\pi + \dots \quad (5.171)$$

for large integer  $n$ . The problem is thus regularised, although of course there will be many unstable modes with smaller  $|\sigma|$  (for sufficiently small  $\delta$ ).

Based on the above discussion, we now solve (5.156) numerically. We write the equation in the form of a pair of differential-delay equations,

$$\begin{aligned} \dot{W} &= U, \\ \nu r \dot{U} &= \Pi - \frac{1}{2}\mu U_1(1 - r)^2 - (\gamma + U^2)r - q_2 - q_3, \end{aligned} \quad (5.172)$$

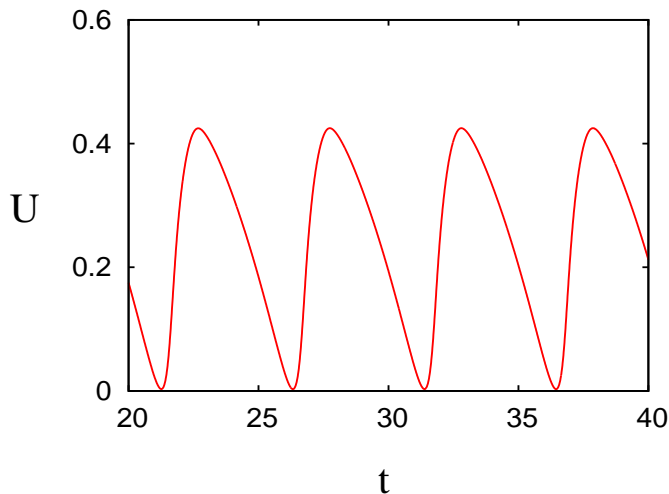


Figure 5.5: Solution of (5.172) with  $\mu = 30$ ,  $\gamma = 2.5$ ,  $\delta = 0.025$ ,  $\Pi = 2$  and  $\nu = 40$ .

where

$$q_2 = \delta\mu U_1(1 - r), \quad q_3 = U_1(2U - U_1)(1 - r), \quad r = W - W_1, \quad (5.173)$$

and the parameter  $\nu = \delta$ , but we wish to use  $\nu$  as an independent parameter in our numerical solution. If we include only the terms discussed above in the regularisation analysis (i. e., put  $\gamma = q_2 = q_3 = 0$ ), then the model is just

$$\begin{aligned} \nu r \dot{U} &= \Pi - \frac{1}{2}\mu U_1(1 - r)^2 - rU^2, \\ \dot{W} &= U, \\ r &= W - W_1, \end{aligned} \quad (5.174)$$

and we will use this below in discussing stability. The solution behaviour for (5.174) is not dramatically different to that of (5.172).

The equations in (5.172) have the appearance of a singularly perturbed system (when  $\nu \ll 1$ ), and it is often challenging to find asymptotic solutions of such equations. In addition, this system has an added twist. If we fix the parameters  $\mu = 30$ ,  $\delta = 0.025$ ,  $\gamma = 2.5$ ,  $\Pi = 2$ , and progressively reduce  $\nu$  from a very high value, we find that the steady state at  $\Pi = 2$ ,  $U = 0.14$  (see figure 5.4) has a Hopf bifurcation to a stable limit cycle as  $\nu$  is reduced through  $\approx 53$ . As  $\nu$  decreases, the amplitude grows until at  $\nu \approx 40$  (as shown in figure 5.5) the inlet velocity decreases to zero, and for  $\nu \lesssim 40$ , reversed flow occurs. The model is not applicable for reversed flow, and indeed the numerical solution breaks down in that case. This appears consistent with theoretical stability results of many authors, which indicate that instability is commonplace at large  $\mu$ . The twist here is that the model itself precludes attainment of the relevant desired asymptotic limit, where  $\nu = \delta \ll 1$ .

### 5.4.7 Stability analysis

In solving (5.172), we have found the following behaviours. Firstly, if we put  $\gamma = q_2 = q_3 = 0$ , as in (5.174), then the steady state is stable for high  $\nu$ , but has limit cycle behaviour at  $\nu \approx 20$ . If we now include gravity, thus  $\gamma = 2.5$ , this behaviour is shifted to  $\nu \approx 35$ . If additionally  $q_2 \neq 0$ , this behaviour is further shifted to  $\nu \approx 40$ , and introduction of  $q_3 \neq 0$  makes little difference to this (as described earlier). So the qualitative behaviour of the simplified model (5.174) and that of the more complete system (5.172) are similar, and in this section we will therefore deal with the simpler one.

If we perturb the equilibrium  $U = r = U^*$ , then the resulting linearised equation has solutions  $U - U^* = e^{\sigma t}$ , providing

$$\nu\sigma^2 + (2V + Ae^{-\sigma})\sigma - B(1 - e^{-\sigma}) = 0, \quad (5.175)$$

where

$$A = \frac{\mu(1 - V)^2}{2V}, \quad B = \mu(1 - V) - V. \quad (5.176)$$

First note that  $\sigma = 0$  is always a solution of this; this represents the invariance of (5.174) to time translation and does not signal instability. Due to Picard's theorem, (5.175) has infinitely many roots  $\sigma(V, \mu, \nu)$  which accumulate at  $\sigma = \infty$ . Moreover, at large  $\nu$  these all have negative real part. Suppose that  $\text{Re } \sigma > 0$  for some  $\sigma$ ; then  $|e^{-\sigma}| < 1$  and so  $|1 - e^{-\sigma}| < 2$  is also bounded. Since from (5.175),

$$\sigma = \frac{1}{2\nu} \left[ -(2V + Ae^{-\sigma}) \pm \left\{ (2V + Ae^{-\sigma})^2 + 4\nu B(2V + Ae^{-\sigma})(1 - e^{-\sigma}) \right\}^{1/2} \right], \quad (5.177)$$

it follows that  $\sigma$

is for large  $\nu$ ; expanding (5.175) for small  $\sigma$  then leads to

$$\sigma \approx -\frac{B - A - 2V}{\nu - A + \frac{1}{2}B}, \quad (5.178)$$

and this is real negative if  $V < \frac{1}{3}$ ; if  $V > \frac{1}{3}$ , it becomes positive if  $\mu > \frac{6V^2}{(1 - V)(3V - 1)}$ ; but this just corresponds to the Ledinegg instability discussed above. Discounting this possibility, it follows that in fact  $\text{Re } \sigma < 0$  for large  $\nu$ .

Thus instability may occur as  $\nu$  is reduced, and this will be of Hopf type (always excluding the Ledinegg case which we have already discussed), and will occur at  $\nu = \nu_c$  where  $\sigma = i\Omega$ , and thus

$$\begin{aligned} \nu &= \frac{A\Omega \sin \Omega + B \cos \Omega}{\Omega^2}, \\ \Omega &= \frac{B \sin \Omega}{2V + A \cos \Omega}. \end{aligned} \quad (5.179)$$

If we confine ourselves to the case where  $\mu$  is large, then

$$\Omega \approx \frac{2V \tan \Omega}{1 - V}. \quad (5.180)$$

Since we discount Ledinegg, we assume  $V < \frac{1}{3}$ . Then (5.180) has an infinite number of non-zero roots  $\pm\Omega_0, \pm\Omega_1, \dots$  with  $\Omega_k \in (k\pi, (k + \frac{1}{2})\pi)$ , and the corresponding values of  $\nu$  are approximately

$$\nu = \frac{\mu(1 - V)}{\Omega^2 \cos \Omega}. \quad (5.181)$$

Instability first occurs for  $\Omega = \Omega_0$ , and thus

$$\nu_c \approx \frac{\mu(1 - V)}{\Omega_0^2 \cos \Omega_0}, \quad (5.182)$$

and is of  $O(\mu)$ , as suggested by the numerical results.

To get a more explicit idea of the dependence on  $\nu$  on  $V$ , we consider the limit  $V \ll 1$ , when  $\Omega_0 \approx \frac{1}{2}\pi - \frac{(1 - V)}{\pi V}$ , and this leads to

$$\nu_c \approx \frac{\mu(1 - V)^2}{\pi V}, \quad (5.183)$$

and it turns out this is an excellent approximation all the way t  $V = 0.25$ , after which it diverges from true value, which tends to infinity as  $V \rightarrow \frac{1}{3}$ . Equally, we can look at the limit  $V \rightarrow \frac{1}{3}$ , when  $\Omega \rightarrow 0$ , and we then find

$$\nu_c \approx \frac{2\mu(1 - V)}{9(1 - 3V)}. \quad (5.184)$$

It is then tempting to look for a uniform approximation, even iif there is no basis for this. But barging ahead with the matched asymptotic expansion idea of adding

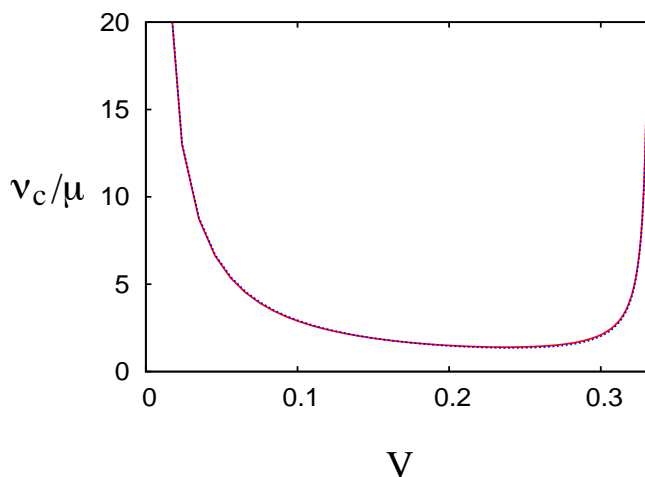


Figure 5.6: The approximation to  $\nu_c/\mu$  in (5.185) (blue) overlying the exact expression (5.182) in red.

the two approximations and subtracting a ‘common part’, we actually find that the expression

$$\nu_c = \mu \left[ \frac{(1-V)^2}{\pi V} + \frac{2(1-V)}{9(1-3V)} - \frac{1}{2} \right] \quad (5.185)$$

provides an essentially perfect uniform approximation to the exact solution! This is shown in figure 5.6.

## Outlook

In practice, of course, we should have  $\nu = \delta$  and small. All of the above indicates that when  $\mu \gg 1$ , the steady state is wildly unstable. Perhaps this is why boilers commonly operate at high pressure, where the density ratio  $\frac{\rho_l}{\rho_g}$ , and thus  $\mu$ , is reduced.

On the other hand, the large value of  $\mu$  implies in itself that a transition to annular flow would occur, and the stability characteristics might be quite different.

## Exercises

5.1 A basic two fluid model of two-phase flow is given by the equations

$$\begin{aligned} (\alpha\rho_g)_t + (\alpha\rho_g v)_z &= \Gamma, \\ \{\rho_l(1-\alpha)\}_t + \{\rho_l(1-\alpha)u\}_z &= -\Gamma, \\ \rho_g[v_t + vv_z] &= -p_z - \frac{M}{\alpha}, \\ \rho_l[u_t + D_l uu_z] &= -p_z + \frac{M}{1-\alpha}, \end{aligned}$$

where  $\alpha$  is void fraction,  $u$  and  $v$  are liquid and gas phase velocities,  $p$  is pressure, and  $\rho_g$  and  $\rho_l$  are gas and liquid densities; the constant  $D_l > 1$  is a profile coefficient, and  $\Gamma$  and  $M$  are interfacial source and drag terms, which are prescribed algebraic functions of the variables.

Explain how to find the characteristics of this system when written in the form

$$A\psi_t + B\psi_x = \mathbf{c}.$$

(i) Assuming  $\rho_g$  and  $\rho_l$  are constant and  $\rho_g \ll \rho_l$ , show that the characteristics are generally real.

(ii) If

$$\frac{d\rho_g}{dp} = \frac{1}{c_g^2}, \quad \frac{d\rho_l}{dp} = \frac{1}{c_l^2},$$

calculate approximate values of the characteristics if  $u, v \ll c_l, c_g$  and  $\rho_g \ll \rho_l$ , and comment on the physical significance of these.

5.2 The shallow water equations are given by

$$\begin{aligned} h_t + (hu)_x &= 0, \\ u_t + uu_x + gh_x &= 0, \end{aligned}$$

By a suitable transformation, show that they can be written in the form

$$\begin{aligned} u_t + uu_x + 2ss_x &= 0, \\ 2s_t + su_x + 2us_x &= 0, \end{aligned}$$

and by defining  $\boldsymbol{\psi} = (u, s)^T$ , write this in the form

$$A\boldsymbol{\psi}_t + B\boldsymbol{\psi}_x = 0.$$

Find the eigenvalues  $\lambda_{\pm}$  and corresponding eigenvectors of  $A^{-1}B$ , and show that the matrix of column eigenvectors  $P$  such that  $BP = APD$ , where  $D = \text{diag}(\lambda_+, \lambda_-)$ , is a constant matrix. Hence show, by defining  $\boldsymbol{\psi} = P\mathbf{v}$ , that  $\mathbf{v}_t + D\mathbf{v}_x = 0$ , and give the Riemann invariants  $v_i$  in terms of  $u$  and  $s$ .

5.3 Consider a two-phase (liquid-gas) flow through a pipe with cross-sectional area  $A$ . The coordinate system is chosen so that the  $z$ -axis points along the centre of the pipe, and  $x$  and  $y$  are the cross-sectional coordinates;  $t$  denotes time. Averaged quantities (denoted by bars) only depend on  $z$  and  $t$ .

(a) Define the indicator function  $X_g(x, y, z, t)$  for the gas phase and use it to derive the mass conservation equation

$$\frac{\partial(\alpha\bar{\rho}_g)}{\partial t} + \frac{\partial(\alpha\bar{\rho}_g\bar{v})}{\partial z} = 0.$$

In your derivation, the gas volume fraction  $\alpha(z, t)$ , the gas average density  $\bar{\rho}_g(z, t)$  and gas average velocity  $\bar{v}(z, t)$  must be defined as integrals over the pipe cross section. What is the analogous equation (and definitions) for the liquid phase with density  $\bar{\rho}_l(z, t)$  and average velocity  $\bar{u}(z, t)$ ?

(b) Now consider an annular flow through a circular pipe of radius  $R$  with a gas core and the liquid flowing along the wall, so that the gas-liquid interface is located at radius  $R\sqrt{\alpha}$ . Assume that  $\rho_g > 0$  and  $\rho_l > 0$  are constant. The momentum conservation equations are

$$\begin{aligned} \rho_g \left[ \frac{\partial(\alpha\bar{v})}{\partial t} + \frac{\partial(\alpha\bar{v}^2)}{\partial z} \right] &= -\alpha \frac{\partial\bar{p}}{\partial z} - \frac{F_{gl}}{A}, \\ \rho_l \left[ \frac{\partial\{(1-\alpha)\bar{u}\}}{\partial t} + \frac{\partial\{(1-\alpha)D_l\bar{u}^2\}}{\partial z} \right] &= -(1-\alpha) \frac{\partial\bar{p}}{\partial z} + \frac{(F_{gl} - F_{lw})}{A}, \end{aligned}$$

where  $D_l > 1$  is a constant.  $F_{gl}$  denotes the interfacial drag on the gas due to the liquid, and  $F_{lw}$  is the drag on the liquid at the wall. Assume that

$$F_{gl} = 2\pi R\sqrt{\alpha}\rho_g f_{gl}(\bar{v} - \bar{u})|\bar{v} - \bar{u}|, \quad F_{lw} = 2\pi R\rho_l f_{lw}\bar{u}|\bar{u}|,$$

where  $f_{gl}$  and  $f_{lw}$  are dimensionless friction factors. At  $z = 0$ , the inlet conditions are  $\alpha = \alpha_0$ ,  $\bar{v} = \bar{v}_0$ ,  $\bar{u} = \bar{u}_0$ , and  $\bar{p} = \bar{p}_0$ .

Now introduce scalings  $R/f_{gl}$  for  $z$  and  $R/f_{gl}U$  for  $t$ , as well as

$$\alpha = 1 - B\beta, \quad \bar{u} = Uu, \quad \bar{v} = Vv, \quad \bar{p} = p_a + Pp,$$

with  $B = \frac{f_{lw}}{f_{gl}}$ ,  $V = \alpha_0 \bar{v}_0$ ,  $P = \rho_g V^2$ ,  $U = \varepsilon V$ , and  $\varepsilon = \left( \frac{\rho_g f_{gl}}{\rho_l f_{lw}} \right)^{1/2}$ .

Non-dimensionalise the four mass and momentum equations, writing the equations in terms of variables  $\beta$ ,  $u$ ,  $v$ ,  $p$  and parameters  $\varepsilon$ ,  $D_l$  and  $B$ . Express the non-dimensional inlet values,  $\beta_0$ ,  $u_0$ ,  $v_0$  and  $p_0$  in terms of given quantities.

(c) Suppose  $0 < D_l - 1 \ll 1$ ,  $B \ll 1$ ,  $\varepsilon \ll 1$ . Derive the leading order equations for the steady state, and find solutions for  $u > 1$ ,  $v > 0$ ,  $\beta > 0$  that satisfy the inlet conditions  $\beta = \beta_0$ ,  $v = 1$ ,  $u = u_0$ .

5.4

5.5 The energy equation for a one-dimensional two-phase flow in a tube is given by

$$\begin{aligned} \Gamma L + \alpha c_{pg}(T_t + vT_z) + (1 - \alpha)\rho_l c_{pl}(T_t + uT_z) - \{(\alpha p_g)_t + (\alpha p_g v)_z\} \\ - [\{(1 - \alpha)p_l\}_t + \{(1 - \alpha)p_l u\}_z] = Q, \end{aligned}$$

where

$$\Gamma = (\alpha \rho_g)_t + (\alpha \rho_g v)_z = -[\{(1 - \alpha)\rho_l\}_t + \{(1 - \alpha)\rho_l u\}_z],$$

and the temperatures of the two phases are assumed equal, and denoted by  $T$ .

The enthalpy of each phase satisfies  $dh_k = c_{pk} dT$ , and is related to the internal energy  $e_k$  by

$$h_k = e_k + \frac{p_k}{\rho_k};$$

$L = h_g - h_l$  is the latent heat. Deduce that the energy equation can be written in the form

$$(\alpha \rho_g e_g)_t + (\alpha \rho_g e_g v)_z + [(1 - \alpha)\rho_l e_l]_t + [(1 - \alpha)\rho_l e_l u]_z = Q.$$

Define the mixture density by

$$\rho = \rho_l(1 - \alpha) + \rho_g \alpha,$$

the mixture pressure by

$$p = (1 - \alpha)p_l + \alpha p_g,$$

the mixture internal energy by

$$\rho e = \alpha \rho_g e_g + (1 - \alpha)\rho_l e_l,$$

and the mixture enthalpy by

$$h = e + \frac{p}{\rho};$$

deduce that

$$\rho h = \alpha \rho_g h_g + (1 - \alpha) \rho_l h_l.$$

If the flow is homogeneous, deduce that

$$\rho \frac{de}{dt} = Q,$$

where  $\frac{d}{dt}$  is the material derivative, and if the pressure drop along the tube  $\Delta p \ll \rho_g L$ , show that  $\frac{de}{dt} \approx \frac{dh}{dt}$ , and deduce that

$$\frac{\partial u}{\partial z} = \frac{(\rho_l - \rho_g)Q}{\rho_g \rho_l L}.$$

- 5.6 Write down the two-fluid model for two-phase flow in a pipe of length  $l$  and diameter  $d$ , including a phase change term and an interfacial drag term, a liquid profile coefficient  $D_l$  of  $O(1)$ , wall friction and gravity. The interfacial drag term is taken to be

$$M = \frac{3C_D \alpha \rho_l}{4d_b} (v - u)^2,$$

where  $d_b$  is bubble diameter and  $C_D$  is a drag coefficient of  $O(1)$ , and the wall friction term is

$$\frac{4f \rho_l u^2}{d},$$

where  $f$  is a friction factor.

Assuming that the phase densities  $\rho_g$  and  $\rho_l$  are constant, the phase pressures are equal, and that a suitable velocity scale is  $U$ , make the model dimensionless, and show that it can be written in the form

$$\begin{aligned} \alpha_t + (\alpha v)_z &= \Gamma, \\ -\alpha_t + \{(1 - \alpha)u\}_z &= -\delta\Gamma, \\ \delta F^2 [(\alpha v)_t + (\alpha v^2)_z] &= -\alpha p_z - \delta\alpha - \frac{\alpha(v - u)^2}{\nu^2}, \\ F^2 [\{(1 - \alpha)u\}_t + \{D_l(1 - \alpha)u^2\}_z] &= -(1 - \alpha)p_z - (1 - \alpha) + \frac{\alpha(v - u)^2}{\nu^2} - \kappa u^2, \end{aligned}$$

and define the parameters  $\delta$ ,  $F$ ,  $\nu$  and  $\kappa$ . For flow in an oil well, suitable choices are  $U = 0.5 \text{ m s}^{-1}$ ,  $l = 10^3 \text{ m}$ ,  $d = 10 \text{ cm}$ ,  $d_b = 1 \text{ cm}$ ,  $C_D = 0.4$ ,  $f = 0.005$ ,  $\rho_g = 1.1 \text{ kg m}^{-3}$ ,  $\rho_l = 10^3 \text{ kg m}^{-3}$ . By using these values, compute the values of the dimensionless parameters, and by neglecting those which are small, derive

a simplified model for  $\alpha$  and  $u$ , assuming boundary conditions  $\alpha = 0$ ,  $u = V(t)$  at  $z = 0$ , and that  $\Gamma$  is constant.

If  $V$  is constant, find the steady state solution, and show that it breaks down ( $\alpha(z)$  becomes multi-valued) if  $\nu > 5^{5/2}V$ .

5.7 An approximate homogeneous two-phase model for density wave oscillations in a pipe of length  $l$  is given by

$$\begin{aligned}\rho_t + u\rho_z &= -u_z\rho, \\ \rho(u_t + uu_z) &= -p_z - \rho g - \frac{4f\rho_l u^2}{d}, \\ \rho(h_t + uh_x) &= Q,\end{aligned}$$

where  $Q$  is constant, and

$$h \approx h^* + \frac{\rho_g L}{\rho}$$

in the two-phase region;  $h^*$ ,  $L$  and  $Q$  are constants,  $\rho_g$  and  $\rho_l$  are (constant) gas and liquid densities,  $h$  is enthalpy, and  $\rho$ ,  $p$  and  $u$  are mixture density, pressure and velocity. For  $h < h_{\text{sat}}$ , the saturation enthalpy, only liquid is present,  $\rho = \rho_l$ , and the above relation for  $h$  is irrelevant.

Boundary conditions for the flow are that

$$\begin{aligned}h &= h_0 < h_{\text{sat}}, \quad u = U(t) \quad \text{at} \quad z = 0, \\ h &= h_{\text{sat}} \quad \text{on} \quad z = r(t),\end{aligned}$$

where the unknown boiling boundary  $r(t)$  is to be determined, and the pressure drop along the pipe,  $\Delta p$ , is prescribed.

Show that

$$r(t) = \int_{t-\tau}^t U(s) ds,$$

and give the definition of  $\tau$ . Show that the pressure drop in the single phase region is

$$\Delta p_{sp} = [\Delta p_i \dot{U} + \Delta p_g + \Delta p_f U^2]r,$$

where

$$\Delta p_i = \rho_l u_0^2, \quad \Delta p_g = \rho_l g l, \quad \Delta p_f = \frac{4f l \rho_l u_0^2}{d}, \quad u_0 = \frac{l}{\tau}.$$

Non-dimensionalise the two-phase model by scaling

$$\rho \sim \rho_l, \quad z, r \sim l, \quad t \sim \tau, \quad u, U \sim u_0,$$

and show that the two-phase velocity and density satisfy

$$u = U + \frac{z-r}{\varepsilon}, \quad z = r + \varepsilon \int_0^{-\ln \rho} U_1(t - \varepsilon \xi) e^\xi d\xi, \quad r = \int_{t-1}^t U(s) ds,$$

where  $U_1(t) = U(t - 1)$ , and give the definition of  $\varepsilon$ . Write down an integral expression for the two-phase pressure drop in the form

$$\Delta p_{tp} = \int_r^1 (\Delta p_i \Phi_i + \Delta p_g \Phi_g + \Delta p_f \Phi_f) dz,$$

where the functions  $\Phi_k$  depend on  $u$  and  $\rho$  and their derivatives.

If  $U = V$  in the steady state, explain why  $0 < V < 1$ . Write down an expression for  $\Delta p$  as a function of  $V$ . Show that if  $V$  is sufficiently close to one,  $\Delta p$  is an increasing function of  $V$ , but that if  $\varepsilon$  is sufficiently small, it is a decreasing function of  $V$  over part of its range.

Now suppose that  $\Delta p_i = \Delta p_g = 0$ . To examine the stability of the steady state (denoted by a suffix zero for  $r$ ,  $u$  and  $\rho$ ), write

$$U = V + v, \quad r = r_0 + r_1, \quad u = u_0 + u_1, \quad \rho = \rho_0 + \rho_1,$$

and linearise the equations. Hence derive expressions for  $r_1$ ,  $u_1$  and  $\rho_1$ .

By taking  $v = e^{\sigma t}$ , derive an algebraic equation for  $\sigma$  from the condition that the perturbation to  $\Delta p$  is zero. If only the single phase pressure drop term is included, show that

$$\sigma = -\frac{1}{2}(1 - e^{-\sigma}),$$

and deduce that the steady state is stable.

If only the two-phase pressure drop is included, and  $\varepsilon$  is assumed to be small, show that

$$\sigma = \gamma(e^\sigma - 1), \quad \gamma = \frac{2(1 - 2V)}{1 - V},$$

and deduce that  $\text{Re } \sigma \rightarrow \infty$  as  $\sigma \rightarrow \infty \in \mathbf{C}$ , and thus that the model is ill-posed.

If both pressure drops are included (and the two-phase approximation for small  $\varepsilon$  is used), show that

$$\sigma = -\frac{\Gamma(1 - e^{-\sigma})}{\delta - e^{-\sigma}}, \quad \delta = \frac{4\varepsilon V^3}{(1 - V)^2}, \quad \Gamma = \gamma + \frac{1}{2}\delta,$$

and deduce that the model is ill-posed for  $\delta < 1$ .

Finally, if the inertial term in the single phase region (only) is included, show that

$$\nu \sigma^2 + \sigma(\delta - e^{-\sigma}) + \Gamma(1 - e^{-\sigma}) = 0, \quad \nu = \frac{2\varepsilon V^2 \Delta p_i}{(1 - V)^2 \Delta p_f},$$

and deduce that the model is well-posed, but the steady state is unstable for small  $\varepsilon$ .

## References

- Aldridge, C. J. and A. C. Fowler 1992 Mathematical modelling of thermosyphons in cryogenic air separation plants. Proc. 6th European Conference on Mathematics in Industry, ed. F. Hodnett; B. G. Teubner, Leipzig, pp. 75-78.
- Baines, P. G. and A. E. Gill 1969 On thermohaline convection with linear gradients. *J. Fluid Mech.* **37**, 289-306.
- Baines, W. D. and J. S. Turner 1969 Turbulent buoyant convection from a source in a confined region. *J. Fluid Mech.* **37**, 51-80.
- Balmforth, N. J., A. Provenzale and J. A. Whitehead 2001 The language of pattern and form. In: Geomorphological fluid mechanics, eds. N. J. Balmforth and A. Provenzale, pp. 3-33. Springer-Verlag, Berlin.
- Barry, R. G. and R. J. Chorley 1998 Atmosphere, weather and climate, 7th ed. Routledge, London.
- Batchelor, G. K. 1967 An introduction to fluid dynamics. C. U. P., Cambridge.
- Charney, J. G. 1947 The dynamics of long waves in a baroclinic westerly current. *J. Meteor.* **4**, 135-163.
- Davies, G. F. 1999 Dynamic Earth: plates, plumes and mantle convection. C. U. P., Cambridge.
- Davies, A. L. and R. Potter 1967 Hydraulic stability: an analysis of the causes of unstable flow in parallel channels. Paper presented at the Symposium on Two-phase Flow Dynamics, Eindhoven EUR4288e, pp. 1,225-1,266.
- Delmastro
- Drew, D. A. 1983 Mathematical modelling of two-phase flow. *Ann. Rev. Fluid Mech.* **15**, 261-291.
- Drew, D. A. and R. T. Wood 1985 Overview and taxonomy of models and methods for workshop on two-phase flow fundamentals. Nat. Bureau of Standards, Gaithersburg, MD, Sept. 22-27.
- Eady, E. T. 1949 Long waves and cyclone waves. *Tellus* **1**, 33-52.
- Fowler, A. 2011 Mathematical geoscience. Springer-Verlag, London.
- Greenspan, H. P. 1968 The theory of rotating fluids. C. U. P., Cambridge.
- Hewitt, G. F. and D. N. Roberts 1969 Studies of two-phase flow patterns by simultaneous flash and X-ray photography. Report no. AERE-M2159, Atomic Energy Research Establishment, Harwell, Oxfordshire, England.

- Holmes, A. 1978 Principles of physical geology. 3rd edition, revised by Doris Holmes. John Wiley and sons, New York.
- Howard, L.N. 1966 Convection at high Rayleigh number. Proc. 11th Int. Cong. Appl. Mech., ed. H.Görtler, pp. 1109-1115. Springer, Berlin.
- Huppert, H. E. 2000 Geological fluid mechanics. In: Batchelor, G. K., H. K. Moffatt and M. G. Worster (eds.), Perspectives in fluid dynamics, pp. 447-506. C. U. P., Cambridge.
- Ishii, M. 1975 Thermo-fluid dynamic theory of two-phase flow. Eyrolles, Paris.
- Jimenez, J. and J. A. Zufiria 1987 A boundary layer analysis of Rayleigh-Bénard convection at large Rayleigh number. J. Fluid Mech. **178**, 53-71.
- Linden, P. F. 2000 Convection in the environment. In: Perspectives in fluid dynamics, eds. G. K. Batchelor, H. K. Moffatt and M. G. Worster, pp. 289-345. C. U. P., Cambridge.
- McBirney, A. R. and R. M. Noyes 1979 Crystallisation and layering of the Skaergaard intrusion. J. Petrol. **20**, 487-554.
- Morton, B. R., G. Taylor and J. S. Turner 1956 Turbulent gravitational convection from maintained and instantaneous sources. Proc. R. Soc. Lond. **A234**, 1-23.
- Pedlosky, J. 1987 Geophysical fluid dynamics. Springer-Verlag, Berlin.
- Roberts, G. O. 1979 Fast viscous Bénard convection. Geophys. Astrophys. Fluid Dynamics **12**, 235-272.
- Rubenstein and Mauri 1986
- Stuhmiller, J. H. 1977 The influence of interfacial pressure forces on the character of two-phase flow model equations. Int. J. Multiphase Flow **3**, 551-560.
- Turcotte, D. L. and E. R. Oxburgh 1967 Finite amplitude convection cells and continental drift. J. Fluid Mech. **28**, 29-42.
- Turcotte, D. L. and G. Schubert 1982 Geodynamics: applications of continuum physics to geological problems. John Wiley, New York.
- Turner, J. S. 1974 Double-diffusive phenomena. Ann. Rev. Fluid Mech. **6**, 37-54.
- Turner, J. S. 1979 Buoyancy effects in fluids. C. U. P., Cambridge.
- Vitagliano, V. and P. A. Lyons 1956 Diffusion coefficients for aqueous solutions of sodium chloride and barium chloride. J. Amer. Chem. Soc. **78** (8), 1,549-1,552.
- Wager, L. R. and G. M. Brown 1968 Layered igneous rocks. Oliver and Boyd, Edinburgh.

Wegener, A.L. 1924 The origin of continents and oceans. 3rd ed., trans. J.G.A. Skerl. Methuen, London.

Ziegler, G. R., A. L. Benado and S. S. H. Rizvi 1987 Determination of mass diffusivity of simple sugars in water by the rotating disk method. J. Food. Sci. **52** (2), 501-502.